# New Pre-Catalysts for Olefin Polymerisation and Ring-Opening Polymerisation of Lactides/Lactones

**Mark Walton**

**2014**

.

# New Pre-Catalysts for Olefin Polymerisation and Ring-Opening Polymerisation of Lactides/Lactones

**Mark Walton**

A thesis submitted in accordance with the requirements for the degree of Doctor of Philosophy by research at the University of East Anglia

**University of East Anglia**

**Department of Chemistry**

**2014**

© This copy of the thesis has been supplied on condition that anyone who consults it is understood to recognise that its copyright rests with the author and that no quotation from the thesis, nor any information derived therefrom, may be published without the author's prior, written consent.

## Abstract

A number of pre-catalysts featuring phenoxyimine, phenolate and calixarene ligand systems have been synthesized, characterised and screened for their ability to polymerize α-olefins or ring open polymerize (ROP) cyclic esters.

The treatment of a number of related phenoxyimine ligands (**L1H** – **L3H**, **L6H** – **L14H**) and bridged phenoxyimines (**L4H$_2$** and **L5H$_2$**) with vanadium trichloride ($VCl_3$), vanadium oxytrichloride ($VOCl_3$) or vanadium oxytripropoxide ($VO(O^nPr)_3$) afforded the compounds **1** – **20**. Compounds **21**, **22** and **23** were isolated from the reaction between $VO(O^nPr)_3$ and diphenolate ligand (**L15H$_2$**) or bridged diphenolates (**L16H$_4$** or **L17H$_4$**) respectively. Treatment of the alkali vanadium compound ($LiVO(OtBu)_4$) with *tert*-butylcalix[6]arene (**L18H$_6$**) afforded compound **24**, while on a number of syntheses, the minor 1D polymeric compound **25** was also obtained. Whilst the reaction between *tert*-butylcalix[8]arene (**L19H$_8$**) and $NaVO(O^tBu)_4$ led to the formation of compound **26**, the use of the alkali free $VO(O^tBu)_3$ resulted in the formation of two solvates of compound **27**.

Imidazole (**L20H**), oxazole (**L21H**), α-diimine (**L22**), iminopyridine (**L23**, **L24**) and phenoxyimine (**L25H** – **L29H**) ligand sets have been treated with group 5 (Nb or Ta) chlorides or oxytrichlorides to afford compounds **28** – **50**, which have been fully characterised. The screening of group 5 compounds **1** – **50** for the polymerisation of α-olefins revealed high activity, significantly in the case of the niobium pre-catalysts which were two orders of magnitude above the previously reported compounds.

The reactions between 1,3-dipropoxy-*p*-*tert*-butyl-calix[4]arene (**L30H$_2$**), hexahomotrioxacalix[3]arene (**L31H$_3$**) or tripropoxy-*p*-*tert*-butylcalix[4]arene (**L32H**) with zinc or magnesium alkyls has been explored, resulting in the isolation of compounds **51** – **58**, which includes a number of heterobimetallic compounds. While all of the zinc and magnesium compounds screened were found to be active for the ring opening polymerisation of either ε-caprolactone or *rac*-lactide, compound **58**, featuring a tripropoxy-*p*-*tert*-butylcalix[4]arene (**L32H**) ligand with a magnesium n-butyl group was found to exhibit exceptional activity and immortal character.

## Acknowledgements

Firstly, I would like to thank my supervisors Professor Carl Redshaw and Dr Simon Lancaster. I thank Professor Carl Redshaw for giving me the opportunity to undertake my PhD; it has been a challenging but very rewarding experience. I thank Dr Simon Lancaster for allowing me to continue my research and for his unwavering interest and discussions on my work. I would also like to thank Dr Gregory Wildgoose for his role as my secondary supervisor.

I would like to thank all of my inorganic colleagues, especially Dr Dave Day, Mr Elliot Lawrence, Mr Tom Dann, Mr James Buttress, Dr Dragoş-Adrian Roşca, Dr Elizabeth Jacobs, Mr James Woods, Miss Chrysoula Pateraki and Mr Angel Bajo-Sanchez. Special thanks go to Dr Oliver Rowe and Dr Lucy Clowes for their constant friendship and support. I would also like to thank many of my organic colleagues for their friendship and discussions.

I am grateful to Dr Myles Cheesman for help with EPR measurements, Dr David Hughes, Dr Anna-Marie Fuller, Dr Joseph Wright and Dr Mark Elsegood for their help with X-ray crystallography as well as Dr Yimin Chao and Dr Alex Walton for X-ray Photoelectron Spectroscopy collection and analysis. I would also like to thank Dr Colin Macdonald for help with NMR experiments.

For their collaboration, I would like to thank Miss Jing Ma and Professor Ke-Quig Zhao at the Sichuan Normal University in china, Mr Kenji Michiue at Mitsui Chemicals and Pertti Elo at the Borealis group.

I am very appreciative to my family and Miss Rowena Maskell for their unconditional support, patience and understanding.

**Abbreviations**

**General**

| | |
|---|---|
| Å | angstrom |
| acac | acetylacetonate |
| Ar | aryl |
| $^{t}$Bu | tertiary butyl |
| $^{t}$BuOH | tertiary butanol |
| Bn | Benzyl |
| °C | degrees Celsius |
| Cp | $\eta^5$ cyclopentadienyl |
| DEAC | diethylaluminium chloride |
| DMAC | dimethylaluminium chloride |
| DMAO | dried methylaluminoxane |
| DSC | differential scanning calorimetry |
| Et | ethyl |
| EADC | ethylaluminium dichloride |
| ETA | ethyltrichloroacetate |
| $Et_2O$ | diethyl ether |
| EtOH | ethanol |
| GPC | gel permeation chromatography |
| h | hour |
| HDPE | high density polyethylene |
| LDPE | low density polyethylene |
| LLDPE | linear low density polyethylene |
| M | metal |
| min | minute |
| MADC | methylaluminium dichloride |
| MAO | methylaluminoxane |
| Me | methyl |
| MeCN | acetonitrile |
| MeOH | methanol |
| *M*n | number average molecular weight |
| *M*w | weight average molecular weight |
| PDI | polydispersity index |

| | |
|---|---|
| PE | polyethylene |
| Ph | phenyl |
| PP | polypropylene |
| $^{i}$Pr | isopropyl |
| PrOH | propanol |
| $P_r$ or $P_m$ | probability of a racemo or meso insertion |
| R | alkyl |
| ROP | ring opening polymerisation |
| rt | room temperature |
| TEA | triethylaluminium chloride |
| THF | tetrahydrofuran |
| TIBA | triisobutylaluminium |
| TMA | trimethylaluminium |

**NMR: Nuclear Magnetic Resonance**

| | |
|---|---|
| br | broad |
| d | doublet |
| J | coupling constant |
| m | multiplet |
| ppm | parts per million |
| q | quartet |
| s | singlet |
| t | triplet |

**IR: Infra-Red**

| | |
|---|---|
| m | mid |
| s | strong |
| w | weak |
| br | broad |

**MS: Mass spectroscopy**

| | |
|---|---|
| CI | chemical ionisation |
| EI | electron impact |
| ESI | electrospray ionisation |

| | |
|---|---|
| MALDI | matrix assisted laser desorption ionisation |
| TOF | time of flight |

# Table of Contents


Abstract iii

Acknowledgements iv

Abbreviations v

**Chapter 1 – Introduction 1**

1.1 Introduction 2

1.1.1 Ziegler-Natta and metallocene polymerization catalysts 2

1.1.1.1 Polymerization of ethylene mechanisms 3

1.1.2 Post-metallocene Catalysts 4

1.1.3 Vanadium Schiff base pre-catalysts for the polymerization of ethylene 4

1.1.3.1 Active species in vanadium polymerization 7

1.1.4 Niobium/Tantalum pre-catalysts for the polymerization of ethylene 10

1.1.5 Biodegradable polymers 11

1.1.5.1 Ring-opening polymerization of cyclic esters 12

1.1.5.2 Living and Immortal polymerization 14

1.1.6 Pre-catalysts for the ROP of cyclic esters 17

1.1.6.1 Zinc and Magnesium 17

1.2 Aims 19

1.3 Overview 20

1.4 References 21

**Chapter 2 – Vanadium Pre-Catalysts 25**

2.1 Introduction 26

2.2 Results and Discussion – Vanadium Phenoxyimine compounds 30

2.2.1 Synthesis and structures 30

2.2.1.1 Silica Immobilisation 41

2.2.2 Vanadium(III) Phenoxyimine Polymerisation Screening 43

2.2.2.1 Schlenk Line Ethylene Screening 43

2.2.2.2 Homogenous Parallel Pressure Reactor Ethylene Screening 44

2.2.2.3 Heterogeneous Parallel Pressure Reactor Ethylene Screening 44

2.2.3 Vanadyl Phenoxyimine Polymerisation Screening 46

2.2.3.1 Schlenk Line Ethylene Screening 46

2.3 Results and Discussion – Di/Tetraphenolate Vanadium Compounds 48

2.3.1 Synthesis and Structures 48

2.3.2 Polymerisation Screening 52

2.4 Results and Discussion – *p-tert*-Butylcalix[6/8]arene Vanadium Compounds 55
2.4.1 Synthesis and Structures 55
2.4.2 Polymerisation Screening 61
2.5 Conclusions 63
2.6 References 65

**Chapter 3 – Niobium and Tantalum Pre-Catalysts 67**

3.1 Introduction 68
3.2 Results and Discussion 69
3.2.1 Synthesis and structures 69
3.2.2 Silica Immobilisation 77
3.2.3 Catalytic Screening 78
3.2.3.1 Homogeneous Catalysis 78
3.2.3.2 Parallel Pressure Reactor screening 83
3.2.3.3 Ethylene PPR polymerisation 84
3.2.3.4 Ethylene/1-hexene copolymerisation 85
3.3 Conclusions 88
3.4 References 89

**Chapter 4 – Zinc and Magnesium Pre-catalysts 90**

4.1 Introduction 91
4.2 Results and Discussion 93
4.2.1 Synthesis of Zinc Calix[4]arene Compounds 93
4.2.2 Synthesis of Magnesium Calix[4]arene Compounds 100
4.2.3 Polymerisation Results using zinc compounds 104
4.2.4 Polymerisation Results using magnesium compounds 106
4.3 Conclusion 109
4.4 References 110

**Chapter 5 – Experimental Section 112**

5.1 General Considerations 113
5.1.1 Synthesis of Known Compounds 114
5.1.2 Synthesis of Vanadium Complexes 114
5.1.2.1 Synthesis of **L1**($VCl_2$) (**3**) 114
5.1.2.2 Synthesis of **L2**($VCl_2$) (**4**) 115
5.1.2.3 Synthesis of **L4**$[VCl_2(THF)_2]_2$ (**7**) 115
5.1.2.4 Synthesis of **L5**$[VCl2(THF)_2]_2$ (**8**) 116
5.1.2.5 Synthesis of (**L3**H)$_2$($VOCl_2$) (**9**) 116

5.1.2.6 Synthesis of **L6**$_2$(VO) (**10**) 117
5.1.2.7 Synthesis of **L7**$_2$(VO) (**11**) 117
5.1.2.8 Synthesis of **L8**$_2$(VO) (**12**) 118
5.1.2.9 Synthesis of **L9**$_2$(VO) (**13**) 118
5.1.2.10 Synthesis of **L10**$_2$(VO) (**14**) 119
5.1.2.11 Synthesis of **L11**$_2$(VO) (**15**) 119
5.1.2.12 Synthesis of **L6**$_2$[(VO)$_2$(μ-O)$_2$] (**16**) 120
5.1.2.13 Synthesis of **L12**$_2$(VO) (**17**) 120
5.1.2.14 Synthesis of **L13**$_2$(VO) (**18**) 121
5.1.2.15 Synthesis of **L14**($VOCl_2$) (**19**) 121
5.1.2.16 Synthesis of **L14**($VO_2$) (**20**) 122
5.1.2.17 Synthesis of **L15**$_2$[(VO)$_2$(μ-O$^n$Pr)]$_2$ (**21**) 122
5.1.2.18 Synthesis of **L16**[VO(O$^n$Pr)(THF)]$_2$ (**22**) 123
5.1.2.19 Synthesis of **L17**[VO(O$^n$Pr)]$_2$ (**23**) 124
5.1.2.20 Synthesis of [Li(NCMe)$_4$][$V_2$(O)$_2$Li(NCMe)(**L18**$H_2$)$_2$]·8MeCN (**24**·8MeCN) 124
5.1.2.21 Synthesis of [$VO_2$($LiMeCN_2$)$_2$(**L18**$H_2$)] (**25**) 125
5.1.2.22 Synthesis of [Na(NCMe)$_5$][(VO)$_2$**L19**H]$^-$4MeCN (**26**.4MeCN) 126
5.1.2.23 Synthesis of [(VO)$_4$L$^8$(μ$^3$-O)$_2$] **27**.3MeCN and **27**.3$CH_2Cl_2$ 126
5.1.3 Synthesis of Niobium/Tantalum Complexes 127
5.1.3.1 Synthesis of **L20**($NbCl_4$) (**28**) 127
5.1.3.2 Synthesis of **L20**[$NbOCl_2$(MeCN)] (**29**) 128
5.1.3.3 Synthesis of **L20**($TaCl_4$) (**30**) 128
5.1.3.4 Synthesis of **L20**[$TaOCl_2$(MeCN)] (**31**) 129
5.1.3.5 Synthesis of **L21**($NbCl_4$) (**32**) 129
5.1.3.6 Synthesis of **L21**[$NbOCl_2$(MeCN)] (**33**) 130
5.1.3.7 Synthesis of **L21**($TaCl_4$) (**34**) 130
5.1.3.8 Synthesis of **L22**($NbCl_4$) (**35**) 131
5.1.3.9 Synthesis of **L24**$_2$($NbCl_2O$)$_2$ (**39**) 131
5.1.3.10 Synthesis of **L25**($NbCl_4$) (**40**) 132
5.1.3.11 Synthesis of **L25**($TaCl_4$) (**41**) 132
5.1.3.12 Synthesis of **L26**($NbCl_4$) (**42**) 133
5.1.3.13 Synthesis of **L26**($TaCl_4$) (**43**) 133
5.1.3.14 Synthesis of **L27**($NbCl_4$) (**44**) 134
5.1.3.15 Synthesis of **L27**($TaCl_4$) (**45**) 134
5.1.3.16 Synthesis of **L28**($NbCl_4$) (**46**) 135
5.1.3.17 Synthesis of **L28**($TaCl_4$) (**47**) 135
5.1.3.18 Synthesis of **L29**($NbCl_4$) (**48**) 136
5.1.3.19 Synthesis of (**L26**$^{-Me}$)($TaCl_3$) (**49**) 136

5.1.3.20 Synthesis of **L27H**($TaCl_5$) (**50**) 137
5.1.4 Synthesis of Zinc/Magnesium Bearing Calix[4]arenes 137
5.1.4.1 Synthesis of **L30**($ZnC_6F_5)_2$ (**51**) 137
5.1.4.2 Synthesis of **L30**[$NaZnN(SiMe_3)_2$] (**53**) 138
5.1.4.3 Synthesis of **L30**[$ZnN(SiMe_3)_2]_2$ (**54**) 139
5.1.4.4 Synthesis of **L31**($ZnC_6F_5)_3$ (**55**) 139
5.1.4.5 Synthesis of (**L31**)$Zn_6(C_6F_5)$(R)(RH)OH·5MeCN (**56**) 141
5.1.4.6 Synthesis of **L30**[Li(THF)$Mg^nBu$)] (**57**) 142
5.1.4.7 Synthesis of **L32**($Mg^nBu$) (**58**) 143
5.1.5 Polymerisation Procedures 143
5.1.5.1 Homogeneous Polyethylene Polymerisation Procedure 143
5.1.5.2 Polycaprolactone Polymerisation Procedure 144
5.1.5.3 Parallel Pressure Reactor Polymerisation Procedure 144
5.1.5.4 Poly(Lactic acid) Polymerisation Procedure 144
5.1.6 X-ray Photoelectron Spectroscopy Analysis 144
5.1.7 Crystallography 145
5.2 References 146

**Chapter 6 – Appendix** **149**

# Chapter 1 – Introduction

## 1.1 Introduction

### *1.1.1 Ziegler-Natta and metallocene polymerization catalysts*

The Nobel Prize in chemistry was awarded to Karl Ziegler and Giulio Natta for their advancement of polymers in 1963, which led to vastly increased production of polyethylene. Low density polyethylene was only produced on a small scale using high temperatures and pressures, Karl Ziegler's discovery of using a mixture of $TiCl_4/AlEt_3$ to produce polymeric $TiCl_3$, allowed for the synthesis of polyethylene using mild conditions.[1] Giulio Natta explored the polymerization of propylene using the same type of catalyst.[2] Whilst use of heterogeneous polymeric $TiCl_3$ for the production of polyethylene was an improvement over the radical mechanisms that were previously used, the catalytic system often gave varying chain length polymer due to a number of different sites present. The unknown mechanism gave the impetus to explore single site homogenous catalysts, which would allow easier investigation. Whilst Breslow had previously investigated the homogeneous titanocene catalyst $Cp_2TiCl_2$, activation using triethylaluminium (TEA) led to a species that exhibited inferior activity when compared with Ziegler's original polymeric $TiCl_3$ and therefore commercially unviable.[3] It was not until Kaminsky and Sinn accidently added water to a bis(cyclopentadienyl)titanium dimethyl and trimethylaluminium polymerization system that they discovered a metallocene that was highly active for polymerization of α-olefins.[4] Subsequent studies revealed the culprit for the higher activities observed was the formation of methylaluminoxane (MAO) which acts as an efficient non-coordinating counter-ion after alkyl extraction (**Scheme 1.1**).[5]

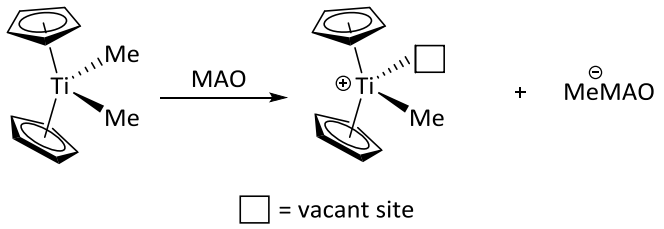


**Scheme 1.1** Activation of $Cp_2TiMe_2$ by MAO.

The 'single site' nature of the metallocene based catalysts allowed not only high activity, 10 – 100 times higher than classical Ziegler-Natta catalysts,[6] but also produced polymers with narrow molecular weight distributions and desirable, predictable properties. The solubility in hydrocarbons and ease of modification of metallocene catalysts allowed the prediction of the polymer properties.

Since the discovery of MAO as activator for metallocene based catalysts, a large number of catalysts have been produced and extensively reviewed.[7-9]

### *1.1.1.1 Polymerization of ethylene mechanisms*

The active catalytic site in olefin polymerization is generally agreed as a coordinatively unsaturated cationic metal alkyl complex which is often generated, such as with MAO, from either the metal halide or alkyl. The Cossee-Arlman mechanism has been widely accepted as the method of polymerization of Ziegler-Natta type catalysts (**Scheme 1.2**), and is applicable to homogeneous catalysts.[10-11] A ethylene monomer co-ordinates to the metal centre, followed by alkyl migration to the 2-position concomitant with regeneration of a vacant site (**Scheme 1.2**).[12-13]

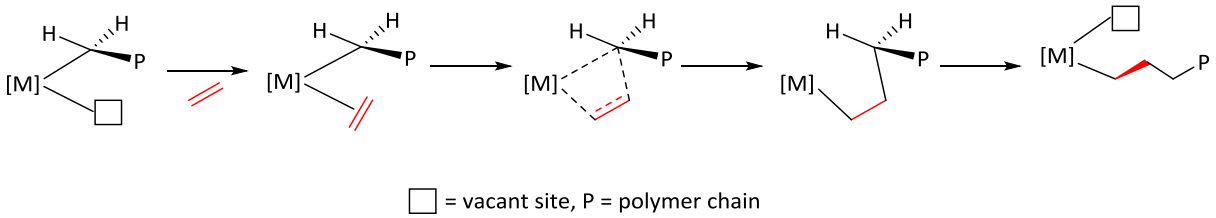


**Scheme 1.2** Cossee-Arlman mechanism for the polymerization of ethylene.

Whilst there are a number of chain transfer reactions, β-hydrogen transfer from the polymer chain to the ethylene monomer is the most dominant (**Scheme 1.3**, (a)).[1] The transfer of β-hydrogen to the metal centre, forming a metal hydride (**Scheme 1.3**, (b)),[1] and chain transfer to the aluminium metal centre will also cause termination of the growing chain (**Scheme 1.3**, (c)).[14-15]

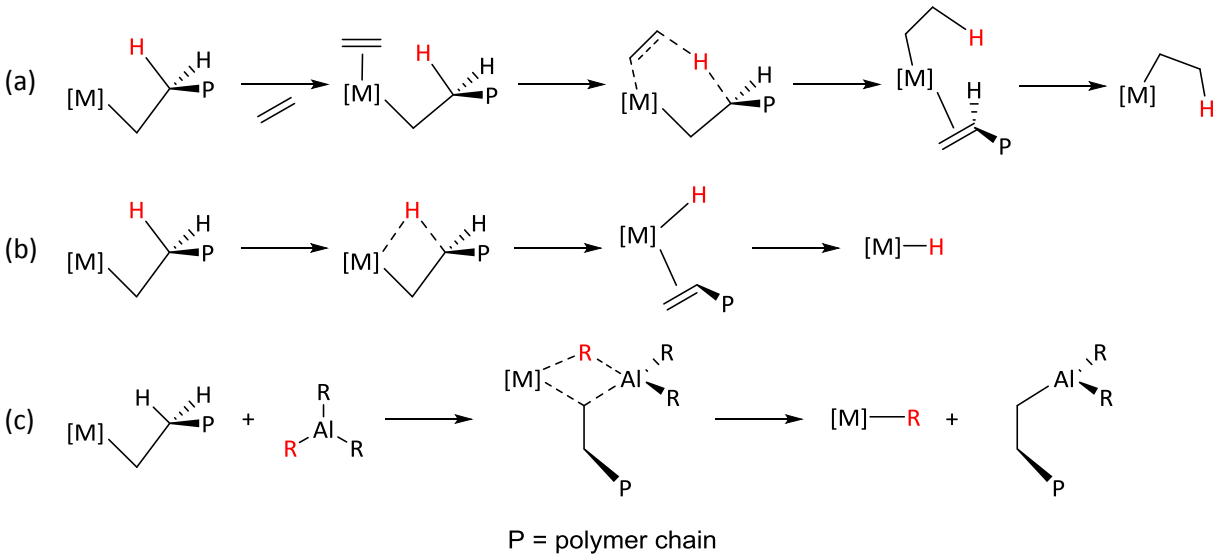


**Scheme 1.3** Chain transfer mechanisms.

### *1.1.2 Post-metallocene Catalysts*

The drive into exploring new metallocene catalysts eventually led to the isolation of *ansa*-metallocenes and constrained geometry catalysts (**Chart 1.1**). The bridge in *ansa*-metallocene catalysts causes the angle between the two cyclopentadienyl rings to open up, decreasing the steric hindrance from the ligand and resulting in higher activities for polymerization,[16] as well as the ability to perform co-polymerizations.[6] Further investigations into the bridge in *ansa*-metallocene catalysts led to the synthesis of constrained geometry catalysts. Compared to metallocenes and *ansa*-metallocenes, the open catalytic site of the constrained geometry catalysts allow for better incorporation of longer α-olefins in the polymer chain while not sacrificing the high molecular mass obtained.[17] A vast number of constrained geometry catalysts have been isolated and screened, many of which have been an extensively reviewed.[18]

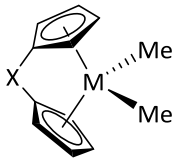


(a)

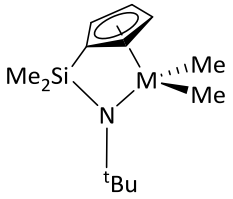


(b)

**Chart 1.1** *Ansa*-metallocene (a) and constrained geometry pre-catalysts (b).

### *1.1.3 Vanadium Schiff base pre-catalysts for the polymerization of ethylene*

While group 4 metallocene, *ansa*-metallocenes and constrained geometry catalysts have been at the forefront of polymerization activity, the search for new catalysts with even greater control over the properties of the resulting polymers has led to investigations of new ligand families. Phenoxyimine based group 4 catalysts have shown promising activities, thermal stabilities and polymer control,[19] the use of tridentate ligands has been explored by the work of Tang *et al.* and the Fujita group,[19-20] while Paolucci *et al.* used a quinoline based titanium catalyst for the polymerization of propylene.[21]

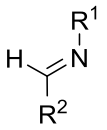


(a) $R^1 \neq H$

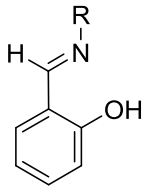


(b)

**Chart 1.2** Schiff Base (a) and Phenoxyimine (b).

Until the seminal work by Fujita and co-workers utilizing a vanadium chloride mononuclear pre-catalyst with two phenoxyimine ligands (**Chart 1.3**, **I**), group 5 Schiff base catalysts gave relatively poor activities.[22-23] Fujita's group found that immobilizing the FI catalysts upon a $MgCl_2$ support restricted the reduction of the vanadium centre to an inactive oxidation state. Li and co-workers further investigated phenoxyimine ligands and compared mono and diligated vanadium compounds; the substituents on the phenoxyimine backbone directly affected the behaviour of the pre-catalysts and were highly active for the polymerization of ethylene (**Chart 1.3**, **II**).[24] Nomura and colleagues investigated an imidovanadium, rather than vanadyl, phenoxyimine compounds (**Chart 1.3**, **III**),[25] which were also highly efficient for the polymerization of ethylene. Redshaw *et al.* have also recently reported phenoxyimine complexes comprising $N_2O_2S_2$-based ligands (**Chart 1.3**, **IV**).[26] In all of these examples alkyl aluminium chlorides are preferred to methylaluminoxane (MAO), use of MAO as co-catalyst generally offers inferior activities.[27] The present discussion on Schiff base ligands in vanadium ethylene polymerization is not exhaustive and comprehensive reviews can be found from the groups of Fujita, Nomura and Redshaw on the use of phenoxyimine type ligand systems.[27-28]

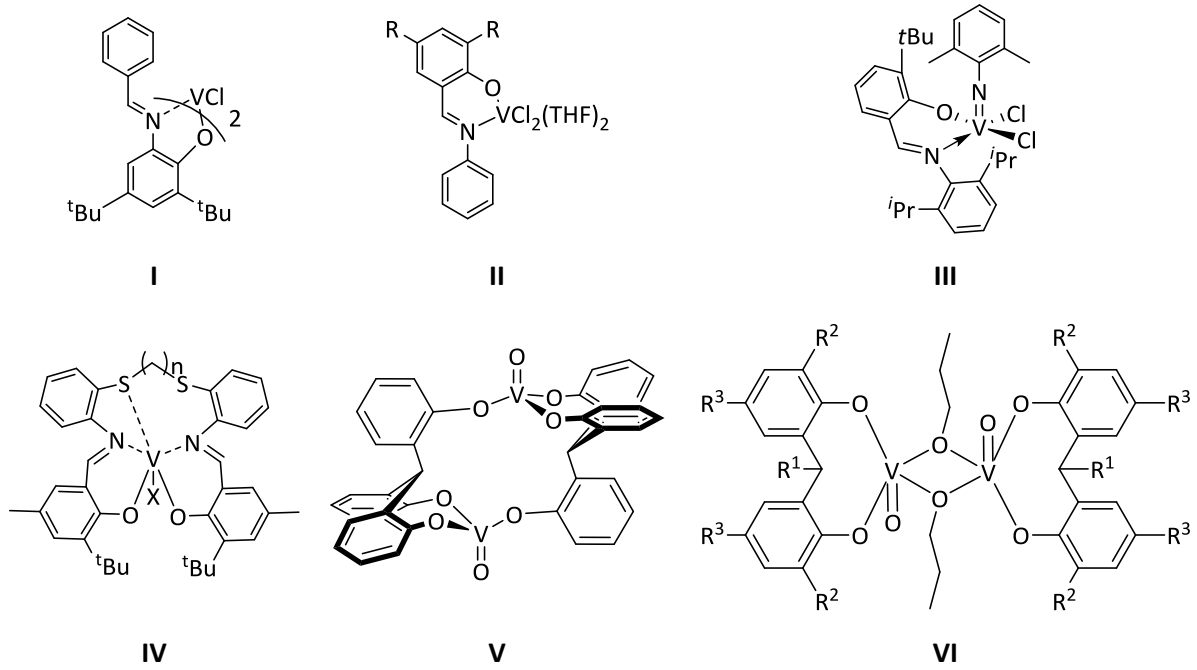


**Chart 1.3** Known phenoxyimine vanadium pre-catalysts.

Similarly to phenoxyimine compounds, Redshaw *et al.* found that use of tridentate C- and N-capped tripodal or diphenolate ligands systems gave highly active vanadium catalysts for ethylene polymerization (**Chart 1.3**, **V** and **VI**),[29-30] of which the tridentate ligands gave higher activity than the diphenolate derivatives.

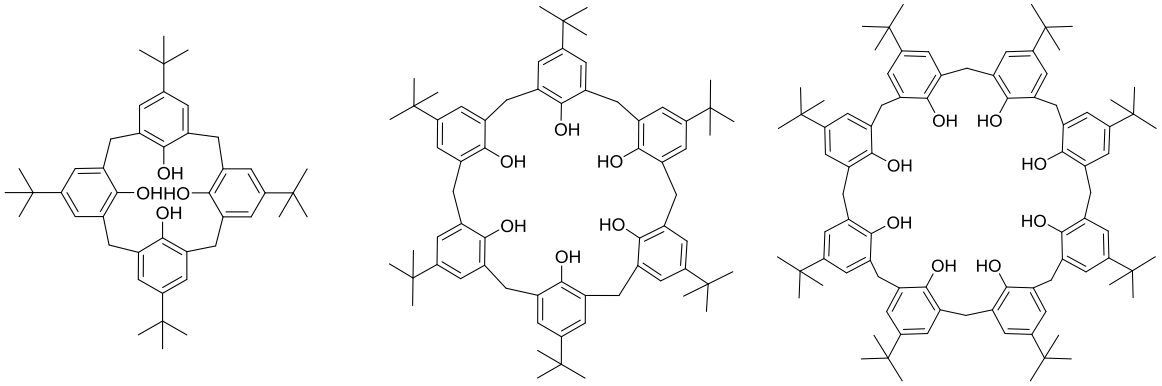


(a) (b) (c)

**Chart 1.4** p-*tert*-Butylcalix[4]arene (a), p-*tert*-butylcalix[6]arene (b) and p-*tert*-butylcalix[8]arene (c).

The discovery of highly active phenolate complexes led to use of calixarene vanadium compounds; calixarenes can be viewed as cyclic analogues of linear phenolates. The term calixarene was originally coined by C. D. Gutsche in 1978 due to the cone conformation adopted by these structures.[31] Gutsche developed a nomenclature for calixarenes to include a bracketed number which indicates the number of phenols making up the calixarene.[32] A one pot procedure for the synthesis of even numbered calixarenes was developed by Gutsche and co-workers in which the phenol starting material contains a p-*tert*-butyl group (**Chart 1.4**).[33-35] *Tert*-butylcalix[4]arene can form four distinct conformations dependent on the relative orientation of the phenol rings (**Chart 1.5**).

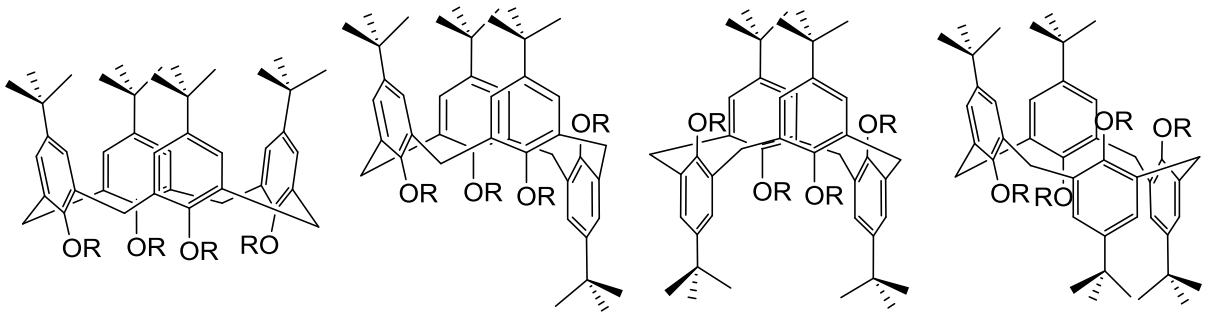


(a) (b) (c) (d)

**Chart 1.5** Conformations of p-*tert*-butylcalix[4]arene: (a) cone, (b) partial cone, (c) 1,3-alternate, (d) 1,2-alternate.

As the *tert*-butylcalix[4]arene version is the easiest to synthesize this derivative dominates the literature. Calix[4]arenes have found use in applications such as mimics for enzymes,[36] and ion recognition.[37] While metal based calix[4]arenes have previously been used as alcohol oxidation catalysts,[38] they have shown limited activity as a polymerisation catalyst (< 100 g/mmol.hr),[39-40] however Redshaw *et al.* utilized a oxacalix[3]arene vanadium compound, where the methylene bridge

has been replaced with $CH_2$—O—$CH_2$, which resulted in activities of 130,000 g/mmol.hr, significantly higher than previous vanadium calixarene catalysts (**Chart 1.6**, **VII**).[41] The high activities obtained using the oxacalix[3]ligand have led to more investigations into the use of vanadium calixarenes,[42-43] however the high activities exhibited by the oxacalix[3]arene have, so far, not been matched. While a number of calix[4]arene vanadium compounds have been explored for the polymerization of ethylene, few calix[6]arene and calix[8]arene vanadium compounds have even been synthesized. Both the Pedersen and Limberg groups have synthesized a divanadyl calix[8]arene cation in which the calix[8]arene wraps around two vanadyl centres in octahedral environments, the structures only differ by the counterion (**Chart 1.6**, **VIII**).[38, 44] A similar neutral calix[8]arene structure was synthesized by Gibson *et al* (**Chart 1.6**, **IX**),[45] which when screened for ethylene polymerization using dimethylaluminium chloride exhibited activities of 50 g/mmol.hr.bar. Gibson *et al.* also utilized a calix[6]arene which resulted in the formation of a trivanadium complex (**Chart 1.6**, **X**).

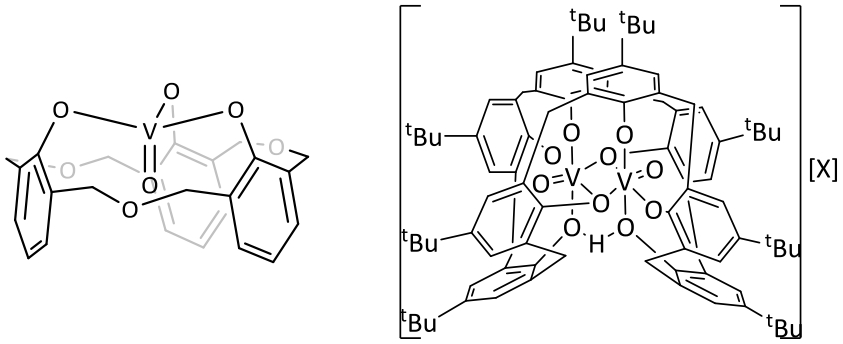

**VII** **VIII**

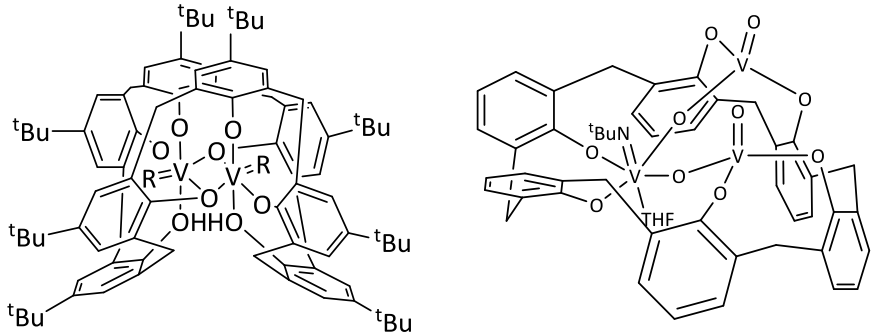

**IX** (R = Ntol) **X**

**Chart 1.6** Calix[6/8]arene vanadium compounds, *tert*-butyl groups on compounds **VII** and **X** have been removed for clarity

### *1.1.3.1 Active species in vanadium polymerization*

Although a number of vanadium catalysts have been employed for the polymerization of α-olefins, the active species responsible is still under discussion. Fujita's and Czaha's work on $MgCl_2$ supported

catalyst systems seemed to exclude the vanadium in oxidation state +2 as the active component,[22] which was further supported by Zambelli *et al.*[46] The study of (acac) vanadium system's by Gambarotta further confirmed the exclusion of V(II) as a probable active species in 2003, with the isolation of $[(acac)_2Al]^+$ obtained through ligand abstraction and a divalent vanadium species incapable of polymerization.[47] Given the reduction of the vanadium precursor by the aluminium co-catalyst it is highly unlikely that a oxidation state of +5 is responsible for the polymerization, as such only +3 and +4 oxidation states remain as options. Soshnikov *et al.* utilized EPR studies of bis(phenoxyimine)vanadyl complexes following reaction with various aluminium co-catalysts to further elucidate the active component.[48] Comparison of the resulting polymerization activities and that the use of trialkyl aluminium as co-catalyst results in an inactive species, led to the assignment of inactive and active structures (**Scheme 1.4**). It should be noted that attempts to prove the vanadium-oxygen double bond is still present after reaction with $AlEt_3$ by IR studies, were unsuccessful due to multiple bands from $AlEt_3$; $AlEt_3$ could and probably does attack at the vanadyl position.

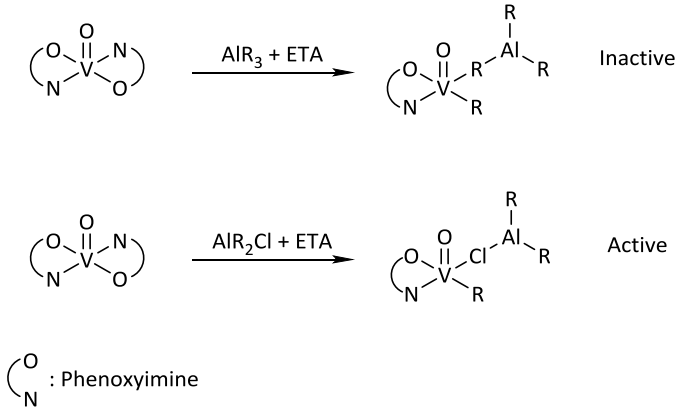


**Scheme 1.4** Active species proposed by Soshnikov for bis(phenoxyimine) based vanadyl catalysts. [48]

The active species predicted by Soshnikov is in somewhat agreement with the work performed by Nomura and co-workers (**Scheme 1.5**),[49] in which the synthesis of a number of vanadium compounds which were active for the polymerization of ethylene using dimethylaluminium chloride were reported, surprisingly the pre-catalysts were active for the dimerization of ethylene when activated with MAO. EPR studies were again used to elucidate the active site however the results suggested an active oxidation state of +3, although the addition of ethyl trichloroacetate, which usually improves the catalyst system by re-oxidising the vanadium centre, resulted in a lower activity signifying a different active site.

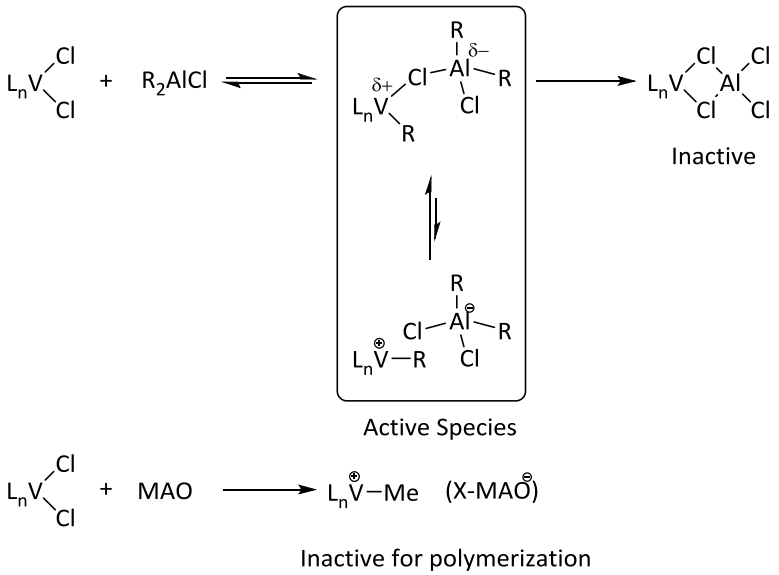


**Scheme 1.5** Assumed catalytically active species by Nomura and co-workers.

Soshnikov *et al.* also investigated the active species in vanadyl compounds containing N- and C-capped tris(phenolate) ligands,[50] again the polymerization activity (with ETA) paralleled the concentration of vanadium in oxidation state +4, as does the loss of activity with reduction of the vanadium oxidation state to +3. Soshnikov *et al.* further investigated the treatment of vanadyl calix[4]arenes (**Scheme 1.6**) with aluminium alkyls.[51] The exploration of the EPR spectrum following treatment led to the assignment of the compounds featured in **Scheme 1.6**. The proposed active species are formed after the aluminium alkyls attack the vanadium-oxygen double bond resulting in cleavage of the oxygen and formation of a vanadium alkyl. It is unlikely that the vanadium-oxygen double bond survives the conditions generally used in polymerization screening. The presence of the chlorine from the co-catalyst is clearly very important in the makeup of the vanadium active species, as using trialkylaluminium or MAO as co-catalyst is rarely successful. Given the parallel trends for concentration of vanadium in oxidation state +4 and activity of polymerization observed by Soshnikov *et al*. it is likely that vanadium in an oxidation state of +4 forms an active part of the propagating species.

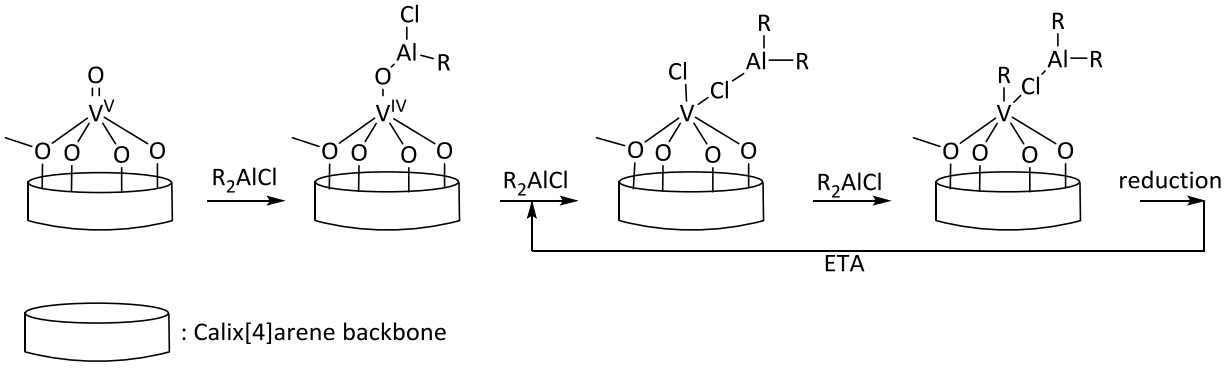


**Scheme 1.6** Active species proposed by Soshnikov *et al.* for calix[4]arene based vanadyl catalysts.

### *1.1.4 Niobium/Tantalum pre-catalysts for the polymerization of ethylene*

While vanadium catalysts have been explored rather extensively, the higher congeners are relatively unknown. In the case of niobium, however, results have been disappointing. A recent review by Galletti and Pampaloni, and the work by Patil, gives overviews of niobium-based pre-catalysts for ethylene polymerization.[52-53] A number of ligands have been treated with niobium precursors, recently including simple alkoxide, diphenolates, oxacalix[3]arene and pentamethylcyclopentadienyl ligands (**Chart 1.7**); the activities of the niobium catalysts produced have been disappointing.

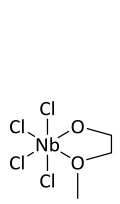

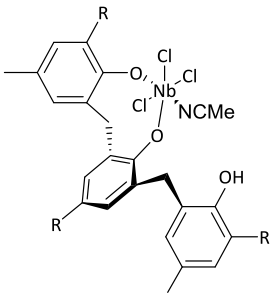

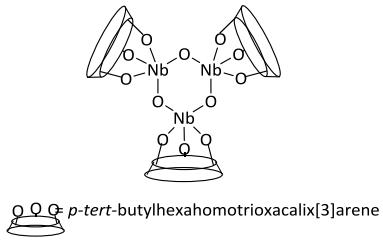


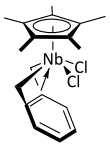

| **XI** [54] | **XII** [55] | **XIII** [56] | **XIV** [57] |
|---|---|---|---|
| 151 g/mmol.hr.bar | 90 g/mmol.hr.bar | 84 g/mmol.hr.bar | 43 g/mmol.hr.bar |
| 600 Al/Nb (DMAO) | 800 Al/Nb (DEAC) | 300 Al/Nb (DEAC) | 800 Al/Nb (DMAC) |
| 50 °C | 50 °C | 45 °C | 45 °C |
| 1 bar | 1 bar | 1 bar | 1 bar |

**Chart 1.7** Previously reported niobium pre-catalysts and their activities.

While the use of niobium catalysts for the polymerization of ethylene has resulted in poorly active compounds the use of tantalum has been much more successful. Redshaw *et al.* explored tantalum calixarene and oxacalixarene systems, however the resulting activities were poor (**Chart 1.8**, **XV**).[56] Michiue *et al.* had much greater success using tris(pyrazolyl)borate ligands achieving 25,700 g/mmol.hr activity (**Chart 1.8**, **XVI**), which is the highest activity obtained using a tantalum based catalyst to date.[58] Whilst Hakala *et al.* synthesized a aminopyridinato tantalum complex which achieved activities of 23,900 g/mmol.hr (**Chart 1.8**, **XVII**),[59] Chakraborty and co-workers utilized phenoxyimine based tantalum compound (**Chart 1.8**, **XVIII**) and Stryker and co-workers utilized mono cyclopentadienyl tantalum compounds (**Chart 1.8**, **XIX**), both of which exhibited low activity for polyethylene polymerization.[60-61] Tantalum compounds have found more success when used for trimerization of ethylene reactions to give 1-hexene, the reduction to a +3 compound resulted in the high selectivity of 1-hexene over polyethylene.[62]

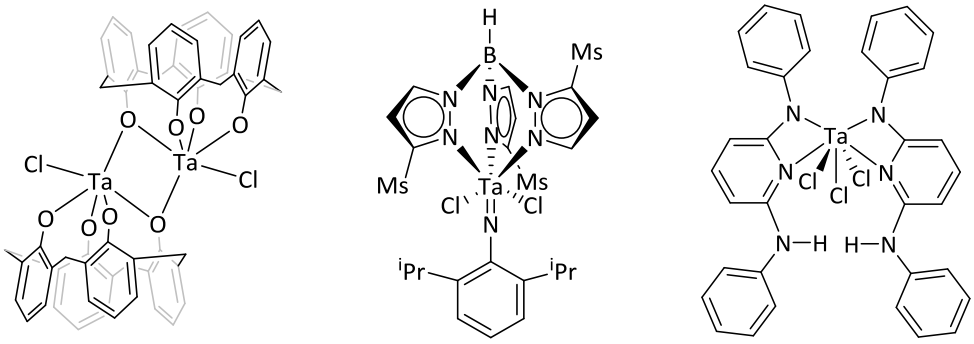

**XV** **XVI** **XVII**

**XVIII** **XIX**

**Chart 1.8** Tantalum pre-catalysts for the polymerization of ethylene

### *1.1.5 Biodegradable polymers*

Polymers with an inherent biodegradability, of which poly(lactic acid) (PLA) and poly(caprolactone) (PCL) are two of the most common, have gained significant interest due to their use in biomedical devices.[63-65] While there are a large number of biodegradable polymers, poly(lactide) is considered the most promising polymer.[66] Poly(lactide) or poly(lactic acid), PLA, is derived from 100% renewable sources such as corn with a view to replacing polyolefin-based plastics, although it should be noted the competition between use of corn as a food source versus the sheer amount of corn required to replace traditional plastics is a limiting factor. While lactide is available from corn (**Scheme 1.7**), ε-caprolactone is generally produced via the Baeyer Villiger oxidation of cyclohexanone, although recent patents give the possibility of synthesis from starch (**Scheme 1.7**).[67]

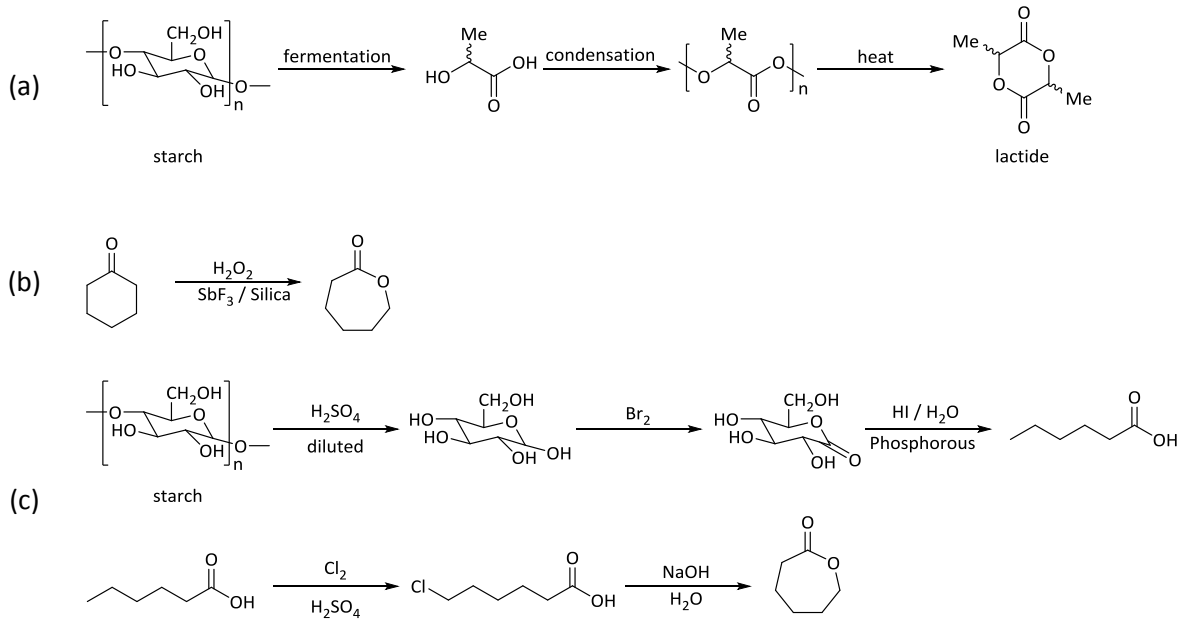


**Scheme 1.7** Synthesis of Lactide from starch (a) and ε-caprolactone from Baeyer Villiger oxidation (b) or from starch (c).[68]

### *1.1.5.1 Ring-opening polymerization of cyclic esters*

There are a number of methods for the production of polyesters such as, polycondensation, anionic and cationic ring opening polymerization.[69] Polycondensation is achievable by the treatment of a diol with a diacid or the condensation of hydroxyl acid, however this produces a stoichiometric amount of water which has to be removed to drive the reaction, while the control of the resulting molecular weight is often poor. This polymerization method also requires good stoichiometric control of the starting materials. Ring opening polymerization does not suffer from such drawbacks; no water is produced during polymerization, a single monomer is required and the resulting molecular weights are often predictable. Ring opening polymerization can follow a number of mechanisms such as cationic, anionic or co-ordination insertion pathways (**Scheme 1.8**); the driving force is the release of ring strain.

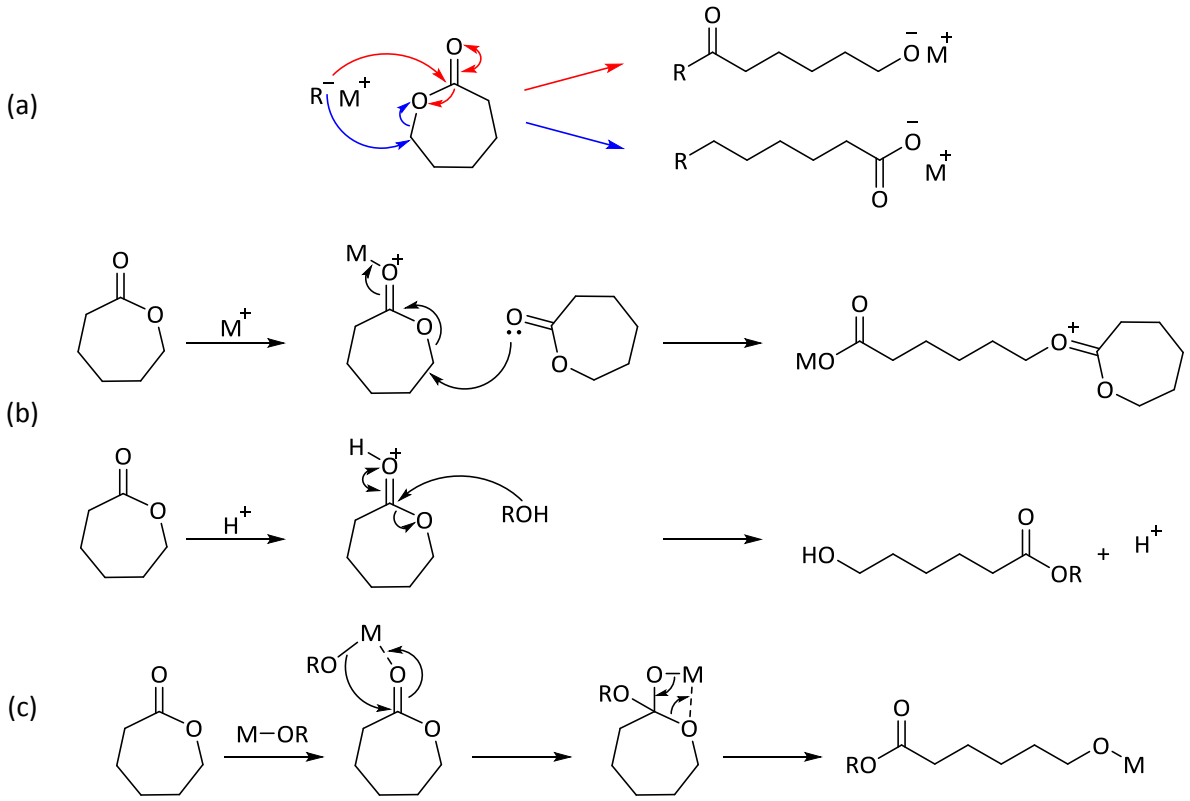


**Scheme 1.8** Anionic (a), Cationic (b) and co-ordination insertion mechanisms (c) for the ring opening polymerization of cyclic esters[70]

Anionic ring-opening polymerization proceeds through nucleophilic attack of a negatively charged species on either the carbonyl carbon or the acyl-oxygen adjacent carbon. (**Scheme 1.8**, (a)) The counter-ion stabilises the negatively charged propagating species. Similarly to anionic polymerization, there are two possible mechanisms in the cationic polymerisation of cyclic esters. A cation can co-ordinate to the oxygen of the carbonyl, activating the carbon position to attack from either an alcohol or another monomer, both of which lead to a new nucleophile for chain propagation (**Scheme 1.8**, (b)). Both anionic and cationic polymerization mechanism often lead to low polymer chain length due to extensive back-biting (*trans*-esterification) reactions (**Scheme 1.9**).

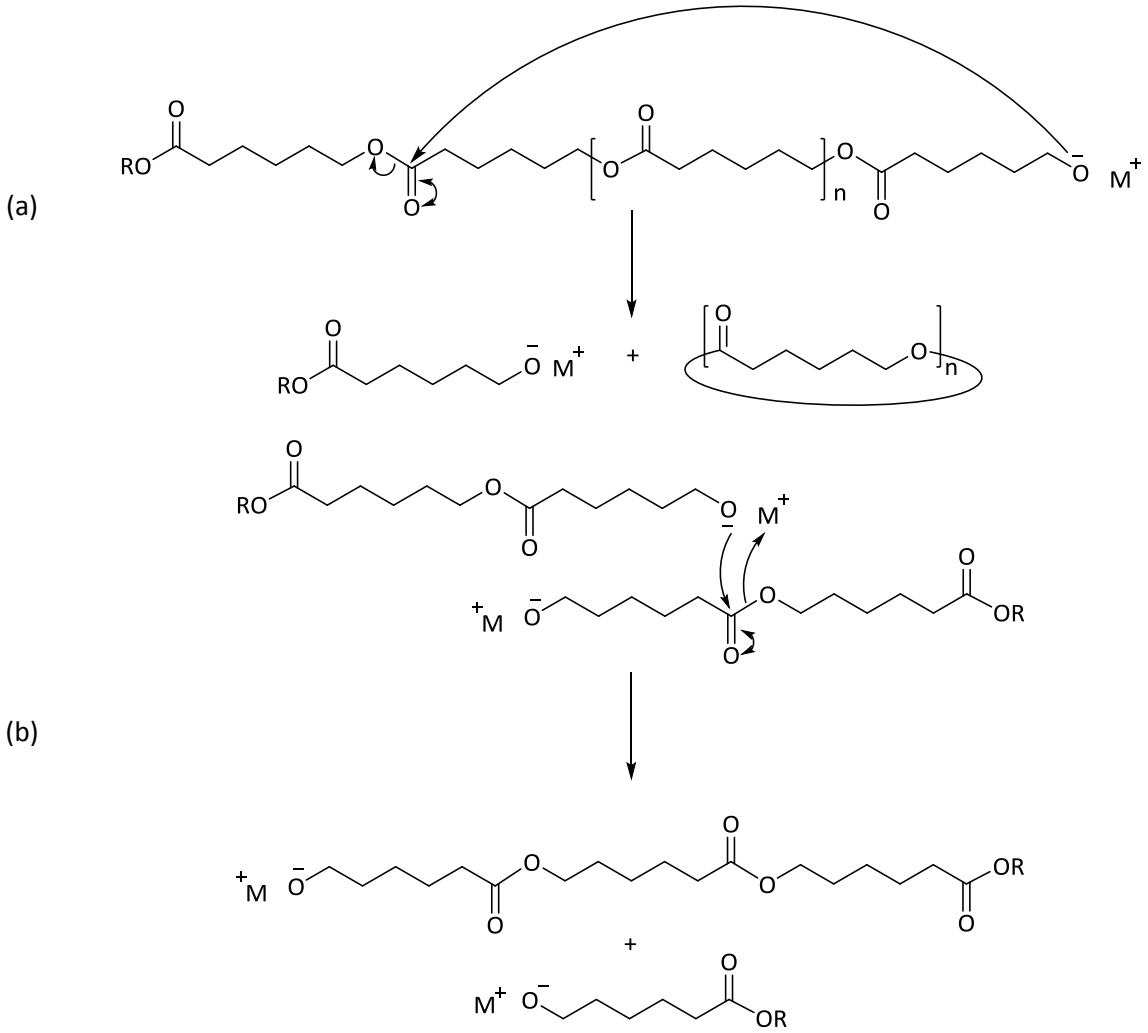


**Scheme 1.9** Intramolecular (a) and intermolecular (b) *trans*-esterification reactions in anionic polymerization

The production of PLA through a co-ordination insertion mechanism by metal based catalysts for ring opening polymerization is considered to be the most convenient preparative route, primarily due to the living polymerization mechanism which controls the molecular weight and low polydispersity (**Scheme 1.10**).[65] In the 'co-ordination insertion' mechanism a Lewis acidic metal co-ordinates the carbonyl oxygen so that a bound alkoxide can attack the activated carbonyl resulting in ring opening polymerization.

*1.1.5.2 Living and Immortal polymerization*

The chain growth during the co-ordination insertion pathway usually follows a living polymerization mechanism due to the fact that each chain grows from every metal centre; the rate of initiation must be faster than the rate of propagation and all of the metal centres should be active at all times, therefore each chain grows at the same speed resulting in a narrow molecular weight distribution or

polydispersity index (PDI). The chain length is dependent on the ratio between monomer and number of metal centres and the degree of polymerization (conversion). Immortal polymerization is a type of living polymerization, where the addition of a chain transfer agent (such as alcohol) disconnects the growing polymer chain to form a dormant polymer chain. The dormant and active polymer chains must be in equilibrium, with an exchange rate faster than the rate of propagation, so that the each chain grows at the same speed, therefore giving narrow PDI values and control of the resulting chain length; the chain length is dependent on the ratio of chain transfer agent to monomer. As immortal polymerization catalysts are no longer dependent on the amount of catalyst, this can be reduced so that little catalyst is present in the resulting polymer; the rate of polymerization is still dependent on the amount of catalyst added.

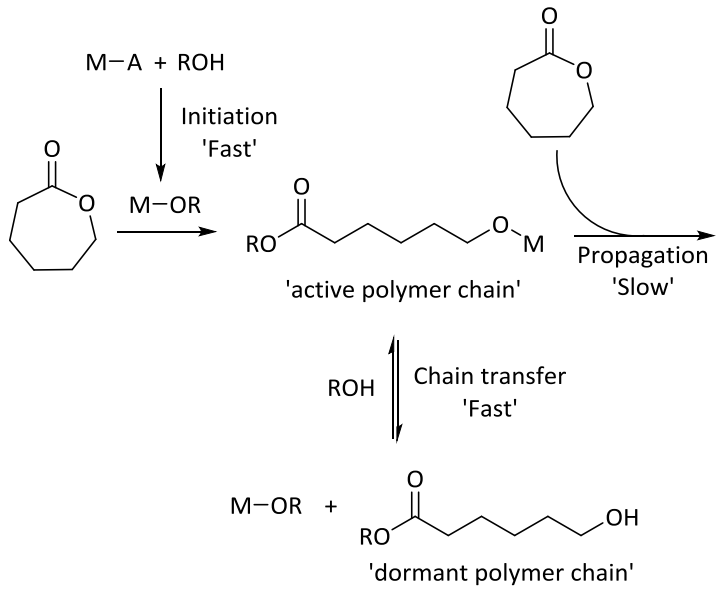


**Scheme 1.10** Immortal polymerization

While ε-caprolactone is a simple cyclic ester, the presence of two stereocentres on lactide allow for the stereoselective production of poly(lactic acid) (**Scheme 1.11**). Originally the optical activity of the polymer was used to assign the formation of isotactic PLA, Munson *et al.* demonstrated that the tacticity of the polymer at tetrad level can be determined from the homodecoupled $^{1}$H NMR (**Figure 1.1**)[71]. The degree of stereoregularity is defined by the probability of *racemic* (syndiotactic) or *meso* (isotactic) enchainment ($P_r$ or $P_m$ respectively); the possibility that the next insertion will reverse (r dyad) or retain (m dyad) the stereoselectivity. The probability of each respective enchainment can be determined from the integration of the tetrad peaks from homodecoupled $^{1}$H NMR spectrum (**Figure 1.1**) which are assigned from the literature;[72] $P_r = 2I_1(I_1 + I_2)$, where $I_1$ = integration of rmr + mmr/rmm, and $I_2$ = integration of mmr/rmm + mmm + mrm.[73] In the case of *rac*-lactide, $P_r = 1$ describes perfect heterotactic polymer, $P_r = 0.5$ atactic polymer, and $P_r = 0$ isotactic polymer. The

microstructure of the polymer produced affects the physical bulk properties of PLA. Heterotactic PLA exhibits a melting point ($T_m$) of 130 °C and no observable glass transition temperature ($T_g$). Whilst PLLA (poly(lactic acid) produced from enantiopure *L*-lactide) has a $T_m$ = 180 °C and a $T_g$ of approximately 50 °C, a 50 : 50 mixture of PLLA and PDLA has a comparable $T_g$ but an increased melting point of 230 °C. [74]

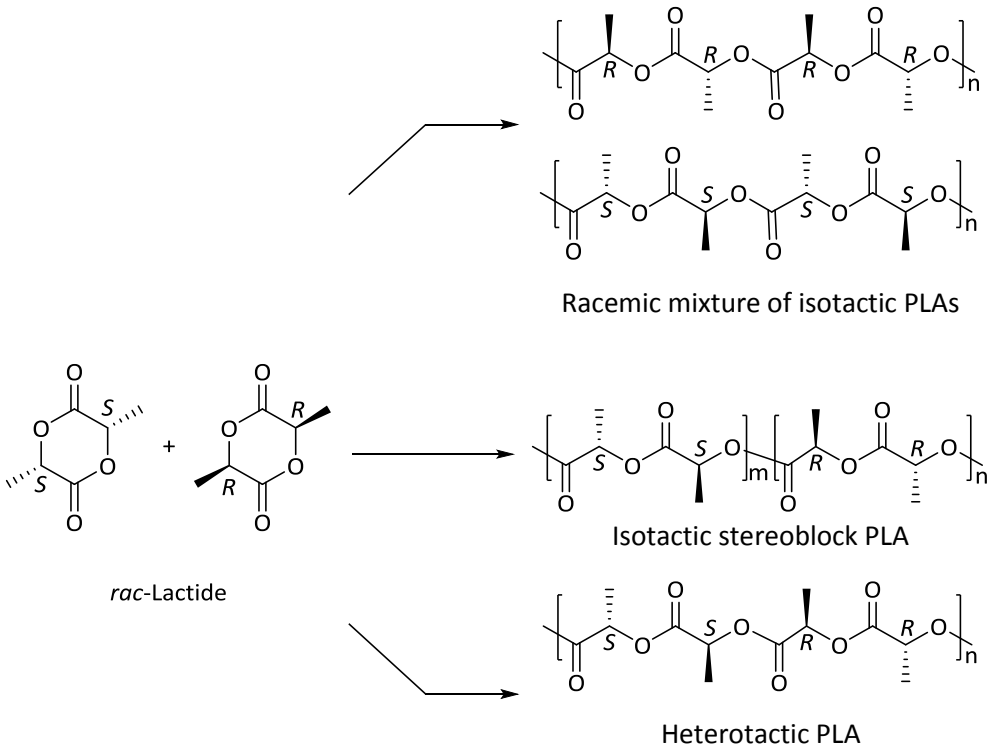


**Scheme 1.11** Stereochemistry of PLA microstructures.

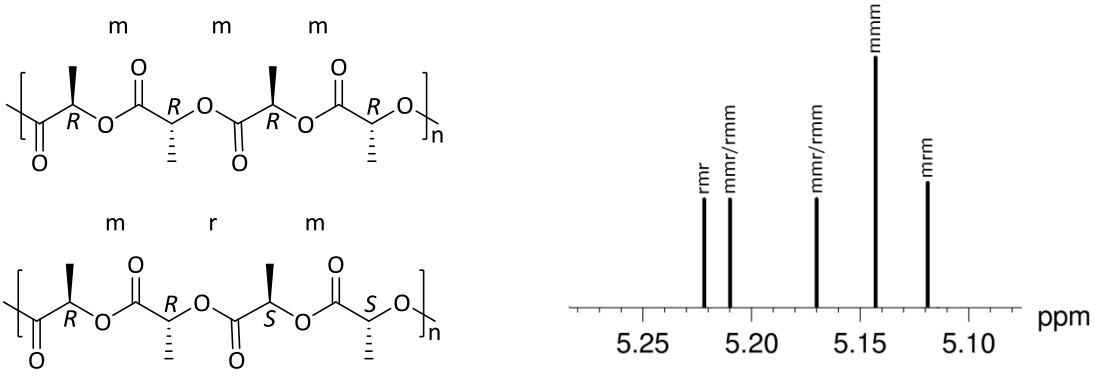


**Figure 1.1** Homodecoupled $^1$H NMR tacticity assignments[74]

### *1.1.6 Pre-catalysts for the ROP of cyclic esters*

#### *1.1.6.1 Zinc and Magnesium*

Since Coates and co-workers published their seminal work on zinc and magnesium β-diiminate complexes, a large number of pre-catalysts have appeared in the literature and much of the periodic table has been utilized for this application, however zinc and magnesium compounds have seen the vast majority of this exposure.[75-76] For a comprehensive overview of lactide and ε-caprolactone pre-catalysts there are a number of detailed reviews.[66, 74, 77-80]

A multitude of ligand systems have been employed, examples of which include phenoxyimines,[81-82] β-diiminates,[76, 83] salan[84] and heteroscorpionates,[85-86] and as such only ligands that are similar to the ones employed herein are reviewed. Calix[4]arene zinc compounds have been relatively unexplored, a zinc alkyl based calix[4]arene synthesised by Vigalok and co-workers was relatively successful and although the dialkoxycalix[4]arene ligand is dianionic when deprotonated its use leads to a dimetallic complex that still contains a nucleophilic group (**Chart 1.9**, **XX**).[87] Recently, a number of catalysts utilizing bispentafluorophenyl zinc derivatives for the polymerization of *rac*-lactide have been investigated, establishing that $Zn(C_6F_5)_2$ can be highly active for ROP polymerization.[88-89]

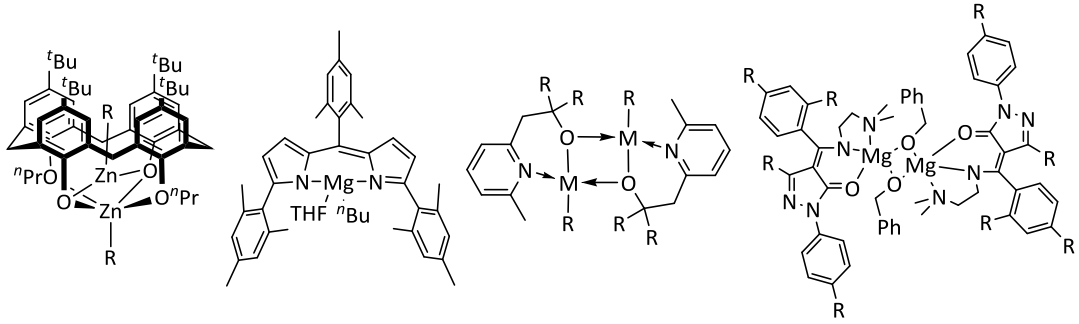


**XX** (R = Me) **XXI** **XXII** **XXIII**

**Chart 1.9** Previously reported zinc and magnesium compounds for the ROP of Lactides

Recently there has been a resurgence of magnesium based catalysts, for example Chisholm *et al.* utilised β-diiminate magnesium compounds, similar to the Coates and co-workers magnesium β-diiminate complexes, for the ROP of *rac*-lactide (**Chart 1.9**, **XXI**).[83] The catalyst exhibited exceptionally high activity as well as hetero-tactic bias when tetrahydrofuran (THF) was added to the polymerization system; however the addition of excess alcohol resulted in solvolysis, ligand loss and as a result the system was unsuitable for 'immortal' polymerization.[83] Wang *et al.* explored the use of pyridyl functionalized alkoxy zinc and magnesium complexes which exhibited immortal

polymerization of *L*-lactide and ε-caprolactone (**Chart 1.9**, **XXII**).[90] The magnesium catalyst employed was able to polymerize ε-caprolactone even in the presence of 500 equivalents of benzyl alcohol as chain transfer agent, giving the expected molecular weight. The pyridyl alkoxy magnesium catalyst also demonstrated immortal character for the ROP of *L*-lactide using triethanolamine as chain transfer/activation agent.[90] Chuang *et al*. have utilized tridentate pyrazolonate magnesium catalysts (**Chart 1.9**, **XXIII**),[91] and although they gave lower activities for the ROP of *rac*-lactide versus the catalysts reported by the groups of Chisholm and Coates,[76, 83] they exhibited immortal and stereo-selective behaviour ($P_r$ = 0.87).

## 1.2 Aims

The main aim of this study is the investigation of a number of vanadium compounds in combination with a number of related ligand systems for the co-/polymerization of ethylene and/or propylene. Vanadium compounds have been shown to be good catalysts for the co-/polymerization of ethylene and/or propylene, however their resulting activities need to be improved to complete with their group 4 counterparts and the modification of the ligand systems in combination with vanadium can achieve this goal.

The resulting activities of the vanadium compounds herein led to the investigation of niobium and tantalum counterparts, of which relatively little research has previously been conducted. Here the exploration of niobium and tantalum compounds for the polymerization of ethylene is presented.

We wanted to apply a number of ligand systems that have shown promise for group 5 ethylene polymerization with metallic species, in this case magnesium and zinc, that are traditionally highly active for ring opening polymerization of cyclic esters. The oxacalix[3]arene vanadium compounds synthesized by Redshaw *et al.* exhibited some of the highest activity for polymerization of ethylene and as such we have used oxacalix[3]arene and the more accessable calix[4]arene ligand systems in combination with magnesium and zinc for the ring opening polymerization of cyclic esters.

All compounds have been fully characterised and where possible their molecular structure has been confirmed by single crystal X-ray diffraction.

## 1.3 Overview

This thesis focuses on the synthesis and activity of a number of group 5 pre-catalysts for the polymerization of ethylene and co-polymerization of 1-propylene/ethylene. The ring opening polymerization of cyclic esters using magnesium/zinc compounds is also presented. The results and discussion chapters are separated by metal.

In the first part of the results and discussion section (**Chapter 2**), the synthesis of vanadium compounds bearing Schiff base, di-/tetra-phenolate and *p-tert*-butylcalix[6/8]arene ligands is discussed with structural considerations and investigated for their ability to polymerise α-olefins. A number of vanadium compounds have also been supported onto silica; the silica supported compounds have also been subjected to ethylene polymerization studies.

The second part of the results and discussion (**Chapter 3**) focuses on a series of niobium and tantalum compounds supported by imidazole, oxazole and Schiff base ligands, their synthesis, structural analysis and ethylene polymerization abilities. A number of niobium and tantalum compounds have been supported on silica to give heterogeneous catalysts, and this effect on the resulting polymerization ability is also presented.

The final chapter of the results and discussion (**Chapter 4**) shifts emphasis to the use of magnesium and zinc calix[4]arene compounds for the ring opening polymerization of ε-caprolactone or *rac*-lactide.

The synthetic procedures, characterization data and polymerization methods have been collated into the experimental section (**Chapter 5**), while the crystallography tables of each crystal structure is contained in the appendix (**Chapter 6**).

## 1.4 References


[1] P. Margl, L. Deng, T. Ziegler, *J. Am. Chem. Soc.,* **1998**, *121*, 154.

[2] G. Natta, P. Pino, G. Mazzanti, P. Longi, *Gazz. Chim. Ital.,* **1957**, *87*, 549.

[3] D. S. Breslow, N. R. Newburg, *J. Am. Chem. Soc.,* **1959**, *81*, 81.

[4] A. Andresen, H.-G. Cordes, J. Herwig, W. Kaminsky, A. Merck, R. Mottweiler, J. Pein, H. Sinn, H.-J. Vollmer, *Angew. Chem., Int. Ed. Engl.,* **1976**, *15*, 630.

[5] H. Sinn, W. Kaminsky, H.-J. Vollmer, R. Woldt, *Angew. Chem., Int. Ed. Engl.,* **1980**, *19*, 390.

[6] W. Kaminsky, O. Sperber, R. Werner, *Coord. Chem. Rev.,* **2006**, *250*, 110.

[7] W. Kaminsky, *J. Chem. Soc., Dalton Trans.,* **1998**, 1413.

[8] M. Bochmann, *J. Chem. Soc., Dalton Trans.,* **1996**, 255.

[9] H. H. Brintzinger, D. Fischer, R. Mülhaupt, B. Rieger, R. M. Waymouth, *Angew. Chem., Int. Ed. Engl.,* **1995**, *34*, 1143.

[10] P. Cossee, *J. Catal.,* **1964**, *3*, 80.

[11] E. J. Arlman, *J. Catal.,* **1964**, *3*, 89.

[12] M. Brookhart, M. L. H. Green, *J. Organomet. Chem.,* **1983**, *250*, 395.

[13] H. Krauledat, H.-H. Brintzinger, *Angew. Chem., Int. Ed. Engl.,* **1990**, *29*, 1412.

[14] L. Resconi, S. Bossi, L. Abis, *Macromolecules,* **1990**, *23*, 4489.

[15] N. Naga, K. Mizunuma, *Polymer,* **1998**, *39*, 5059.

[16] B. Wang, *Coord. Chem. Rev.,* **2006**, *250*, 242.

[17] J. Suhm, M. J. Schneider, R. Mülhaupt, *J. Mol. Catal. A: Chem.,* **1998**, *128*, 215.

[18] H. Braunschweig, F. M. Breitling, *Coord. Chem. Rev.,* **2006**, *250*, 2691.

[19] C. Redshaw, Y. Tang, *Chem. Soc. Rev.,* **2012**, *41*, 4484.

[20] Y. Suzuki, S. Kinoshita, A. Shibahara, S. Ishii, K. Kawamura, Y. Inoue, T. Fujita, *Organometallics,* **2010**, *29*, 2394.

[21] G. Paolucci, A. Zanella, L. Sperni, V. Bertolasi, M. Mazzeo, C. Pellecchia, *J. Mol. Catal. A: Chem.,* **2006**, *258*, 275.

[22] Y. Nakayama, H. Bando, Y. Sonobe, Y. Suzuki, T. Fujita, *Chem. Lett.,* **2003**, *32*, 766.

[23] Y. Nakayama, H. Bando, Y. Sonobe, T. Fujita, *J. Mol. Catal. A: Chem.,* **2004**, *213*, 141.

[24] J.-Q. Wu, L. Pan, N.-H. Hu, Y.-S. Li, *Organometallics,* **2008**, *27*, 3840.

[25] Y. Onishi, S. Katao, M. Fujiki, K. Nomura, *Organometallics,* **2008**, *27*, 2590.

[26] D. M. Homden, C. Redshaw, D. L. Hughes, *Inorg. Chem.,* **2007**, *46*, 10827.

[27] H. Makio, H. Terao, A. Iwashita, T. Fujita, *Chem. Rev.,* **2011**, *111*, 2363.

[28] K. Nomura, S. Zhang, *Chem Rev,* **2011**, *111*, 2342.

[29] C. Redshaw, M. A. Rowan, D. M. Homden, S. H. Dale, M. R. J. Elsegood, S. Matsui, S. Matsuura, *Chem. Commun.,* **2006**, 3329.

[30] C. Redshaw, L. Warford, S. H. Dale, M. R. J. Elsegood, *Chem. Commun.,* **2004**, 1954.

[31] C. D. Gutsche, R. Muthukrishnan, *J. Org. Chem.,* **1978**, *43*, 4905.

[32] C. D. Gutsche, *Calixarenes, A Versatile Class of Macrocyclic Compounds*, Kluwer Academic Publishers, Dordrecht, Netherlands, **1990**.

[33] C. D. Gutsche, J. H. Munch, *Org. Synth.,* **1990**, *68*, 243.

[34] C. D. Gutsche, B. Dhawan, M. Leonis, D. Stewart, *Org. Synth.,* **1990**, *68*, 238.

[35] C. D. Gutsche, M. Iqbal, *Org. Synth.,* **1990**, *68*, 234.

[36] D. T. Schühle, J. A. Peters, J. Schatz, *Coord. Chem. Rev.,* **2011**, *255*, 2727.

[37] J. P. Chinta, B. Ramanujam, C. P. Rao, *Coord. Chem. Rev.,* **2012**, *256*, 2762.

[38] C. Limberg, *Eur. J. Inorg. Chem.,* **2007**, 3303.

[39] O. V. Ozerov, N. P. Rath, F. T. Ladipo, *J. Organomet. Chem.,* **1999**, *586*, 223.

[40] C. Capacchione, P. Neri, A. Proto, *Inorg. Chem. Commun.,* **2003**, *6*, 339.

[41] C. Redshaw, M. A. Rowan, L. Warford, D. M. Homden, A. Arbaoui, M. R. J. Elsegood, S. H. Dale, T. Yamato, C. P. Casas, S. Matsui, S. Matsuura, *Chem. Eur. J.,* **2007**, *13*, 1090.

[42] C. Redshaw, L. Clowes, D. L. Hughes, M. R. J. Elsegood, T. Yamato, *Organometallics,* **2011**, *30*, 5620.

[43] L. Clowes, C. Redshaw, D. L. Hughes, *Inorg. Chem.,* **2011**, *50,* 7838.

[44] G. E. Hofmeister, F. E. Hahn, S. F. Pedersen, *J. Am. Chem. Soc.,* **1989**, *111*, 2318.

[45] V. C. Gibson, C. Redshaw, M. R. J. Elsegood, *J. Chem. Soc., Dalton Trans.,* **2001**, 767.

[46] A. Zambelli, I. Sessa, F. Grisi, R. Fusco, P. Accomazzi, *Macromol. Rapid Commun.,* **2001**, *22*, 297.

[47] S. Gambarotta, *Coord. Chem. Rev.,* **2003**, *237*, 229.

[48] I. E. Soshnikov, N. V. Semikolenova, K. P. Bryliakov, A. A. Shubin, V. A. Zakharov, C. Redshaw, E. P. Talsi, *Macromol. Chem. Phys.,* **2009**, *210*, 542.

[49] A. Igarashi, S. Zhang, K. Nomura, *Organometallics,* **2012**, *31*, 3575.

[50] I. E. Soshnikov, N. V. Semikolenova, K. P. Bryliakov, V. A. Zakharov, C. Redshaw, E. P. Talsi, *J. Mol. Catal. A: Chem.,* **2009**, *303*, 23.

[51] I. E. Soshnikov, N. V. Semikolenova, A. A. Shubin, K. P. Bryliakov, V. A. Zakharov, C. Redshaw, E. P. Talsi, *Organometallics,* **2009**, *28*, 6714.

[52] A. M. Raspolli Galletti, G. Pampaloni, *Coord. Chem. Rev.,* **2010**, *254*, 525.

[53] Y. R. Patil, *Olefins Polymerisation Reactivity of Niobium-Based Metal Complexes*, LAP Lambert Acad. Publ., **2011**.

[54] F. Marchetti, G. Pampaloni, Y. Patil, A. M. R. Galletti, S. Zacchini, *J. Polym. Sci., Part A: Polym. Chem.,* **2011**, *49*, 1664.

[55] C. Redshaw, D. M. Homden, M. A. Rowan, M. R. J. Elsegood, *Inorg. Chim. Acta,* **2005**, *358*, 4067.

[56] C. Redshaw, M. Rowan, D. M. Homden, M. R. Elsegood, T. Yamato, C. Perez-Casas, *Chem. Eur. J.,* **2007**, *13*, 10129.

[57] K. Mashima, Y. Nakayama, M. Kaidzu, N. Ikushima, A. Nakamura, *J. Organomet. Chem.,* **1998**, *557*, 3.

[58] K. Michiue, T. Oshiki, K. Takai, M. Mitani, T. Fujita, *Organometallics,* **2009**, *28*, 6450.

[59] K. Hakala, B. Löfgren, M. Polamo, M. Leskelä, *Macromol. Rapid Commun.,* **1997**, *18*, 635.

[60] T. K. Saha, M. Mandal, M. Thunga, D. Chakraborty, V. Ramkumar, *Dalton Trans.,* **2013**, *42*, 10304.

[61] D. M. Antonelli, A. Leins, J. M. Stryker, *Organometallics,* **1997**, *16*, 2500.

[62] R. Arteaga-Müller, H. Tsurugi, T. Saito, M. Yanagawa, S. Oda, K. Mashima, *J. Am. Chem. Soc.,* **2009**, *131*, 5370.

[63] S. Mecking, *Angew. Chem., Int. Ed.,* **2004**, *43*, 1078.

[64] E. S. Place, J. H. George, C. K. Williams, M. M. Stevens, *Chem. Soc. Rev.,* **2009**, *38*, 1139.

[65] O. Dechy-Cabaret, B. Martin-Vaca, D. Bourissou, *Chem. Rev.,* **2004**, *104*, 6147.

[66] M. J. L. Tschan, E. Brule, P. Haquette, C. M. Thomas, *Polym. Chem.,* **2012**, *3*.

[67] M. Minami, S. Kozaki, US Patent, 2003/0023026 A1, 2003

[68] L. Clowes (2011). *Group V pro-catalysts for the polymerisation of ethylene and ε-caprolactone*. University of East Anglia.

[69] A. J. R. Lasprilla, G. A. R. Martinez, B. H. Lunelli, A. L. Jardini, R. M. Filho, *Biotechnol. Adv.,* **2012**, *30*.

[70] K. M. Stridsberg, M. Ryner, A.-C. Albertsson, *Adv. Polym. Sci*, **2002**, *157*, 41.

[71] M. T. Zell, B. E. Padden, A. J. Paterick, K. A. M. Thakur, R. T. Kean, M. A. Hillmyer, E. J. Munson, *Macromolecules,* **2002**, *35*, 7700.

[72] T. K. Sen, A. Mukherjee, A. Modak, S. K. Mandal, D. Koley, *Dalton Trans.,* **2013**, *42*, 1893.

[73] F. d. r. Drouin, P. O. Oguadinma, T. J. J. Whitehorne, R. E. Prud'homme, F. Schaper, *Organometallics,* **2010**, *29*, 2139.

[74] M. J. Stanford, A. P. Dove, *Chem. Soc. Rev.,* **2010**, *39*, 486.

[75] M. Cheng, A. B. Attygalle, E. B. Lobkovsky, G. W. Coates, *J. Am. Chem. Soc.,* **1999**, *121*, 11583.

[76] B. M. Chamberlain, M. Cheng, D. R. Moore, T. M. Ovitt, E. B. Lobkovsky, G. W. Coates, *J. Am. Chem. Soc.,* **2001**, *123*, 3229.

[77] I. dos Santos Vieira, S. Herres-Pawlis, *Eur. J. Inorg. Chem.,* **2012**, 765.

[78] J. Wu, T.-L. Yu, C.-T. Chen, C.-C. Lin, *Coord. Chem. Rev.,* **2006**, *250*, 602.

[79] M. H. Chisholm, *Inorg. Chim. Acta,* **2009**, *362*, 4284.

[80] A. Arbaoui, C. Redshaw, *Polym. Chem.,* **2010**, *1*, 801.

[81] W. Yi, H. Ma, *Inorg. Chem.,* **2013**, *52*, 11821.

[82] M. Bouyhayi, Y. Sarazin, O. L. Casagrande, J. F. Carpentier, *Appl. Organomet. Chem.,* **2012**, *26*, 681.

[83] M. H. Chisholm, K. Choojun, J. C. Gallucci, P. M. Wambua, *Chem. Sci.,* **2012**, *3*, 3445.

[84] S. Song, H. Ma, Y. Yang, *Dalton Trans.,* **2013**, *42*, 14200.

[85] L. F. Sánchez-Barba, A. Garcés, J. Fernández-Baeza, A. Otero, C. Alonso-Moreno, A. Lara-Sánchez, A. M. Rodríguez, *Organometallics,* **2011**, *30*, 2775.

[86] A. Garcés, L. F. Sánchez-Barba, J. Fernández-Baeza, A. Otero, M. Honrado, A. Lara-Sánchez, A. M. Rodríguez, *Inorg. Chem.,* **2013**, *52*, 12691.

[87] E. Bukhaltsev, L. Frish, Y. Cohen, A. Vigalok, *Org. Lett.,* **2005**, *7*, 5123.

[88] G. Schnee, C. Fliedel, T. Avilés, S. Dagorne, *Eur. J. Inorg. Chem.,* **2013**, *2013*, 3699.

[89] E. Piedra-Arroni, C. Ladaviere, A. Amgoune, D. Bourissou, *J. Am. Chem. Soc.,* **2013**, *135*, 13306.

[90] Y. Wang, W. Zhao, D. T. Liu, S. H. Li, X. L. Liu, D. M. Cui, X. S. Chen, *Organometallics,* **2012**, *31*, 4182.

[91] H.-J. Chuang, H.-L. Chen, J.-L. Ye, Z.-Y. Chen, P.-L. Huang, T.-T. Liao, T.-E. Tsai, C.-C. Lin, *J. Polym. Sci., Part A: Polym. Chem.,* **2013**, *51*, 696.

# Chapter 2 – Vanadium Pre-Catalysts

## 2.1 Introduction

Vanadium-based pre-catalysts for olefin polymerisation catalysis have generated a great deal of interest from both academia and industry,[1-9] due to their catalytic activities and thermal stability, and the ability to perform co- and ter-polymerisation reactions.[10-12] Whilst a number of beneficial co-operative effects have previously been reported using polynuclear nickel and group IV based catalysts,[13] leading to either improved or different catalytic performance, few catalysts featuring multiple vanadium metal centres have been explored.[14] The development of a number of mono- and multi-metallic vanadium compounds for the polymerisation of ethylene is explored herein. The chapter is separated into sub-sections based on the ligand set. In the first section phenoxyimine based vanadium compounds are discussed followed by di/tetraphenolate and finally *p-tert*-calix[6/8]arene vanadium compounds.

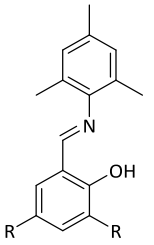

**L1H** R = $^t$Bu
**L2H** R = H

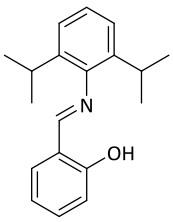

**L3H**

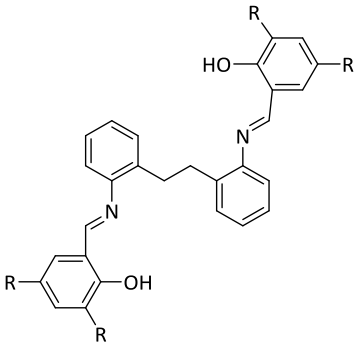

**L4H$_2$** R = $^t$Bu
**L5H$_2$** R = H

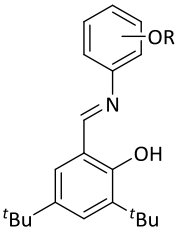

**L6H** R = *o*-OMe
**L7H** R = *m*-OMe
**L8H** R = *p*-OMe
**L9H** R = *o*-OEt
**L10H** R = *o*-$OCF_3$
**L11H** R = *o*-OPh

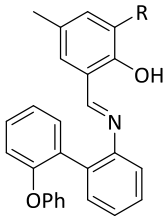

**L12H** (R = Ad)
**L13H** (R = $CMe_2Ph$)

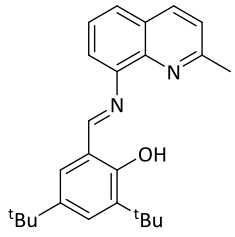

**L14H**

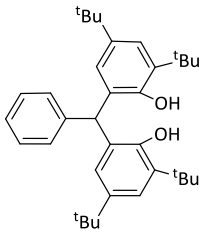

**L15H$_2$**

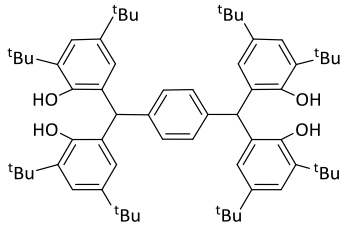

**L16H$_4$**

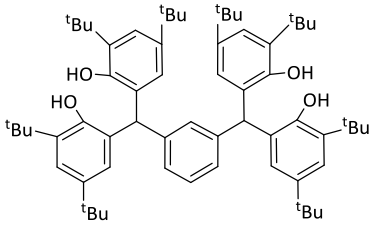

**L17H$_4$**

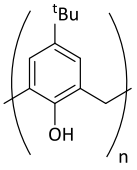

**L18H$_6$** n = 6
**L19H$_8$** n = 8

**Chart 2.1** Pre-ligands used for synthesis of vanadium complexes utilized in this study.

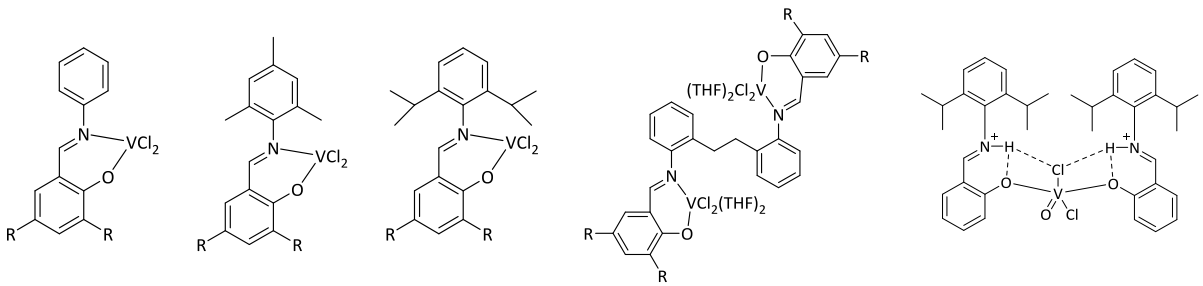

**1** (R = $^{t}$Bu) **3** (R = $^{t}$Bu) **5** (R = $^{t}$Bu) **7** (R = $^{t}$Bu) **9**
**2** (R = H) **4** (R = H) **6** (R = H) **8** (R = H)

**Chart 2.2** Vanadium(III) trichloride phenoxyimine compounds utilized in this study.

As previously discussed in **chapter 1**, the emergence of or phenoxyimine-type (FI, salicylaldiminato) ligands used for the polymerisation of ethylene has produced a number of early transition metal catalytic systems. In most examples featuring phenoxyimine ligand sets, the pre-catalysts form a mononuclear species. The recently published work on zinc,[15] in which multiple zinc centres are held in close proximity, led to the use of the ligand family $[C_6H_4N{=}CH(ArO)]_2(\mu\text{-}CH_2CH_2)$ (**Chart 2.1**, Ar = 2,4-*t*-$Bu_2C_6H_2$ **L4H$_2$**, $C_6H_4$ **L5H$_2$**), and upon treatment with vanadium trichloride, binuclear catalysts (**Chart 2.2**, **7** – **8**) were isolated. Similarly sterically hindered mononuclear vanadium catalysts (**Chart 2.2**, **1** – **6** and **9**) have been isolated and compared with the binuclear catalysts for polyethylene screening. Compounds **7** – **8** were investigated in collaboration with Dr Lucy Clowes.[16] Compounds **4** and **6** have also been supported on silica, giving **S-4** and **S-6** respectively, and screened for the polymerisation of ethylene.

We have extended our investigation of the phenoxyimine ligand set to include a third heteroatom capable of binding to the metal centre and treated these compounds with vanadium(V) precursors. In many catalytic systems variation of the ancillary ligands surrounding the metal centre can transform the behaviour of the catalyst.[7] The treatment of the Schiff base ligands **L6H** – **L14H** with vanadium oxytripropoxide or oxytrichloride led to the isolation of compounds **10** – **20** (**Chart 2.3**). Unexpectedly, treatment with ligands (**L6H** – **L13H**) led to the reduction of the vanadium centre and di-ligation. Compounds **10** – **20** have been investigated for the polymerisation of ethylene. Compounds **10**, **11**, **13**, **14**, **17** and **18** were synthesized in collaboration with the University of Sichuan Normal University in Chengdu (China). This work has been published.[17]

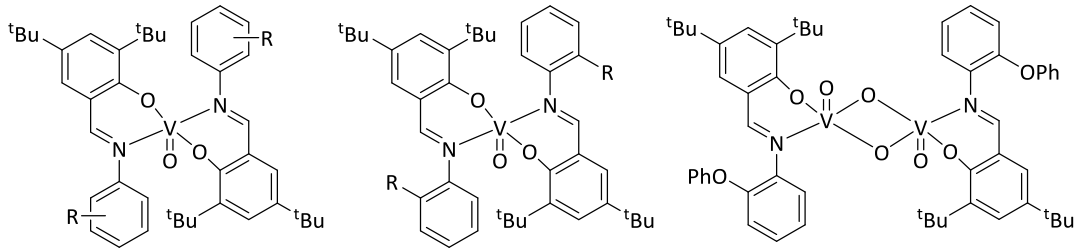

**10** (R = *o*-OMe)
**11** (R = m-OMe)
**12** (R = *p*-OMe)

**13** (R = OEt)
**14** (R = $OCF_3$)
**15** (R = OPh)

**16**

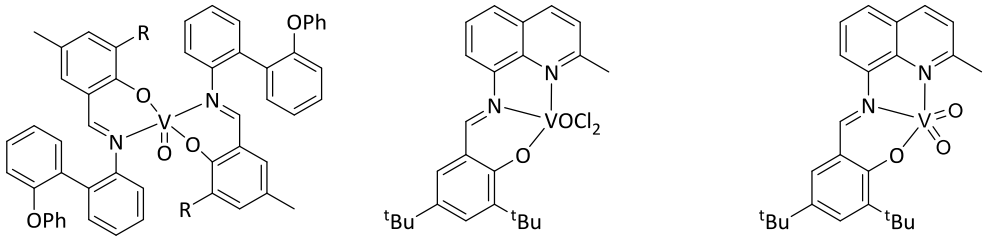

**17** (R = Ad)
**18** (R = $CMe_2Ph$)

**19**

**20**

**Chart 2.3** Vanadyl phenoxyimine pre-catalysts investigated in this study

In **chapter 1**, a number of diphenolate and trisphenolate vanadium pre-catalysts which have shown very high activity for the polymerisation of ethylene is presented, wanting to explore the effect of a polynuclear vanadium compound featuring this type of ligand system resulted in the synthesis of bridging vanadium diphenolates (tetraphenolates) for the polymerisation of ethylene. We have synthesized two isomers of phenyl bridged diphenolate vanadium compounds (**Chart 4**, **22** and **23**) and the synthesis of a similar vanadium diphenolate compound (**Chart 4**, **21**). Compounds **21** – **23** have been screened for polymerisation of ethylene and ethylene/propylene and the effect of the bridging ligand scaffold is explored in the second section of the results and discussion.

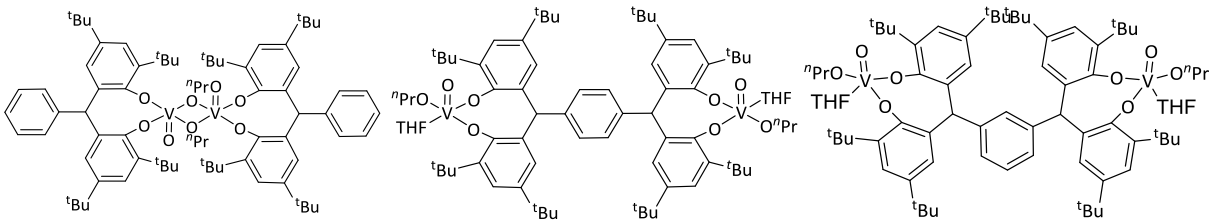

**21**

**22**

**23**

**Chart 2.4.** Tetraphenolate vanadium pre-catalysts investigated in this study.

In the third section of this chapter, *p-tert*-butylcalix[6/8]arene vanadium pre-catalysts for the polymerisation of ethylene and co-polymerisation of ethylene/propylene are explored. Calix[4]arene compounds can be envisaged as cyclic phenolate ligands that form a 'vase' structure, however the increased flexibility of calix[6]arene, and especially calix[8]arene, results in adoption of more complex conformations.[18]

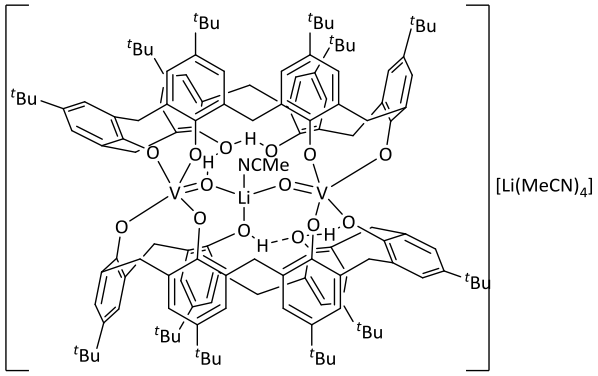


**24**

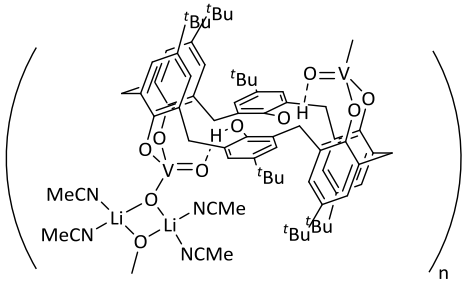


**25**

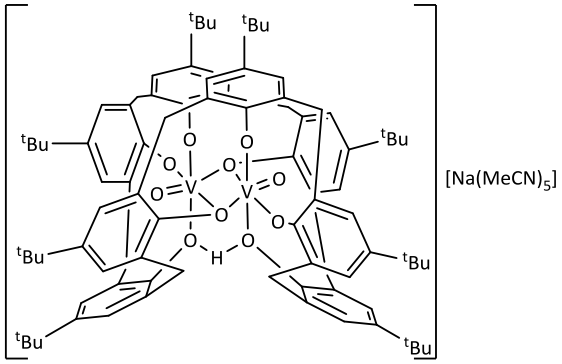


**26**

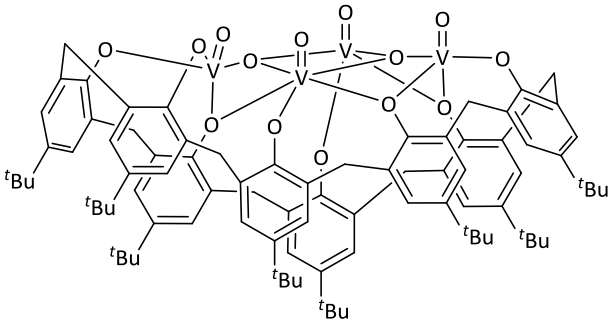

**27**

**Chart 2.5** Calixarene vanadium compounds synthesized and screened in this study.

As discussed in **chapter 1**, while there are a number of examples in the literature of calix[4]arene and oxacalix[3]arene vanadium compounds as pre-catalysts exhibiting high activities for the polymerisation of ethylene, few group 5 *p-tert*-butylcalix[6/8]arene compounds have been reported for this application or even synthesized.[19] This may be due to the increased costs associated with the preparation of these larger ligands, however the ability for the calix[6/8]arenes to coordinate multiple metal centres have led to increased interest. As stated previously, the ability to coordinate multiple metal centres in close proximity has the potential to lead to useful cooperative effects in catalysis,[13, 20] herein the synthesis of vanadium calix[6/8]arene compounds featuring alkali metal centres is presented (**Chart 2.5**). The treatment of *p-tert*-butylcalix[6/8]arenes with alkali vanadyl precursors ($MVO(Ot\text{-}Bu)_4$, M = alkali metal) in toluene afforded compounds **24** – **27** in good yield (38 – 63%) after extraction using acetonitrile. On a number of occasions the polymeric compound **25** crystallised as a minor product (<10% yield) from the synthesis of compound **24**. Compounds **24** – **27** were screened for polymerisation of ethylene and co-polymerisation of ethylene/propylene and the results reported herein.

## 2.2 Results and Discussion – Vanadium Phenoxyimine compounds

### *2.2.1 Synthesis and structures*

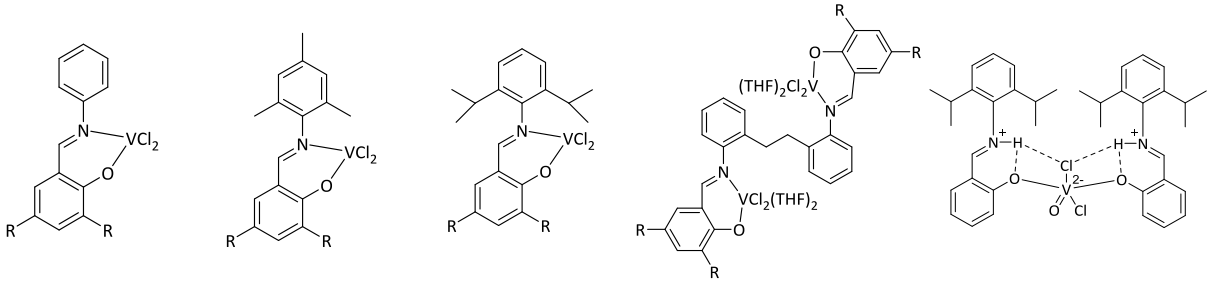

**1** (R = $^{t}$Bu) **3** (R = $^{t}$Bu) **5** (R = $^{t}$Bu) **7** (R = $^{t}$Bu) **9**
**2** (R = H) **4** (R = H) **6** (R = H) **8** (R = H)

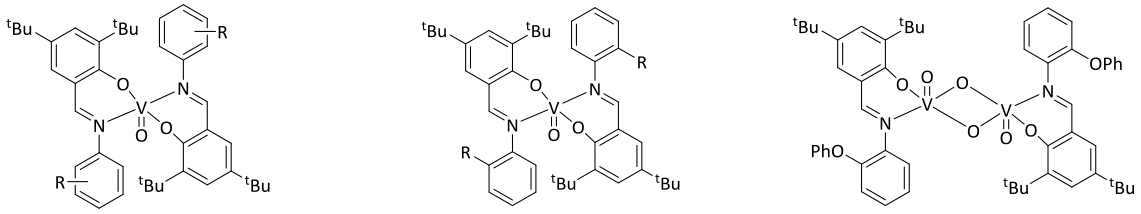

**10** (R = *o-OMe*) **13** (R = OEt) **16**
**11** (R = *m-OMe*) **14** (R = $OCF_3$)
**12** (R = *p-OMe*) **15** (R = OPh)

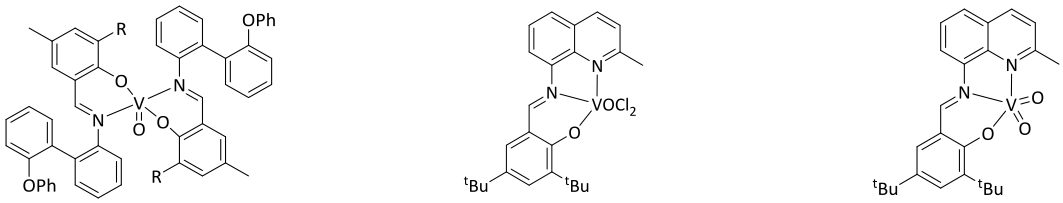

**17** (R = Ad) **19** **20**
**18** (R = CMe2Ph)

**Chart 2.6** Vanadium phenoxyimine compounds synthesized and screened in this section.

The ligands **L1H** – **L14H** required for each of the corresponding vanadium complexes **1** – **20** (**Chart 2.6**) were obtained in good yields *via* standard condensation of the requisite aniline with one or two equivalents of either salicylaldehyde or 3,5-di-*tert*-butyl-2-hydroxybenzaldehyde. The treatment of **L1H** – **L5H$_2$** with the required quantity of $VCl_3$.3THF in tetrahydrofuran (see **Scheme 2.1**), led to the isolation of compounds **1** – **8**, the addition of triethylamine drives the reaction by removing the hydrogen chloride which is produced as a side product. Compounds **1**, **2**, **5** and **6** have previously been isolated and fully characterised by Li and co-workers.[4] Compounds **1** – **8** have been

characterised by mass spectrometry, IR, elemental analysis and magnetic moment and where possible single crystal X-ray diffraction.

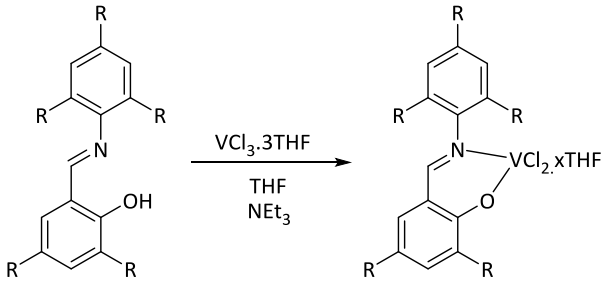


**Scheme 2.1** Li's method for the synthesis of phenoxyimine vanadium dichlorides.[4]

Single crystals of compound **7** suitable for X-ray diffraction studies were grown from the diffusion of light petroleum into a THF solution; an ORTEP representation is shown in **Figure 2.1**. The vanadium metal centres bind to the ligand through the imine nitrogen and phenolate oxygen with loss of two equivalents of hydrogen chloride; there are two co-ordinated THF molecules to each vanadium *trans* to the Schiff base ligand. The octahedral geometry acquired by the two vanadium centres is completed by the remaining chlorine atoms which are *trans* to each other. The phenoxyimine moieties are related by an inversion centre, and have a bite angle of 89.56(9)°.

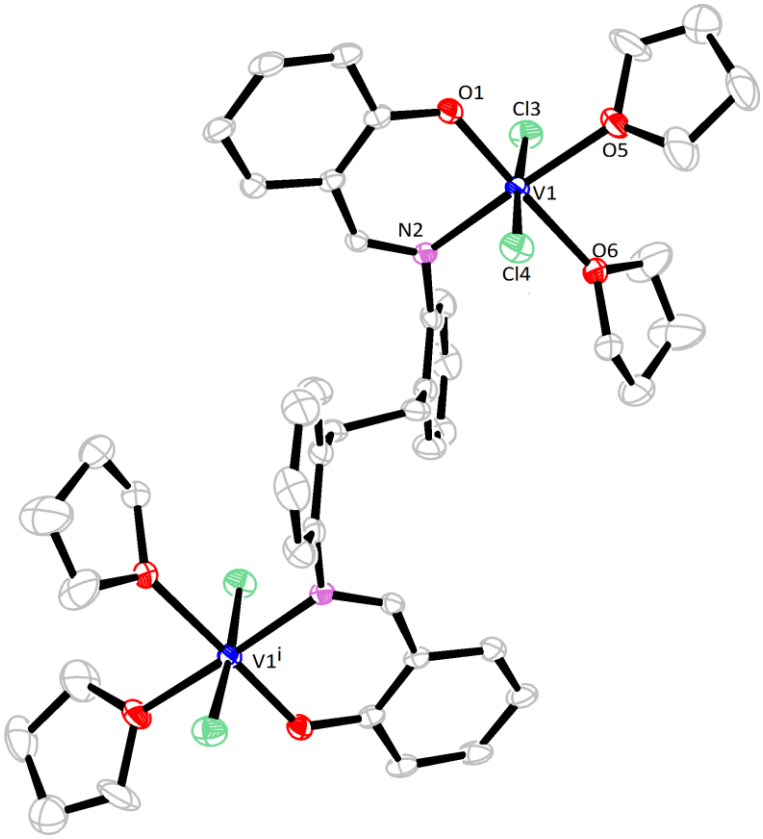


**Figure 2.1** ORTEP representation of compound **7**. Hydrogen atoms and *tert*-butyl groups have been omitted for clarity. Displacement ellipsoids are drawn at the 50% probability level. Selected bond lengths (Å) and angles (°):V—O(1) 1.870(2), V—N(2) 2.087(2), V—Cl(3) 2.3546(9), V—Cl(4) 2.3581(9), V—O(5) 2.107, V—O(6) 2.117(2), O(1)—V—N(2) 89.56(9), O(1)—V—O(5) 92.12(9), O(1)—V—O(6) 177.31(9), N(2)—V—O(5) 177.87(9), N(2)—V—O(6) 92.60(9), Cl(3)—V—Cl(4) 176.20(4).

Whilst compound **6** was synthesized following the reported literature method, complex **9** was formed using 'wet' ligand (**L3H** that had been dried insufficiently; ligand used for formation of compound **6** had been dried *in vacuo* in excess of 16 hours) in moderate yield (*ca* 37%). Single crystals of **9** were grown from a saturated acetonitrile solution on prolonged standing at ambient temperature. The vanadium atom in complex **9** (**Figure 2.2**) is five-coordinate with an approximately square-pyramidal geometry. The chloride ligands and phenolate oxygen occupy the corners of the base with the vanadyl oxygen, O(5), at the apex. The two phenolate ligands are approximately mirrored about the central $VOCl_2$ plane. The compound is dizwitterionic with the nitrogen containing hydrogen bonds between the chloride and the phenolate oxygen atoms. There are also two solvent (acetonitrile) molecules in the asymmetric unit of the cell.

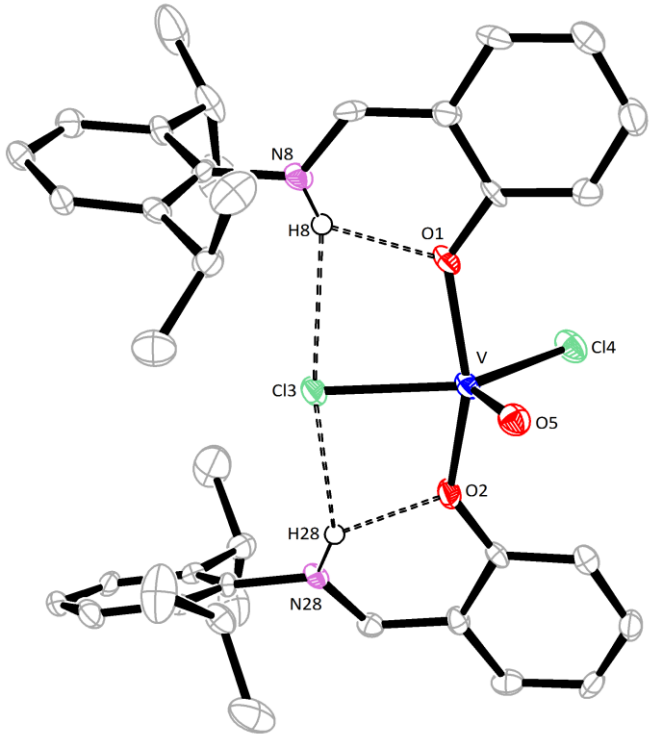


**Figure 2.2** ORTEP representation of dizwitterionic complex **9**.2$CH_3CN$, indicating the atom numbering scheme. Hydrogen atoms which do not undergo hydrogen bonding and solvent molecules have been removed for clarity. Displacement ellipsoids are drawn at the 50% probability level. Selected bond lengths (Å) and angles (°): V—O(1) 1.987(3), V—O(2) 1.978(3), V—Cl(3) 2.3594(14), V—Cl(4) 2.3265(12), V—O(5) 1.573(3), O(2)—V—O(1) 155.91(14), O(1)—V—Cl(3) 82.08(10), O(1)—V—Cl(4) 90.33(9), O(5)—V—O(1) 101.11(15), O(2)—V—Cl(3) 81.64(9), O(2)—V—Cl(4) 90.26(9), O(5)—V—O(2) 101.43(15), Cl(4)—V—Cl(3) 138.69(5), O(5)—V—Cl(3) 112.20(12), O(5)—V—Cl(4) 109.12(12), C(7)—N(8) 1.312(6), C(27)—N(28) 1.291(6), H(8)···O(1) 1.97, N(8)—H(8)···O(1) 130.0, H(8)···Cl(3) 2.59, N(8)—H(8)···Cl(3) 149.1, H(28)···O(2) 1.95, N(28)—H(28)···O(2) 132.6, H(28)···Cl(3) 2.68, N(28)—H(28)···Cl(3) 153.2.

Compounds **10** – **15**, **17** and **18** were synthesized by the treatment of the required amount of **L6H** – **L14H** with vanadium oxytripropoxide in refluxing toluene, unexpectedly, the vanadium metal centre is reduced from oxidation state +5 to +4. The vanadium catalysed oxidation of alcohols has been extensively explored,[21-26] and there are a number of proposed mechanisms. Whilst the mechanism is facilitated by the presence of base, the similar structures and products observed by Hanson and co-workers (**Scheme 2.2**, (b))[23-26] imply that it is highly probable that the propoxide ligand is undergoing oxidation with the concomitant reduction of the vanadium centre. It should be noted that the 8-quinolate vanadium compound utilized by Hanson and co-workers was ineffective for the oxidation of aliphatic alcohols,[24] the proposed oxidation of 1-propanol in the absence of base for the synthesis of

compounds **10** – **15**, **17** and **18**, suggest these compounds may be highly active for the oxidation of alcohols.

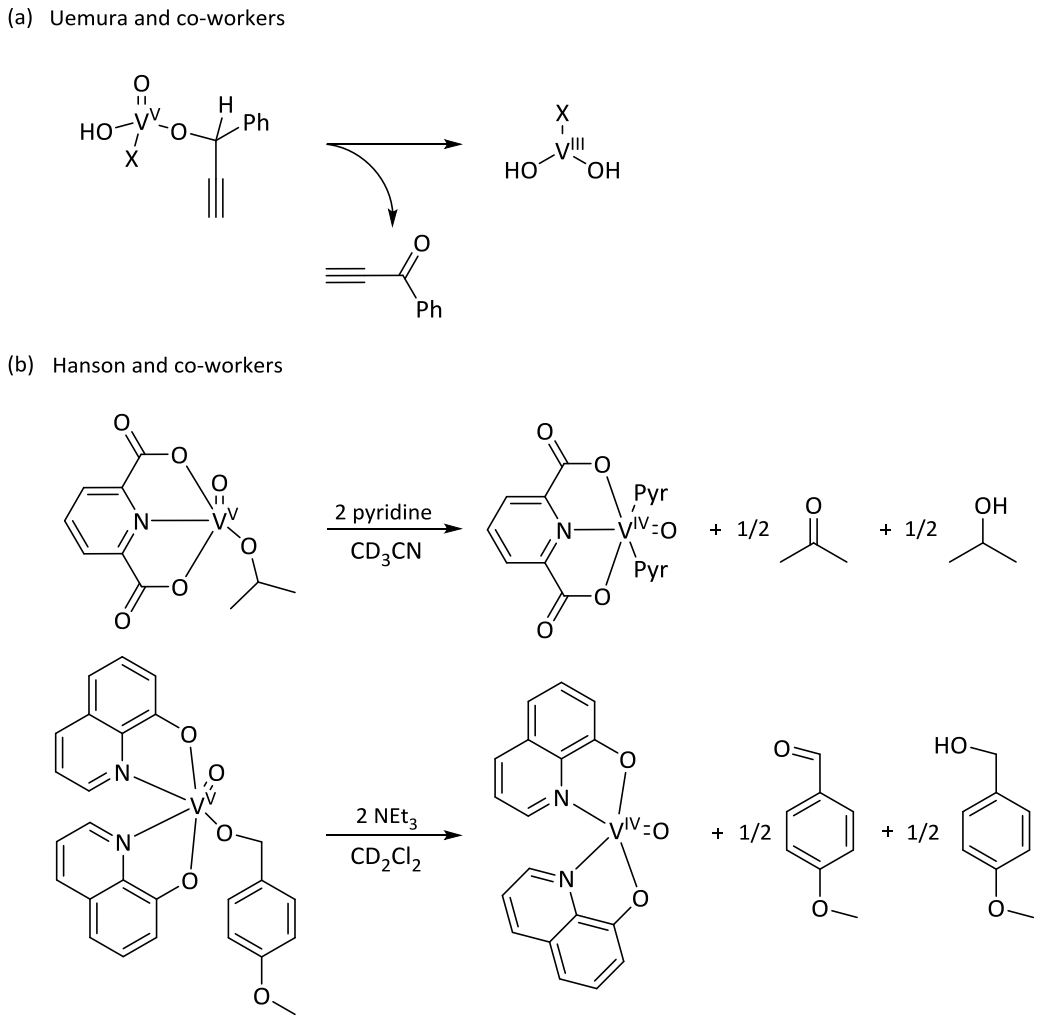


**Scheme 2.2** Reduction of vanadium centres during alcohol oxidation catalysis as explored by (a) Uemura and co-workers and (b) Hanson and co-workers.

Crystals of compounds **10** – **15** suitable for single crystal X-ray diffraction studies were grown from saturated acetonitrile solutions (**Figure 2.3**). All compounds are very similar with distorted trigonal bipyramidal geometry, the N(1)—V(1)—N(2) bond angle diverges from linearity in each case (167.82(9)° – 173.60(14)°), the oxygen atoms occupy the equatorial positions whilst the N atoms axial. All complexes possess $C_2$ symmetry around the V=O bond. The vanadyl bond lengths are typical, as are the imine to vanadium dative bonds (see **Table 2.1**).[27] Although originally the third heteroatom was intended to participate in binding to the vanadium centre, in compounds **10** – **15**, the OR group is rotated away from the vanadium metal centre and does not participate in dative bonding.

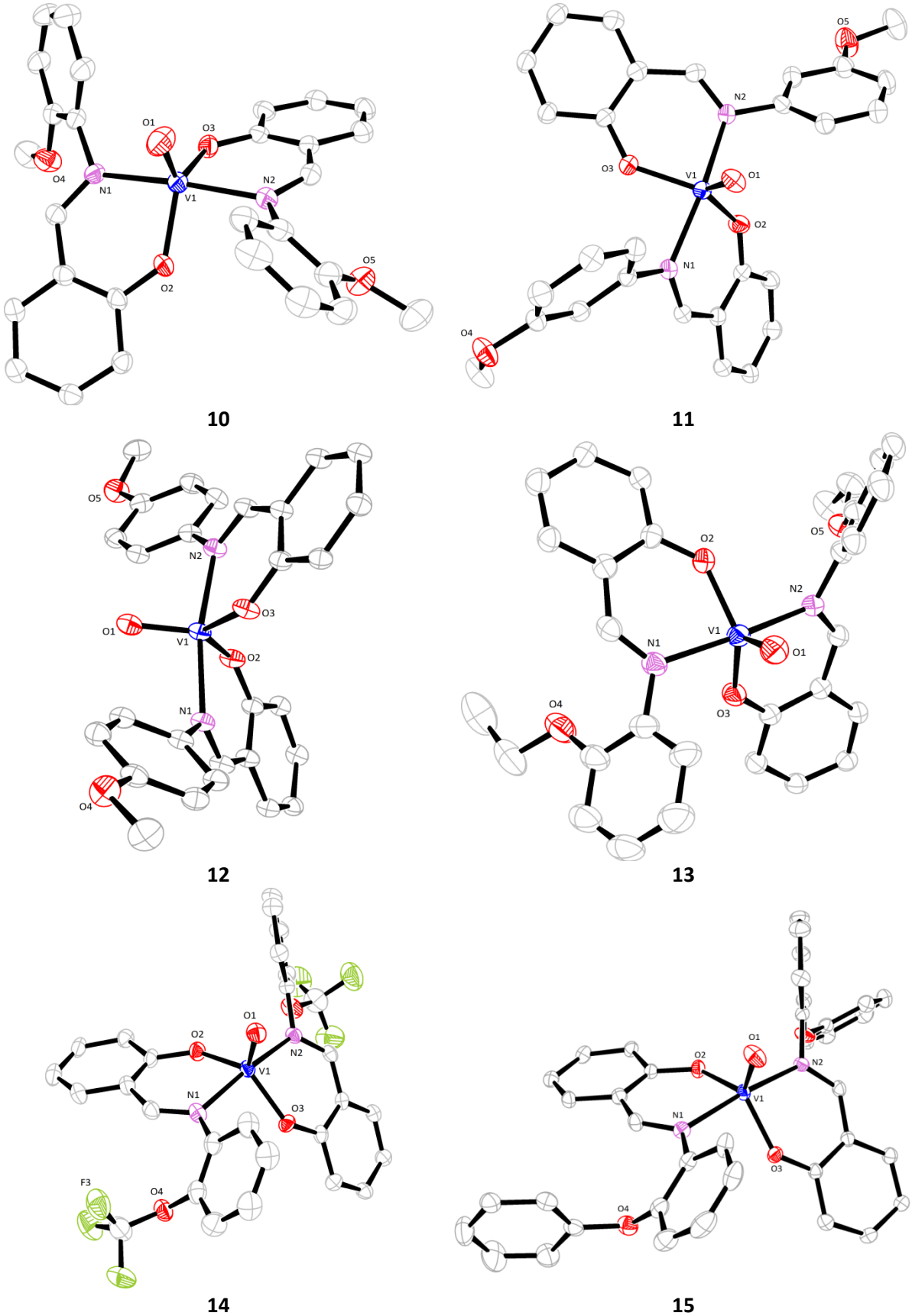


**Figure 2.3** ORTEP representation of compounds **10** – **15**. Displacement ellipsoids are drawn at the 50% probability level. Hydrogen atoms, *tert*-butyl groups and solvent molecules have been removed for clarity.

**Table 2.1**. Selected bond lengths (Å) and angles (°) for complexes **10** – **15**.

| | **10** | **11** | **12** | **13** | **14** | **15** |
|---|---|---|---|---|---|---|
| V(1)-O(1) | 1.596(3) | 1.597(2) | 1.596(2) | 1.603(3) | 1.605(4) | 1.596(2) |
| V(1)-O(2) | 1.915(3) | 1.905(2) | 1.9165(19) | 1.925(3) | 1.904(4) | 1.907(2) |
| V(1)-O(3) | 1.904(3) | 1.905(2) | 1.9109(19) | 1.908(3) | 1.913(4) | 1.897(2) |
| V(1)-N(1) | 2.129(3) | 2.118(3) | 2.126(2) | 2.139(3) | 2.134(5) | 2.134(2) |
| V(1)-N(2) | 2.135(4) | 2.126(3) | 2.119(2) | 2.138(3) | 2.125(5) | 2.126(2) |
| | | | | | | |
| O(1)-V(1)-O(3) | 118.06(16) | 118.77(11) | 115.50(10) | 117.76(15) | 118.20(19) | 120.01(11) |
| O(1)-V(1)-O(2) | 118.87(16) | 119.60(10) | 120.63(9) | 119.99(14) | 114.7(2) | 116.39(11) |
| O(3)-V(1)-O(2) | 123.06(13) | 121.64(10) | 123.87(9) | 122.24(13) | 127.08(17) | 123.58(9) |
| O(1)-V(1)-N(1) | 92.77(15) | 95.17(10) | 95.74(9) | 93.90(14) | 92.5(2) | 93.31(10) |
| O(3)-V(1)-N(1) | 88.99(13) | 87.50(9) | 88.28(8) | 89.31(12) | 87.77(18) | 87.90(9) |
| O(2)-V(1)-N(1) | 87.75(13) | 87.66(9) | 86.54(9) | 87.03(12) | 88.27(18) | 87.65(9) |
| O(1)-V(1)-N(2) | 93.59(16) | 93.78(10) | 96.22(9) | 93.58(14) | 96.4(2) | 94.01(10) |
| O(3)-V(1)-N(2) | 88.53(13) | 87.02(9) | 88.61(8) | 87.58(12) | 86.87(17) | 86.73(9) |
| O(2)-V(1)-N(2) | 88.66(13) | 89.09(9) | 85.43(9) | 88.87(12) | 89.19(17) | 90.86(9) |
| N(1)-V(1)-N(2) | 173.60(14) | 170.94(9) | 167.82(9) | 172.50(13) | 170.99(18) | 172.41(9) |

In an attempt to synthesize a vanadium compound containing only one ligand to each vanadium, **L11H** was treated with 1 equivalent of $VO(O^nPr)_3$ in refluxing toluene, which resulted in the formation of compound **16**. Single crystals of **16** were grown from a saturated acetonitrile solution. The crystal structure is shown in **Figure 2.4** and the selected bond lengths are presented in the legend. Compound **16** is a centrosymmetric molecule and contains two vanadium centres, which are linked via oxo bridges, and the two deprotonated ligands. The source of the oxo bridges is most likely adventitious hydrolysis. The vanadium metal centre adopts a distorted square pyramidal geometry; the corners of the square are made up from the oxo bridges and the Schiff base ligands, the vanadyl oxygen is at the apex. The chelating rings form a six-membered ring adopting an envelope conformation with the V atom as the tip of the flap and with a bite angle of 82.30(4)$^o$.

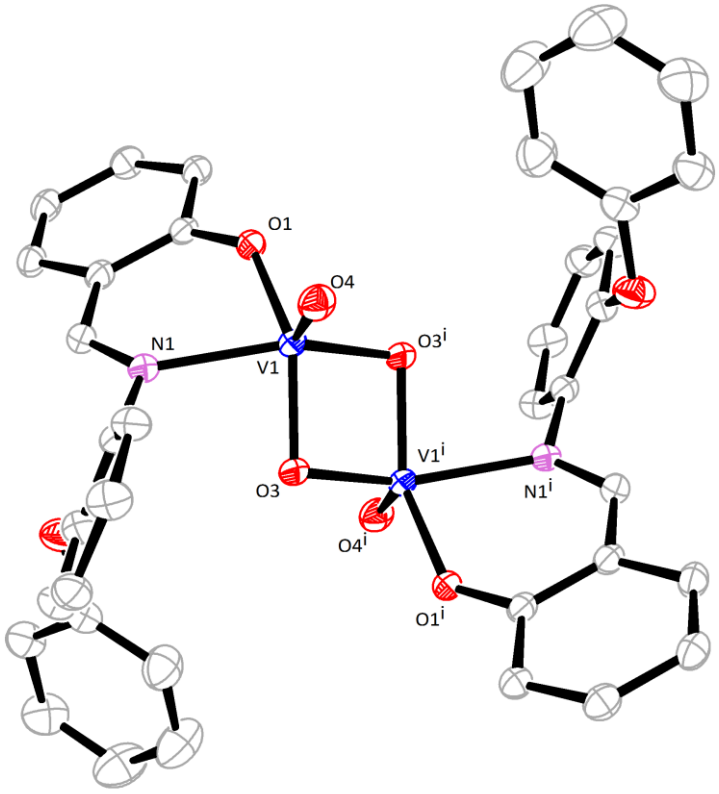


**Figure 2.4** ORTEP representation of the dinuclear μ–oxo complex **16** showing the atom numbering scheme. Hydrogen atoms and *t*-butyl groups have been omitted for clarity. Displacement ellipsoids are drawn at the 50% probability level. Selected bond lengths (Å) and angles (°): V(1)—O(1) 1.5952(10), V(1)—O(3$^{i}$) 1.8084(10), V(1)—O(3) 1.8247(9), V(1)—O(2) 1.8334(9), V(1)—N(1) 2.1371(11), V(1)···V(1$^{i}$) 2.7157(4), O(1)—V(1)—O(3$^{i}$) 107.30(5), O(1)—V(1)—O(3) 109.76(5), O(3$^{i}$)—V(1)—O(3) 83.25(4), O(1)—V(1)—O(2) 107.13(5), O(3$^{i}$)—V(1)—O(2) 95.93(4), O(3)—V(1)—O(2) 141.55(5), O(1)—V(1)—N(1) 99.71(5), O(3$^{i}$)—V(1)—N(1) 152.13(5), O(3)—V(1)—N(1) 81.27(4), O(2)—V(1)—N(1) 82.30(4), O(1)—V(1)—V(1$^{i}$), 115.16(4), O(3$^{i}$)—V(1)—V(1$^{i}$) 41.86(3), O(3)—V(1)—V(1$^{i}$) 41.40(3), O(2)—V(1)—V(1$^{i}$) 126.52(3), N(1)—V(1)—V(1$^{i}$) 119.12(3).

The use of an extended *ortho* derivative, such as in **L12** and **L13**, resulted in the formation of complexes **17** and **18** (**Figure 2.5** and **Figure 2.6**), which are similar to that of **10** – **15**. Again the third heteroatom does not participate in dative bonding. The two complexes possess distorted trigonal bipyramidal geometry, with the N(1)—V(1)—N(2) bond angle diverging from linearity in each case (See **Table 2.2**).

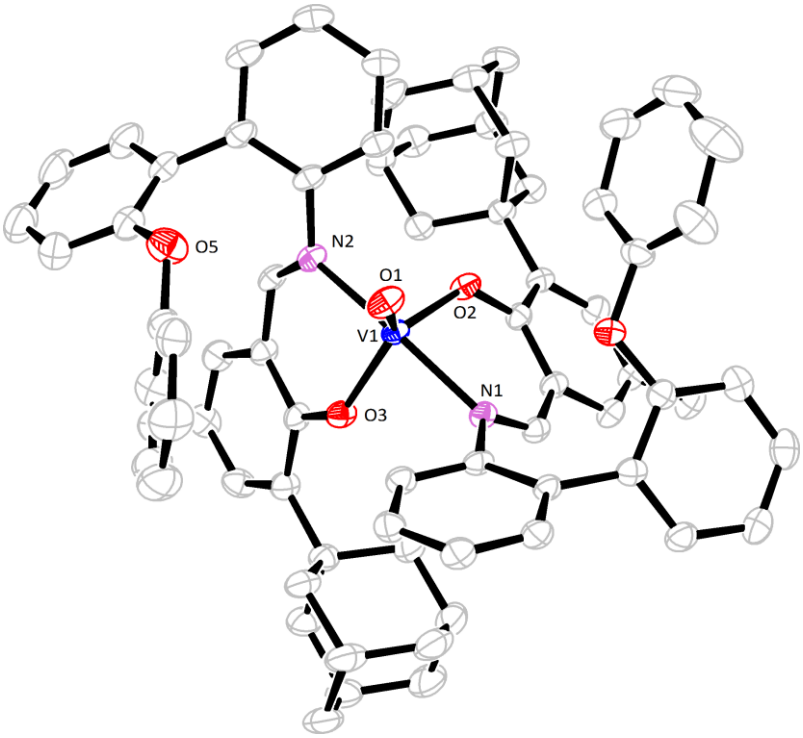


**Figure 2.5** ORTEP representation of **17** showing the atom numbering scheme. Hydrogen atoms and *tert*-butyl groups have been removed for clarity.

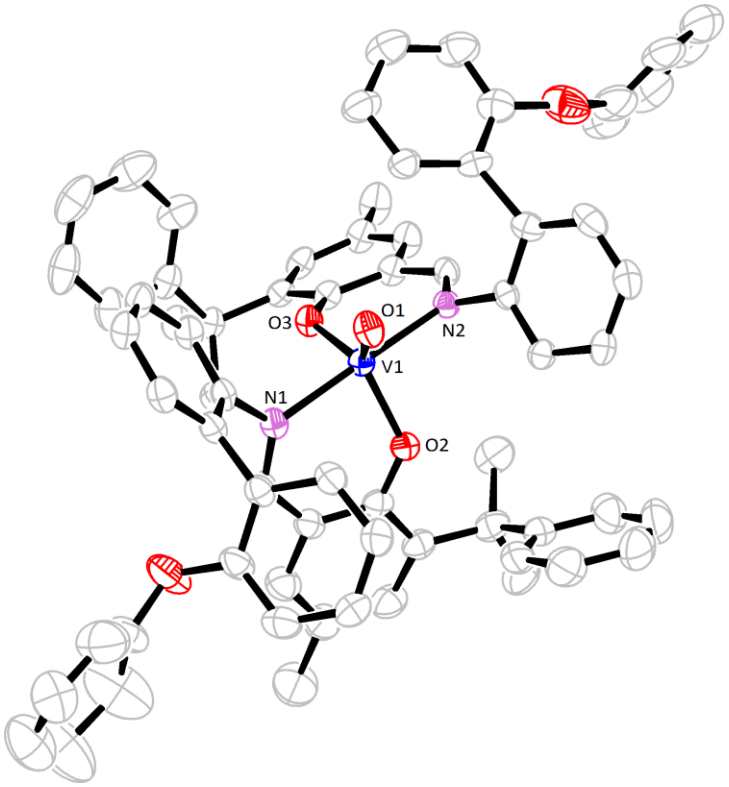


**Figure 2.6** ORTEP representation of **18** showing the atom numbering scheme. Hydrogen atoms and *tert*-butyl groups have been removed for clarity.

**Table 2.2**. Selected bond lengths (Å) and angles (°) for complexes **17** and **18**.

| | **17** | **18** |
|---|---|---|
| V(1)-O(1) | 1.593(2) | 1.595(2) |
| V(1)-O(2) | 1.911(2) | 1.912(2) |
| V(1)-O(3) | 1.903(2) | 1.915(2) |
| V(1)-N(1) | 2.113(2) | 2.093(3) |
| V(1)-N(2) | 2.113(2) | 2.113(3) |
| O(1)-V(1)-O(3) | 125.65(11) | 123.94(12) |
| O(1)-V(1)-O(2) | 122.19(11) | 123.33(12) |
| O(3)-V(1)-O(2) | 112.15(10) | 112.73(10) |
| O(1)-V(1)-N(1) | 95.34(10) | 92.93(11) |
| O(3)-V(1)-N(1) | 86.07(9) | 89.74(10) |
| O(2)-V(1)-N(1) | 87.07(9) | 86.76(10) |
| O(1)-V(1)-N(2) | 95.16(10) | 92.14(11) |
| O(3)-V(1)-N(2) | 87.79(9) | 86.90(10) |
| O(2)-V(1)-N(2) | 87.37(9) | 90.98(10) |
| N(1)-V(1)-N(2) | 169.50(9) | 174.89(10) |

The reaction of the quinoline based ligand, **L14H**, with vanadium oxytrichloride resulted in the isolation of compound **19**, whereas use of vanadium oxytripropoxide formed the dioxo vanadium compound **20**. The brown complex [$VOCl_2$**L14**] (**19**) was obtained in 68% isolated yield from a saturated acetonitrile solution at ambient temperature. Single crystal X-ray diffraction studies revealed the molecular structure (**Figure 2.7**), with selected bond lengths and angles given in the legend. Whereas treatment of **L14H** with [$VO(O^nPr)_3$] in refluxing toluene afforded the yellow complex [$VO_2$**L14**] (**20**) in 64% isolated yield. Again acetonitrile was utilized to recrystallize compound **20**; single crystal X-ray diffraction studies revealed the structure (**Figure 2.8**) with selected bond lengths and angles given in the legend. The metal centre of compound **19** possesses distorted octahedral geometry with the tridentate ligand binding in *mer* fashion and with the vanadyl group *trans* to the imino nitrogen. By contrast, compound **20** adopts distorted trigonal bipyramidal geometry; the imine nitrogen and the dioxo oxygens fill the equatorial plane with the phenolate oxygen and quinoline nitrogen atoms in axial positions. Presumably the presence of the second oxo group arises *via* fortuitous hydrolysis, liberating propanol.

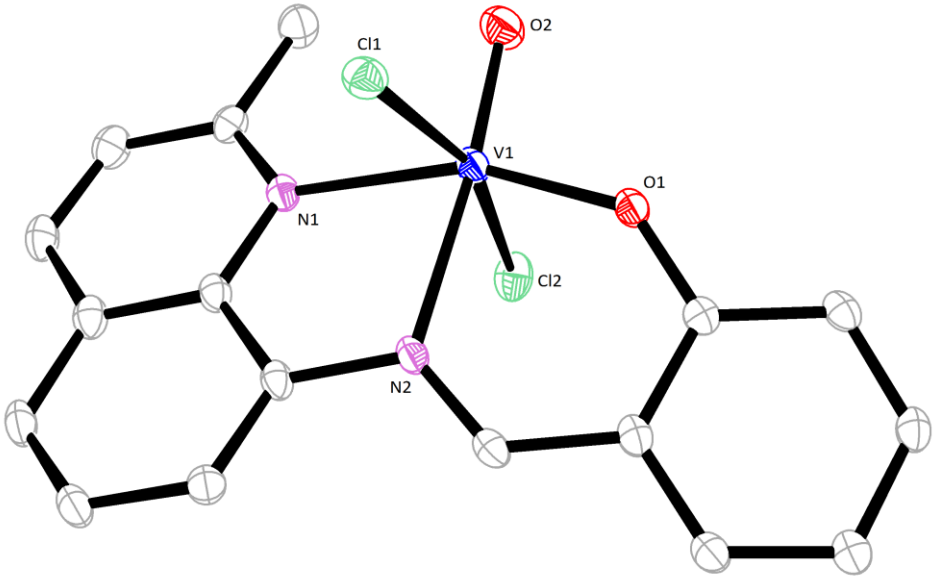


**Figure 2.7** ORTEP representation of **19** showing the atom numbering scheme. Hydrogen atoms and *tert*-butyl groups have been removed for clarity. Selected bond lengths (Å) and angles (°): V(1)—O(1) 1.8105(14), V(1)—O(2) 1.5911(14), V(1)—N(1) 2.1669(17), V(1)—N(2) 2.2090(16), V(1)—Cl(1) 2.3610(6), V(1)—Cl(2) 2.3147(6); O(1)—V(1)—N(1) 158.23(6), O(2)—V(1)—N(2) 173.64(7), Cl(1)—V(1)—Cl(2) 162.72(2).

The use of **L14H** seems to inhibit the dimerization of five-co-ordinate vanadium dioxo species to a structure similar to compound **16**. The ligand again binds in *mer* fashion. The main source of distortion is due to the rigidity of the quinoline nitrogen which is displaced from the ideal axial position, in a similar fashion to previous examples of quinoline dioxovanadium species.[28] The unit cell contains three unique complexes that vary only in the twist between the quinolinyl group and the phenolate aromatic ring; 39.94(9)° for complex containing V1, 31.07(9)° for V2 and 30.96(9)° for V3, respectively. The reaction was repeated to avoid hydrolysis, however the dioxo complex was again formed; structure **20'** differs from **20** due to the presence of only one unique complex in the unit cell and the degree of solvation. Compounds **10** – **20** have been characterised by EPR (**10** – **15**, **17** and **18**) or NMR (**16**, **19** and **20**), IR, mass spectroscopy, elemental analysis and where possible single crystal X-ray diffraction.

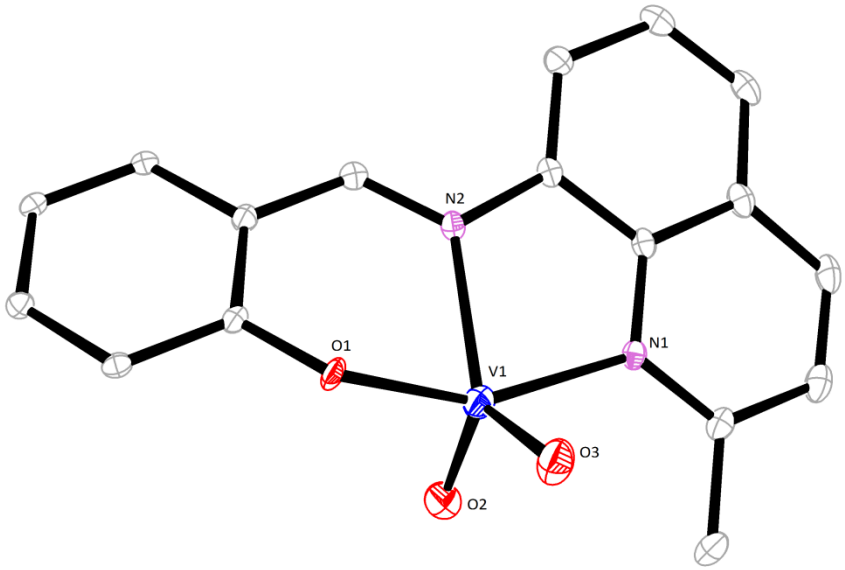


**Figure 2.8** ORTEP representation **20**.2/3(MeCN) showing the atom numbering scheme. Hydrogen atoms and *tert*-butyl groups have been removed for clarity. Displacement ellipsoids are drawn at the 50% probability level. Selected bond lengths (Å) and angles (°): V(1)—O(1) 1.624(3), V(1)—O(2) 1.628(4), V(1)—O(3) 1.913(3), V(1)—N(1) 2.139(4), V(1)—N(2) 2.164(4); O(1)—V(1)—N(1) 134.67(17), O(2)—V(1)—N(2) 98.21(15), O(3)—V(1)—N(2) 152.79(14).

### *2.2.1.1 Silica Immobilisation*

The supported structures **S-4** and **S-6** were synthesized by immobilising compounds **4** and **6** on dried silica, the $SiO_2$ had been heated to 350 °C under dynamic vacuum for 48 hr. X-ray photoelectron spectroscopy (XPS) analysis was used to assign the percentage composition of vanadium, from the V-2$p_{3/2}$ peak at 517.0 ± 0.02 eV, in the supported structures (**Figure 2.9**). The resulting concentration of vanadium was shown to be 0.054% of the bulk sample. The C-*1s* peak at 284.7 eV was used to calibrate the spectrum; however the calculated carbon concentration in the sample is much higher than expected, now assigned to the presence of adventitious carbon. Confirmation that the ligand has not been leached from the system was ascertained from the identification of N-*1s* and Cl-2*p* peaks at binding energies of 401.0 eV (0.089 %) and 199.7 eV (0.162 %).

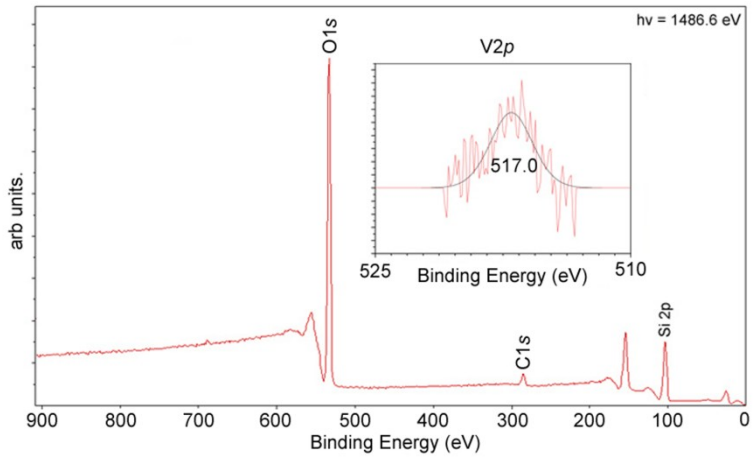


**Figure 2.9** X-ray photoelectron survey spectrum of **S-4**. The vanadium V2*p* energy window 525 – 510 eV is shown inset.

### *2.2.2 Vanadium(III) Phenoxyimine Polymerisation Screening*

#### *2.2.2.1 Schlenk Line Ethylene Screening*

**Table 2.3** Ethylene polymerisation results[a]

| Run | Pre-catalyst[b] | Polymer[c] | Activity[d] | $M_w$[e] | $M_n$[f] | PDI[g] | $M_p$[h] |
|---|---|---|---|---|---|---|---|
| 1 | **1** | 0.98 | 3,920 | 273,000 | 47,600 | 5.7 | 143.7 |
| 2 | **2** | 1.31 | 5,240 | 168,000 | 39,200 | 4.3 | 142.6 |
| 3 | **3** | 0.55 | 2,210 | - | - | - | - |
| 4 | **4** | 0.80 | 3,190 | - | - | - | - |
| 5 | **5** | 0.48 | 1,920 | - | - | - | - |
| 6 | **6** | 0.71 | 2,850 | - | - | - | - |
| 7 | **7** | 2.38 | 9,520 | 445,000 | 181,000 | 2.5 | 140.6 |
| 8 | **8** | 1.2 | 4,800 | 170,000 | 30,500 | 5.6 | 143.1 |
| 9 | **9** | 0.41 | 1,640 | - | - | - | - |

[a] **Conditions**: 1 bar ethylene; toluene (100 mL); 4000 equivalents DMAC; ETA (0.1 mL); reaction quenched with dilute HCl, washed with methanol (20 mL) and dried for 12 h in a vacuum oven at 80 °C. [b] 0.5μmol. [c] Grams of polymer. [d] Grams of polymer/mmol.hr.bar [e] Weight average molecular weight. [f] Number average molecular weight. [g] Polydispersity index. [h] °C determined by DSC. All runs carried out at 25 °C, 30 min. and Al/V (Molar ratio) 4000.

Complexes **1** – **9** have been evaluated as pre-catalysts for the polymerisation of ethylene, employing DMAC (dimethylaluminium chloride) as co-catalyst, and ETA (ethyltrichloroacetate) as a re-activator. Polymerisations were carried out in toluene (100 mL) using 4000 molar equiv. of co-catalyst at 25 °C over 30 minutes (**Table 2.3**). Screening using complexes **1** to **9** gave highly active polymerisation catalysts, however they are disappointing in terms of other recently reported vanadium pre-catalysts based on the same system (DMAC/ETA).[29] The polymerisation screening revealed for the mononuclear pre-catalysts that the activity of the *tert*-butyl counterparts (**Table 2.3**, complexes **1**, **3** and **5**), were lower than their salicylaldehyde counterparts (complexes **2**, **4** and **6**). The general trend for **1** to **6**, where the *ortho* position is progressively more sterically demanding, shows a decrease in activity. On comparing bi-metallic complex **7** with the mononuclear vanadium pre-catalysts, there is a suggestion of a co-operative effect in **7** as the observed activities for **1** to **6** suggest that this is not simply a steric effect. In the case of R = H (**4** and **8**), the beneficial cooperative effect in **8** is far less pronounced.

*2.2.2.2 Homogenous Parallel Pressure Reactor Ethylene Screening*

**Table 2.4** Homogenous PPR Ethylene polymerisation results[a]

| Run | Pre-catalyst[b] | Temperature[c] | Yield[d] | Activity[e] |
|---|---|---|---|---|
| 1 | **7** (0.10) | 60 | 0.0436 | 65 |
| 2 | **7** (0.15) | 60 | 0.0382 | 38 |
| 3 | **7** (0.20) | 60 | 0.0408 | 31 |
| 4 | **7** (0.25) | 60 | 0.0455 | 27 |
| 5 | **7** (0.10) | 80 | 0.0363 | 54 |
| 6 | **7** (0.20) | 80 | 0.0475 | 36 |
| 7 | **7** (0.25) | 80 | 0.0461 | 28 |

[a] **Conditions**: 6.67 bar ethylene, 1 hr reaction time, Al/V (Molar ratio) 4000 (MAO). [b] (mmol). [c] °C. [d] Grams of polymer. [e] g/mmol.hr.bar

The activity of compound **7** was further explored for the polymerisation of ethylene using a parallel pressure reactor. Methylaluminoxane (MAO) was used as a co-catalyst and produced moderately active catalysts for the polymerisation of ethylene (**Table 2.4**). Using a larger equivalent of catalyst loading was detrimental to the activity. Clearly, DMAC is the co-catalyst of choice when compared with MAO. It should be noted that varying the co-catalyst for vanadium polymerisation was explored by Nomura *et al*,[30] who suggested that the size of MAO forces the catalyst to form discrete ions, whereas use of DMAC results in the formation of chloro-bridged species which are more active for polymerisation.

*2.2.2.3 Heterogeneous Parallel Pressure Reactor Ethylene Screening*

**Table 2.5** PPR, Homopolymerisation of **S-4** and **S-6**[a]

| Run | Pre-Catalyst[b] | Metal Content[c] | Final Ethylene Uptake[d] |
|---|---|---|---|
| 1 | **S-4** (0.3) | 3.17 | 5.04 |
| 2 | **S-4** (0.8) | 8.44 | 4.88 |
| 3 | **S-4** (0.8)[e] | 8.44 | 3.82 |
| 4 | **S-6** (0.3) | 3.17 | 6.26 |
| 5 | **S-6** (0.8) | 8.44 | 4.12 |
| 6 | **S-6** (0.8)[e] | 8.44 | 1.07 |

[a] **Conditions**: 80°C, 5µmol TIBA as co-catalyst, 0.5 mol/L ethylene concentration, ethylene pressure: 92 psi, 1 hour polymerisation run; reaction quenched with $CO_2$; [b]mg, [c] determined by XPS (µmol, $x10^{-3}$), [d] psi, [e] Repeated Run.

The silica supported compounds **S-4** and **S-6** were subjected to homo-polymerisation (ethylene) and co-polymerisation (1-hexene and ethylene), over a one hour period. Triisobutyl aluminium (TIBA) or ethylaluminium dichloride (EADC) were used as co-catalysts, with the addition of ethyl trichloroacetate (ETA) where required. The metal content contained in the bulk sample was determined by XPS and this value was used to determine the catalytic activity of the supported catalysts. The Homo-polymerisation results show the two pre-catalysts to be inactive for the polymerisation of ethylene using TIBA (**Table 2.5**, runs 1 – 6); the resulting uptake of ethylene (psi) was due to saturation of heptane rather than polymerisation. Co-polymerisation was more successful, where **S-6** outperformed **S-4** with peak activities of 1,744 and 757 g/mmol.hr.bar respectively (**Table 2.6**, runs 8 and 2), using EADC as co-catalyst and the addition of ETA. Use of ETA indeed gave higher activities on a number of runs, as did use of EADC rather than TIBA. However the resulting activities and ethylene uptakes from repeated runs show a large divergence, as such repeated runs are shown instead of the averaged values (**Table 2.6**).

**Table 2.6** PPR, Copolymerisation using **S-4** or **S-6** with co-catalyst EADC and ETA[a]

| Run | Pre-Catalyst[b] | Metal Content[c] | Yield[d] | Activity[e] | Final Ethylene uptake[f] | ETA:Metal ratio |
|---|---|---|---|---|---|---|
| 1 | **S-4** (0.3) | 3.17 | 0.0054 | 269 | 10.38 | 1440 |
| 2 | **S-4** (0.3)[e] | 3.17 | 0.0152 | 757 | 16.03 | 1440 |
| 3 | **S-4** (0.8) | 8.44 | 0.0017 | 32 | 3.51 | 1440 |
| 4 | **S-4** (0.8)[e] | 8.44 | 0.0038 | 71 | 5.04 | 1440 |
| 5 | **S-6** (0.3) | 3.17 | 0.0288 | 1435 | 18.77 | 720 |
| 6 | **S-6** (0.3) | 3.17 | 0.004 | 199 | 8.09 | 1440 |
| 7 | **S-6** (0.3)e | 3.17 | 0.0085 | 424 | 7.94 | 1440 |
| 8 | **S-6** (0.3)[e] | 3.17 | 0.035 | 1744 | 25.64 | 1440 |
| 9 | **S-6** (0.3)[e] | 3.17 | 0.0125 | 623 | 11.14 | 1440 |
| 10 | **S-6** (0.8) | 8.44 | 0.0086 | 161 | 10.38 | 1440 |
| 11 | **S-6** (0.8)[e] | 8.44 | 0.0081 | 151 | 8.70 | 1440 |

[a] **Conditions**: 80°C, 5µmol EADC as co-catalyst, 0.5 mol/L ethylene concentration, ethylene pressure: 92 psi, 1 hour polymerisation run; ETA added as a solution in heptane; reaction quenched with $CO_2$; [b]mg, [c] determined by XPS (µmol, x$10^{-3}$), [d]grams, [e](g/(mmol.hr)), [f]psi.

### *2.2.3 Vanadyl Phenoxyimine Polymerisation Screening*

#### *2.2.3.1 Schlenk Line Ethylene Screening*

The polymerisation screening of compounds **10** – **20** were performed at the University of Sichuan Normal University in Chengdu (China) and the results interpreted herein. Firstly, complex **18** was screened to ascertain the polymerisation conditions resulting in the highest activities for ethylene polymerisation at 1 bar (**Table 2.7**). Diethylaluminium chloride (DEAC) was used as co-catalyst and ethyltrichloroacetate (ETA) as re-activator. The polymerisation screening indicated that the highest activity was obtained using 16,000 equivalents of DEAC to vanadium at 20 °C, although it should be noted the activities are somewhat similar. The activity of complex **18** increased with temperature and peaked at 80 °C, however the polymer molecular weight appeared to drop by an order of magnitude above 30 °C (≈135,600 g/mol at 20 °C, **Table 2.7** run 4 *versus* ≈15,800 g/mol at 30 °C, **Table 2.7** run 7). The catalyst system was short-lived with the activity dropping to below 50% after 60 minutes. Complexes **10** – **20** were screened using the conditions resulting in the highest activity, determined by the screening of complex **18**, *ie* 16,000 equivalents DEAC, 0.1 mL ETA, 80 °C; the results are presented in **Table 2.8.**

**Table 2.7** Optimization of catalysis conditions using pre-catalyst **18** at 1 bar.[a]

| Run | Al/V | T[b] | Time[c] | Yield[d] | Activity[e] | $M_w$ | $M_n$ | PDI | $T_m$[f] |
|---|---|---|---|---|---|---|---|---|---|
| 1 | 4000 | 20 | 30 | 0.382 | 1,530 | 102,000 | 54,500 | 1.9 | 137.1 |
| 2 | 8000 | 20 | 30 | 0.437 | 1,750 | 119,000 | 66,000 | 1.8 | 134.9 |
| 3 | 12000 | 20 | 30 | 0.452 | 1,810 | 126,000 | 63,200 | 2.0 | 135.5 |
| 4 | 16000 | 20 | 30 | 0.478 | 1,910 | 136,000 | 74,100 | 1.8 | 135.9 |
| 5 | 20000 | 20 | 30 | 0.432 | 1,730 | 106,000 | 52,400 | 2.0 | 135.4 |
| 6 | 24000 | 20 | 30 | 0.335 | 1,340 | 117,000 | 60,000 | 2.0 | 136.2 |
| 7 | 16000 | 30 | 30 | 0.669 | 2,680 | 15,800 | 6,000 | 2.6 | 130.5 |
| 8 | 16000 | 40 | 30 | 0.830 | 3,320 | 8,100 | 2,700 | 3.0 | 127.0 |
| 9 | 16000 | 50 | 30 | 0.982 | 3,930 | 8,100 | 2,200 | 3.7 | 126.9 |
| 10 | 16000 | 60 | 30 | 1.104 | 4,420 | 7,700 | 2,000 | 3.9 | 126.0 |
| 11 | 16000 | 70 | 30 | 1.308 | 5,230 | 8,000 | 2,100 | 3.8 | 126.3 |
| 12 | 16000 | 80 | 30 | 1.648 | 6,590 | 13,200 | 2,700 | 4.9 | 128.1 |
| 13 | 16000 | 90 | 30 | 1.077 | 4,310 | 22,000 | 1,900 | 11 | 127.0 |
| 14 | 16000 | 100 | 30 | 0.431 | 1,730 | 5,400 | 1,100 | 4.9 | 128.0 |
| 15 | 16000 | 110 | 30 | 0.172 | 690 | 6,400 | 900 | 7.1 | 121.6 |
| 16 | 16000 | 80 | 10 | 0.775 | 9,300 | 4,900 | 1,500 | 3.3 | 124.9 |
| 17 | 16000 | 80 | 20 | 1.195 | 7,170 | 3,600 | 1,300 | 2.8 | 124.2 |
| 18 | 16000 | 80 | 60 | 2.033 | 4,070 | 5,200 | 1,600 | 3.3 | 125.4 |

[a] Conditions: 0.5 $\mu$mol of [V] per run, 30 mL of toluene, 0.1ml ETA per run, 1 bar of ethylene. GPC analysis was conducted in 1,2,4-trichlorobenzene, [b] °C, [c](min), [d] grams, [e] g/(mmol.hr), [f] °C polymer melting point.

All of the complexes were found to be highly active for the polymerisation of ethylene. The polymer molecular weights ($M_w$) were in the range 2,400 – 11,700 with PDI values of between 2.6 and 5.6. The activities of the compounds were all somewhat similar; all of the complexes give activities in the range of 3,800 – 8,700 g/mmol.hr. The melting points of the polymers produced are somewhat low; $^{13}$C NMR studies of the polymer produced using pre-catalyst **20** revealed that there is no branching in the polymer chain, and no alkene carbons present. The minor peaks have been assigned as the result of the polymer end group (see **Figure 2.10**).[31] This indicates that the termination of the growing polymer chain does not proceed through β-hydride transfer, but more likely from chain transfer to the aluminium.

**Table 2.8** Catalysis runs using compounds **10** – **20** pre-catalysts under optimized conditions at 1 bar.[a]

| Run | Complex | Yield[b] | Activity[c] | $M_w$ | $M_n$ | PDI | $T_m$[d] |
|---|---|---|---|---|---|---|---|
| 1 | **10** | 1.134 | 6,800 | 4,500 | 1,500 | 3.0 | 124.9 |
| 2 | **11** | 0.868 | 5,210 | 9,900 | 2,000 | 5.0 | 127.2 |
| 3 | **12** | 0.956 | 5,740 | 8,400 | 2,000 | 4.2 | 126.7 |
| 4 | **13** | 0.871 | 5,230 | 3,400 | 1,100 | 3.1 | 123.8 |
| 5 | **14** | 0.801 | 4,810 | 5,800 | 1,600 | 3.6 | 125.7 |
| 6 | **15** | 1.006 | 6,030 | 11,700 | 2,100 | 5.6 | 128.0 |
| 7 | **16** | 0.640 | 3,840 | 7,800 | 1,800 | 4.3 | 126.2 |
| 8 | **17** | 1.284 | 7,700 | 7,100 | 1,800 | 3.9 | 126.3 |
| 9 | **18** | 1.195 | 7,170 | 3,600 | 1,300 | 2.8 | 124.2 |
| 10 | **19**[e] | 0.217 | 8,690 | 7,600 | 2,500 | 3.0 | 127.9 |
| 11 | **20**[e] | 0.141 | 5,640 | 10,900 | 3,700 | 3.0 | 129.7 |

[a] Conditions: 0.5 $\mu$mol of [V] per run, 30 mL of toluene, 80 °C, 16,000 equivalents of $Et_2AlCl$, 0.1 mL of ETA, 20 min, 1 bar of ethylene. GPC analysis was conducted in 1,2,4-trichlorobenzene. [b] grams, [c] g/(mmol.hr), [d] °C polymer melting point, [e] 20,000 equivalents of $Et_2AlCl$, 0.1 $\mu$mol of [V].

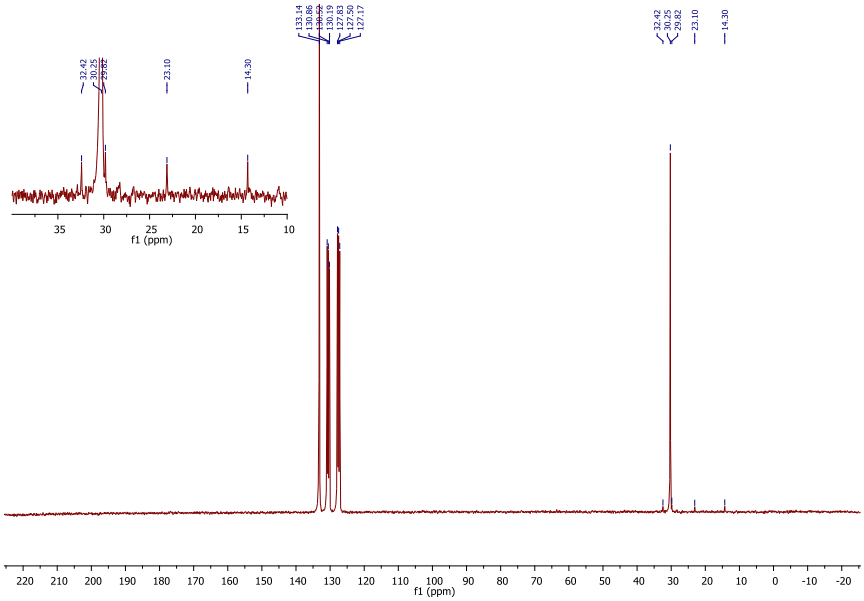


**Figure 2.10** $^{13}$C NMR spectrum of polymer produced using compound **20.**

## 2.3 Results and Discussion – Di/Tetraphenolate Vanadium Compounds

### *2.3.1 Synthesis and Structures*

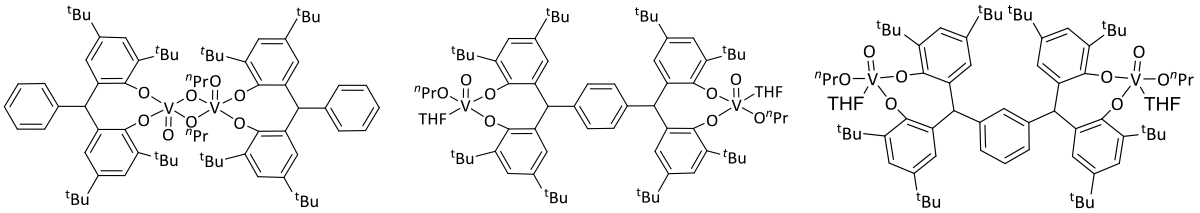

**21** **22** **23**

**Chart 2.7** Diphenolate and tetraphenolate vanadium pre-catalysts investigated in this study.[32]

Compounds **21 – 23** were synthesized in good yield (35 – 75%) from the treatment of **L15H$_2$** – **L17H$_4$** with vanadium oxytripropoxide in THF. **L15H$_2$** – **L17H$_4$** were synthesized following the reported literature method (see for example, **Scheme 2.3**).[32] Treatment of the bidentate ligand **L15H$_2$** with VO(O$^n$Pr)$_3$ led to the formation of compound **21**. Compound **21** was crystallised from light petroleum to give red needles which were suitable for single crystal X-ray diffraction. The crystal structure revealed that compound **21** forms a dimer in the solid state (see **Figure 2.11**).

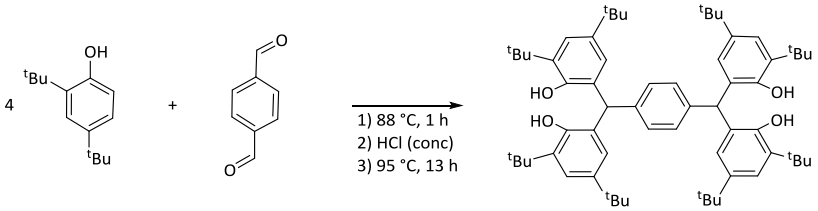


**Scheme 2.3** Synthesis of ligand **L16H$_4$.**

The vanadium oxytripropoxide loses two equivalents of propanol to bind the bidentate ligand. The dimer is centrosymmetric and contains two vanadyl moieties in a *trans* arrangement that are bridged by the two remaining *n*-propoxide ligands. Each vanadium metal centre is in trigonal bipyramidal geometry; the bidentate ligand and one of the *n*-propoxide ligands occupying the equatorial positions, the vanadyl oxygen and second *n*-propoxide occupy the axial positions. The diphenolate ligands third phenyl ring is rotated away with the methine hydrogen, which is directed toward the vanadium centre. Compound **21** has also been characterised by elemental analysis, NMR and IR spectroscopy. The molecular ion observed in the mass spectrum matches the monomer rather than the dimer.

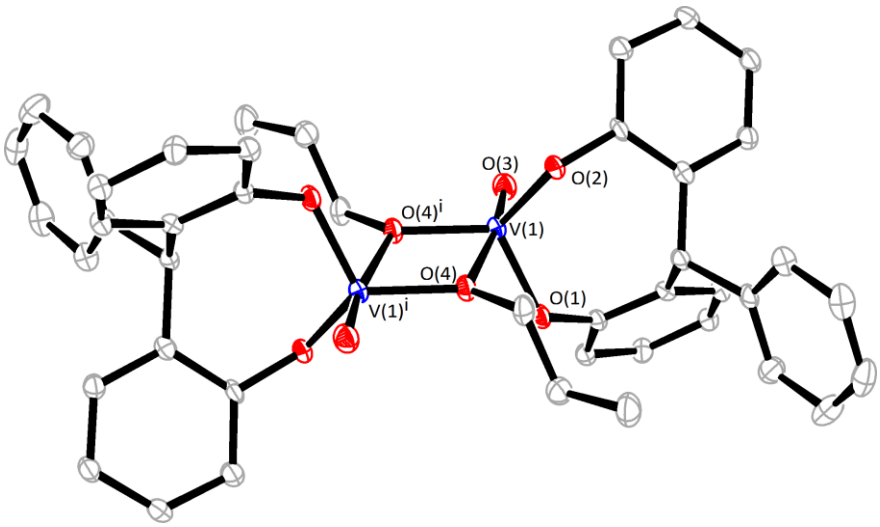


**Figure 2.11** ORTEP representation of complex **21**, indicating the atom numbering scheme. *Tert*-Butyl groups, hydrogen and solvent molecules have been removed for clarity. Displacement ellipsoids are drawn at the 50% probability level. Selected bond lengths (Å) and angles (°): O(1)—V(1) 1.8117(15), O(2)—V(1) 1.8165(16), O(3) —V(1) 1.5869(15), O(4) —V(1)′ 1.8348(15), O(4) —V(1) 2.2917(14), V(1)—O(4)′ 1.8348(15), V(1)′—O(4)—V(1) 108.23(6), O(3)—V(1)—O(1) 100.19(7), O(3)—V(1)—O(2) 100.58(8), O(1)—V(1)—O(2) 113.14(7), O(3)—V(1)—O(4)′ 100.35(7), O(1)—V(1)—O(4)′ 115.74(7), O(2)—V(1)—O(4)′ 121.56(7), O(3)—V(1)—O(4) 172.06(7), O(1)—V(1)—O(4) 84.55(6), O(2)—V(1)—O(4) 83.19(6), O(4)′—V(1)—O(4) 71.77(6).

Treatment of the tetradentate ligand (**L16H$_4$**) with vanadium oxytripropoxide leads to the formation of compound **22** concomitant with the loss of two equivalents of propanol. Crystals suitable for single crystal X-ray diffraction of compound **22** were grown by slow diffusion of light petroleum into THF; the crystal structure is presented in **Figure 2.12**. The vanadium complex has trigonal bipyramidal geometry. The two sets of diphenolates across the central phenyl ring are arranged in a *trans* fashion related by an inversion centre. A single *n*-propoxide ligand remains per vanadium centre and the fifth position is occupied by a THF molecule. The elemental analysis, mass spectrometric, IR and NMR characterisation data is consistent with the crystal structure.

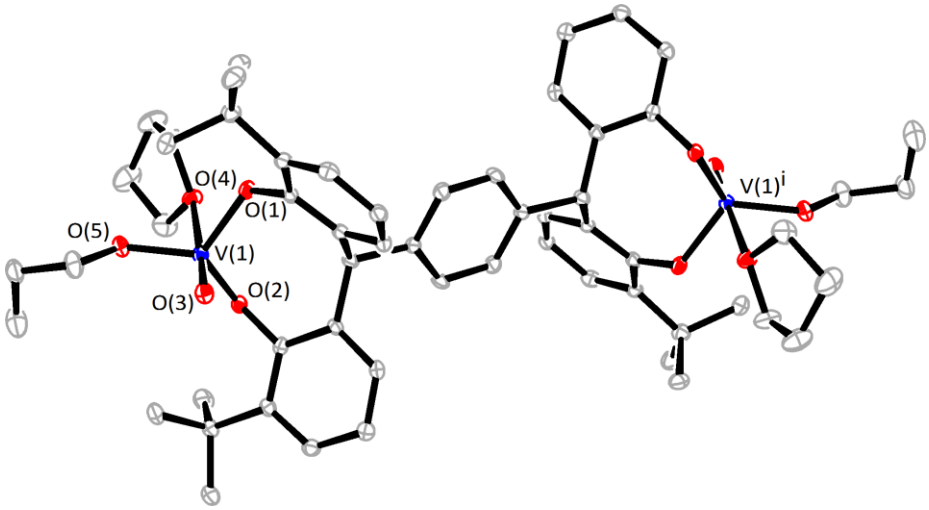


**Figure 2.12.** ORTEP representation of complex **22**.2$C_4H_8O$, indicating the atom numbering scheme. *Tert*-butyl groups and hydrogen atoms have been removed for clarity. Displacement ellipsoids are drawn at the 50% probability level. Selected bond lengths (Å) and angles (°): V(1)—O(3) 1.5871(14), V(1)—O(5) 1.7878(15), V(1)—O(2) 1.8187(15), V(1)—O(1) 1.8256(16), V(1)—O(4) 2.3307(13), O(3)—V(1)—O(5) 100.20(7), O(3)—V(1)—O(2) 100.05(7), O(5)—V(1)—O(2) 119.29(7), O(3)—V(1)—O(1) 99.63(7), O(5)—V(1)—O(1) 120.16(7), O(2)—V(1)—O(1) 111.73(7), O(3)—V(1)—O(4) 178.12(7), O(5)—V(1)—O(4) 78.36(6), O(2)—V(1)—O(4) 81.73(6), (1)—V(1)—O(4) 80.16(6).

Compound **23** was synthesized in the same manner as compound **22**, using the *meta*-derived tetradentate ligand (**L17H$_4$**) rather than the *para*-tetraphenolate; however the data collected for crystals grown from diffusion of light petroleum into THF were only suitable in defining the connectivity of the structure. The vanadium centres are in trigonal bipyramidal geometry with a THF molecule occupying the fifth position. The $^1$H NMR spectrum indicates that the compound contains two vanadium centres per ligand, as expected from compound **22**, and contains one *n*-propoxide per vanadium centre, however there are no THF peaks present. The $^{13}$C NMR, elemental analysis, mass spectra and IR characterisation is consistent with the structure after loss of THF, suggesting the THF molecule is labile enough to be removed under vacuum. The bond lengths for both compounds are typical and similar to the other vanadium complexes in trigonal bipyramidal geometry reported in this chapter.

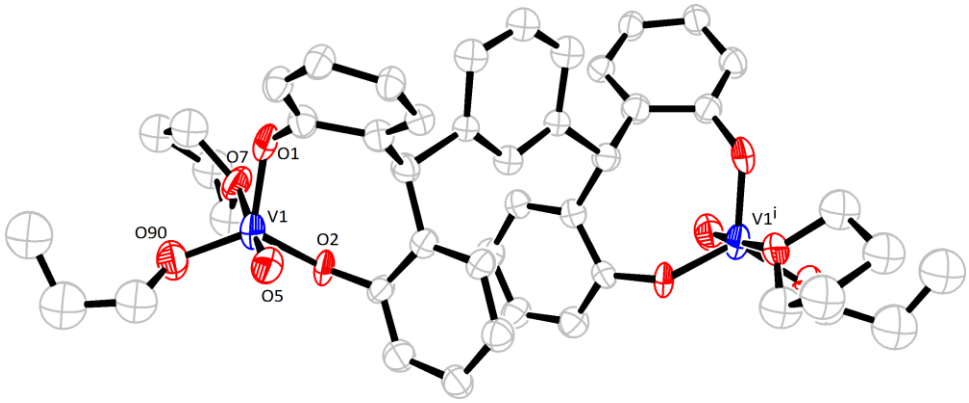


**Figure 2.13.** ORTEP representation of complex **23**, indicating the atom numbering scheme. *Tert*-butyl groups and hydrogen atoms have been removed for clarity. Displacement ellipsoids are drawn at the 20% probability level. Selected bond lengths (Å) and angles (°): O(1)—V(1) 1.816(16), O(2)—V(1) 1.828(13), O(5)—V(1) 1.662(18), O(7)—V(1) 2.205(19), O(90)—V(1) 1.741(17), O(5)—V(1)—O(90) 100.6(8), O(5)—V(1)—O(1) 97.0(8), O(90)—V(1)—O(1) 120.4(7), O(5)—V(1)—O(2) 96.6(7), O(90)—V(1)—O(2) 120.3(8), O(1)—V(1)—O(2) 113.3(6), O(5)—V(1)—O(7) 177.3(7), O(90)—V(1)—O(7) 81.7(7), O(1)—V(1)—O(7) 80.5(7), O(2)—V(1)—O(7) 83.5(6).

### *2.3.2 Polymerisation Screening*

Compounds **21** – **23** and $VO(OEt)Cl_2$, were screened for the polymerisation of ethylene and the co-polymerisation of ethylene/propylene at Mitsui Chemicals, Japan. Each catalyst has been screened for polymerisation using different co-catalysts, dimethylaluminium chloride (DMAC), diethylaluminium chloride (DEAC), ethylaluminium chloride (EADC) or ethylaluminium sesquichloride (EASC) and with addition of ETA (ethyl trichloroacetate).

**Table 2.9**. Selected results for the effect of co-catalyst and ETA on compounds **21** – **23**.[a]

| Run | Pre-Cat | Co-Cat | Al/V | ETA/V | T[c] | Yield[b] | Activity[d] | $M_w$ | $M_n$ | PDI |
|---|---|---|---|---|---|---|---|---|---|---|
| 1 | **21** | DMAC | 5000 | - | 30 | 0.068 | 13,600 | | | |
| 2 | | | 20000 | - | 30 | 0.128 | 25,600 | 2,260,000 | 548,000 | 4.1 |
| 3 | | | 5000 | 5000 | 30 | 0.454 | 90,800 | | | |
| 4 | | | 20000 | 20000 | 30 | 0.534 | 106,800 | 974,000 | 117,000 | 8.3 |
| 5 | | DEAC | 5000 | 5000 | 30 | 0.36 | 72,000 | | | |
| 6 | | | 20000 | 20000 | 10[e] | 0.811 | 486,600 | 73,000 | 25,700 | 2.9 |
| 7 | | EADC | 5000 | 5000 | 30 | 0.304 | 60,800 | | | |
| 8 | | | 20000 | 20000 | 30 | 0.338 | 67,600 | 750,000 | 206,000 | 3.7 |
| 9 | | EASC | 5000 | 5000 | 30 | 0.292 | 58,400 | | | |
| 10 | | | 20000 | 20000 | 30 | 0.358 | 71,600 | 667,000 | 161,000 | 4.2 |
| 11 | **22** | DMAC | 5000 | 5000 | 30 | 0.388 | 77,600 | | | |
| 12 | | | 20000 | 20000 | 30 | 0.45 | 90,000 | 866,000 | 82,000 | 11 |
| 13 | | DEAC | 5000 | 5000 | 30 | 0.323 | 64,600 | | | |
| 14 | | | 20000 | 20000 | 30 | 0.494 | 98,800 | 268,000 | 45,400 | 5.9 |
| 15 | | EADC | 5000 | 5000 | 30 | 0.31 | 62,000 | | | |
| 16 | | | 20000 | 20000 | 30 | 0.472 | 94,400 | 750,000 | 70,400 | 11 |
| 17 | | EASC | 5000 | 5000 | 30 | 0.297 | 59,400 | | | |
| 18 | | | 20000 | 20000 | 30 | 0.438 | 87,600 | 273,000 | 27,800 | 9.8 |
| 19 | **23** | DMAC | 5000 | 5000 | 30 | 0.343 | 68,600 | | | |
| 20 | | | 20000 | 20000 | 30 | 0.423 | 84,600 | 1,068,000 | 121,000 | 8.8 |
| 21 | | DEAC | 5000 | 5000 | 30 | 0.303 | 60,600 | | | |
| 22 | | | 20000 | 20000 | 15[e] | 0.527 | 210,800 | 111,000 | 26,100 | 4.2 |
| 23 | | EADC | 5000 | 5000 | 30 | 0.3232 | 64,640 | | | |
| 24 | | | 20000 | 20000 | 23[e] | 0.538 | 140,348 | 548,000 | 135,546 | 4.0 |
| 25 | | EASC | 5000 | 5000 | 30 | 0.2947 | 58,940 | | | |
| 26 | | | 20000 | 20000 | 22[e] | 0.4951 | 135,027 | 217,000 | 29,600 | 7.3 |
| 27 | **$VO(OEt)Cl_2$** | DMAC | 5000 | 5000 | 30 | 0.368 | 73,600 | | | |
| 28 | | | 20000 | 20000 | 30 | 0.429 | 85,800 | 1,787,000 | 385,000 | 4.6 |
| 29 | | DEAC | 5000 | 5000 | 30 | 0.257 | 51,400 | | | |
| 30 | | | 20000 | 20000 | 30 | 0.343 | 68,600 | 139,000 | 48,600 | 2.9 |
| 31 | | EADC | 5000 | 5000 | 30 | 0.272 | 54,400 | | | |
| 32 | | | 20000 | 20000 | 30 | 0.375 | 75,000 | 711,000 | 188,000 | 3.8 |
| 33 | | EASC | 5000 | 5000 | 30 | 0.317 | 63,400 | | | |
| 34 | | | 20000 | 20000 | 30 | 0.341 | 68,200 | 388,000 | 100,000 | 3.9 |

[a] **Conditions**: 50 °C, 5 mL toluene, 0.01 µmol V, 8 bar ethylene, reaction quenched with $CO_2$; [b]grams, [c]minutes, [d](g/(mmol.hr)), [e]polymerisation was stopped due to consumption of stock ethylene.

From the co-catalyst screening (**Table 2.9**), the addition of ETA to the catalytic system is beneficial; the activity of the runs including an addition of ETA was always higher than with no addition (**Table 2.9**, runs 1 – 4). It should be noted that the runs in which no ETA was added also gave much higher molecular weight polyethylene; possibly due to a larger ethylene to vanadium ratio, as the bulk vanadium is quickly reduced to an inactive oxidation state. The addition of larger equivalence of ETA and co-catalyst lead to improved activity (**Table 2.9**).

**Table 2.10**. Effect of temperature on compounds **21** – **23** and $VO(OEt)Cl_2$.[a]

| Run | Pre-Cat | Co-Cat | T[c] | Time[d] | Yield[b] | Activity[e] | $M_w$ | $M_n$ | PDI | $T_m$[f] |
|---|---|---|---|---|---|---|---|---|---|---|
| 1 | **21** | DMAC | 50 | 30 | 0.422 | 169,000 | 467,000 | 67,300 | 6.9 | 137.2 |
| 2 | | | 80 | 30 | 0.41 | 164,000 | 136,000 | 44,500 | 3.1 | 133.2 |
| 3 | | | 110 | 30 | 0.081 | 32,000 | | | | 134.8 |
| 4 | | | 140 | 30 | - | - | | | | |
| 5 | | DEAC | 50 | 30 | 0.283 | 113,000 | 254,000 | 38,900 | 6.5 | 135.4 |
| 6 | | | 80 | 30 | 0.355 | 142,000 | 136,000 | 20,600 | 6.6 | 136.1 |
| 7 | | | 110 | 30 | 0.07 | 28,000 | | | | 132.2 |
| 8 | | | 140 | 30 | 0.031 | 12,000 | | | | 130.2 |
| 9 | **22** | DMAC | 50 | 30 | 0.357 | 143,000 | 536,000 | 93,900 | 5.7 | 132.0 |
| 10 | | | 80 | 30 | 0.301 | 120,000 | 174,000 | 60,400 | 2.9 | 133.0 |
| 11 | | | 110 | 30 | 0.062 | 24,400 | | | | 135.0 |
| 12 | | | 140 | 30 | - | - | | | | |
| 13 | | DEAC | 50 | 30 | 0.218 | 87,000 | 555,000 | 84,000 | 6.6 | 134.0 |
| 14 | | | 80 | 30 | 0.046 | 18,400 | 367,000 | 34,900 | 10.5 | 133.0 |
| 15 | | | 110 | 30 | - | - | | | | |
| 16 | | | 140 | 30 | - | - | | | | |
| 17 | **23** | DMAC | 50 | 30 | 0.311 | 124,000 | 784,000 | 115,000 | 6.8 | |
| 18 | | | 80 | 30 | 0.402 | 161,000 | 188,000 | 67,800 | 2.8 | |
| 19 | | | 110 | 30 | 0.065 | 26,000 | | | | |
| 20 | | | 140 | 30 | 0.002 | 800 | | | | |
| 21 | | DEAC | 50 | 30 | 0.215 | 86,000 | 672,000 | 88,100 | 7.6 | |
| 22 | | | 80 | 30 | 0.056 | 22,000 | 314,000 | 35,800 | 8.8 | |
| 23 | | | 110 | 30 | 0.02 | 8,000 | | | | |
| 24 | | | 140 | 30 | 0.005 | 2,000 | | | | |
| 25 | **$VO(OEt)Cl_2$** | DMAC | 50 | 30 | 0.374 | 150,000 | 946,000 | 169,000 | 5.6 | 134.7 |
| 26 | | | 80 | 30 | 0.354 | 142,000 | 138,000 | 45,700 | 3.0 | 133.3 |
| 27 | | | 110 | 30 | 0.097 | 39,000 | | | | 134.5 |
| 28 | | | 140 | 30 | - | - | | | | |
| 29 | | DEAC | 50 | 30 | 0.483 | 193,000 | 317,000 | 56,800 | 5.6 | 134.4 |
| 30 | | | 80 | 30 | 0.237 | 95,000 | 209,000 | 27,200 | 7.7 | 134.0 |
| 31 | | | 110 | 30 | 0.087 | 35,000 | | | | 133.8 |
| 32 | | | 140 | 30 | 0.018 | 7,000 | | | | 128.9 |

[a] **Conditions**: 5 mL toluene, 0.005 µmol V, 8 bar ethylene, 20000 equivalents Co-catalyst, 20000 equivalents ETA, reaction quenched with $CO_2$; [b]grams, [c] °C, [d] minutes, [e] (g/(mmol.hr)), [f] °C polymer melting point.

Use of different chloro-aluminium alkyls indicated, for compounds **21**, DEAC was the co-catalyst of choice giving the highest activity and lowest PDI values (**Table 2.9**, run 6); compound **22** gave similar activities for each co-catalyst, whereas surprisingly, given the similarities with **22**, compound **23** gave much higher activities when using the ethyl derived aluminium chloride co-catalysts (see **Table 2.9**, runs 19 – 26). For compounds **21** and **22**, EADC and EASC gave lower activities than DEAC and lower molecular weights than DMAC. The highest molecular weight polyethylene was obtained using DMAC as co-catalyst; however the PDI values were high for each pre-catalyst employed suggesting multiple active species.

Using the conditions established in **Table 2.9** (20,000 equivalence DEAC or DMAC, 20,000 equivalence ETA) compounds **21** – **23** and the reference compound ($VO(OEt)Cl_2$) were screened over a series of temperatures (**Table 2.10**). When DMAC was used as co-catalyst, pre-catalysts **21**, **22** and $VO(OEt)Cl_2$ showed optimal activity at 50 °C, whereas pre-catalyst **23** gave highest activity at 80 °C; each compound also showed lower PDI values at 80 °C. In the runs that DEAC was employed as co-catalyst again 50 °C was the temperature of choice, except for compound **21** where a temperature of 80 °C showed increased activity; the PDI values increased with increasing temperature. The co-polymerisation of propylene and ethylene using compounds **21** – **23** at 50 °C revealed that DMAC was a more efficient co-catalyst than DEAC, achieving an activity greater than 100,000 $gmol^{-1}$ for all pre-catalysts screened, the molecular weight of the polymer produced was also much higher when DMAC was employed. In each run the PDI values were in the range 1.8 – 2.4 and the propylene incorporation between 8 – 10%.

**Table 2.11** Ethylene/propylene co-polymerisations using compounds **21** – **23**.[a]

| Run | Pre-Cat | Co-Cat | Yield[b] | Activity[c] | %C3 | $M_w$ | $M_n$ | PDI | $T_m$[d] |
|---|---|---|---|---|---|---|---|---|---|
| 1 | **21** | DMAC | 0.361 | 144,000 | 8.5 | 325,000 | 134,000 | 2.4 | 90.4 |
| 2 | | DEAC | 0.206 | 82,400 | 8.3 | 88,800 | 46,400 | 1.9 | 93.4 |
| 3 | **22** | DMAC | 0.338 | 135,000 | 8.2 | 291,000 | 123,000 | 2.4 | 90.9 |
| 4 | | DEAC | 0.116 | 46,400 | 7.6 | 98,000 | 43,200 | 2.3 | 95.0 |
| 5 | **23** | DMAC | 0.274 | 110,000 | 8.2 | 311,000 | 137,000 | 2.3 | 90.9 |
| 6 | | DEAC | 0.189 | 75,600 | 7.7 | 99,000 | 53,000 | 1.9 | 93.6 |
| 7 | **$VO(OEt)Cl_2$** | DMAC | 0.391 | 156,000 | 10.0 | 241,000 | 86,600 | 2.8 | 88.9 |
| 8 | | DEAC | 0.191 | 76,400 | 9.8 | 75,700 | 42,700 | 1.8 | 90.0 |

[a] **Conditions**: 5 mL toluene, 30 minutes, 50 °C, 0.005 µmol V, 4 bar ethylene, 0.4 MPa propylene, 20000 equivalents co-catalyst, 20000 equivalents ETA, reaction quenched with $CO_2$; [b]grams, [c](g/(mmol.hr)), [d] °C polymer melting point.

## 2.4 Results and Discussion – *p-tert*-Butylcalix[6/8]arene Vanadium Compounds

### *2.4.1 Synthesis and Structures*

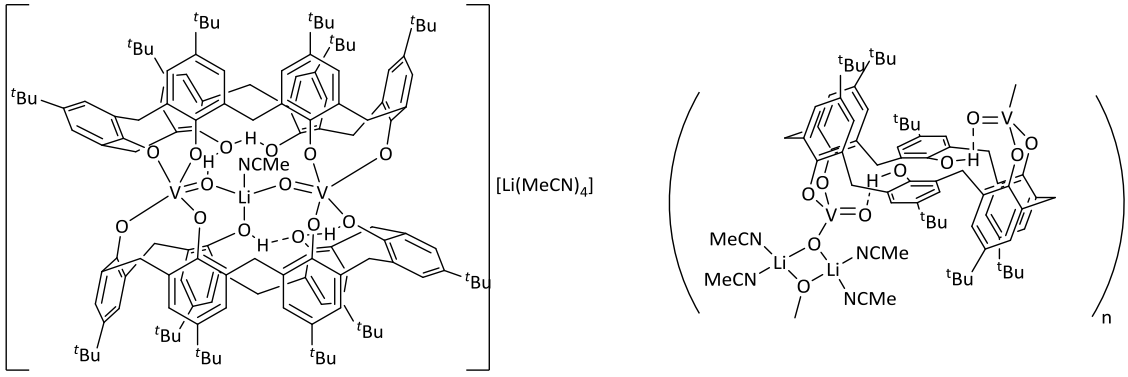


**24** **25**

**Chart 2.8** Vanadium *p-tert*-butylcalix[6]arene compounds synthesized, screened and reported in this chapter.

The ligands *p-tert*-butylcalix[6]arene and *p-tert*-butylcalix[8]arene were synthesized following the literature procedure.[33] The alkali/vanadium precursors, [MVO(O*t*-Bu)$_4$], used in the following reactions were synthesized by an adaptation of a procedure described by Wilkinson and co-workers;[34] vanadium oxytrichloride and four equivalents of MO*t*-Bu were stirred in diethylether (or THF) at –78 °C for 12 h, prior to the addition of the *p-tert*-butylcalix[6/8]arene. Compound **24** was synthesized by treatment of *p-tert*-butylcalix[6]arene with 1 equivalent of [LiVO(O*t*-Bu)$_4$], generated *in situ*, in refluxing toluene. Green blocks of compound **24**, suitable for single crystal X-ray diffraction, were isolated from a saturated acetonitrile solution. On a number of repeated syntheses a small amount (<10%) of yellow needles were found amongst the green blocks of compound **24**. The yellow needles were subjected to single crystal X-ray diffraction studies, revealing the structure of compound **25**, however due to the low yield and contamination with compound **24**, the full characterisation could not be completed. Attempts to synthesize compound **25** as the major product, by using a 2 : 1 ratio of LiVO(OtBu)$_4$ to calixarene, were unsuccessful and resulted in a mixture of products that were not separable. A second solvate of compound **24** was also isolated (**24**′) which only differs by the number of molecules of crystallisation.

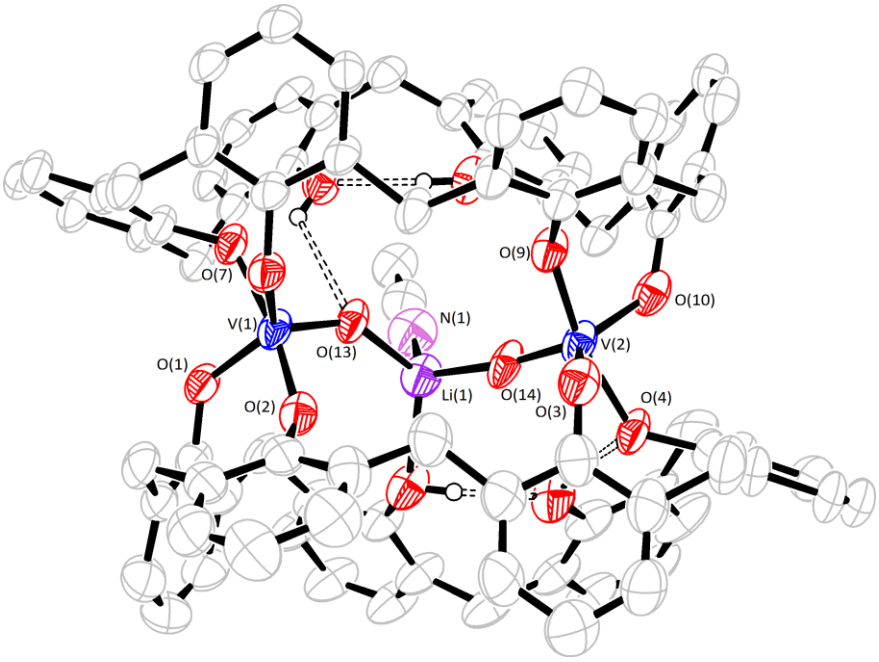


**Figure 2.14** View of compound **24**.8$CH_3CN$. Displacement Hydrogen atoms, other than those undergoing hydrogen bonding, *tert*-butyl groups, minor disordered components and the $Li(MeCN)_4$ counter-ion have been removed for clarity. Selected bond lengths (Å) and angles (°): V(1)—O(1) 1.861(4), V(1)—O(2) 1.805(5), V(1)—O(13) 1.606(4), V(1)—O(7) 1.916(4), V(1)—O(8) 1.870(4), Li(1)—O(6) 2.078(12), Li(1)—O(13) 1.948(11), O(1)—V(1)—O(13) 113.29(19), O(2)—V(1)—O(7) 168.17(18), V(1)—O(1)—C(1) 126.3(4), V(1)—O(2)—C(12) 144.9(4), V(1)—O(7)—C(67) 134.3(4), V(1)—O(8)—C(78) 125.6(4), V(1)—O(13)—Li(1) 143.1(4).

The single crystal X-ray diffraction study of compound **24** revealed two *p-tert*-butylcalix[6]arene ligands bound to two vanadyl distorted square-based pyramidal centres. Each vanadium centre forms two oxygen—vanadium bonds with each calixarene, the remaining two oxygen atoms on each calixarene are still protonated and form hydrogen bonds. The vanadyl oxygen atoms are at the apex of the square-based pyramids (O(13) and O(14)) and bridge to each other through a 4-coordinate lithium cation. The coordination sphere of the lithium cation is completed by a protonated phenoxy oxygen atom and a solvent molecule (acetonitrile). To balance the charge a second lithium cation bound to 4 acetonitrile molecules is found within the cavity of one of the calixarene ligands. The molecular structure of complex **24** is presented in **Figure 2.14**, and selected bond length and angles are given in the legend. Compound **24** was also characterised using elemental analysis, mass spectrometry, IR and NMR techniques. The $^1H$ NMR spectrum features two broad singlets at 10.54 (1H) and 6.74 (3H) ppm which are assigned to the hydrogen bonded protons. There are also a number of doublets for the methylene bridges, aromatic protons and *tert*-butyl groups due to the break in symmetry from the parent calixarene.

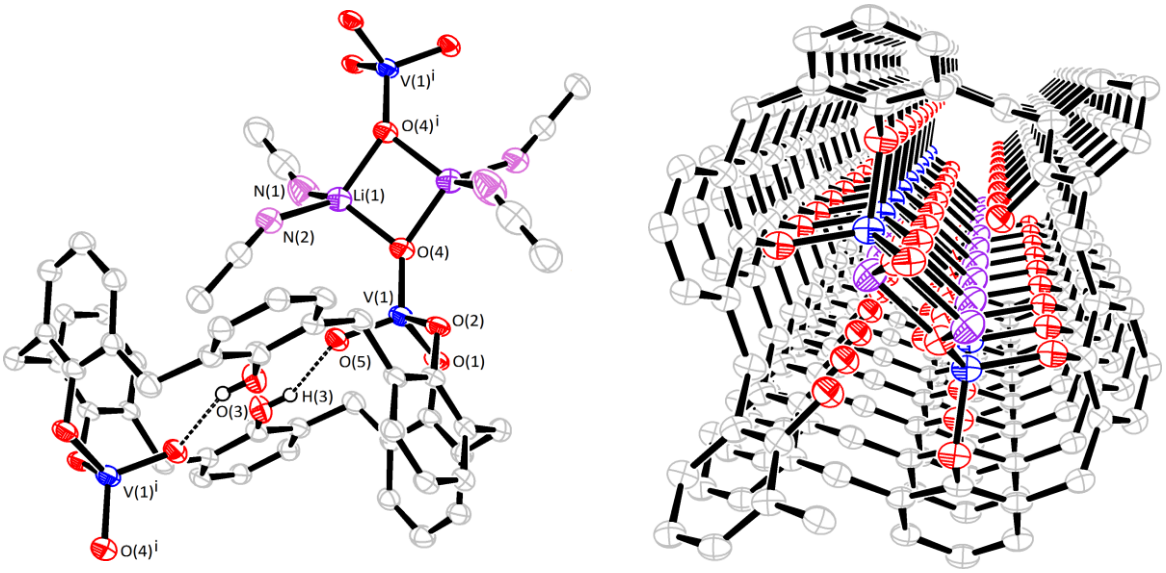


**Figure 2.15** Views of 1D polymer compound **25**.$CH_3CN$. Hydrogen atoms, other than those undergoing hydrogen bonding, *tert*-butyl groups and minor disordered components have been removed for clarity. Selected bond lengths (Å) and angles (°): V(1)—O(1) 1.814(3), V(1)—O(2) 1.816(3), V(1)—O(4) 1.652(3), V(1)—O(5) 1.612(3), Li(1)—O(4) 1.973(8), Li(1B)—O(4) 1.972(8), O(4)—V(1)—O(5) 111.55(15), V(1)—O(1)—C(1) 120.3(2), V(1)—O(2)—C(12) 124.2(2), V(1)—O(4)—Li(1) 141.9(3), V(1)—O(4)—Li(1B) 128.5(3).

The molecular structure of complex **25**, formed amongst crystals of **24** but with much lower yield (<10%), revealed a 1D polymeric structure. A single calix[6]arene ligand is present with a chair conformation consisting of two up, two flat and two down phenolates. The 'up' and 'down' phenolate oxygens each bind to a 4-coordinate vanadyl centre in tetrahedral geometry, which in turn is linked to a $Li_2O_2$ diamond unit and then onto the next vanadium centre completing the polymer chain. Each lithium centre is also bound to two acetonitrile solvent molecules. The two 'flat' phenolates are still protonated and undergo hydrogen bonding with the vanadyl oxygen. Further characterisation of compound **25** was prevented by the low yield and the presence of large excesses of compound **24**.

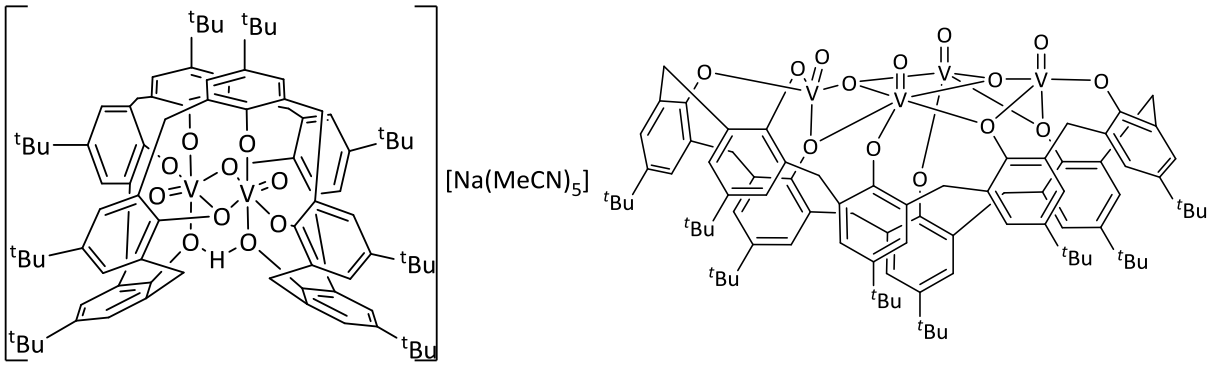


**26** **27**

**Chart 2.9** Vanadium *p-tert*-butylcalix[8]arene compounds synthesized and screened in this chapter.

Compound **26** was synthesized in a similar fashion to compound **24**; *p-tert*-butylcalix[8]arene was treated with two equivalents of [NaVO(O*t*-Bu)$_3$] to give compound **26** as a dark brown solid. Block crystals suitable for single crystal X-ray diffraction were grown from a saturated acetonitrile solution. The molecular structure is presented in **Figure 2.16**, and selected bond lengths and angles in the legend. Pedersen and co-workers and Limberg and co-workers have previously prepared ammonium and phosphonium salts, respectively, that are similar to compound **26**.[35] There are two vanadium centres in the internal cavities of the saddle-shaped calix[8]arene. The vanadyl centres are octahedral and bridged through two oxygen atoms of the calixarene, and are in *trans* orientation to each other. One phenolic oxygen on the calix[8]arene scaffold remains protonated and forms a hydrogen bond to another phenolic oxygen. A sodium counter-ion is present in the unit cell and is solvated by five acetonitrile molecules. Compound **26** has also been characterised by $^1$H NMR, IR, elemental analysis and mass spectrometry. The $^1$H NMR spectrum shows a broad singlet at 15.49 ppm which is assigned to the bridging hydrogen, a similar structure characterised by Gibson *et al*, also assigned a similar upfield proton as the bridging hydrogen.[36]

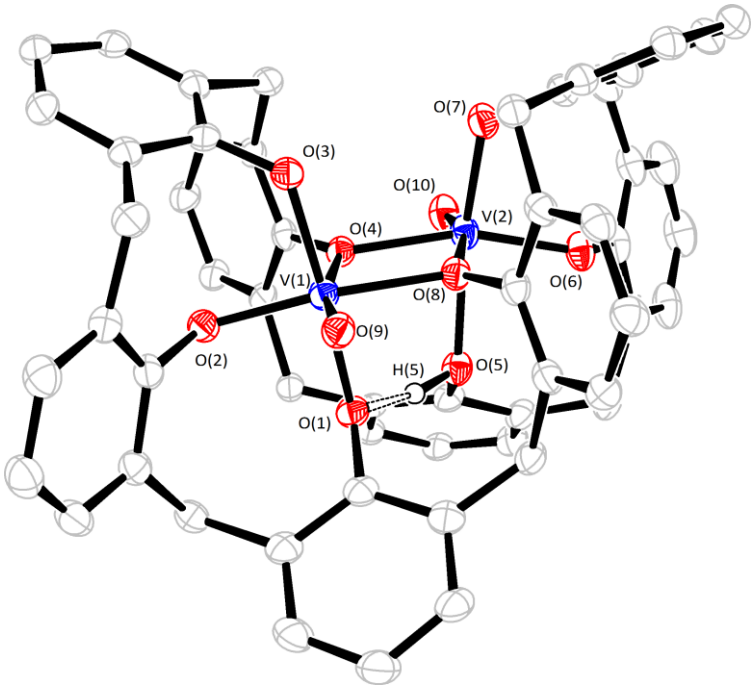


**Figure 2.16.** View of compound **26**.4$CH_3CN$. Hydrogen atoms, other than those undergoing hydrogen bonding, *tert*-butyl groups, the sodium counter-ion and minor disordered components have been removed for clarity. Selected bond lengths (Å) and angles (°): V(1)—O(1) 2.0148(19), V(1)—O(2) 1.8452(19), V(1)—O(3) 1.855(2), V(1)—O(4) 2.181(2), V(1)—O(8) 1.9916(19), V(1)—O(9) 1.589(2), V(1)···V(2)[a] 3.3695(7), O(1)—V(1)—O(3) 163.56(9), O(4)—V(1)—O(8) 72.11(7), O(4)—V(1)—O(9) 165.81(9), V(1)—O(4)—V(2) 108.33(9), V(1)—O(8)—V(2) 107.28(8).

Treatment of *p-tert*-butylcalix[8]arene and four equivalents of [VO(O*t*-Bu)$_3$] (generated *in-situ* from [$VOCl_3$] and 3KO*t*Bu) afforded the green complex, **27**. Two solvates, after crystallisation of compound **27** from either acetonitrile or dichloromethane were studied using single crystal X-ray diffraction. Both solvates **27**.3MeCN and **27**.3$CH_2Cl_2$, have very similar structures and only differ significantly by solvent molecules in the unit cell (see **Table 2.12**), and as such only the dichloromethane solvate is discussed. The *p-tert*-butylcalix[8]arene ligand is fully deprotonated and adopts a shallow saddle-shaped conformation (**Figure 2.17**), the phenolate oxygens are bound to four *penta*-coordinated vanadyl centres that are arranged in a ladder-like configuration. In both molecules, the geometry around each vanadium centre is square-pyramidal. Diffraction data for both solvates of **27** were collected using synchrotron radiation.

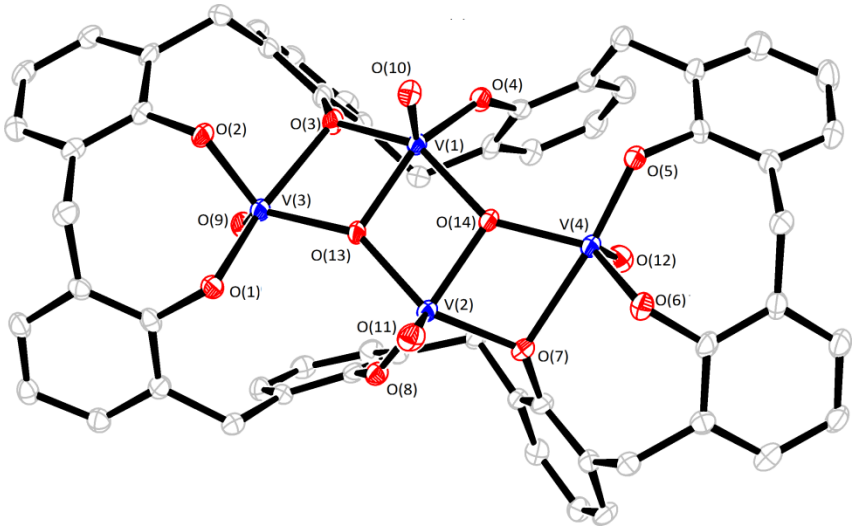


**Figure 2.17** View of compound **27**.3$CH_2Cl_2$. Hydrogen atoms have been omitted for clarity. Selected bond lengths (Å) and angles (°) are listed in **Table 2.12**.

**Table 2.12** Selected structural data for the solvates **27**.3MeCN and **27**.3$CH_2Cl_2$**.**

| Bond lengths (Å)/Angle ($^{O}$) | **27**.3MeCN | **27**.3$CH_2Cl_2$ |
|---|---|---|
| V(1)-O(3) | 1.914(5) | 1.914(3) |
| V(1)-O(4) | 1.776(6) | 1.762(3) |
| V(1)-O(10) | 1.572(6) | 1.573(3) |
| V(1)-O(13) | 1.946(6) | 1.939(3) |
| V(1)-O(14) | 1.931(5) | 1.949(3) |
| V(3)-O(1) | 1.799(6) | 1.798(3) |
| V(3)-O(2) | 1.786(6) | 1.788(2) |
| V(3)-O(3) | 2.214(6) | 2.200(3) |
| V(3)-O(9) | 1.562(6) | 1.580(3) |
| V(3)-O(13) | 1.878(5) | 1.884(3) |
| | | |
| V(1)-O(3)-V(3) | 98.7(2) | 97.56(12) |
| V(1)-O(13)-V(3) | 110.3(3) | 108.36(14) |
| V(1)-O(13)-V(2) | 103.2(2) | 104.62(13) |
| V(1)-O(14)-V(4) | 145.2(3) | 143.97(17) |

### *2.4.2 Polymerisation Screening*

Compounds **24**, **26** and **27** were screened for polymerisation of ethylene and co-polymerisation of ethylene/propylene using dimethylaluminium chloride (DMAC) or diethylaluminium chloride (DEAC) as co-catalyst at Mitsui Chemicals, Japan. Temperature screening of compound **24**, **26** and **27** revealed, when using DMAC, compounds **24** and **26** show optimum polymerisation activity at 80 °C (**Table 2.13**, runs 1 – 4 and runs 10 – 14); compound **27** is more active at 50 °C (**Table 2.13**, run 19). When using temperatures above 80 °C the activity of each catalyst depreciated dramatically. The catalysis, when DMAC is employed, is however more controlled at temperatures higher than 50 °C for each pre-catalyst; the PDI values obtained were in the range, 2.1 – 3.2, however the molecular weight of the resulting polymers was higher at 50 °C (600,000 – 800,000 $gmol^{-1}$) than at 80 °C (100,000 – 160,000 $gmol^{-1}$). Use of DEAC as co-catalyst was detrimental to the resulting activity and thermal stability.

**Table 2.13** Selected results for the effect of co-catalyst and ETA on compounds **24**, **26** and **27**.[a]

| Run | Pre-Cat | Co-Cat | T[c] | Yield[b] | Activity[d] | $M_w$ | $M_n$ | PDI | $T_m$[e] |
|---|---|---|---|---|---|---|---|---|---|
| 1 | **24** | DMAC | 50 | 0.306 | 122,000 | 641,000 | 97,700 | 6.6 | 134.3 |
| 2 | | | 80 | 0.506 | 202,000 | 105,000 | 40,200 | 2.6 | 133.9 |
| 3 | | | 110 | 0.171 | 68,500 | 30,200 | 14,400 | 2.1 | 133.9 |
| 4 | | | 140 | 0.003 | 1,160 | - | - | - | 130.1 |
| 5 | | DEAC | 50 | 0.256 | 102,000 | 490,000 | 79,000 | 6.2 | 130.7 |
| 6 | | | 80 | 0.107 | 43,000 | 835,000 | 40,600 | 20.6 | 131.6 |
| 7 | | | 110 | 0.039 | 15,600 | 198,000 | 15,300 | 13.0 | 133.2 |
| 8 | | | 140 | 0.007 | 2,800 | - | - | - | 130.3 |
| 10 | **26** | DMAC | 50 | 0.331 | 132,000 | 789,000 | 176,000 | 4.5 | 134.5 |
| 12 | | | 80 | 0.408 | 163,000 | 133,000 | 55,600 | 2.4 | 132.9 |
| 13 | | | 110 | 0.067 | 26,800 | 30,800 | 14,500 | 2.1 | 132.8 |
| 14 | | | 140 | - | - | - | - | - | - |
| 15 | | DEAC | 50 | 0.184 | 73,600 | 554,000 | 115,000 | 4.8 | 131.6 |
| 16 | | | 80 | 0.015 | 6,000 | 316,000 | 12,300 | 25.7 | 132.0 |
| 17 | | | 110 | 0.011 | 4,400 | 112,000 | 5,710 | 19.5 | 130.4 |
| 18 | | | 140 | - | - | - | - | - | - |
| 19 | **27** | DMAC | 50 | 0.251 | 101,000 | 752,000 | 118,000 | 6.4 | 136.5 |
| 20 | | | 80 | 0.202 | 80,800 | 158,000 | 67,700 | 2.3 | 136.9 |
| 21 | | | 110 | 0.021 | 8,240 | 27,300 | 8,550 | 3.2 | 132.8 |
| 22 | | | 140 | - | - | - | - | - | - |
| 23 | | DEAC | 50 | 0.149 | 59,400 | 663,000 | 126,000 | 5.3 | 132.1 |
| 24 | | | 80 | 0.021 | 8,480 | 375,000 | 37,600 | 10.0 | 133.0 |
| 25 | | | 110 | - | - | - | - | - | |
| 26 | | | 140 | - | - | - | - | - | |

[a] **Conditions**: 30 minutes, 5 mL toluene, 0.005 µmol V, 0.8 MPa ethylene, 20000 equivalents co-catalyst, 20000 equivalents ETA, reaction quenched with $CO_2$; [b] grams, [c] °C, [d](g/(mmol.hr)), [e] °C polymer melting point.

Compounds **24**, **26** and **27** were also subjected to co-polymerisation screening of ethylene/propylene with either DEAC or DMAC as co-catalyst at 50 °C (see **Table 2.14**). Again DMAC was the co-catalyst of choice in terms of activity and polymer chain length with all three catalysts when compared with DEAC, however the catalytic system is more controlled, as indicated by the PDI values (**Table 2.14**, 1.9 – 2.0, for DEAC, 2.2 – 2.9, for DMAC). Compound **27** gave the highest polymer molecular weight (321,000 $gmol^{-1}$), whilst compounds **24** and **26** gave similar molecular weight polymer (≈195,000 $gmol^{-1}$). The incorporation of propylene in the polymer chain is similar for all three pre-catalysts (7.8 – 10.9%) as are the melting points of the polymers (89.8 – 93.7 °C).

**Table 2.14** Ethylene/propylene co-polymerisations using compounds **24**, **26** and **27**.[a]

| Run | Pre-Cat | Co-Cat | Yield[b] | Activity[c] | %C3 | $M_w$ | $M_n$ | PDI | $T_m$[d] |
|---|---|---|---|---|---|---|---|---|---|
| 1 | **24** | DMAC | 0.268 | 107,000 | 8.2 | 195,000 | 90,200 | 2.2 | 92.3 |
| 2 | | DEAC | 0.206 | 82,400 | 9.8 | 63,600 | 32,300 | 2.0 | 89.8 |
| 3 | **26** | DMAC | 0.163 | 65,100 | 10.9 | 198,000 | 69,500 | 2.9 | 90.3 |
| 4 | | DEAC | 0.070 | 28,000 | 8.2 | 105,000 | 53,000 | 2.0 | 93.7 |
| 5 | **27** | DMAC | 0.105 | 41,800 | 7.8 | 321,000 | 122,000 | 2.6 | 92.9 |
| 6 | | DEAC | 0.071 | 28,200 | 7.8 | 88,700 | 46,800 | 1.9 | 93.7 |

[a] **Conditions**: 5 mL toluene, 30 minutes, 50 °C, 0.005 µmol V, 0.4 MPa ethylene, 0.4 MPa propylene, 20000 equivalents co-catalyst, 20000 equivalents ETA, reaction quenched with $CO_2$; [b] grams, [c] (g/(mmol.hr)), [d] °C polymer melting point.

## 2.5 Conclusions

A number of novel vanadium compounds based on phenoxyimine, di/tetraphenolate and calix[6/8]arene ligand scaffolds have been synthesised and screened for the polymerisation of ethylene. The phenoxyimine vanadium (III) dichloride compounds **1** – **9**, when used in combination with ETA and DMAC, were highly active for the polymerisation of ethylene (1,000 – 10,000 g/mmol.hr.bar). Comparison of the bimetallic compound **7** with monometallic derivatives suggested a co-operative effect. Supporting vanadium complexes **4** and **6** upon silica (forming **S-4** and **S-6**) was detrimental to the polymerisation activity.

We have prepared vanadium Schiff base catalysts, complexes **10** – **20**, using vanadyl tripropoxide/trichloride as precursors. The reaction of 2 equivalents of ligands, **L6H** – **L13H**, with vanadium oxytripropoxide resulted in the formation of vanadyl bis(chelates) with the reduction of the vanadium metal centre from +5 to +4. Mechanistic investigations by Hanson and co-workers suggest alcohol oxidation of the propoxide ligand with the concomitant reduction of the vanadium centre is occurring.[24] The attempted synthesis of a monoligated phenoxyimine, after treatment vanadium oxytripropoxide, resulted in the formation of the oxo bridged compound **16**, when **L9H** was utilized, and the dioxo compound **20**, from **L14H**, which are related as compound **16** is essentially the dimerization of a dioxo compound. The fixed third position of compound **20** seems to prevent dimerization. Screening of the vanadyl bis(chelates) resulted in activities that were somewhat similar.

Unlike the vanadyl bis(chelates), treatment of di/tetraphenolate ligand **L15H$_2$ – L17H$_4$** with vanadium oxytripropoxide, did not lead to the reduction of the vanadium centre. Whilst the tetraphenolate compound **22**, forms a monomeric bimetallic structure in the solid state, single crystal X-ray diffraction studies of the diphenolate compound **21**, revealed a dimeric structure with bridging μ-O$^n$Pr ligands. The presence of THF in the fifth co-ordination site seems to inhibit the formation of the dimer of compound **22**. Screening of compounds **21** – **23** for the polymerisation of ethylene revealed that higher additions of ETA and co-catalyst lead to higher activity; however the resulting polymer chain length is much lower. Compounds **21** – **23** exhibited different activities depending on the co-catalyst employed, compound **21** was found to be exceptionally active when DEAC was utilized (486,000 g/mmol.hr); the polymer produced also possessed the lowest PDI values of the catalytic systems (2.85). Whilst compound **23** gave highest activities when ethyl aluminium chloride co-catalysts were employed, compound **22** gave similar activities regardless of co-catalyst. The PDI values for the polymer produced were often high for the pre-catalysts employed suggesting multiple active species. The reference compound (VO(OEt)Cl$_2$) gave slightly lower activities than the pre-catalysts **21** – **23**.

When DMAC was employed, optimal activity was achieved at 50 °C using compounds **21**, **22** and $VO(OEt)Cl_2$, whereas compound **23** was more active at 80 °C. Compounds **21 – 23** were highly active for the co-polymerisation of ethylene and propylene achieving activities greater than 100,000 $gmol^{-1}$ for each pre-catalyst with low PDI values (1.8 – 2.4) and propylene incorporation between 8 – 10%.

The treatment of *p-tert*-butylcalix[6]arene with $LiVO(OtBu)_4$ led to the isolation of two compounds, complex **24** (major) and **25** (minor). Compound **25** is presumably formed due to a higher than expected $LiVO(OtBu)_4$ to calixarene ratio, although steps to isolate this compound as the major product were unsuccessful. Whilst, compound **26** was synthesized from the reaction between *p-tert*-butylcalix[8]arene and $NaVO(OtBu)_4$, use of $VO(OtBu)_3$ led to the isolation of compound **27**. Screening of compounds **24**, **26** and **27** using 20,000 equivalents of DMAC gave highly active catalysts for the polymerisation of ethylene (≈80,000 – 200,000 g/mmol.hr, at 80°C) and co-polymerisation of ethylene/propylene (≈40,000 – 110,000 g/mmol.hr, at 50 °C).

## 2.6 References


[1] H. Hagen, J. Boersma, G. van Koten, *Chem. Soc. Rev.,* **2002**, *31*, 357.

[2] S. Gambarotta, *Coord. Chem. Rev.,* **2003**, *237*, 229.

[3] Y. Onishi, S. Katao, M. Fujiki, K. Nomura, *Organometallics,* **2008**, *27*, 2590.

[4] J.-Q. Wu, L. Pan, N.-H. Hu, Y.-S. Li, *Organometallics,* **2008**, *27*, 3840.

[5] C. Redshaw, *Dalton Trans.,* **2010**, *39*, 5595.

[6] K. Nomura, S. Zhang, *Chem. Rev.,* **2010**, *111*, 2342.

[7] J.-Q. Wu, Y.-S. Li, *Coord. Chem. Rev.,* **2011**, *255*, 2303.

[8] Y. Nakayama, H. Bando, Y. Sonobe, Y. Suzuki, T. Fujita, *Chem. Lett.,* **2003**, *32*, 766.

[9] Y. Nakayama, H. Bando, Y. Sonobe, T. Fujita, *J. Mol. Catal. A: Chem.,* **2004**, *213*, 141.

[10] D. L. Christman, G. I. Keim, *Macromolecules,* **1968**, *1*, 358.

[11] Y. Doi, S. Suzuki, K. Soga, *Macromolecules,* **1986**, *19*, 2896.

[12] E. Adisson, A. Deffieux, M. Fontanille, K. Bujadoux, *J. Polym. Sci., Part A: Polym. Chem.,* **1994**, *32*, 1033.

[13] M. Delferro, T. J. Marks, *Chem. Rev.,* **2011**, *111*, 2450.

[14] J. Du, M. Yang, J. Wang, *J. Phys. Chem. A,* **2011**, *115*, 10259.

[15] D. J. Doyle, V. C. Gibson, A. J. P. White, *Dalton Trans.,* **2007**, 358.

[16] L. Clowes (2011). *Group V pro-catalysts for the polymerisation of ethylene and ε-caprolactone*. University of East Anglia.

[17] L. Clowes, M. Walton, C. Redshaw, Y. Chao, A. Walton, P. Elo, V. Sumerin, D. L. Hughes, *Catal. Sci. Technol.,* **2013**, *3*, 152.

[18] R. D. McIntosh, S. M. Taylor, S. Sanz, C. M. Beavers, S. J. Teat, E. K. Brechin, S. J. Dalgarno, *Dalton Trans.,* **2011**, *40*, 12265.

[19] C. Redshaw, M. Rowan, D. M. Homden, M. R. J. Elsegood, T. Yamato, C. Pérez-Casas, *Chem. Eur. J.,* **2007**, *13*, 10129.

[20] S. Singh, H. W. Roesky, *Dalton Trans.,* **2007**, 1360.

[21] Y. Maeda, N. Kakiuchi, S. Matsumura, T. Nishimura, T. Kawamura, S. Uemura, *J. Org. Chem.,* **2002**, *67*, 6718.

[22] S. Velusamy, T. Punniyamurthy, *Org. Lett.,* **2003**, *6*, 217.

[23] S. K. Hanson, R. T. Baker, J. C. Gordon, B. L. Scott, L. A. P. Silks, D. L. Thorn, *J. Am. Chem. Soc.,* **2010**, *132*, 17804.

[24] S. K. Hanson, R. Wu, L. A. P. Silks, *Org. Lett.,* **2011**, *13*, 1908.

[25] G. Zhang, B. L. Scott, R. Wu, L. A. P. Silks, S. K. Hanson, *Inorg. Chem.,* **2012**, *51*, 7354.

[26] B. N. Wigington, M. L. Drummond, T. R. Cundari, D. L. Thorn, S. K. Hanson, S. L. Scott, *Chem. Eur. J.,* **2012**, *18*, 14981.

[27] C. Redshaw, L. Warford, S. H. Dale, M. R. J. Elsegood, *Chem. Commun.,* **2004**, 1954.

[28] G. Asgedom, A. Sreedhara, J. Kivikoski, E. Kolehmainen, C. P. Rao, *J. Chem. Soc. Dalton Trans.,* **1996**, 93.

[29] C. Redshaw, M. A. Rowan, L. Warford, D. M. Homden, A. Arbaoui, M. R. J. Elsegood, S. H. Dale, T. Yamato, C. P. Casas, S. Matsui, S. Matsuura, *Chem. Eur. J.,* **2007**, *13*, 1090.

[30] W. Wang, K. Nomura, *Macromolecules,* **2005**, *38*, 5905.

[31] H. N. Cheng, D. A. Smith, *Macromolecules,* **1986**, *19*, 2065.

[32] L. Tang, E. P. Wasserman, D. R. Neithamer, R. D. Krystosek, Y. Cheng, P. C. Price, Y. He, T. J. Emge, *Macromolecules,* **2008**, *41*, 7306.

[33] D. Parker, *Macrocycle Synthesis: A Practical Approach*, Oxford University Press, Incorporated, **1996**.

[34] M. Bochmann, G. Wilkinson, G. B. Young, M. B. Hursthouse, K. M. A. Malik, *J. Chem. Soc. Dalton Trans.,* **1980**, 1863.

[35] G. E. Hofmeister, F. E. Hahn, S. F. Pedersen, *J. Am. Chem. Soc.,* **1989**, *111*, 2318.

[36] V. C. Gibson, C. Redshaw, M. R. J. Elsegood, *J. Chem. Soc., Dalton Trans.,* **2001**, 767.

# Chapter 3 – Niobium and Tantalum Pre-Catalysts

## 3.1 Introduction

In **chapter 2**, we explored the activity of a number of Schiff base vanadium complexes for the polymerisation of ethylene. The high activity achieved by the vanadium based catalysts led us to use the heavier congeners of group 5 with similar ligands as well as imidazole and oxazole type backbones (**Chart 3.1**). Ligands that are identical in chapter 2 have been renumbered in this section, the numbered compounds are sequential throughout to avoid confusion. The treatment of imidazole/oxazole ligands (**L20H** and **L21H**) with $NbCl_5$, $NbOCl_3$(dme), $TaCl_5$ or $TaOCl_3$(dme) in refluxing toluene led to the isolation of compounds **28** – **34**, while treatment of **L22** with $NbCl_4$(THF) in tetrahydrofuran led to the isolation of compound **35**. The structurally related known compounds (**Chart 3.2, 36** – **38**) featuring α-diimines and bis(imino)pyridine ligand scaffolds have been synthesized to compare the activity of novel compounds, while the reactivity of 2-acetyl-6-iminopyridine with $NbOCl_3$(dme) in THF is also explored (Compound **39**). The reaction between **L25** – **L29H** and $NbCl_5$ and $TaCl_5$ in refluxing toluene led to the isolation of compounds **40** – **48** as well as a number of unexpected products (compounds **49** – **50**). The molecular structures of pre-catalysts **28**, **29**, **30**, **33**, **39**, **40**, **41**, **42**, **44**, **49** and **50** are presented with structural considerations. Compounds **28** – **50** have been screened for ethylene polymerisation activity and the results discussed herein. Compounds **28** – **30** and **32** – **34** were investigated in collaboration with Dr Lucy Clowes.[1] The results described in this chapter have been published.[2]

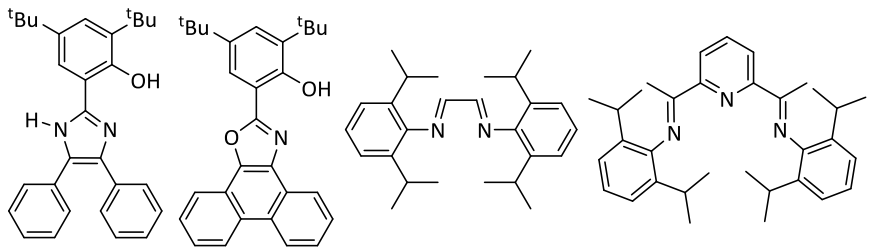


**L20H** **L21H** **L22** **L23**

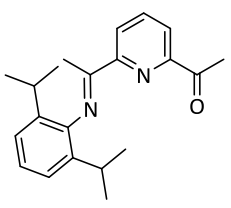


**L24**

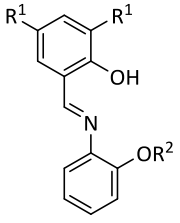


**L25H** $R^1$ = $^t$Bu $R^2$ = Ph
**L26H** $R^1$ = $^t$Bu $R^2$ = Me
**L27H** $R^1$ = Cl $R^2$ = Ph
**L28H** $R^1$ = Cl $R^2$ = Me
**L29H** $R^1$ = $^t$Bu $R^2$ = $CF_3$

**Chart 3.1** Ligands (**L20H** – **L29H**) utilized in this study.

## 3.2 Results and Discussion

### *3.2.1 Synthesis and structures*

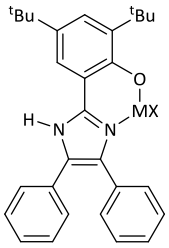

**28** MX = $NbCl_4$
**29** MX = $NbOCl_2$.NCMe
**30** MX = $TaCl_4$
**31** MX = $TaOCl_2$.NCMe

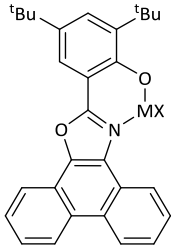

**32** MX = $NbCl_4$
**33** MX = $NbOCl_2$.NCMe
**34** MX = $TaCl_4$

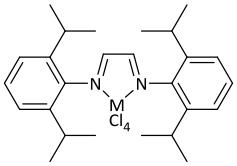

**35** M = Nb
**36** M = Ta

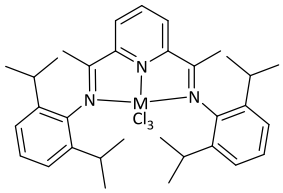

**37** M = Nb
**38** M = Ta

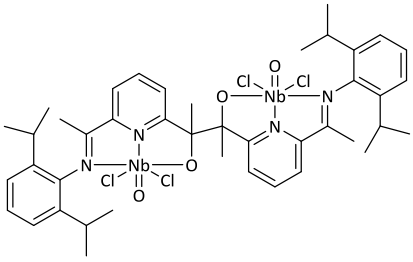

**39**

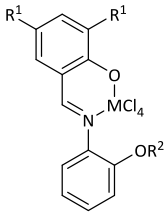

**40** $R^1$ = $^t$Bu, $R^2$ = Ph, M = Nb
**41** $R^1$ = $^t$Bu, $R^2$ = Ph, M = Ta
**42** $R^1$ = $^t$Bu, $R^2$ = Me, M = Nb
**43** $R^1$ = $^t$Bu, $R^2$ = Me, M = Ta
**44** $R^1$ = Cl, $R^2$ = Ph, M = Nb
**45** $R^1$ = Cl, $R^2$ = Ph, M = Ta
**46** $R^1$ = Cl, $R^2$ = Me, M = Nb
**47** $R^1$ = Cl, $R^2$ = Me, M = Ta
**48** $R^1$ = Cl, $R^2$ = $CF_3$, M = Nb

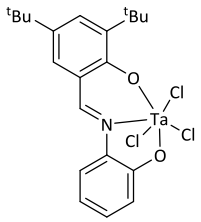

**49**

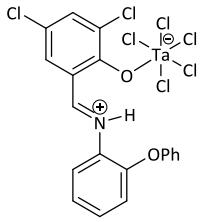

**50**

**Chart 3.2** Complexes synthesized in this section.

Ligands **L20H** and **L21H** were synthesized from the treatment of 3,5-di-*tert*-butyl-2-hydroxybenzaldehyde and either benzyl (1,2-diphenylethane-1,2-dione) or 9,10-phenanthrenequinone in glacial acetic acid in the presence of ammonium acetate and confirmed by comparison to the published characterisation data.[3] The treatment of **L20H** and **L21H** with niobium or tantalum pentachlorides/oxytrichlorides in refluxing toluene led to the isolation of **28** – **31** and **32** – **34** (see **Chart 3.2**). Single crystals of compounds **28** – **30** and **33** suitable for X-ray diffraction studies were grown from saturated acetonitrile solutions.

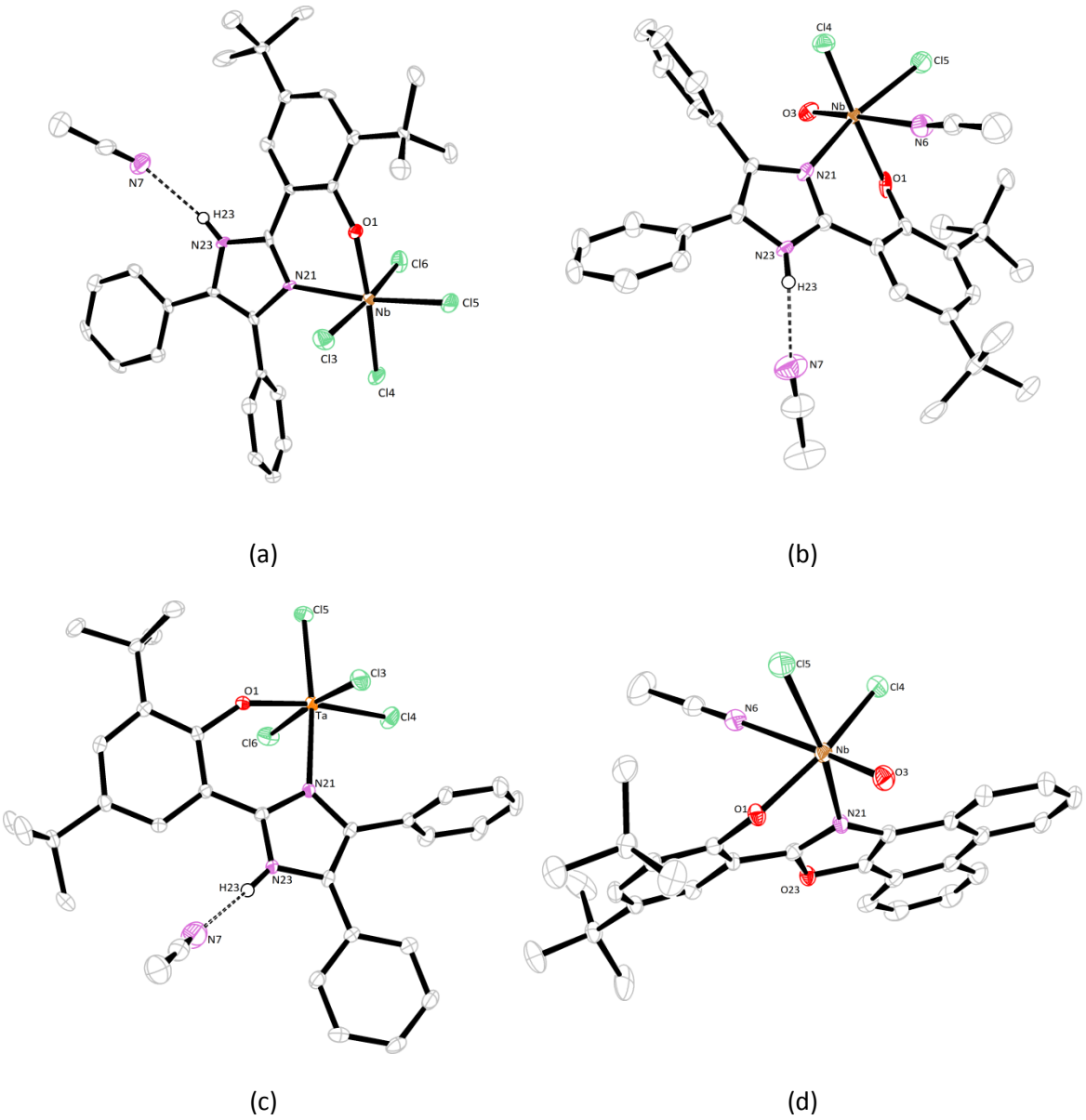


**Figure 3.1** ORTEP representations of **28** (a), **29** (b), **30** (c) and **33** (d) indicating the atom numbering scheme. Hydrogen atoms are removed for clarity except those which participate in hydrogen bonding. Displacement ellipsoids are drawn at the 50% probability level. Selected bond lengths (Å) and angles ($^{o}$) are presented in **Table 3.1**.

The crystal structures of compounds **28**, **29**, **30** and **33** are presented in **Figure 3.1**, in each case the metal centre adopts an octahedral geometry with the oxazole/imidazole ligand bound to the metal centre in *cis* arrangement. In each compound, the oxazole/imidazole ligand always binds to the metal centre through the dative co-ordination of the unsaturated imine nitrogen and the phenolic oxygen. The amine of the imidazole is still protonated and undergoes hydrogen bonding with an acetonitrile molecule. The bond between the ligand phenol and the metal centre (M(1)—O(1)) is always longer in

the oxydichloride derivatives, whereas the imine metal bond is similar in each case, as is the ligand bite angle (see **Table 3.1**). Each compound has also been characterised by elemental analysis, IR spectroscopy, NMR spectroscopy and mass spectroscopy.

**Table 3.1** Selected bond lengths and angles for compounds **28**, **29**, **30** and **33.**

| **Compound** | **28** | **29** | **30** | **33** |
|---|---|---|---|---|
| M(1)—O(1) | 1.863(2) | 1.951(6) | 1.8706(13) | 1.9319(16) |
| M(1)—O(3) | - | 1.705(4) | - | 1.6899(16) |
| M(1)—N(6) | - | 2.493(5) | - | 2.558(2) |
| M(1)—N(21) | 2.267(3) | 2.234(4) | 2.2507(16) | 2.2727(18) |
| M(1)—Cl(3) | 2.3576(9) | - | 2.3532(6) | - |
| M(1)—Cl(4) | 2.3092(8) | 2.3889(15) | 2.3116(5) | 2.3696(7) |
| M(1)—Cl(5) | 2.3083(9) | 2.3773(16) | 2.3136(5) | 2.3741(6) |
| M(1)—Cl(6) | 2.3843(9) | - | 2.3789(6) | - |
| O(1)—M(1)—N(21) | 79.09(9) | 78.3(2) | 79.58(6) | 78.78(7) |
| O(1)—M(1)—Cl(4) | 169.31(7) | 154.24(19) | 170.83(5) | 152.50(5) |
| N(21)—M(1)—Cl(5) | 171.36(7) | 163.66(12) | 171.23(4) | 166.02(5) |
| Cl(3)—M(1)—Cl(6) | 172.09(4) | - | 172.89(2) | - |
| N(6)—M(1)—O(3) | - | 177.38(18) | - | 177.79(8) |

The α-diimine ligand **L22** was treated with $NbCl_4(THF)_2$ in tetrahydrofuran to give the pre-catalyst **35**; however the attempted synthesis of **36** following the same procedure was unsuccessful and as such **36** was synthesized following the recently reported literature procedure, in which the α-diimine ligand **L22** was treated with $(TaCl_4)_n$ in toluene.[4] The known bis(imino)pyridine complexes (**37** and **38**) were synthesized following the methods of Nakayama *et al.* using **L23**.[5] In a similar experiment, 2-acetyl-6-iminopyridine (**L24**) was treated with $NbCl_3$(dme), however compound **39** was isolated in which the $NbCl_3$(dme) is acting as a pinacol coupling agent, as previously explored in the literature (see **Scheme 3.1**).[6-7]

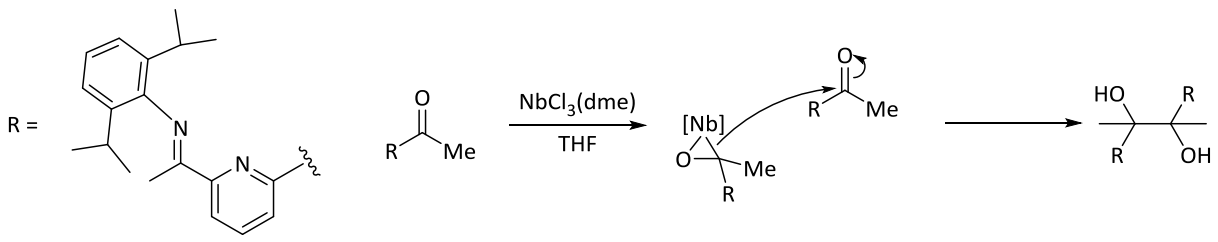


**Scheme 3.1** Mechanism for pinacol coupling using $NbCl_3$(dme).

The molecular structure of **39** is shown in **Figure 3.2**, with selected bond lengths and angles given in the legend. The structure is dimeric about an inversion centre and is coupled through a bridging C—C bond [C(32)—C(32') 1.576(6) Å]. The two niobium metal centres are in octahedral geometry, bound to the ligand through the alkoxide, pyridine and imino nitrogen in *mer* arrangement. Each of the other bond lengths and angles are as expected.[8-9] Attempts to form the analogous tantalum complex were unsuccessful, resulting in a mixture of compounds that could not be separated. Compound **39** was characterised by $^{1}$H NMR, IR spectroscopy and elemental analysis; the molecular ion, from mass spectroscopy analysis, was not observed.

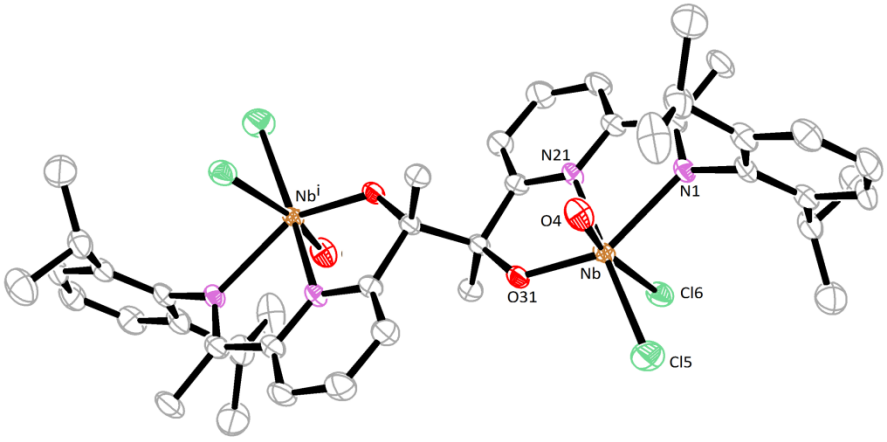


**Figure 3.2** ORTEP representation of a molecule of **39**, indicating the atom numbering scheme. Displacement ellipsoids are drawn at the 50% probability level. Selected bond lengths (Å) and angles (°): Nb—N(1) 2.279(2), Nb—N(21) 2.217(2), Nb—O(31) 1.9076(18), Nb—O(4) 1.708(2) , Nb—Cl(5) 2.3806(9), Nb—Cl(6) 2.5781(8); N(1)—Nb—N(21) 69.67(8), N(1)—Nb—O(31) 142.01(9), N(21)—Nb—O(31) 72.35(8), N(21)—Nb—Cl(5) 165.18(7), N(1)—Nb—O(4) 86.58(9), N(1)—Nb—Cl(6) 83.11(6), O(31)—Nb—Cl(5) 104.79(6), O(4)—Nb—Cl(6) 169.17(7).

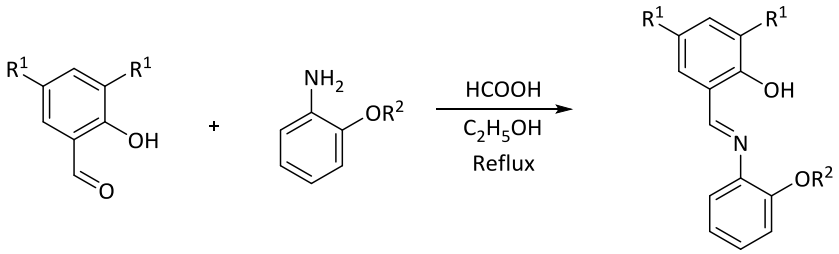


**Scheme 3.2** Synthesis of ligands, **L25H** – **L29H**.

The ligand systems **L25H** – **L29H**, see **Scheme 3.2**, were synthesized by the condensation reaction of the corresponding aldehyde and *o*-methoxy-/*o*-phenoxy-/*o*-trifluoromethyl-aniline in high yields (*ca* 80%), and then treated with either $NbCl_5$ (**40**, **42**, **44**, **46**, **51**) or $TaCl_5$ (**41**, **45**, **47**) in refluxing toluene. Unexpectedly, reaction of the ligand **L26H** with $TaCl_5$ in refluxing toluene led to loss of methyl chloride to afford the phenoxide (**49**, see **Figure 3.3**); similar Lewis acid assisted cleavage of ethers has been utilized in calixarene chemistry as a means of controlling the charge of the ligand set.[10] Demethylation can be avoided by carrying out the synthesis at room temperature, which affords the expected complex **43**. In all cases, crystalline solids can be isolated as yellow/orange to red solids in moderate-to-good yields (*ca* 35 – 72%), and have been characterised by elemental analysis, $^1$H NMR, IR spectroscopy, mass spectrometry and where possible single crystal X-ray diffraction.

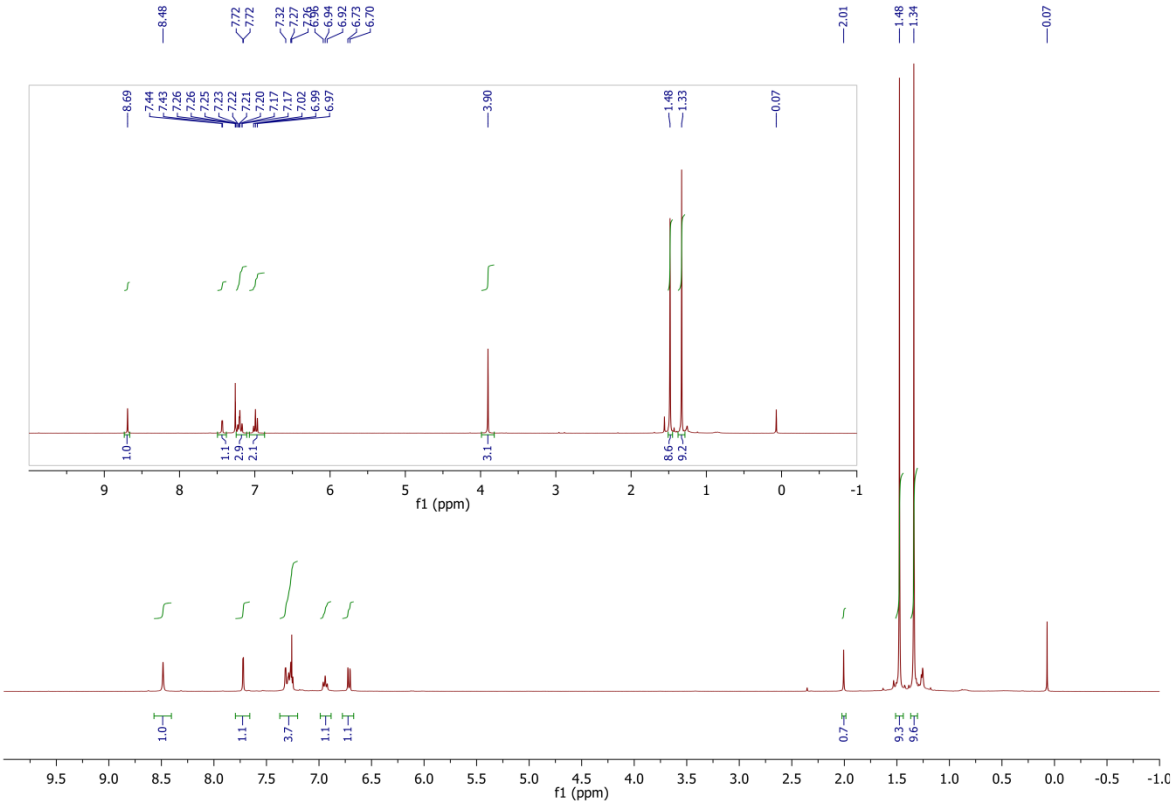


**Figure 3.3** $^1$H NMR spectra of compound **49** and **L26H** (inset).

Single crystals of **40**, **41**, **42** and **44** suitable for X-ray crystallography were grown from their respective saturated acetonitrile solutions, and their structures were determined; **Figure 3.4**, **40**, **Figure 3.5**, **41**, **Figure 3.6**, **42** and **Figure 3.7**, **44**. For each of these samples, there are two independent molecules in the crystal. In each case, the octahedral metal centre is bound to both the nitrogen and oxygen atoms of the Schiff-base ligand. The M—O and M—N bonds have typical dimensions.[9, 11] The $OR^2$ groups are located in similar positions relative to the metal centre. Principal dimensions are compared in **Figure 3.8**. Interestingly, repeating the preparation of **45** in a sealed

reaction vessel over a shorter reaction time yielded the Zwitterionic species **50** (**Figure 3.9**), in which the iminium hydrogen atom was clearly identified in a $N^{+}$–H···N(acetonitrile) hydrogen bond.

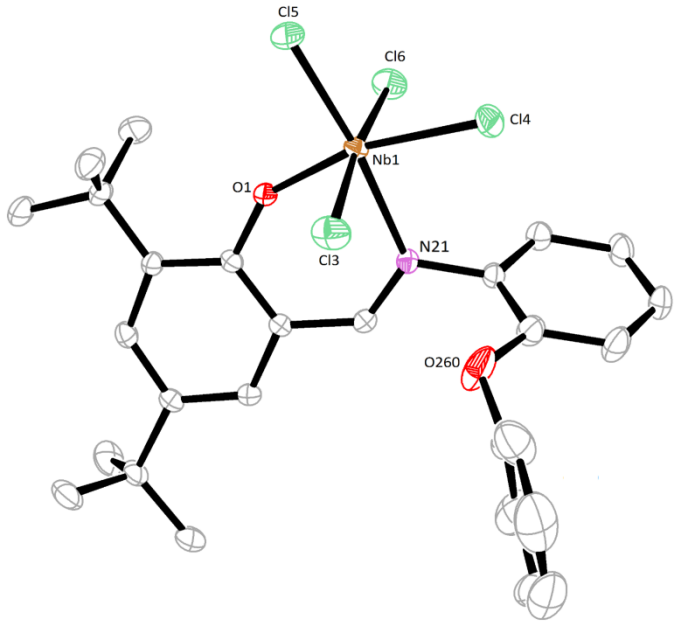


**Figure 3.4** ORTEP representation a molecule of **40**, indicating the atom numbering scheme. Hydrogen atoms are removed for clarity. Displacement ellipsoids are drawn at the 50% probability level. Selected bond lengths (Å) and angles (°) are listed in **Figure 3.8**.

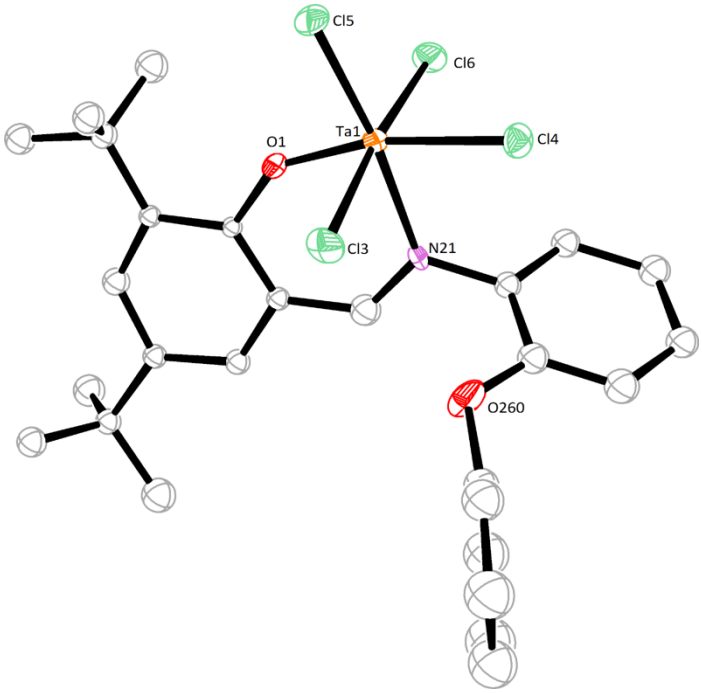


**Figure 3.5** ORTEP representation a molecule of **41**, indicating the atom numbering scheme. Hydrogen atoms are removed for clarity. Displacement ellipsoids are drawn at the 50% probability level. Selected bond lengths (Å) and angles (°) are listed in **Figure 3.8**.

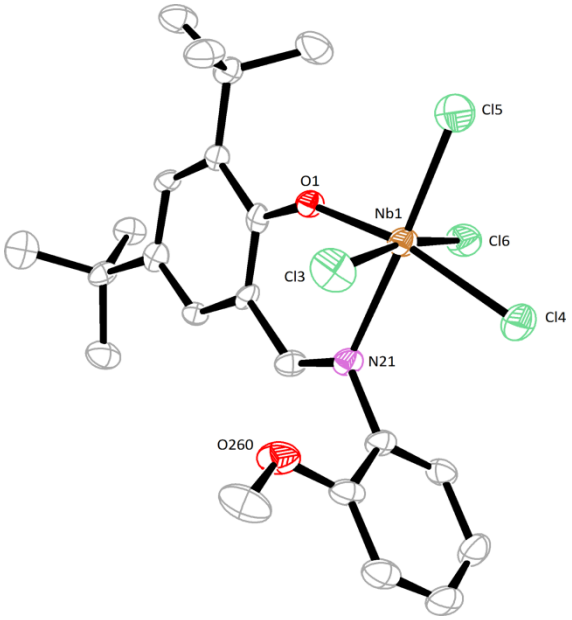


**Figure 3.6** ORTEP representation a molecule of **42**, indicating the atom numbering scheme. Hydrogen atoms are removed for clarity. Displacement ellipsoids are drawn at the 50% probability level. Selected bond lengths (Å) and angles (°) are listed in **Figure 3.8**.

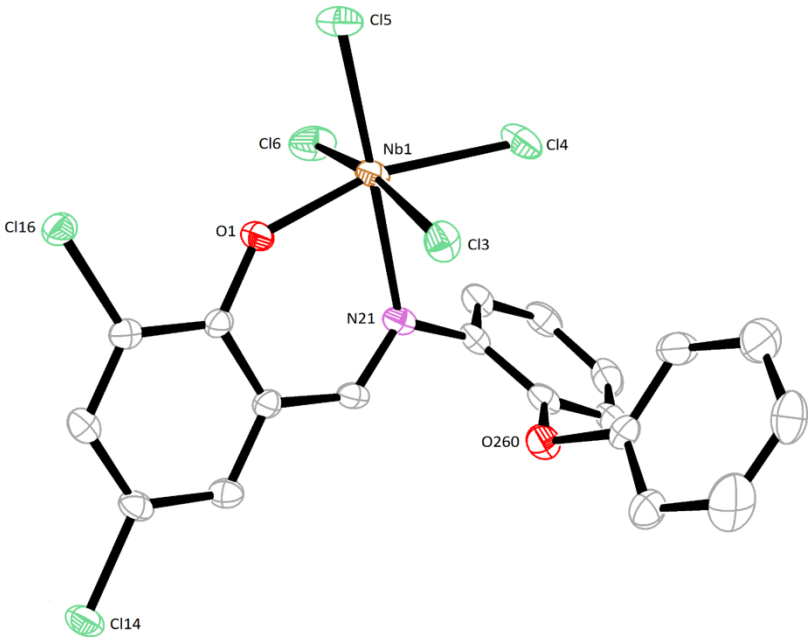


**Figure 3.7** ORTEP representation a molecule of **44**, indicating the atom numbering scheme. Hydrogen atoms are removed for clarity. Displacement ellipsoids are drawn at the 50% probability level. Selected bond lengths (Å) and torsion angles (°) are listed in **Figure 3.8**.

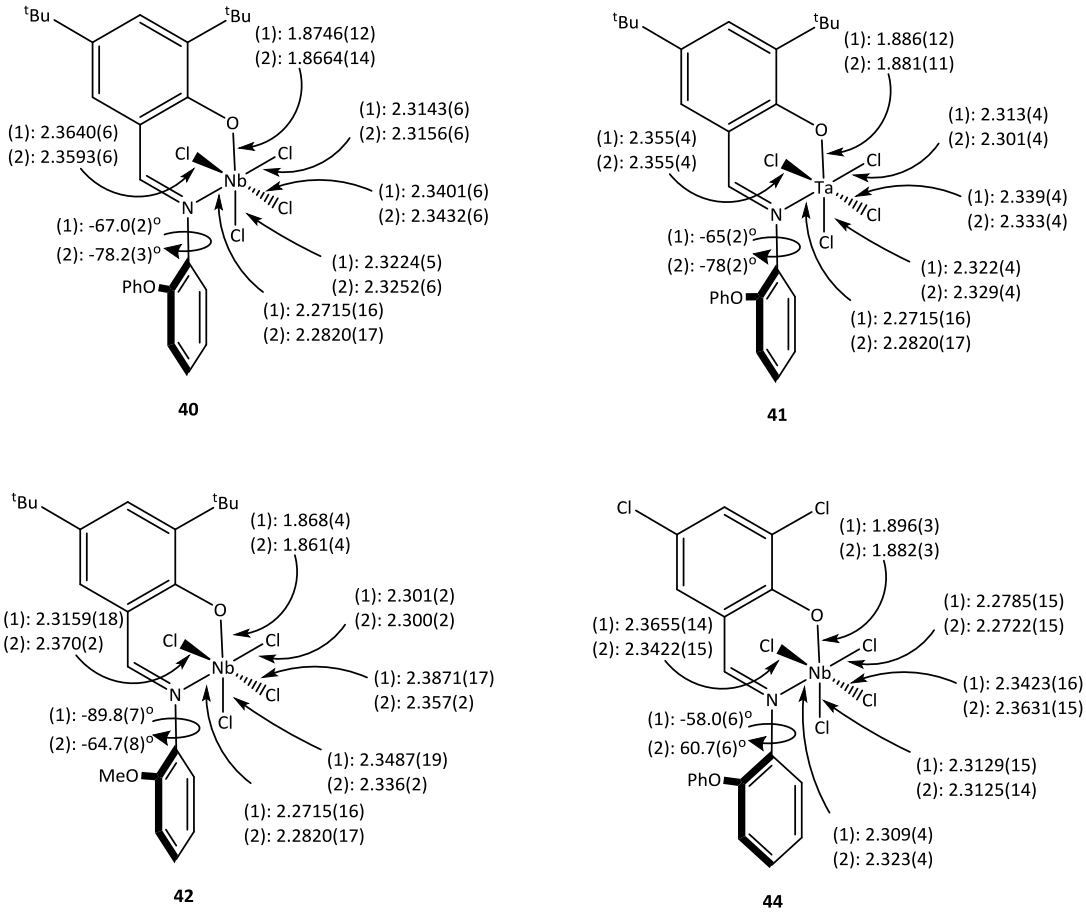


**Figure 3.8** Comparison of bond lengths and torsion angles of structures **40**, **41**, **42** and **44**. Labels (1) and (2) indicate the two independent molecules in each of these structures. Rotation of the bottom phenyl ring about the N—C bond is also shown.

In compound **50**, the tantalum metal centre is in octahedral geometry and bound to the Schiff base only through the oxygen. The phenol is deprotonated and protonated imine nitrogen participates in hydrogen bonding with an acetonitrile molecule. The imine is, however, rotated away from the metal. The isolated structure seems to be an intermediate in the formation of compound **45**; the sealed vessel limits the loss of hydrogen chloride. As such compound **50** can be further refluxed, in an open vessel, under $N_2$ to give compound **45** (**Scheme 3.3**).

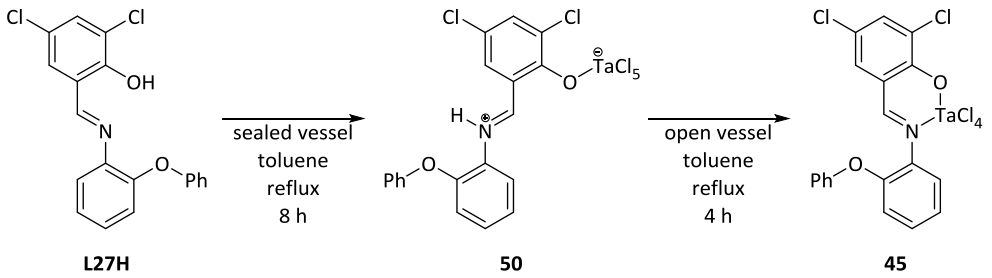


**Scheme 3.3** Synthesis of compound **50** and **45**.

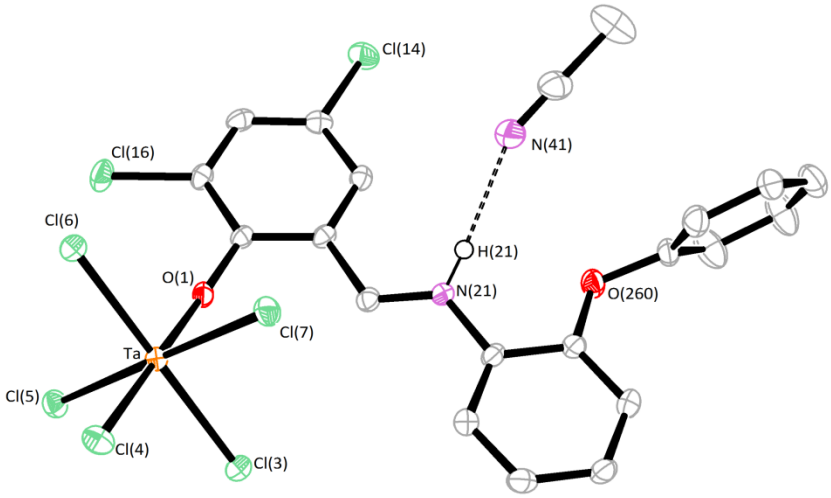


**Figure 3.9** ORTEP representation a molecule of **50**, indicating the atom numbering scheme. Hydrogen atoms are removed for clarity except those which participate in hydrogen bonding. Displacement ellipsoids are drawn at the 50% probability level. Selected bond lengths (Å) and angles (°): Ta—O1 1.904(2), Ta—Cl(5) 2.3510(10), Ta—Cl(6) 2.3576(10), Ta—Cl(4) 2.3579(10), Ta—Cl(3) 2.3630(10), Ta—Cl(7) 2.3911(10); O(1)—Ta—Cl(4) 176.71(7), Cl(6)—Ta—Cl(4) 87.66(3), Cl(3)—Ta—Cl(6) 176.95(3), Cl(5)—Ta—Cl(7) 178.85(3), N(21)—C(31) 1.297(4); hydrogen bond: N(21)—H(21) 0.86, H(21)···N(41) 2.15, N(21)—H(21)···N(41) 157.7.

### *3.2.2 Silica Immobilisation*

Compounds **37**, **38, 43** and **49** were immobilised on pre-treated silica; the $SiO_2$ had been heated to 350 °C under dynamic vacuum for 48 hr, and afforded the supported structures **S-37**, **S-38, S-43** and **S-49**. To calculate the amount of niobium or tantalum bound to the silica surface, X-ray photoelectron spectroscopy (XPS) analysis was employed and performed by Dr Alex Walton at the Leeds EPSRC Nanoscience and Nanotechnology Research Equipment Facility. X-ray photoelectron survey spectra are shown in **Figure 3.10**. Analysis of the resulting photoelectron spectrum of **S-37** showed an Nb3*d* peak with two components at 206.9 and 209.6 eV. The resulting concentration of niobium was shown to be 2.92% of the bulk sample. The presence of peaks at 399.7 eV (0.896%) of the bulk sample) and 198.7 eV (1.07%) correspond to N*1s* and Cl2*p* peaks. The photoelectron spectra of **S-38, S-43** and **S-49** each show two Ta4*d* peaks at 242.2 eV and 230.6 eV (1.13% of the bulk sample), 241.7 eV and 230.1 eV (1.35%), 241.9 eV and 230.6 eV (0.495%) respectively. The spectra also confirmed the presence of Cl2*p* peaks with 0.729, 1.06 and 0.729% of **S-38, S-43** and **S-49** assignable to chlorine. In each of the Ta based samples, the percentage of nitrogen could not be determined. All values were recorded within 0.1 eV.

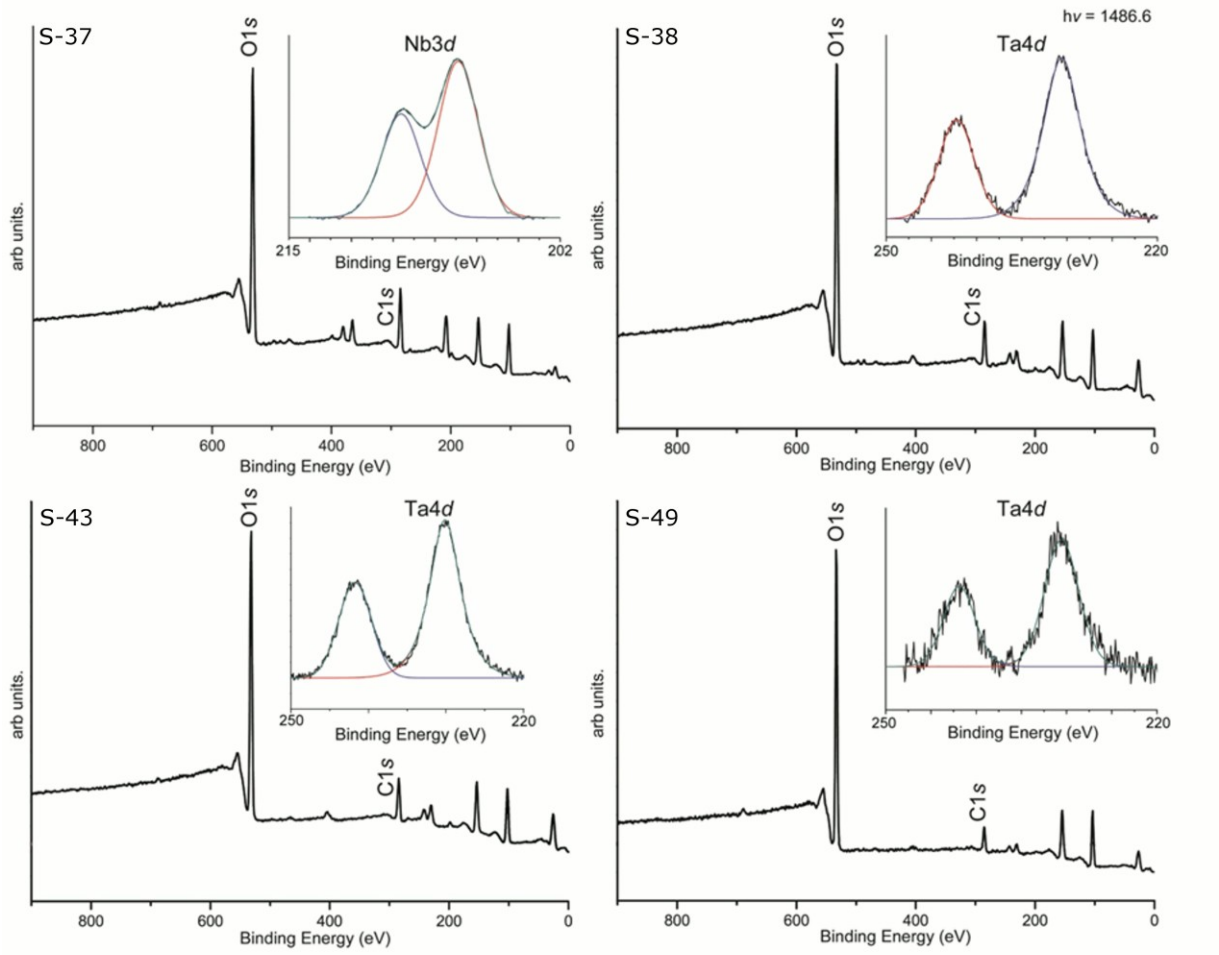


**Figure 3.10** X-ray photoelectron spectra of **S-37**, **S-38, S-43** and **S-49**. Nb3*d* and Ta4*d* energy windows are shown inset. The C*1s* peak was used to calibrate the spectra.

### *3.2.3 Catalytic Screening*

#### *3.2.3.1 Homogeneous Catalysis*

The polymerisation screening in this chapter was performed in collaboration with Dr Lucy Clowes. The imidazole/oxazole compounds, **28** – **34**, were screened employing either MADC or DMAC as co-catalyst for ethylene polymerisation. The activities, in general, can be described as very high, **Table 3.2**; only activities lower than 1,000 g/mmol.hr.bar were achieved during runs 1, 7 and 8. Firstly, to attain the optimum conditions **29** was screened using MADC or DMAC at various temperature and equivalents. MADC was found to give better activities than DMAC (**Table 3.2**, runs 4 – 6 *vs.* runs 7 – 9), with optimum activities exhibited with increasing Al : Nb ratio. We did not explore higher than 8000 equivalents co-catalyst. Similarly to results in **chapter 2** the use of ETA as re-activator was beneficial to the catalytic system (**Table 3.2**, run 1 *vs.* 2).

**Table 3.2** Results for selected ethylene polymerisation runs for pre-catalysts **28** – **34**.

| Run | Pre-cat (µmol) | Co-cat | [Al]/[M] | Temp[b] | Time[c] | Yield[d] | Activity[e] | $M_w$[f] | $M_n$[g] | PDI[h] |
|---|---|---|---|---|---|---|---|---|---|---|
| 1[a] | **28** (0.5) | MADC | 8000 | 20 | 30 | 0.11 | 440 | | | |
| 2 | **28** (0.5) | MADC | 8000 | 20 | 30 | 0.287 | 1,150 | | | |
| 3 | **28** (0.5) | MADC | 8000 | 40 | 15 | 0.119 | 1,900 | | | |
| 4 | **29** (0.25) | MADC | 2000 | 20 | 15 | 0.2 | 1,600 | | | |
| 5 | **29** (0.25) | MADC | 4000 | 20 | 15 | 0.379 | 3,030 | | | |
| 6 | **29** (0.25) | MADC | 6000 | 20 | 15 | 0.525 | 4,200 | | | |
| 7 | **29** (0.25) | DMAC | 4000 | 20 | 15 | 0.089 | 710 | | | |
| 8 | **29** (0.25) | DMAC | 6000 | 20 | 15 | 0.09 | 720 | | | |
| 9 | **29** (0.25) | DMAC | 8000 | 40 | 5 | 0.067 | 1,610 | 1,030,000 | 371,000 | 2.8 |
| 10 | **29** (0.25) | DMAC | 8000 | 40 | 20 | 0.172 | 1,030 | 775,000 | 228,000 | 3.4 |
| 11 | **29** (0.25) | DMAC | 8000 | 40 | 30 | 0.386 | 1,540 | 764,000 | 164,000 | 4.6 |
| 12 | **29** (0.25) | MADC | 8000 | 60 | 5 | 0.228 | 5,470 | 555,000 | 146,000 | 3.8 |
| 13 | **29** (0.25) | MADC | 8000 | 60 | 10 | 0.202 | 2,420 | 490,000 | 200,000 | 2.5 |
| 14 | **29** (0.25) | MADC | 8000 | 60 | 30 | 0.615 | 2,460 | 496,000 | 109,000 | 4.6 |
| 15 | **29** (0.25) | MADC | 8000 | 40 | 15 | 0.332 | 5,310 | | | |
| 16 | **29** (0.25) | MADC | 8000 | 60 | 30 | 0.615 | 2,460 | | | |
| 17 | **29** (0.25) | MADC | 8000 | 80 | 15 | 0.557 | 8,910 | | | |
| 18 | **30** (0.25) | MADC | 8000 | 30 | 15 | 0.16 | 2,580 | | | |
| 19 | **30** (0.25) | MADC | 8000 | 40 | 15 | 0.200 | 3,200 | | | |
| 20 | **30** (0.25) | MADC | 8000 | 50 | 15 | 0.309 | 4,940 | | | |
| 21 | **30** (0.25) | MADC | 8000 | 80 | 15 | 0.210 | 3,360 | 307,000 | 122,000 | 2.5 |
| 22 | **31** (0.25) | MADC | 8000 | 20 | 15 | 0.388 | 6,210 | | | |
| 23 | **31** (0.25) | MADC | 8000 | 40 | 15 | 0.272 | 4,350 | | | |
| 24 | **31** (0.25) | MADC | 8000 | 60 | 15 | 0.098 | 1,570 | | | |
| 25 | **31** (0.25) | MADC | 8000 | 80 | 15 | - | - | | | |
| 26 | **32** (0.25) | MADC | 8000 | 40 | 15 | 0.215 | 3,180 | | | |
| 27 | **33** (0.25) | DMAC | 8000 | 50 | 15 | 0.097 | 1,550 | 1,720,000 | 768,000 | 2.2 |
| 28 | **33** (0.25) | MASC | 8000 | 50 | 15 | 0.220 | 3,520 | | | |
| 29 | **33** (0.25) | MADC | 8000 | 50 | 15 | 0.741 | 11,900 | | | |
| 30 | **34**(0.25) | MADC | 8000 | 20 | 15 | 0.205 | 3,280 | 567,000 | 50,200 | 11.3 |
| 31 | **34** (0.25) | MADC | 8000 | 40 | 15 | 0.211 | 3,380 | | | |
| 32 | **34** (0.25) | MADC | 8000 | 60 | 15 | 0.621 | 9,940 | | | |

*Conditions:*1 bar ethylene Schlenk tests carried out in toluene (100 ml) in the presence of ETA (0.05 ml), reaction was quenched with dilute HCl, washed with methanol (50 ml) and dried for 12 hr at 80 °C. [a] Without ETA, [b] °C, [c] minutes, [d] grams, [e] g/mmol.hr.bar, [f] Weight average molecular weight. [g] Number average molecular weight. [h] Polydispersity index: $M_w/M_n$

Comparison of the imidazole ligated compounds, **28** – **31**, in identical conditions, indicated that at 40 °C the oxydichloride derivatives gave slightly higher activities than the tetrachloride versions (**Table 3.2**, runs 3, 15, 19, and 23); although the activities are similar.

We further investigated the lifetime of pre-catalyst **29** using either DMAC (**Table 3.2**, runs 9 – 11, 40 °C) or MADC (**Table 3.2**, runs 12 – 14, 60 °C). The activity when using DMAC remained approximately the same; however the runs using MADC as co-catalyst showed the activity at 5 minutes dropped to 50% within 10 minutes and remained at this level until the 30 minute mark. There was also a slight increase in polydispersity with time in both sets of runs. As somewhat expected, considering the activities associated with DMAC and MADC, the use of MASC resulted in activities in-between those of DMAC and MADC (**Table 3.2**, runs 27 – 29); higher activities were associated with increased chloride content in the co-catalyst.

The oxazole ligand set appeared to exhibit slighty higher activities for either the niobium tetrachlorides (**Table 3.2**, runs 3 *vs* 26) or oxydichlorides (**Table 3.2**, runs 4 – 17 *vs.* runs 27 – 29); comparable activities were observed for the tantalum tetrachlorides (**Table 3.2**, run 19 *vs* 31).

The tantalum systems showed comparable activities to their niobium counterparts (**34**, **Table 3.2**, runs 30 – 32, vs. **32** run 26). When investigating the chain length using **29**, we found higher molecular weights (>750,000 g/mol) when employing DMAC as the co-catalyst (**Table 3.2**, runs 9 – 11). It should be noted that a number of polymer samples from runs utilizing DMAC/MADC contained some polymer that was insoluble for analysis using GPC, suggesting exceptionally high molecular weight polyethylene.

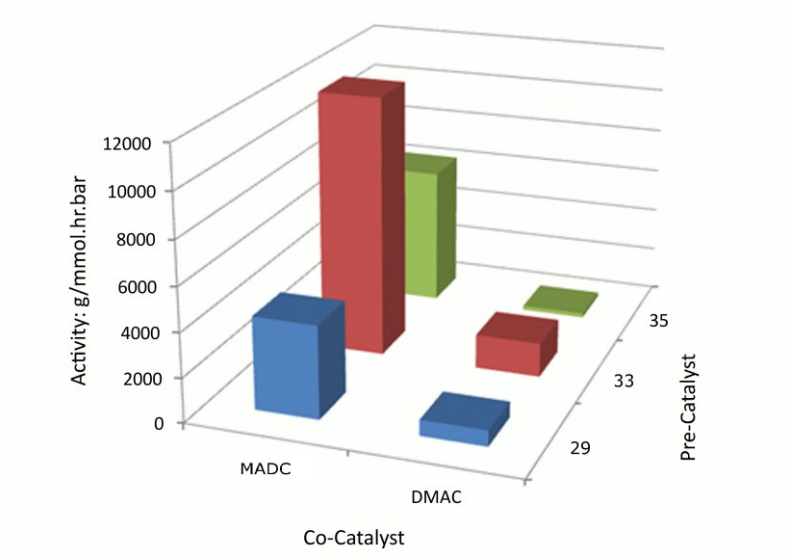


**Figure 3.11** Effect of varying the co-catalyst on pre-catalysts **29**, **33**, and **35.** (For conditions, see **Table 3.2**, run 6 *vs* 8 (**29**), runs 27 *vs* 29 (**33**); **Table 3.3**, runs 2 *vs* 3 (**35**)).

**Table 3.3** Results for ethylene polymerisation runs for pre-catalysts **35** – **39**.

| Run | Pre-cat(µmol) | Co-cat | [Al]/[M] | Temp[a] | Time[b] | Yield PE[c] | Activity[d] | $M_w$[e] | $M_n$[f] | PDI[g] |
|---|---|---|---|---|---|---|---|---|---|---|
| 1 | **35** (0.25) | DMAC | 6000 | 20 | 15 | 0.034 | 540 | 418,000 | 181,000 | 2.3 |
| 2 | **35** (0.25) | DMAC | 8000 | 20 | 15 | 0.012 | 190 | - | - | - |
| 3 | **35** (0.25) | MADC | 8000 | 20 | 15 | 0.393 | 6,290 | 358,000 | 138,000 | 2.5 |
| 4 | **35** (0.25) | MADC | 8000 | 60 | 15 | 0.160 | 2,560 | - | - | - |
| 5 | **35** (0.25) | MADC | 8000 | 80 | 15 | 0.100 | 1,600 | 230,000 | 90,800 | 2.5 |
| 6 | **36** (0.25) | MADC | 8000 | 20 | 15 | 0.400 | 6,400 | - | - | - |
| 7 | **36** (0.25) | MADC | 8000 | 40 | 15 | 0.620 | 9,920 | - | - | - |
| 8 | **36** (0.25) | MADC | 8000 | 60 | 15 | 0.470 | 7,520 | - | - | - |
| 9 | **36** (0.25) | MADC | 8000 | 80 | 15 | 0.065 | 1,040 | - | - | - |
| 10 | **37** (0.25) | DMAC | 6000 | 20 | 15 | 0.037 | 590 | - | - | - |
| 11 | **37** (0.25) | DMAC | 8000 | 20 | 15 | 0.069 | 1,100 | - | - | - |
| 12 | **37** (0.25) | MADC | 4000 | 20 | 15 | 0.130 | 2,080 | 1,070,000 | 257,000 | 4.2 |
| 13 | **37** (0.25) | MADC | 8000 | 40 | 15 | 0.212 | 3,390 | - | - | - |
| 14 | **37** (0.25) | MADC | 8000 | 60 | 15 | 0.170 | 2,720 | 183,000 | 63,000 | 2.9 |
| 15 | **37** (0.25) | MADC | 8000 | 80 | 15 | - | - | - | - | - |
| 16 | **38** (0.25) | MADC | 8000 | 20 | 15 | 0.352 | 5,632 | - | - | - |
| 17 | **38** (0.25) | MADC | 8000 | 40 | 15 | 0.645 | 10,320 | - | - | - |
| 18 | **38** (0.25) | MADC | 8000 | 60 | 15 | 0.128 | 2,050 | - | - | - |
| 19 | **38** (0.25) | MADC | 8000 | 80 | 15 | - | - | - | - | - |
| 20 | **39** (0.25) | MADC | 8000 | 20 | 15 | 0.191 | 1,530 | - | - | - |
| 21 | **39** (0.25) | MADC | 8000 | 40 | 15 | 0.109 | 870 | - | - | - |
| 22 | **39** (0.25) | MADC | 8000 | 60 | 15 | 0.133 | 1,060 | - | - | - |
| 23 | **39** (0.25) | MADC | 8000 | 80 | 15 | 0.162 | 1,100 | - | - | - |

*Conditions:*1 bar ethylene Schlenk tests carried out in toluene (100 ml) in the presence of ETA (0.05 ml), reaction was quenched with dilute HCl, washed with methanol (50 ml) and dried for 12 hr at 80 °C. [a] °C, [b] minutes, [c] grams, [d] g/mmol.hr.bar, [e] Weight average molecular weight. [f] Number average molecular weight. [g] Polydispersity index: $M_w/M_n$

Polymerisation studies (Table 3.3) showed similar activities of **35** and **36** at room temperature, approximately 6,000 g/mmol.hr.bar (runs 3 and 6). However the tantalum species showed increased stability at higher temperatures (*e.g.* 7,520 *vs* 2,560 g/mmol.hr.bar, Table 3.3, runs 8 and 4). In the case complexes **37** and **38**, use of *tert*-butyl modified methylaluminoxane afforded activities ≤ 70 g/mmol.hr.bar. [12] Here, we found that use of **37** with MADC, in the presence of ETA, afforded activities as high as 3390 g/mmol.hr.bar (Table 3.3, run 13). When comparing use of co-catalysts MADC and DMAC for polymerisation, it is clear that MADC is the co-catalyst of choice (Figure 3.11).

The screening of the imidazole/oxazole based complexes revealed high activity for niobium/tantalum compounds and as such a number of the Schiff base ligands, some of which were included in **chapter 2**, were screened for ethylene polymerisation. The polymerisation system MADC/ETA, which had been shown in **Table 3.2** and **Table 3.3** to be the most promising, was then used to assess pre-catalysts **40** – **47** for polyethylene production.

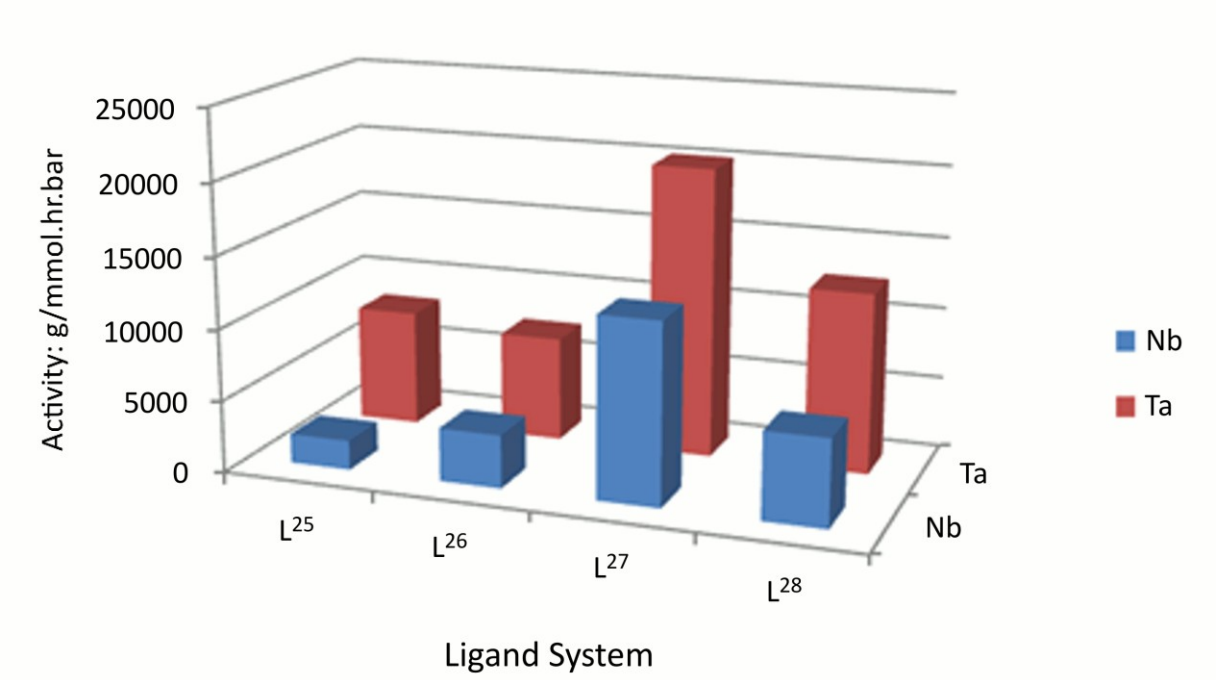


**Figure 3.12** Effect of $R^1$ and $R^2$ on the Activity of Nb/Ta Schiff Bases (for conditions, see **Table 3.4**, run 4).

The niobium derivatives of pre-catalysts **40** – **50** possessed similar activities to **28** – **39**; however the tantalum analogues were slightly more active. These Schiff-base type catalysts (**40** – **49**, but not **50**) were active up to 80 °C (**Table 3.4**, runs 5, 11 and 19), although a noticeable drop-off in activity for **47** was observed above 60 °C. The molecular weight of the polyethylene decreased with increasing temperature (**Table 3.4**, runs 15 *vs* 19). Interestingly, catalyst system **47** had one of the highest activities of the pre-catalysts studied herein (run 18, activity ≈18,450 g/mmol.hr.bar). Modification of the $R^1$ and $R^2$ groups of the Schiff base backbone had some influence on the polymerisation activity of the metal centre involved. The catalysts with chloro groups at the $R^1$ position, those incorporating **L27** and **L28**, generally afforded higher activities than their *tert*-butyl counterparts, **L25** and **L26**, **Figure 3.12**. The highest activity obtained utilized pre-catalyst **45** with an activity of approximately 20,000 g/mmol.hr.bar, while compound **49** gave polymer with molecular weight of over 1,000,000 g/mol.

**Table 3.4** Temperature dependence of activity for pre-catalysts **40** – **50**.

| Run | Pre-cat (µmol) | $R^1$ | $R^2$ | Metal Centre | Temp[a] | Time[b] | Yield[c] | Activity[d] | $M_w$[e] | $M_n$[f] | PDI[g] |
|---|---|---|---|---|---|---|---|---|---|---|---|
| 1 | **40** (0.25) | *t*Bu | Ph | Nb | 20 | 15 | 0.054 | 860 | 552,000 | 143,000 | 3.9 |
| 2 | **40** (0.25) | *t*Bu | Ph | Nb | 30 | 15 | 0.053 | 850 | | | |
| 3 | **40** (0.25) | *t*Bu | Ph | Nb | 40 | 15 | 0.074 | 1,180 | | | |
| 4 | **40** (0.25) | *t*Bu | Ph | Nb | 50 | 15 | 0.129 | 2,060 | | | |
| 5 | **40** (0.25) | *t*Bu | Ph | Nb | 80 | 15 | 0.197 | 3,150 | 108,000 | 41,700 | 2.6 |
| 6 | **41** (0.25) | *t*Bu | Ph | Ta | 50 | 15 | 0.509 | 8,140 | | | |
| 7 | **42** (0.25) | *t*Bu | Me | Nb | 50 | 15 | 0.231 | 3,700 | | | |
| 8 | **43** (0.25) | *t*Bu | Me | Ta | 20 | 15 | 0.36 | 5,760 | | | |
| 9 | **43** (0.25) | *t*Bu | Me | Ta | 40 | 15 | 0.485 | 7,760 | | | |
| 10 | **43** (0.25) | *t*Bu | Me | Ta | 50 | 15 | 0.456 | 7,300 | | | |
| 11 | **43** (0.25) | *t*Bu | Me | Ta | 80 | 15 | 0.33 | 5,280 | | | |
| 12 | **44** (0.25) | Cl | Ph | Nb | 50 | 15 | 0.786 | 12,580 | 101,000 | 14,700 | 6.9 |
| 13 | **45** (0.25) | Cl | Ph | Ta | 50 | 15 | 1.263 | 20,200 | | | |
| 14 | **46** (0.25) | Cl | Me | Nb | 50 | 15 | 0.378 | 6,050 | | | |
| 15 | **47** (0.25) | Cl | Me | Ta | 20 | 15 | 0.5 | 8,000 | 322,000 | 64,200 | 5.0 |
| 16 | **47** (0.25) | Cl | Me | Ta | 40 | 15 | 0.708 | 11,300 | | | |
| 17 | **47** (0.25) | Cl | Me | Ta | 50 | 15 | 0.785 | 12,600 | | | |
| 18 | **47** (0.25) | Cl | Me | Ta | 60 | 15 | 1.153 | 18,500 | | | |
| 19 | **47** (0.25) | Cl | Me | Ta | 80 | 15 | 0.547 | 8,750 | 70,300 | 11,600 | 6.0 |
| 20 | **48** (0.25) | Cl | $CF_3$ | Nb | 20 | 15 | 0.092 | 1,470 | | | |
| 21 | **48** (0.25) | Cl | $CF_3$ | Nb | 40 | 15 | 0.168 | 2,690 | | | |
| 22 | **48** (0.25) | Cl | $CF_3$ | Nb | 60 | 15 | 0.113 | 1,810 | | | |
| 23 | **48** (0.25) | Cl | $CF_3$ | Nb | 80 | 15 | - | - | | | |
| 24 | **49** (0.25) | *t*Bu | - | Ta | 20 | 15 | 0.25 | 4,000 | 1,150,000 | 403,000 | 2.9 |
| 25 | **49** (0.25) | *t*Bu | - | Ta | 40 | 15 | 0.327 | 5,230 | 421,000 | 48,700 | 8.6 |
| 26 | **49** (0.25) | *t*Bu | - | Ta | 50 | 15 | 0.923 | 14,800 | | | |
| 27 | **49** (0.25) | *t*Bu | - | Ta | 80 | 15 | 1.034 | 16,500 | 495,000 | 206,000 | 2.4 |
| 28 | **50** (0.25) | Cl | Ph | Ta | 20 | 15 | 0.329 | 5,260 | | | |
| 29 | **50** (0.25) | Cl | Ph | Ta | 40 | 15 | 0.274 | 4,380 | | | |
| 30 | **50** (0.25) | Cl | Ph | Ta | 60 | 15 | 0.027 | 432 | | | |
| 31 | **50** (0.25) | Cl | Ph | Ta | 80 | 15 | - | . | | | |

*Conditions:* 1 bar ethylene Schlenk tests carried out in toluene (100 ml) in the presence of ETA (0.05 ml), reaction was quenched with dilute HCl, washed with methanol (50 ml) and dried for 12 hr at 80 °C. [a] °C, [b] minutes, [c] grams, [d] g/mmol.hr.bar, [e] Weight average molecular weight. [f] Number average molecular weight. [g] Polydispersity index: $M_w/M_n$

### *3.2.3.2 Parallel Pressure Reactor screening*

A number of the pre-catalysts described herein were subjected to homo- and hetero-geneous parallel pressure reactor screening (PPR) at the Borealis group, Finland, employing methylaluminoxane (MAO) as co-catalyst.[13-14] The results for ethylene polymerisation using pre-catalysts **28** and **40** are given in

**Table 3.5**, whilst pre-catalysts **29**, **30**, **32**, and **35** have been employed in the co-polymerisation of ethylene with 1-hexene (**Table 3.6**). The supported catalysts **S-37**, **S-38, S-43** and **S-49** were subjected to both homo-polymerisation (ethylene) using tri-isobutyl aluminium (TIBA) as co-catalyst, and co-polymerisation (1-hexene and ethylene) using TIBA or ethyl aluminium dichloride (EADC) as co-catalyst (**Table 3.7**). The effect of the addition of ethyl trichloroacetate (ETA) was also investigated (**Table 3.8**).

*3.2.3.3 Ethylene PPR polymerisation*

Both pre-catalysts **28** and **40** were moderately active for the polymerisation of ethylene under the conditions employed. The lower results here are thought to be associated with the use of MAO as co-catalyst. Nomura and co-workers have proposed for vanadium-based catalyst systems/MAO the formation of discrete ion-pairs, which led to lower activities.[15] Increasing the catalyst loading was detrimental to the observed activity, suggesting that the concentration of the active species could have an upper limit.

**Table 3.5** Parallel Pressure Reactor Ethylene polymerisation screening of pre-catalysts **28** and **40**.

| Run | Pre-Catalyst (µmol) | Temp[a] | Time[b] | Yield[c] | Activity[d] |
|---|---|---|---|---|---|
| 1 | **28** (0.4) | 80 | 1.0 | 0.035 | 13.2 |
| 2 | **40** (0.1) | 60 | 1.0 | 0.040 | 60.4 |
| 3 | **40** (0.15) | 60 | 1.0 | 0.040 | 40.0 |
| 4 | **40** (0.2) | 60 | 0.6 | 0.040 | 59.1 |
| 5 | **40** (0.2) | 60 | 1.0 | 0.041 | 30.9 |
| 6 | **40** (0.2) | 80 | 1.0 | 0.033 | 25.0 |
| 7 | **40** (0.2) | 80 | 1.0 | 0.032 | 24.1 |
| 8 | **40** (0.25) | 80 | 1.0 | 0.030 | 19.5 |
| 9 | **40** (0.3) | 80 | 1.0 | 0.031 | 15.7 |
| 10 | **40** (0.35) | 80 | 1.0 | 0.031 | 12.3 |

*Conditions:* 6.68 bar ethylene, 1hr reaction time, co-catalyst: methylaluminoxane, 4000 equivalents, heptane as solvent; [a] °C, [b] minutes, [c] grams, [d] g/mmol.hr.bar.

*3.2.3.4 Ethylene/1-hexene copolymerisation*

**Table 3.6** PPR co-polymerisation screening of pre-catalysts **29**, **30**, **32** and **35** with MAO as co-catalyst.

| Run | Pre-cat (µmol) | Temp[a] | Yield[b] | Activity[c] |
|---|---|---|---|---|
| 1 | **29** (0.2) | 80 | 0.035 | 26.4 |
| 2 | **29** (0.3) | 80 | 0.031 | 15.6 |
| 3 | **29** (0.35) | 80 | 0.032 | 13.8 |
| 4 | **29** (0.4) | 80 | 0.040 | 14.8 |
| 5 | **30** (0.2) | 80 | 0.034 | 25.6 |
| 6 | **30** (0.3) | 80 | 0.034 | 18.0 |
| 7 | **30** (0.35) | 80 | 0.035 | 14.7 |
| 8 | **32** (0.2) | 80 | 0.035 | 26.1 |
| 9 | **32** (0.25) | 80 | 0.036 | 21.6 |
| 10 | **35** (0.2) | 80 | 0.078 | 58.2 |
| 11 | **35** (0.3) | 80 | 0.036 | 18.1 |
| 12 | **35** (0.35) | 80 | 0.035 | 15.0 |
| 13 | **35** (0.4) | 80 | 0.038 | 14.2 |

*Conditions:* 6.68 bar ethylene, 1hr reaction time; for co-polymerisations, 54 µL 1-hexene, co-catalyst: methylaluminoxane, 4,000 equivalents, heptane as solvent; [a] °C, [b] grams, [c] g/mmol.hr.bar.

For 1-hexene/ethylene co-polymerisation, pre-catalysts **29**, **30**, **32** and **35** exhibited low activity when activated using MAO as co-catalyst (**Table 3.6**). Pre-catalyst **35** displayed the highest activity at ≈60 g/mmol.hr.bar (**Table 3.6**, run 10) for a catalyst loading of 0.2 µmol, though the activity was far less (≈15 g/mmol.hr.bar) for increased catalysts loadings (≤ 0.4 µmol). When TIBA and EADC were employed as co-catalyst (**Table 3.7**), the activity for compounds **29** and **30** were somewhat similar. The activities for compound **32** and **35** were improved when TIBA was employed, and lower with EADC. The highest activity obtained was 288 g/mmol.hr.bar for compound **35** (**Table 3.7**, run 11).

**Table 3.7** PPR co-polymerisation screening of pre-catalysts **29**, **30**, **32** and **35** using TIBA and EADC.

| Run | Pre-catalyst (mg) | Co-catalyst | Metal Content[a] | Yield[b] | Activity[c] | Ethylene Consumption[d] |
|---|---|---|---|---|---|---|
| 1 | **29** (0.4) | TIBA | 0.1262 | 0.0028 | 22.1 | 3.97 |
| 2 | **29** (0.8) | TIBA | 0.2523 | 0.0073 | 28.9 | 6.26 |
| 3 | **30** (0.4) | TIBA | 0.0250 | 0.001 | 40.0 | 5.65 |
| 4 | **30** (0.8) | TIBA | 0.0499 | 0.0014 | 28.0 | 3.36 |
| 5 | **30** (1.0) | TIBA | 0.0624 | 0.0013 | 20.8 | 9.31 |
| 6 | **32** (0.4) | TIBA | 0.0296 | 0.0013 | 43.9 | 7.94 |
| 7 | **32** (0.8) | TIBA | 0.0592 | 0.0014 | 23.6 | 3.05 |
| 8 | **32** (1.0) | TIBA | 0.0740 | 0.0101 | 136.4 | 8.55 |
| 9 | **35** (0.4) | TIBA | 0.0110 | 0.0011 | 100 | 4.12 |
| 10 | **35** (0.8) | TIBA | 0.0219 | 0.001 | 45.6 | 2.29 |
| 11 | **35** (1.0) | TIBA | 0.0274 | 0.0079 | 288 | 11.75 |
| 12 | **29** (0.4) | EADC | 0.1262 | 0.0022 | 17.4 | 2.59 |
| 13 | **29** (0.8) | EADC | 0.2523 | 0.0032 | 12.7 | 5.04 |
| 14 | **29** (1.0) | EADC | 0.3154 | 0.002 | 6.34 | 5.04 |
| 15 | **30** (0.8) | EADC | 0.0499 | 0.0012 | 24.0 | 10.38 |
| 16 | **30** (1.0) | EADC | 0.0624 | 0.0016 | 25.6 | 5.04 |
| 17 | **32** (0.4) | EADC | 0.0296 | 0.0009 | 30.4 | 5.80 |
| 18 | **32** (0.8) | EADC | 0.0592 | 0.0014 | 23.6 | 10.23 |
| 19 | **32** (1.0) | EADC | 0.0740 | 0.0013 | 17.6 | 13.89 |
| 20 | **35** (0.4) | EADC | 0.0110 | 0.001 | 91.2 | 2.75 |
| 21 | **35** (0.8) | EADC | 0.0219 | 0.0019 | 86.7 | 6.26 |
| 22 | **35** (1.0) | EADC | 0.0274 | 0.0006 | 21.9 | 4.43 |

*Conditions:* 6.68 bar ethylene, 1hr reaction time, 54 µL 1-hexene, 4,000 equivalents co-catalyst, heptane as solvent; [a] µmol, [b] grams, [c] g/mmol.hr.bar, [d] psi.

The supported pre-catalysts **S-37**, **S-38, S-43** and **S-49** were found to be inactive for the homo-polymerisation of ethylene when using TIBA as co-catalyst (results not shown). However, these pre-catalysts were found to be active for the co-polymerisation of 1-hexene and ethylene, though the runs gave complicated, poor and unpredictable results (**Table 3.8**). In general, supported pre-catalysts **S-43** and **S-49** were the most active with either TIBA or EADC; however, drawing more specific conclusions is difficult given the poor reproducibility of the data. Repeated runs of each pre-catalyst are shown (rather than being averaged) in the table due to the lower reproducibility. The activities of pre-catalysts **S-37**, **S-43** and **S-49** were monitored through their consumption of ethylene (**Figure 3.13**). The pre-catalysts were first allowed a long contact time with EADC and ETA before the addition of ethylene. The consumption of ethylene initially rises and then plateaus after approximately one minute, thus indicating that the catalyst is only active for the first minute of the polymerisation and then is effectively dead for the remainder of the run.

**Table 3.8** Co-polymerisation screening of pre-catalysts **S-37**, **S-38, S-43** and **S-49** using EADC/ETA.

| Run | Pre-catalyst (mg) | Metal Content (µmol)[a] | yield (g) | Activity[b] | Ethylene Consumption (psi) | ETA:M |
|---|---|---|---|---|---|---|
| 1 | **S-37** (0.3) | 9.46 | 0.0013 | 13.7 | 6.10 | 1440 |
| 2 | **S-37** (0.3)[c] | 9.46 | 0.0015 | 15.9 | 4.88 | 1440 |
| 3 | **S-37** (0.8) | 25.2 | 0.0017 | 6.74 | 4.88 | 1440 |
| 4 | **S-38** (0.8)[c] | 4.99 | 0.0015 | 30.0 | 3.97 | 1440 |
| 5 | **S-38** (0.8)[c] | 4.99 | 0.0015 | 30.0 | 7.48 | 1440 |
| 6 | **S-38** (0.3) | 0.822 | 0.0009 | 110 | 4.73 | 1440 |
| 7 | **S-43** (0.3) | 2.22 | 0.011 | 495 | 10.2 | 360 |
| 8 | **S-43** (0.3)[c] | 2.22 | 0.0045 | 203 | 6.41 | 360 |
| 9 | **S-43** (0.3)[c] | 2.22 | 0.003 | 135 | 5.65 | 720 |
| 10 | **S-43** (0.3)[c] | 2.22 | 0.0041 | 185 | 3.51 | 720 |
| 11 | **S-43** (0.3)[c] | 2.22 | 0.0014 | 63.0 | 5.49 | 1440 |
| 12 | **S-43** (0.3)[c] | 2.22 | 0.001 | 45.0 | 8.09 | 1440 |
| 13 | **S-43** (0.3)[c] | 2.22 | 0.0015 | 67.5 | 7.63 | 1440 |
| 14 | **S-43** (0.8) | 5.92 | 0.0012 | 20.2 | 5.95 | 1440 |
| 15 | **S-43** (0.8)[c] | 5.92 | 0.0023 | 38.8 | 5.80 | 1440 |
| 16 | **S-49** (0.3) | 0.822 | 0.0024 | 291 | 4.58 | 1440 |
| 17 | **S-49** (0.8)[c] | 2.19 | 0.0019 | 86.7 | 4.73 | 1440 |

*Conditions:* 6.68 bar ethylene, 1 h reaction time, 54 µL 1-hexene added, 4000 equivalents EADC as co-catalyst, heptane as solvent; [a] $\times 10^2$, [b] g/mmol.hr.bar; [c] repeated run.

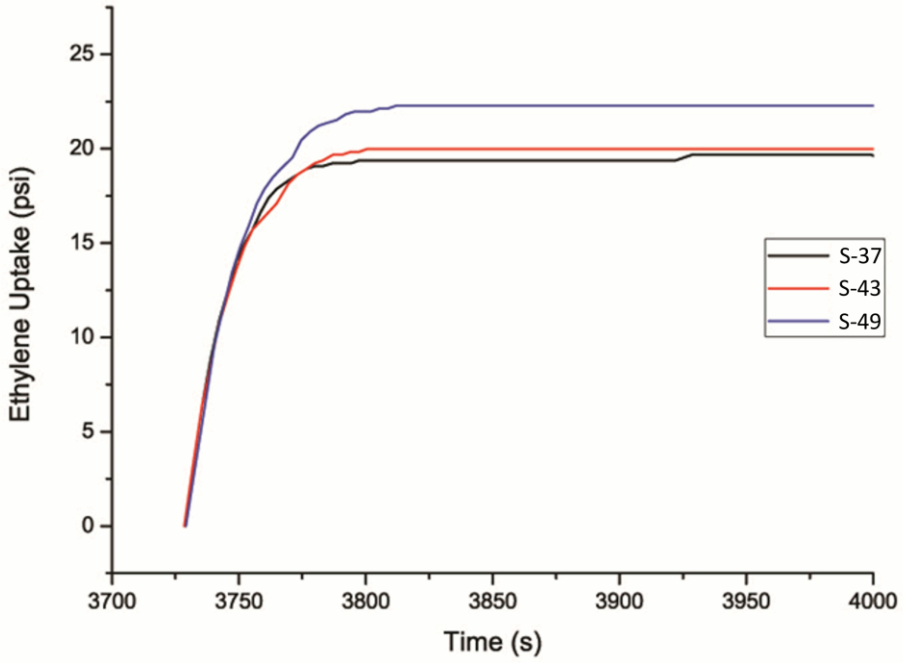


**Figure 3.13** Consumption profiles of **S-37**, **S-43** and **S-49** with EADC as co-catalyst and ETA as re-activator. Ethylene consumption is recorded after premixing of co-catalyst and pre-catalyst (≈ 1 h).

## 3.3 Conclusions

The representative results of the ethylene polymerisation screening show that, under homogeneous conditions, the combination of a niobium or tantalum pre-catalysts bearing an imine-based ligand set and the co-catalyst $MeAlCl_2$ (MADC) is capable, in the presence of ETA, of polymerizing ethylene with activities in excess of 11,000 g/mmol.hr.bar for niobium and 20,000 g/mmol.hr.bar for tantalum. High activity is maintained at elevated temperatures when the ligand set also contains a phenoxide moiety. In the case of niobium, such activities are two orders of magnitude greater than any previously reported systems. Use of $Me_2AlCl$ (DMAC) or $Me_3Al_2Cl_3$ (MASC) as the co-catalyst also yields highly active systems; activities also increase with increasing chloride content in the co-catalyst. Under more robust industrial conditions, use of MAO as co-catalyst for either the polymerisation of ethylene or co-polymerisation of ethylene with 1-hexene resulted in moderately active systems.

## 3.4 References


[1] L. Clowes (2011). *Group V pro-catalysts for the polymerisation of ethylene and ε-caprolactone*. University of East Anglia.

[2] C. Redshaw, M. Walton, L. Clowes, D. L. Hughes, A. M. Fuller, Y. M. Chao, A. Walton, V. Sumerin, P. Elo, I. Soshnikov, W. Z. Zhao, W. H. Sun, *Chem. Eur. J.,* **2013**, *19*, 8884.

[3] A. O. Eseola, W. Li, R. Gao, M. Zhang, X. Hao, T. Liang, N. O. Obi-Egbedi, W. H. Sun, *Inorg. Chem.,* **2009**, *48*, 9133.

[4] H. Tsurugi, T. Saito, H. Tanahashi, J. Arnold, K. Mashima, *J. Am. Chem. Soc.,* **2011**, *133*, 18673.

[5] Y. Nakayama, N. Maeda, T. Shiono, in *Stud. Surf. Sci. Catal., Vol. Volume 161* (Eds.: K. N. Takeshi Shiono, T. Minoru), Elsevier, **2006**, pp. 165-170.

[6] E. J. Roskamp, S. F. Pedersen, *J. Am. Chem. Soc.,* **1987**, *109*, 6551.

[7] J. Szymoniak, J. Besançon, C. Moïse, *Tetrahedron,* **1994**, *50*, 2841.

[8] K. Mashima, Y. Nakayama, N. Ikushima, M. Kaidzu, A. Nakamura, *J. Organomet. Chem.,* **1998**, *566*, 111.

[9] C. Redshaw, D. M. Homden, M. A. Rowan, M. R. J. Elsegood, *Inorg. Chim. Acta,* **2005**, *358*, 4067.

[10] A. Zanotti-Gerosa, E. Solari, L. Giannini, C. Floriani, N. Re, A. Chiesi-Villa, C. Rizzoli, *Inorg. Chim. Acta,* **1998**, *270*, 298.

[11] C. Redshaw, M. Rowan, D. M. Homden, M. R. Elsegood, T. Yamato, C. Perez-Casas, *Chem. Eur. J.,* **2007**, *13*, 10129.

[12] Y. R. Patil, *Olefins Polymerisation Reactivity of Niobium-Based Metal Complexes*, LAP Lambert Acad. Publ., **2011**.

[13] V. Murphy, X. Bei, T. R. Boussie, O. Brümmer, G. M. Diamond, C. Goh, K. A. Hall, A. M. Lapointe, M. Leclerc, J. M. Longmire, J. A. W. Shoemaker, H. Turner, W. H. Weinberg, *Chem. Rec.,* **2002**, *2*, 278.

[14] T. R. Boussie, G. M. Diamond, C. Goh, K. A. Hall, A. M. LaPointe, M. Leclerc, C. Lund, V. Murphy, J. A. Shoemaker, U. Tracht, H. Turner, J. Zhang, T. Uno, R. K. Rosen, J. C. Stevens, *J. Am. Chem. Soc.,* **2003**, *125*, 4306.

[15] W. Wang, K. Nomura, *Macromolecules,* **2005**, *38*, 5905.

# Chapter 4 – Zinc and Magnesium Pre-catalysts

## 4.1 Introduction

In **chapter 2**, calixarene compounds in combination with vanadium were explored for the polymerisation of ethylene. Whilst a great number of zinc and magnesium catalysts have been explored since the seminal work by Coates and co-workers,[1] most have ligand systems such as diphenolates,[2-3] and Schiff bases,[4] relatively few calix[4]arene-based catalysts for the ring opening polymerisation of lactide/ε-caprolactone have been examined,[5] and indeed, in the case of magnesium, there are few reported calix[4]arene complexes (See **Chapter 1**, pg 17 for details on previous magnesium and zinc based catalysts).[6] Generally ligands that are monoanionic are chosen for reaction with zinc/magnesium precursors as they will inevitably lead to a metal that still contains a viable nucleophilic group for ROP, which may be the reason *p-tert*-calix[4]arenes have rarely been utilized. Vigalok and co-workers have had success with zinc alkyl based calix[4]arenes and although the dialkoxycalix[4]arene ligand is dianionic when deprotonated its use leads to a dimetallic complex that still contain nucleophilic groups.[7]

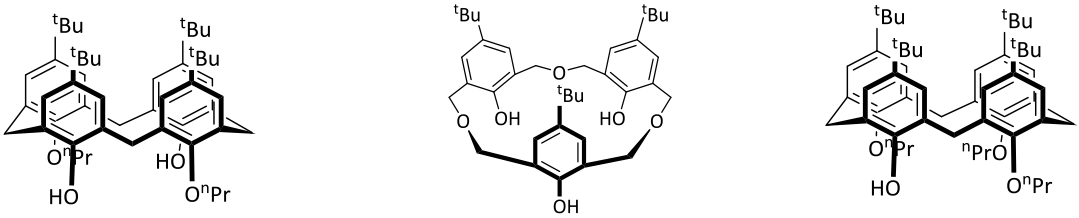


**L30H$_2$** **L31H$_3$** **L32H**

**Chart 4.1** Ligands utilized in this chapter.

Initially, calix[4]arene and oxacalix[3]arene ligands (See **Chart 4.1**) utilized for the synthesis of zinc and magnesium compounds and their subsequent polymerisation activity explored (**Chart 4.2**). While zinc compounds are often synthesized due to their higher tolerance of water, magnesium compounds generally give higher activities as ROP catalysts due to the more polarised M—O bond, and as such the synthesis of calix[4]arene compounds containing magnesium alkyls were targeted (**Chart 4.2**). Zinc compounds have been subjected to both ε-caprolactone and *rac*-lactide, while magnesium compounds have been utilized for *rac*-lactide polymerisation only. The effect of additional chain transfer agents and the tacticity of the resulting polymers are also presented.

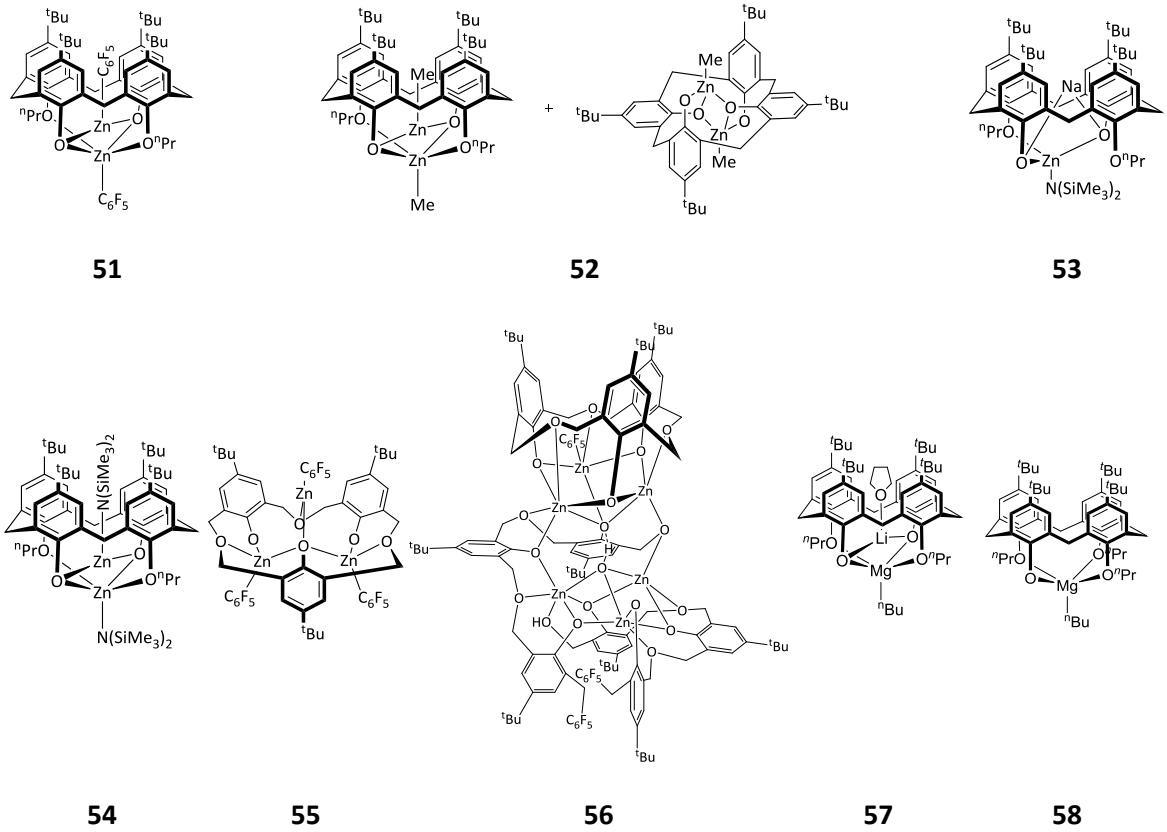


**Chart 4.2** Calixarene magnesium/zinc compounds reported in this chapter.

## 4.2 Results and Discussion

### *4.2.1 Synthesis of Zinc Calix[4]arene Compounds*

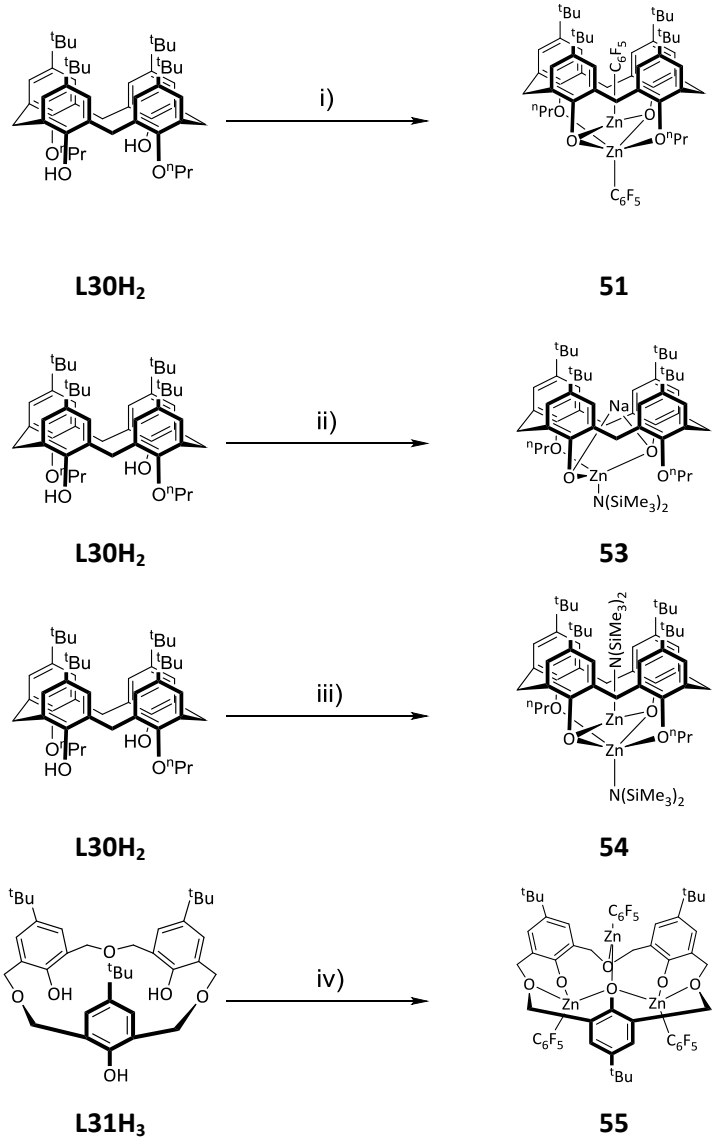


**Scheme 4.1** Synthesis of zinc compounds **51** – **55**. i) 2 $Zn(C_6F_5)_2$.tol, toluene, reflux, 16 h. ii) 2 $Zn(N(SiMe_3)_2)_2$, toluene, reflux, 72 h. iii) 1) 2 NaH, THF, 16hr, room temperature, 2) $ZnCl_2$, THF, 2hr, RT, 3) $Na(N(SiMe_3)_2)$, THF, 2 hr, RT. iv) 3 $Zn(C_6F_5)_2$.tol, toluene, RT, 2 h.

1,3-dipropoxy-*p*-*tert*-butyl-calix[4]arene (**L30H$_2$**) and *p*-*tert*-butylhexahomotrioxacalix[3]arene (**L31H$_3$**) ligands were synthesized following the known procedures.[8-9] The treatment of 1,3-dipropoxy-*p*-*tert*-butyl-calix[4]arene with $Zn(C_6F_5)_2$.toluene in refluxing toluene led to the isolation of compound **51**.

The *n*-propoxy calix[4]arene derivative was employed since Vigalok and co-workers had shown that the calixarene derivatives containing smaller alkyl chains led to more complex products, including partial and 1,3-alternate cone conformations, indeed in this case the cone conformation was isolated exclusively.[10] Crystallization of compound **51** from hot acetonitrile led to formation of clear blocks which were suitable for single crystal diffraction. Compound **51** crystallises with two pentafluorophenyl zinc fragments, one outside from the calix[4]arene backbone and one within the cavity. The protruding zinc metal centre is five co-ordinate in a trigonal bipyramidal geometry bonding to all four of the calix[4]arene oxygen, whereas the encapsulated zinc is trigonal planar and only binds to the non-propoxy oxygen atoms. The structure of compound **51** is depicted in **Figure 4.1**, selected bond lengths/angles are given in the legend.

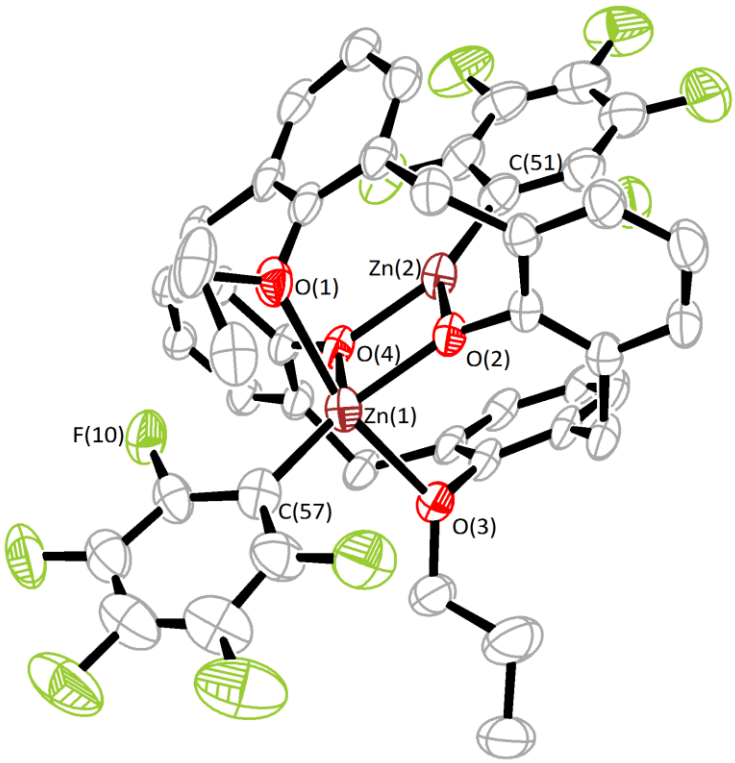


**Figure 4.1** ORTEP representation of compound **51**. Hydrogen atoms, *tert*-butyl groups and minor disordered components have been removed for clarity. Displacement ellipsoids are drawn at the 50% probability level. Selected bond lengths (Å) and angles (°): Zn(1)—O(1) 2.346(2), Zn(1)—O(2) 1.9680(19), Zn(1)—O(3) 2.312(2), Zn(1)—O(4) 1.964(2), Zn(2)—O(2) 1.955(2), Zn(2)—O(4) 1.931(2), Zn(1)—C(57) 1.941(13), Zn(1)—C(57X) 1.996(12), Zn(2)—C(51) 1.944(3), O(4)—Zn(1)—O(2) 79.15(8), O(4)—Zn(2)—O(2) 80.25(8), Zn(2)—O(2)—Zn(1) 99.80(8), Zn(2)—O(4)—Zn(1) 100.80(8).

Disappointingly, the polymerisation screening of compound **51** indicated no reaction between the benzyl alcohol (BnOH) and the Zn—$C_6F_5$ moiety, which is also the conclusion obtained by Schnee *et al* and Piedra-Arroni *et al.*[11-12] The catalyst is behaving through an 'activated monomer' rather than 'co-ordination insertion' pathway and also exhibits a much lower activity than the previous Zn—$C_6F_5$ containing compounds.[11-12] To ensure that the polymerisation would proceed through a 'co-ordination insertion' mechanism the replacement of the pentafluorophenyl group with a more nucleophilic group (such as an alkoxide or amide) was targeted. To isolate a zinc alkoxide, firstly the methyl zinc derivative was synthesized following the literature procedure (compound **52**).[7] In the literature report single crystals of compound **52** were not isolated. In constrast we isolated crystals suitable for single crystal X-ray diffraction from a saturated light petroleum solution.

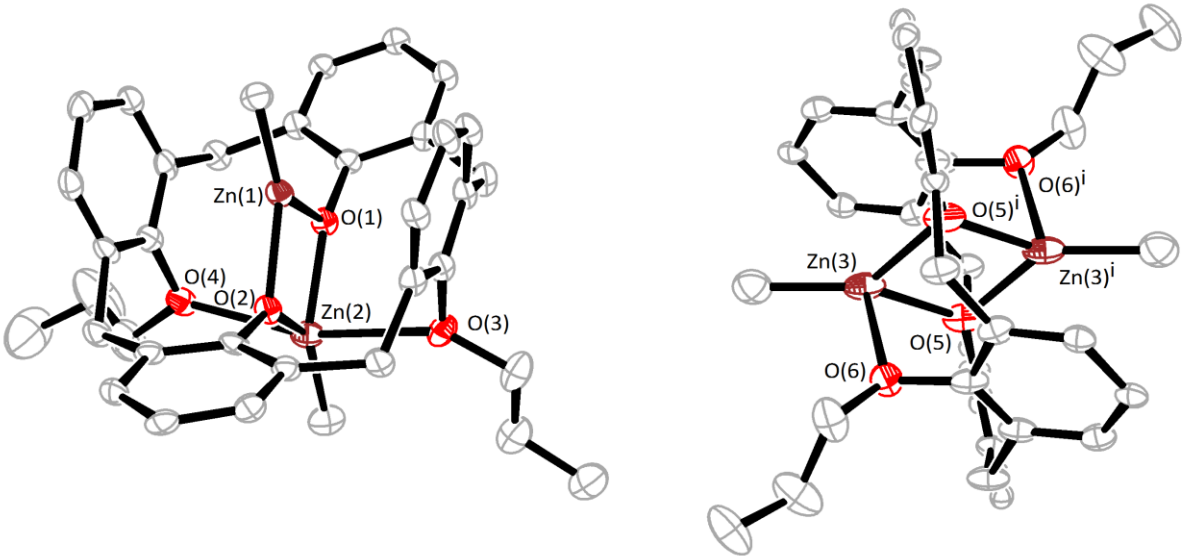


**Figure 4.2** ORTEP representation of compound **52**. Hydrogen atoms, *tert*-butyl groups and minor disordered components have been removed for clarity. Thermal ellipsoids are drawn at the 50% probability level. Selected bond lengths (Å) and angles (°): Cone: C(51)—Zn(1) 1.942(5), C(52)—Zn(2) 1.955(5), O(1)—Zn(1) 1.972(3), O(1)—Zn(2) 1.978(3), O(2)—Zn(1) 1.970(3), O(2)—Zn(2) 1.984(3), O(4)—Zn(2) 2.360(3), Zn(1)—O(1)—Zn(2) 101.26(14), Zn(1)—O(2)—Zn(2) 101.12(13), O(2)—Zn(1)—O(1) 78.95(13), C(52)—Zn(2)—O(1) 139.96(19), C(52)—Zn(2)—O(2) 141.36(19), O(1)—Zn(2)—O(2) 78.47(13). Partial Cone: C(78)—Zn(3) 1.941(6), C(78)—Zn(3) 1.941(6), O(5)—Zn(3) 1.981(4), O(5)—Zn(3)$^i$ 1.985(4), O(6)—Zn(3) 2.211(3), Zn(3)—O(5)$^i$ 1.985(4), Zn(3)—O(5)—Zn(3)$^i$ 104.49(16), O(5)—Zn(3)—O(5)$^i$ 75.51(16), O(5)—Zn(3)—O(6) 86.70(13), O(5)$^i$—Zn(3)—O(6) 90.36(14).

The structure of compound **52** was assigned based on $^1$H NMR data and similarity to the ethyl derivative.[7] Surprisingly the crystal structure of compound **52** shows both the cone and partial cone conformations within the unit cell (although the partial cone is better described as a chair

conformation); the $^{1}$H NMR spectrum ($CDCl_3$) indicates that only the cone conformation is present in solution, which matches the literature characterisation data.[7] The cone conformation is very similar to compound **51**, again the *exo*-Zn is trigonal bipyramidal and the *endo*-Zn is trigonal planar. In the chair conformation, there is a centre of inversion in the middle of the calix[4]arene. The zinc metal centres are in the base of a trigonal pyramid with the *n*-propoxy oxygen at the apex.

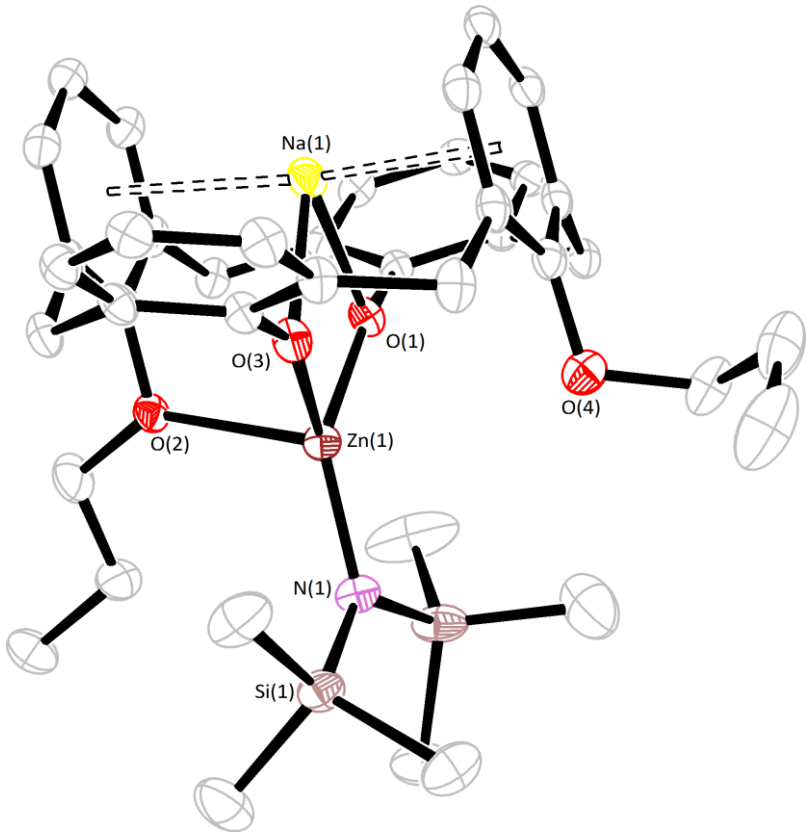


**Figure 4.3** ORTEP representation of compound **53**. Hydrogen atoms, *tert*-butyl groups and disorder have been removed for clarity. Thermal ellipsoids are drawn at the 50 % probability level. Selected bond lengths (Å) and angles (°): Zn(1)—N(1) 1.8929(13), Zn(1)—O(1) 1.9297(10), Zn(1)—O(3) 1.9402(10), Zn(1)—O(2) 2.2760(10), N(1)—Zn(1)—O(1) 131.42(5), N(1)—Zn(1)—O(3) 134.32(5), O(1)—Zn(1)—O(3) 88.46(5), N(1)—Zn(1)—O(2) 109.26(5), O(1)—Zn(1)—O(2) 87.08(4), O(3)—Zn(1)—O(2) 91.34(4).

The treatment of (compound **52**) with alcohol (MeOH, $^{i}$PrOH) at -80 °C does not form the alkoxide; only starting material is detected. At higher temperatures free calix[4]arene is formed suggesting the alcohol displaces the calix[4]arene, a similar result was reported by Drouin *et al*.[13] Zinc silylamides have previously been shown to be active for ROP of *L*-lactide and as such the synthesis of a calixarene zinc silylamide was targeted. Treatment of 1,3-dipropoxy-*p*-*tert*-butyl-calix[4]arene with

$Zn(N(SiMe_3)_2)_2$, synthesized *in situ*, in refluxing toluene led to the isolation of compound **53**. Rather than the expected formation of a dizinc silylamide species, where one Zn—$N(SiMe_3)_2$ fragment is present in the cavity, compound **53** contains a sodium cation within the cavity. The sodium cation is believed to originate from unreacted sodium hexamethyldisilazane from the *in situ* synthesis of $Zn(N(SiMe_3)_2)_2$.

The stepwise reaction of 1,3-dipropoxy-*p*-*tert*-butylcalix[4]arene and sodium hydride, followed by $ZnCl_2$ and finally $NaN(SiMe_3)_2$ led to the formation of compound **53** in good yield (50%). The crystal structure was determined by X-ray diffraction (**Figure 4.3**). The zinc metal centre is bound to three of the oxygen from the calixarene, the two phenolic oxygen and one of the *n*-propoxy oxygen atoms. The dative O—Zn bond length is significantly longer than the other two as expected, 2.2760(10) *vs.* 1.9297(10) and 1.9402(10). The N—Zn bond is 1.8929(13). The sodium cation occupies the calix[4]arene cavity and contains π interactions with two opposite aryl rings, both $\eta^6$, the centroid distances are 2.741 and 2.607 Å. The interaction between the sodium cation and one of the $\eta^6$-centroids causes a pinching of the calixarene so that the final OR group is far enough that it doesn't participate in dative bonding to the zinc metal; the zinc metal centre is therefore in the base of a trigonal pyramid rather than in trigonal bipyramidal geometry seen in compound **51**. The sodium and zinc centres are 3.1725(7) Å apart. The originally envisaged dizinc silylamide, compound **54**, was synthesized from the reaction between two equivalents of zinc bis(hexamethyldisilyl amide), and 1,3-dipropoxy-*p*-*tert*-butylcalix[4]arene in toluene. Attempts to crystalize the product from THF/light petroleum, acetonitrile and pentane were unsuccessful; the compound was exceptionally soluble in each solvent. The volatiles from the reaction were removed *in vacuo* to give a yellow solid. The $^1$H NMR spectrum, elemental analysis and mass spectrum all match the structure as depicted in **Scheme 4.1**. The $^1$H NMR spectra is consistent with the calix[4]arene in cone conformation and is similar to the recorded spectrum from compound **51**.

We have further explored oxacalix[3]arene based zinc compounds. The reaction between three equivalents of $Zn(C_6F_5)_2$.toluene and oxacalix[3]arene at room temperature led to formation of compound **55** after removal of volatiles, however the attempted crystallisation from hot acetonitrile caused the ring opening of the parent oxacalix[3]arene and rearrangement to complex **56**. The ability for a metallic species to open the ether linkages of the oxacalix backbone is not unheard of, Iglesia and co-workers proposed a similar product from a $Ti/SiO_2$ grafted oxacalix[3]arene,[14] however this is the first structurally defined result. Unfortunately, suitable single crystals of compound **55** could not be grown. The $^1$H NMR spectrum shows that the complex exists in a partial cone conformation; there are three distinct sets of doublets for each of the methylene bridges and there is a two to one

integration for the two discrete *tert*-butyl peaks. The $^{19}F$ NMR spectra also show a two to one integration for each of *ortho*- and *para*-fluorine signals; the *meta*-fluorine signals overlap. Compound **55** has also been characterised by mass spectrometry and elemental analysis matching the structure depicted in **Scheme 4.1**.

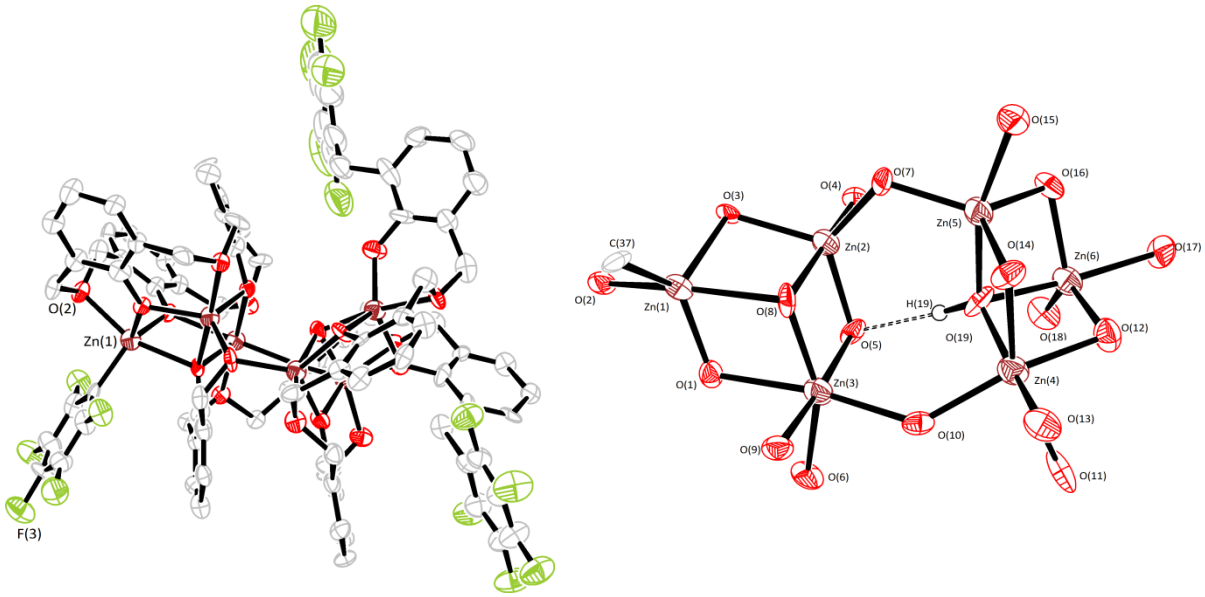


**Figure 4.4** ORTEP representation of compound **56** (left) and core of compound **56** (right). Hydrogen atoms except for those participating in hydrogen bonding in the core of compound **56** (H19), *tert*-butyl groups, solvent molecules and disorder have been removed for clarity. Selected bond lengths (Å): Zn1—O1 1.965 (9), Zn1—C37 2.000 (13), Zn1—O3 2.047 (8), Zn1—O2 2.155 (8), Zn1—O8 2.240 (7), Zn2—O7 1.942 (8), Zn2—O4 2.014 (8) Zn2—O3 2.040 (7), Zn2—O5 2.043 (9), Zn2—O8 2.100 (8), Zn3—O8 2.019 (9), Zn3—O6 2.047 (8), Zn3—O10 2.100 (8), Zn3—O5 2.105 (8), Zn3—O9 2.148 (8), Zn3—O1 2.270 (7), Zn4—O19 2.028 (8), Zn4—O13 2.052 (10), Zn4—O10 2.066 (8), Zn4—O12 2.071 (8), Zn4—O14 2.120 (9), Zn5—O7 1.941 (7), Zn5—O14 1.968 (8), Zn5—O16 2.028 (8), Zn5—O19 2.042 (8), Zn5—O15 2.154 (9), Zn6—O18 1.895 (8), Zn6—O12 2.014 (9), Zn6—O16 2.020 (8), Zn6—O19 2.025 (8), Zn6—O17 2.133 (8).

The ring opened oxacalix[3]arene compound **56** was analysed by single crystal X-ray diffraction and shows three separate oxacalix[3]arene ligands within the molecule, two of which have been ring opened with formation of two carbon—$C_6F_5$ bonds and a protonated oxygen that hydrogen bonds to a MeCN molecule or an oxygen anion that forms two short bonds with two $Zn^{2+}$ (See **Figure 4.4**). The remaining oxacalix[3]arene is intact. There are six zinc metal centres within the compound, one of which is bound to a $C_6F_5$ ring. The core of the molecule consists of two $Zn_3O_4$ cubes missing one corner linked via two O atoms and supported with an O—H···O hydrogen bond. The resulting $^1H$ NMR spectra is complex due to the lack of symmetry, there are nine separate *tert*-butyl signals. The $^{19}F$ NMR spectrum consists of nine peaks indicating three unique $C_6F_5$ fragments. The elemental analysis

results are within 1.2% of the expected values, while the molecular ion was not observable using mass spectrometry. Compounds **51**, **53** – **55** were tested for the polymerisation of ε-caprolactone and *rac*-lactide.

### *4.2.2 Synthesis of Magnesium Calix[4]arene Compounds*

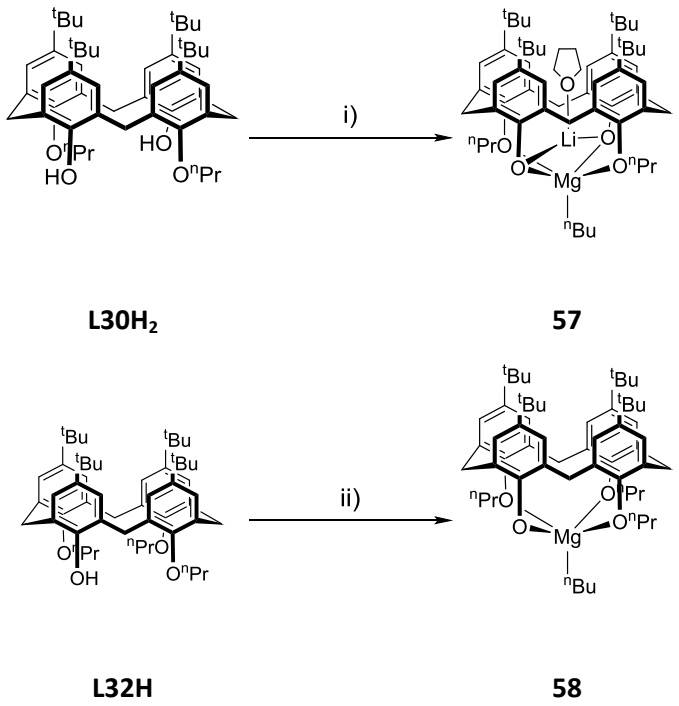


**Scheme 4.2** Synthesis of magnesium compounds **57** and **58**. i) 1) 2 *n*-BuLi, THF, 0 °C, 1 hr, 2) *n*-BuMgBr, THF, 0 °C, 1 hr. ii) *n*-$Bu_2Mg$, THF, 3 hr, 0 °C.

Given that magnesium compounds have been shown to have exceptional activity for the ring opening polymerisation of *rac*-lactide, higher than their zinc counterparts,[1, 15-16] we initially attempted the synthesis of a di(alkyl magnesium)calix[4]arene, similar to the zinc methyl species of Vigalok and co-workers (compound **52**),[7] by reaction of two equivalents of di-*n*-butyl magnesium and 1,3-dipropoxy-*p-tert*-butyl-calix[4]arene in tetrahydrofuran at 0 °C. However, this led to the immediate formation of a white precipitate which was insoluble in common solvents. It is possible one equivalent of the magnesium methyl precursor was reacting with two of the phenolic groups rather than forming a bimetallic calix[4]arene as previously encountered in zinc chemistry.[7] To overcome this, first the 1,3-dipropoxy-*p-tert*-butyl-calix[4]arene was lithiated by treatment with *n*-butyllithium in THF, thereby removing any phenolic protons, and subsequently reacting the lithiated calix[4]arene with two equivalents of *n*-BuMgBr. The reaction proceeded without formation of a precipitate, while it is probable there is formation of a so called 'turbo-Grignard reagent' with any excess Grignard reagent,[17] the fate of the presumably formed lithium bromide is currently unknown. Reaction of the lithiated calix[4]arene with an excess of *n*-BuMgBr led to the same product. Crystals of compound **57** suitable for single crystal X-ray crystallography (see **Figure 4.5**) were grown from the slow diffusion of

light petroleum into a THF solution. Rather than formation of a di-magnesium alkyl complex, only one of the lithiated oxygen reacted with the Grignard reagent, thus forming a hetero-bimetallic complex. The lithium cation was found to reside inside the calix[4]arene cavity, similarly to previous observations of other metallocalix[4]arene systems,[18-21] the magnesium centre bearing an *n*-butyl group is bound to the four oxygens of the lower rim; the Mg—O bonds to the alkoxy groups [O(1)/O(3)] at ≈ 2.34 Å are, as expected, somewhat longer than those to the phenolic groups [O(2)/O(4)] at ≈ 1.93 Å. The magnesium and lithium metal centres are 2.670(5) Å apart, with the magnesium metal centre adopting distorted trigonal bipyramidal geometry. The THF oxygen, lithium, magnesium and carbon of the *n*-butyl group are all essentially linear as represented by the angles between O(5)—Li(1)—Mg(1) and C(61)—Mg(1)—Li(1), 176.77(16) and 179.2(3), respectively. There is also a slight difference in angle around the magnesium between the non-propoxy oxygen atoms O(2)/O(4) and C(61) in the equatorial plane, the angle between O(2) and C(61) is slightly larger than that of O(4) and C(61), 137.75(13)° *vs*. 131.36(13)°.

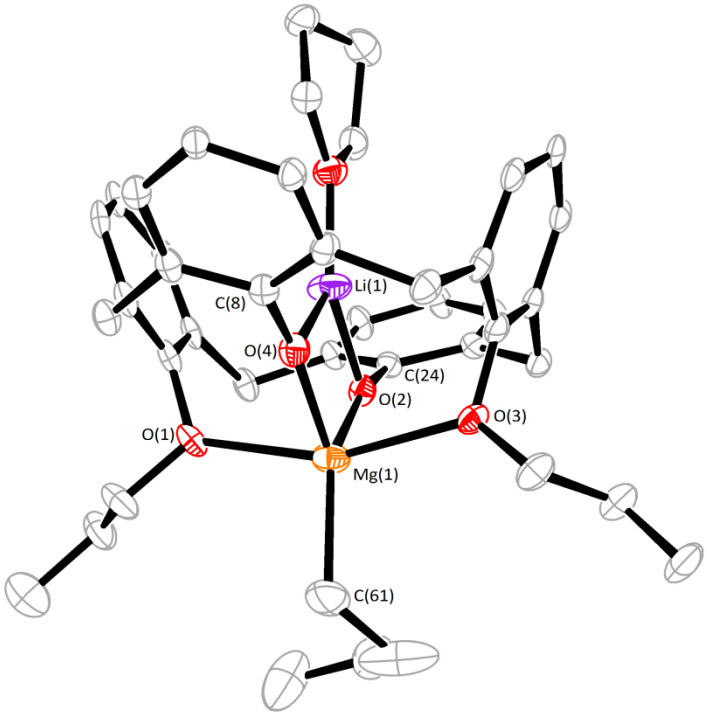


**Figure 4.5** ORTEP representation of compound **57**. Hydrogen atoms, *tert*-butyl groups and minor disordered components have been removed for clarity. Displacement ellipsoids are drawn at the 50% probability level. Selected bond lengths (Å) and angles (°): Li(1)—O(5) 1.867(5), Li(1)—O(2) 1.903(5), Li(1)—O(4) 1.904(5), Mg(1)—O(1) 2.373(2), Mg(1)—O(2) 1.9261(19), Mg(1)—O(3) 2.302(2), Mg(1)—O(4) 1.9356(19). Mg(1)—C(61) 2.146(3). C(61)—Mg(1)—Li(1) 176.77(16), O(5)—Li(1)—Mg(1) 179.2(3), O(2)—Mg(1)—C(61) 137.75(13), O(4)—Mg(1)—C(61), 131.36(13).

**Table 4.1** Selected structural data for **57** and **XIX**. [6]

| Bond length (Å)/Angle (°) | 57 | XIX |
|---|---|---|
| Mg(1)—O(1)/(3) | 2.373(2)/2.302(2) | 2.232(4) |
| Mg(1)—O(2)/O(4) | 1.9261(19)/1.9356(19) | 1.849(4) |
| Mg(1)—L | 2.146(3) | 2.033(4) |
| C(24)—O(2)—Mg(1) | 166.04(16) | 147.2(4) |
| C(8)—O(4)—Mg(1) | 162.96(16) | 147.2(4) |

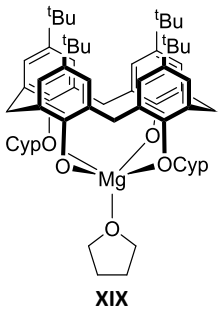


**XIX**

Similar structures based on alkali and alkali earth metals have previously been reported by Floriani and co-workers;[6] in particular the treatment of 1,3-dicyclopentoxy-*p*-*tert*-butyl-calix[4]arene with magnesium anthracene led to the formation of [(*p*-$^t$Bu-calix[4]-$(OCyp)_2$-$(O)_2$)Mg(thf)] (see **Table 4.1**, **XIX**). The structure of **XIX** is similar to compound **57**; compound **57** contains both a lithium and THF molecule within the cavity whereas **XIX** contains only a THF molecule. The presence of the lithium centre within the cavity of **57** forces the calixarene further into an elliptical conformation as shown by the bond angles between C(24)—O(2)—Mg(1)/C(8)—O(4)—Mg(1). Each of the Mg—O bonds are extended in compound **57** *vs.* **XIX** (see **Table 4.1**). Compound **57** has also been characterised by $^1$H and $^{13}$C NMR spectroscopy, mass spectrometry, elemental analysis and IR spectroscopy.

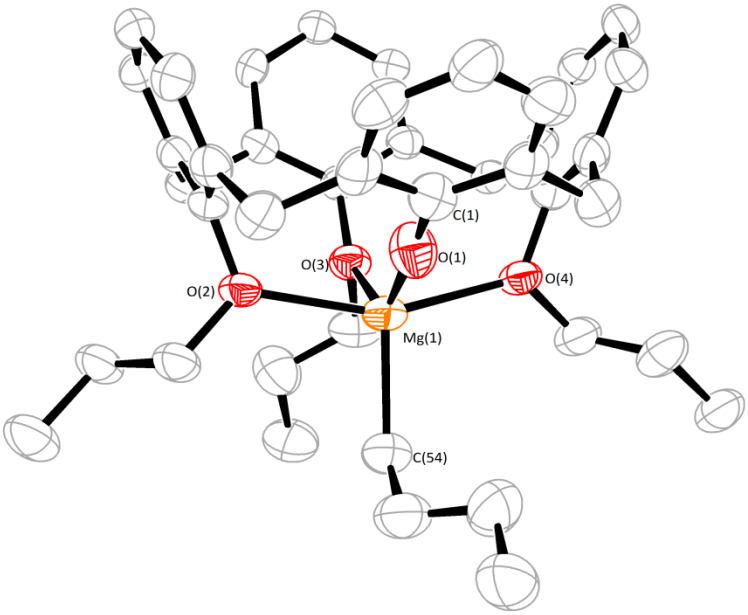


**Figure 4.6** ORTEP representation of compound **58**·(pentane)**.** Hydrogen atoms, *tert*-butyl groups and a pentane molecule located in the calixarene cavity have been removed for clarity. Displacement ellipsoids are drawn at the 50 % probability level. Selected bond lengths (Å) and angles (°): Mg(1)—O(1) 1.860(4), Mg(1)—O(2) 2.247(3), Mg(1)—O(3) 2.145(3), Mg(1)—O(4) 2.255(3), Mg(1)—C(54)

2.152(5), O(1)—C(1) 1.309(5), O(1)—Mg(1)—O(3) 128.07(15), O(1)—Mg(1)—C(54) 127.0(2), O(3)—Mg(1)—C(54) 104.89(17), O(2)—Mg(1)—C(54) 101.62(18), O(4)—Mg(1)—C(54) 100.88(18), C(1)—O(1)—Mg(1) 175.8(3), O(2)—Mg(1)—O(4) 156.69(12).

To synthesize a mono-metallic magnesium species, we employed a tripropoxy-*p*-*tert*-butylcalix[4]arene ligand. Tripropoxy-*p*-*tert*-butylcalix[4]arene (**L32H**) was synthesized according to the method of Zhong *et al*,[22] and was then treated with one equivalent of di-*n*-butyl magnesium in THF. Single crystals of the product **58**.pentane, [**L32**Mg(*n*-Bu)] with a disordered alkyl molecule, suitable for X-ray diffraction, were grown from a saturated light petroleum solution (**Figure 4.6**). We note that although the electron density from single crystal X-ray diffraction indicate a disordered pentane molecule; it is probable that a number of different alkane molecules, from the petroleum fraction used, occupy the calixarene cavity. The solid structure of the compound contains disordered solvent within the cavity, and a magnesium *n*-butyl fragment is again bound to the lower rim of the calix[4]arene. The magnesium centre adopts a disordered trigonal bipyramidal geometry, the axial O(2)—Mg—O(4) bond angle is 156.69(12)°. The bond length for the phenolic oxygen and magnesium, O(1)—Mg(1), 1.860(4) Å is significantly shorter than the OR bond lengths, 2.145(3) – 2.255(3) Å, as expected. The equatorial RO-Mg bond, O(3)—Mg(1), is the shortest of the three, 2.145(3) *vs.* 2.255(3) and 2.247(3). The C(1)—O(1)—Mg(1) bond angle is almost linear, 175.8(3)°; in contrast the Calix-OR-Mg angles are 121.1(2) – 121.6(2)° for the axial and 133.8(2)° for the equatorial positions. Compound **58** has also been characterised by $^{1}$H and $^{13}$C NMR spectroscopy, mass spectrometry, elemental analysis and IR spectroscopy. Compounds **57** and **58** were screened for *rac*-lactide ring opening polymerisation studies and the results reported in **Table 4.3**.

### *4.2.3 Polymerisation Results using zinc compounds*

**Table 4.2** ROP of ε-caprolactone/*rac*-lactide using zinc compounds **51** – **55**.

| Run | Pre- Cat | Solvent | Monomer | T (°C) | M : BnOH | Time (hr) | Conv[a] (%) | $M_{n,GPC}$ | $M_{n,Cal}$ | PDI |
|---|---|---|---|---|---|---|---|---|---|---|
| 1 | **51** | Toluene | ε-caprolactone | 20 | 25 : 1 | 24 | - | | | |
| 2 | **51** | THF | ε-caprolactone | 20 | 25 : 1 | 24 | - | | | |
| 3 | **51** | $CH_2Cl_2$ | ε-caprolactone | 20 | 25 : 1 | 24 | - | | | |
| 4 | **51** | Toluene | ε-caprolactone | 60 | 25 : 1 | 24 | - | | | |
| 5 | **51** | Toluene | ε-caprolactone | 80 | 25 : 1 | 3 | 96 | | | |
| 6 | **51** | Toluene | ε-caprolactone | 100 | 25 : 0 | 2 | 95 | | | |
| 7 | **51** | Toluene | ε-caprolactone | 100 | 25 : 1 | 1 | 98 | | | |
| 8 | **51** | Toluene | ε-caprolactone | 100 | 100 : 1 | 3 | 85 | 4,760 | 9,700 | 1.06 |
| 9 | **51** | Toluene | ε-caprolactone | 100 | 200 : 1 | 4 | 90 | 7,600 | 20,500 | 1.48 |
| 10 | **53** | THF | ε-caprolactone | 20 | 100 : 1 | 24 | 21 | | | |
| 11 | **53** | Toluene | ε-caprolactone | 20 | 100 : 1 | 24 | 21 | | | |
| 12 | **54** | THF | ε-caprolactone | 20 | 100 : 1 | 4 | 27 | | | |
| 13 | **54** | Toluene | ε-caprolactone | 20 | 100 : 1 | 4 | 65 | 11,900 | 7,920 | 1.27 |
| 14 | **54** | Toluene | ε-caprolactone | 20 | 100 : 2 | 4 | 49 | 4,740 | 2,800 | 1.27 |
| 15 | **54** | Toluene | ε-caprolactone | 20 | 200 : 4 | 4 | 47 | 4,500 | 2,680 | 1.18 |
| 16 | **55** | Toluene | ε-caprolactone | 20 | 100 : 1 | 24 | - | | | |
| 17 | **55** | Toluene | ε-caprolactone | 40 | 100 : 1 | 24 | - | | | |
| 18 | **55** | Toluene | ε-caprolactone | 80 | 100 : 1 | 2 | 77 | 2,800 | 8,800 | 1.07 |
| 19 | **55** | Toluene | ε-caprolactone | 100 | 100 : 1 | 1 | 95 | 2,970 | 10,800 | 1.11 |
| 20 | **51** | Toluene | *rac*-lactide | 100 | 100 : 1 | 3 | 90 ($P_r$ = 0.62) | 1,440 | 13,000 | 1.26 |
| 21 | **54** | Toluene | *rac*-lactide | 20 | 100 : 1 | 5 | 64 ($P_r$ = 0.54) | 8,970 | 9,220 | 1.13 |
| 22 | **55** | Toluene | *rac*-lactide | 100 | 100 : 1 | 3 | 52 | | | |

**Conditions**: Polymerisation carried out using 60 µmol catalyst at 20 °C, $[Monomer]_0$ = 0.6 M, 10 mL solvent, ROH taken from a ROH/toluene solution. [a] Determined by NMR spectroscopy, [b] Calculated from ($[Monomer]_0/[OH]_0$) x conv.(%) x Monomer molecular weight + ROH. $M_n$ GPC values corrected considering Mark-Houwink factors (0.58 polylactide/0.56 poly(ε-caprolactone)) from polystyrene standards in THF.[23-24]

Compound **51** was screened for the polymerisation of ε-caprolactone and at room temperature compound **51** was inactive using dichloromethane, tetrahydrofuran and toluene (**Table 4.2**, runs 1 – 3). Only at temperatures greater than 80 °C was compound **51** found to be active for the polymerisation of ε-caprolactone; polymerisation without benzyl alcohol was detrimental to the catalytic system (**Table 4.2**, 5 – 7). Compound **51** only active for the ROP of *rac*-lactide at high temperature, in both cases (ε-caprolactone and *rac*-lactide screening) high conversion rates can be achieved at high temperature, however the resulting polymer molecular weight is much lower than

expected; this indicates that there are significant *trans*-esterification reactions occurring at this temperature. Screening of compound **54**, featuring a $N(SiMe_3)_2$ group, was active at room temperature and can convert 100 equivalents of ε-caprolactone to 65% completion in 4 hours in toluene (**Table 4.2**, run 11), the polymer molecular weight is close to the expected values; lower activity was observed using THF. Compound **53**, which differs from compound **54** by replacement of the $Zn—N(SiMe_3)_2$ in the calix[4]arene cavity with a sodium cation, was not active under the same conditions as compound **54**. Comparably to compound **51**, compound **55** was only active for the ROP of *rac*-lactide and ε-caprolactone at high temperatures (100 °C) and gave molecular weight ε-caprolactone much lower than expected. The polymerisation using compound **55** is further complicated due to the probability of forming a species similar to compound **56**, which we did not screen for polymerisation studies. All of the zinc compounds screened have low PDI values (1.06 – 1.48).

### *4.2.4 Polymerisation Results using magnesium compounds*

Initially, the ring opening polymerisation of *rac*-lactide was attempted using benzyl alcohol (BnOH) as an activator for compound **57** (100 : 1 : 1) in THF (10 mL), however quenching this reaction with excess methanol led to the formation of methyl-(*RS*)-lactate rather than any polymerisation products (See **Scheme 4.3**). Clearly polymerisation has not occurred and a species capable of ring-opening *rac*-lactide is generated on quenching. Sobota and co-workers have recently reported a magnesium catalyst for the chemo-selective ring opening of *rac*-lactide related to our failed quenching method.[25] For subsequent screening we used a drop of dilute hydrochloric acid (0.1 M) to quench the polymerisation. We found that using one equivalent of MeOH in combination with compound **57** was more active for ROP of *rac*-lactide in dichloromethane ($CH_2Cl_2$) rather than THF or toluene (**Table 4.3**, runs 1 – 3, 55% *vs.* 35% and 9.4%, 100 equivalents *rac*-lactide, 60 min). The molecular weight of the polymer obtained in $CH_2Cl_2$ was almost double the expected values. The degradation of a magnesium butyl compound in $CH_2Cl_2$ was also observed by Chisholm *et al*;[16] the magnesium butyl group has presumably reacted with the dichloromethane to form a magnesium chloride moiety incapable of ROP, leading to a higher than expected monomer : catalyst ratio. Compound **57** exhibited low activity when isopropanol, *tert*-butanol or benzyl alcohol were used instead of methanol, and was inactive without the addition of any alcohol.

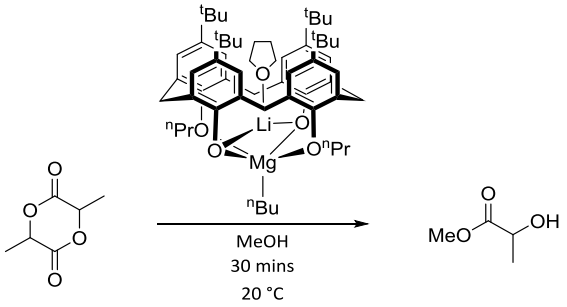


**Scheme 4.3** Reaction of compound **57** with *rac*-lactide in excess MeOH

In contrast to **57**, compound **58** showed increased activities in THF and toluene, rather than $CH_2Cl_2$ (**Table 4.3**, runs 10 – 12). The molecular weight was higher than expected in all three solvents, much more so in $CH_2Cl_2$ than in THF or toluene indicating a degradation of the catalyst. Addition of i-PrOH, t-BuOH or BnOH rather than MeOH led to increased activities, especially in the case of BnOH which gave 92% conversion of 100 equivalents of *rac*-lactide over 3 min (**Table 4.3**, run 16). Compound **58** was also more active without the addition of MeOH in THF, indicating the MeOH can deactivate the catalytic system. The molecular weight of the polymers obtained in THF using i-PrOH, t-BuOH and

BnOH were close to the expected values, and additional benzyl alcohol also acts as a chain transfer agent controlling the resultant chain length giving the catalytic system 'immortal' character (**Table 4.3**, runs 16 – 18). The use of toluene as solvent with BnOH also gives a highly active catalytic system with complete conversion of *rac*-lactide over 5 minutes (**Table 4.3**, runs 20 – 22) with good chain length control and 'immortal' character.

**Table 4.3** ROP of *rac*-lactide using magnesium compounds **57** and **58**

| Run | Cat | Solvent | M : ROH | Time (min) | Conv[a] (%) | $P_r$[a,b] | $M_{n,GPC}$ | $M_{n,Cal}$ | PDI |
|---|---|---|---|---|---|---|---|---|---|
| 1 | **57** | toluene | 100 : 1 (MeOH) | 60 | 9.4 | - | | | |
| 2 | **57** | THF | 100 : 1 (MeOH) | 60 | 35 | - | 2,330 | 5,080 | 1.09 |
| 3 | **57** | $CH_2Cl_2$ | 100 : 1 (MeOH) | 60 | 55 | - | 15,400 | 7,960 | 1.22 |
| 4 | **57** | $CH_2Cl_2$ | 100 : 0 | 480 | trace | - | | | |
| 5 | **57** | $CH_2Cl_2$ | 100 : 1 ($^{i}$PrOH) | 60 | 6.3 | - | | | |
| 6 | **57** | $CH_2Cl_2$ | 100 : 1 ($^{t}$BuOH) | 60 | 12 | - | | | |
| 7 | **57** | $CH_2Cl_2$ | 100 : 1 (BnOH) | 60 | 8.8 | - | | | |
| 8 | **57** | $CH_2Cl_2$ | 100 : 2 (MeOH) | 90 | 80 | 0.41 | 4,460 | 5,780 | 1.15 |
| 9 | **57** | $CH_2Cl_2$ | 100 : 4 (MeOH) | 120 | 94 | 0.42 | 1,790 | 3,400 | 1.19 |
| 10 | **58** | $CH_2Cl_2$ | 100 : 1 (MeOH) | 120 | 55 | 0.49 | 15,500 | 7,960 | 1.12 |
| 11 | **58** | THF | 100 : 1 (MeOH) | 120 | 65 | 0.73 | 12,400 | 9,400 | 1.44 |
| 12 | **58** | Toluene | 100 : 1 (MeOH) | 120 | 61 | 0.30 | 11,700 | 8,820 | 1.98 |
| 13 | **58** | THF | 100 : 0 | 30 | 28 | - | | | |
| 14 | **58** | THF | 100 : 1 ($^{i}$PrOH) | 30 | 97 | 0.79 | 13,600 | 14,000 | 1.46 |
| 15 | **58** | THF | 100 : 1 ($^{t}$BuOH) | 30 | 95 | 0.79 | 15,600 | 13,800 | 1.40 |
| 16 | **58** | THF | 100 : 1 (BnOH) | 3 | 92 | 0.85 | 14,800 | 13,400 | 1.25 |
| 17 | **58** | THF | 100 : 2 (BnOH) | 5 | 95 | 0.78 | 8,920 | 6,900 | 1.34 |
| 18 | **58** | THF | 100 : 4 (BnOH) | 5 | 93 | 0.80 | 3,610 | 3,380 | 1.32 |
| 19 | **58** | Toluene | 100 : 1 (BnOH) | 5 | 94 | 0.35 | 10,500 | 13,500 | 1.54 |
| 20 | **58** | Toluene | 100 : 2 (BnOH) | 5 | 99 | 0.35 | 6,170 | 7,200 | 1.54 |
| 21 | **58** | Toluene | 100 : 4 (BnOH) | 5 | 99 | 0.36 | 3,570 | 2,820 | 1.50 |

**Conditions**: Polymerisation carried out using 60 µmol catalyst at 20 °C, $[La]_0$ = 0.6 M, 10 mL solvent, ROH taken from a ROH/toluene solution. [a] Determined by NMR spectroscopy, [b] Probability of forming a *r* dyad, [c] Calculated from $([LA]_0/[Mg]_0) \times$ conv.(%) × 144.13; with the addition of alcohol, $([LA]_0/[ROH]_0) \times$ conv.(%) × 144.13 + ROH. $M_n$ GPC values corrected considering Mark-Houwink factors (0.58) from polystyrene standards in THF.[23-24]

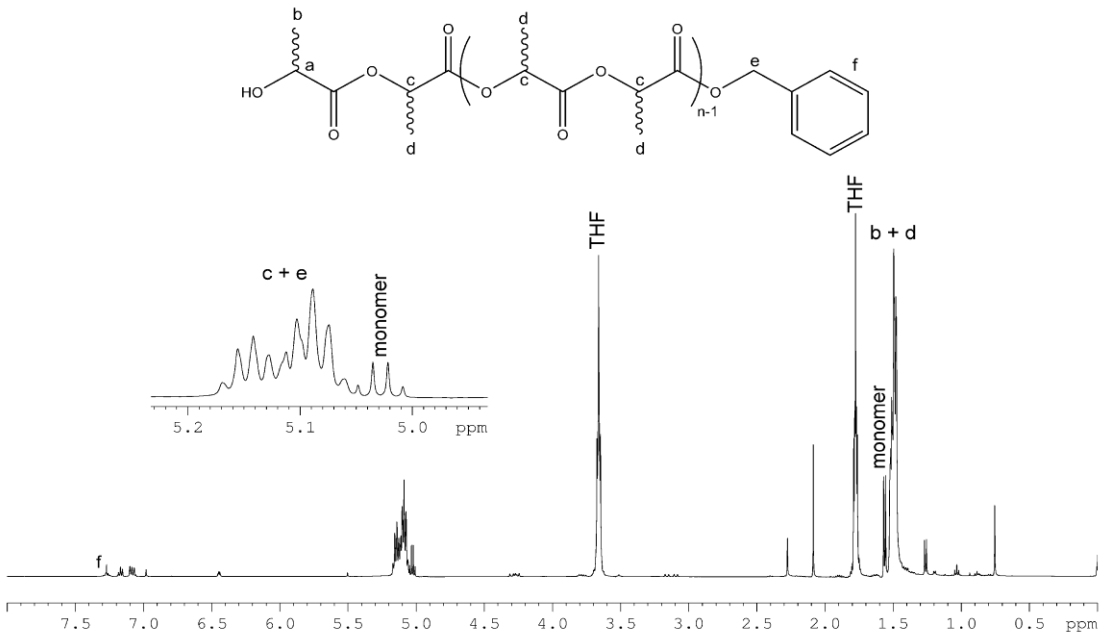


**Figure 4.7** $^{1}$H NMR spectrum from quenched PLA (**Table 4.3**, run 16).

To assign the stereoselectivity of the polymer produced 2D J-resolved $^{1}$H NMR spectroscopy was utilized rather than the more common homonuclear decoupled spectroscopy. 2D J-res spectroscopy separates the 1D spectrum of PLA (see **Figure 4.8**) so that the coupling constants appear on the y axis.[26] A projection on to the x axis essentially removes all coupling from the entire spectrum. The stereoselectivity of the polymer can be easily assigned by reference to the literature.[27] This has the advantage over the traditional homonuclear decoupled spectroscopy used to assign stereoselectivity that no manual information has to be entered, allowing an automated experiment. The resulting spectrum from 2D J-res spectroscopy for the assignment of PLA is shown in **Figure 4.8**. Compounds **51**, **54**, **57** and **58** give essentially atactic PLA (**51**, **54**, **Table 4.2**, runs 20 and 21, Pr = 0.54 – 0.62; **57, 58**, **Table 4.3**, runs 8 – 10, $P_r$ = 0.41 – 0.49). Compound **58** shows a high selectivity for heterotactic PLA in THF (**Table 4.3**, run 14 – 18, $P_r$ = 0.78 – 0.85), and rather surprisingly isotactic PLA in toluene (**Table 4.3**, run 12 and 19 – 21, $P_r$ = 0.30 – 0.36). The effect of THF on the selectivity has previously been discussed by Chisholm *et al,*[16] and there are many other examples.[28-31] We do not as yet have an explanation for the reverse selectivity involving toluene. Although a number of magnesium catalysts have been explored for the immortal and highly active polymerisation of *L*-lactide,[15, 32-34] **2** is the only catalyst that has exhibits both highly active immortal and stereoselective ring opening polymerisation of *rac*-lactide of which we are aware.

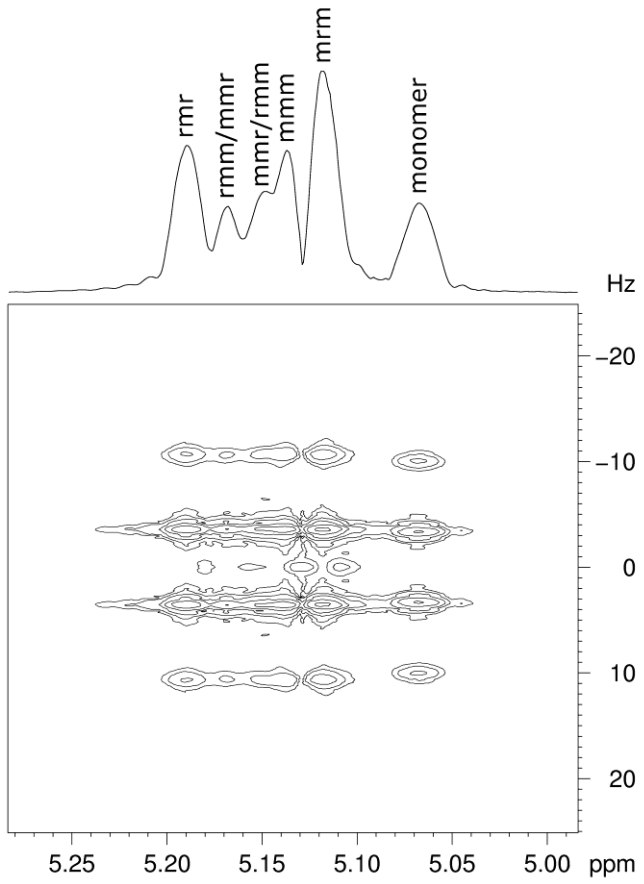


**Figure 4.8** 2D J-resolved $^{1}$H NMR of the methine region (**Table 4.3**, run 16)

## 4.3 Conclusion

A number of zinc and magnesium based calix[4]arene and oxacalix[3]arene compounds using either 1,3-dipropoxy-*p*-*tert*-butyl-calix[4]arene (**L30H$_2$**), tripropoxy-*p*-*tert*-butylcalix[4]arene (**L31H$_3$**) or hexahomotrioxacalix[3]areneH$_3$ (**L32H**) have been synthesized. Compounds **51**, **52**, **53**, **57** and **58** were characterized by single crystal X-ray diffraction as well as the unusual ring opened compound **56**. Compounds featuring a Zn—$C_6F_5$ fragment were poor ROP pre-catalysts as they did not react with benzyl alcohol to form an alkoxide. Compound **54**, which contains a zinc silylamide, was the most active of the zinc based calix[4]arene compounds, however was greatly outperformed by the magnesium catalyst **58**. Compound **58** is a highly active and selective ROP catalyst, 100 equivalents of *rac*-lactide can be converted to PLA ($P_r$ = 0.85, 92%) in 3 minutes, and also reveals 'immortal' polymerisation of *rac*-lactide when activated with excess BnOH (**Table 4.3**, runs 16 – 21). Compound **58** also gives either isotactic or heterotactic bias PLA depending on the solvent employed (THF: **Table 4.3**, runs 16 – 18, $P_r$ = 0.79 – 0.85; toluene: run 12 and 19 – 21, $P_r$ = 0.30 – 0.36).

## 4.4 References


[1] B. M. Chamberlain, M. Cheng, D. R. Moore, T. M. Ovitt, E. B. Lobkovsky, G. W. Coates, *J. Am. Chem. Soc.,* **2001**, *123*, 3229.

[2] C. Y. Li, P. S. Chen, S. J. Hsu, C. H. Lin, H. Y. Huang, B. T. Ko, *J. Organomet. Chem.,* **2012**, *716*, 175.

[3] M. Bouyhayi, Y. Sarazin, O. L. Casagrande, J. F. Carpentier, *Appl. Organomet. Chem.,* **2012**, *26*, 681.

[4] L. H. Yao, L. Wang, J. F. Zhang, N. Tang, J. C. Wu, *J. Mol. Catal. A: Chem.,* **2012**, *352*, 57.

[5] D. M. Homden, C. Redshaw, *Chem. Rev.,* **2008**, *108*, 5086.

[6] G. Guillemot, E. Solari, C. Rizzoli, C. Floriani, *Chem. Eur. J.,* **2002**, *8*, 2072.

[7] E. Bukhaltsev, L. Frish, Y. Cohen, A. Vigalok, *Org. Lett.,* **2005**, *7*, 5123.

[8] K. Iwamoto, K. Araki, S. Shinkai, *Tetrahedron,* **1991**, *47*, 4325.

[9] M. Miah, N. N. Romanov, P. J. Cragg, *J. Org. Chem.,* **2002**, *67*, 3124.

[10] E. Bukhaltsev, I. Goldberg, A. Vigalok, *Organometallics,* **2004**, *23*, 4540.

[11] E. Piedra-Arroni, C. Ladaviere, A. Amgoune, D. Bourissou, *J. Am. Chem. Soc.,* **2013**, *135*, 13306.

[12] G. Schnee, C. Fliedel, T. Avilés, S. Dagorne, *Eur. J. Inorg. Chem.,* **2013**, *2013*, 3699.

[13] F. D. R. Drouin, P. O. Oguadinma, T. J. J. Whitehorne, R. E. Prud'homme, F. Schaper, *Organometallics,* **2010**, *29*, 2139.

[14] J. M. Notestein, L. R. Andrini, V. I. Kalchenko, F. G. Requejo, A. Katz, E. Iglesia, *J. Am. Chem. Soc.,* **2007**, *129*, 1122.

[15] Y. Wang, W. Zhao, D. T. Liu, S. H. Li, X. L. Liu, D. M. Cui, X. S. Chen, *Organometallics,* **2012**, *31*, 4182.

[16] M. H. Chisholm, K. Choojun, J. C. Gallucci, P. M. Wambua, *Chem. Sci.,* **2012**, *3*, 3445.

[17] D. R. Armstrong, P. García-Álvarez, A. R. Kennedy, R. E. Mulvey, J. A. Parkinson, *Angew. Chem., Int. Ed. Engl.,* **2010**, *49*, 3185.

[18] A. Arbaoui, C. Redshaw, M. R. J. Elsegood, V. E. Wright, A. Yoshizawa, T. Yamato, *Chem. Asian J.,* **2010**, *5*, 621.

[19] C. Redshaw, D. Homden, D. L. Hughes, J. A. Wright, M. R. J. Elsegood, *Dalton Trans.,* **2009**, 1231.

[20] C. Redshaw, X. M. Liu, S. Z. Zhan, D. L. Hughes, H. Baillie-Johnson, M. R. J. Elsegood, S. H. Dale, *Eur. J. Inorg. Chem.,* **2008**, 2698.

[21] V. C. Gibson, C. Redshaw, W. Clegg, M. R. J. Elsegood, *Chem. Commun.,* **1997**, 1605.

[22] Y. Shen, Q. Tang, C. Zhang, W. Zhong, *Synlett,* **2012**, *23*, 741.

[23] I. Barakat, P. Dubois, R. Jérôme, P. Teyssié, *J. Polym. Sci., Part A: Polym. Chem.,* **1993**, *31*, 505.

[24] J. Baran, A. Duda, A. Kowalski, R. Szymanski, S. Penczek, *Macromol. Rapid Commun.,* **1997**, *18*, 325.

[25] A. Grala, J. Ejfler, L. B. Jerzykiewicz, P. Sobota, *Dalton Trans.,* **2011**, *40*, 4042.

[26] C. Ludwig, M. R. Viant, *Phytochem. Anal.,* **2010**, *21*, 22.

[27] T. K. Sen, A. Mukherjee, A. Modak, S. K. Mandal, D. Koley, *Dalton Trans.,* **2013**, *42*, 1893.

[28] W. Yi, H. Ma, *Inorg. Chem.,* **2013**, *52*, 11821.

[29] H.-Y. Chen, L. Mialon, K. A. Abboud, S. A. Miller, *Organometallics,* **2012**, *31*, 5252.

[30] H.-J. Chuang, H.-L. Chen, J.-L. Ye, Z.-Y. Chen, P.-L. Huang, T.-T. Liao, T.-E. Tsai, C.-C. Lin, *J. Polym. Sci., Part A: Polym. Chem.,* **2013**, *51*, 696.

[31] A. Garcés, L. F. Sánchez-Barba, J. Fernández-Baeza, A. Otero, M. Honrado, A. Lara-Sánchez, A. M. Rodríguez, *Inorg. Chem.,* **2013**, *52*, 12691.

[32] V. Poirier, T. Roisnel, J.-F. Carpentier, Y. Sarazin, *Dalton Trans.,* **2011**, *40*, 523.

[33] C. Romain, V. Rosa, C. Fliedel, F. Bier, F. Hild, R. Welter, S. Dagorne, T. Aviles, *Dalton Trans.,* **2012**, *41*, 3377.

[34] Y. Wang, W. Zhao, X. Liu, D. Cui, E. Y. X. Chen, *Macromolecules,* **2012**, *45*, 6957.

# Chapter 5 – Experimental Section

## 5.1 General Considerations

All manipulations involving vanadium, niobium, tantalum, zinc or magnesium were carried out under an atmosphere of nitrogen using standard Schlenk and cannula techniques or in a conventional nitrogen-filled glove-box. Toluene was refluxed over sodium, dichloromethane and acetonitrile were refluxed over calcium hydride, tetrahydrofuran, diethyl ether and light petroleum were dried over sodium/benzophenone; all solvents were distilled and degassed prior to use. Elemental analyses were performed by the microanalytical services of the London Metropolitan University. NMR spectra were recorded on Bruker Ascend 500/300 MHz spectrometers or a Varian VXR 400 S spectrometer at 298 K; chemical shifts are referenced to the residual protio impurity of the deuterated solvent ($^{1}$H NMR/$^{13}$C NMR), coupling constants are reported in Hz; IR spectra (nujol mulls, KBr windows, ATR) were recorded on Perkin-Elmer 577 and 457 grating spectrophotometers. The $^{51}$V NMR spectra were calibrated to an external $VOCl_3$/$CDCl_3$ reference. Solution state magnetic susceptibility was measured by Evans' method on a Varian VXR 400 S spectrometer using a 5% $d_{12}$-cyclohexane/95% $d_2$-dichloromethane solution. Polymer melting point measurements were carried out using a TA Instruments DSC 2920. GPC analysis was performed on a Polymer Laboratories, PL-GPC 50 using THF at 0.5 ml/min flow rate and 30 °C, corrected by the Mark-Houwink factor (PLA: 0.58, PCL: 0.56) and calibrated using polystyrene standards. Ethylene was dried by passing through phosphorus pentoxide, 4Å molecular sieves and a triethyl aluminium suspension supported in paraffin oil. ε-Caprolactone was dried over calcium hydride and distilled prior to use. *rac*-Lactide was purchased from Sigma Aldrich and used without further purification. Vanadium oxytriproproxide ($VO(O^nPr_3)$), vanadium oxytrichloride ($VOCl_3$), niobium pentachloride ($NbCl_5$), tantalum pentachloride ($TaCl_5$), *n*-butyllithium ($^n$BuLi), ethyl trichloroacetate, methylaluminium dichloride (1.0 M in hexanes), Ethylaluminium dichloride (1.0M in hexanes), dimethylaluminium chloride (1.0M in hexanes), diethylaluminium chloride (1.0 M in hexanes) and di-*n*-butylmagnesium ($^nBu_2Mg$) were purchased from Sigma Aldrich and were used as received. $VCl_3$.3THF,[1] $NbCl_3$.dme,[2] $NbCl_4$.2THF,[3] $Zn(C_6F_5)_2$.tol[4] and $Zn(N(SiMe_3)_2)_2$[5] were synthesized following the literature procedures.

### *5.1.1 Synthesis of Known Compounds*

Schiff Base ligands were synthesized by following the reported procedures **L1H – L3H**,[6], **L4H –L5H**,[7] **L6H – L8H**,[8] **L9H – L11H**,[9-10] **L12H – L13H**,[9] **L26H**,[8] **L27H – L28H**,[11] by the standard condensation of the corresponding amine with one or two equivalents as required of either salicylaldehyde or 3,5-di-*tert*-butyl-2-hydroxybenzaldehyde in acidified (formic acid) ethanol by the method reported by Jones *et al*.[12] (*E*)-2-(2-methylquinolin-8-ylimino)-4,6-di-*tert*-butylphenol (**L14H**), 2-(α-(2-hydroxy-3,5-di-*tert*-butylphenyl)benzyl)-4,6-di-*tert*-butylphenol (**L15H$_2$**), α,α,α′,α′-tetrakis(3,5-di-*tert*-butyl-2-hydroxyphenyl)-*p*-xylene (**L16H$_4$**), α,α,α′,α′-tetrakis(3,5-di-*tert*-butyl-2-hydroxyphenyl)-*m*-xylene (**L17H**), *p*-*tert*-butylcalix[6]areneH$_6$ (**L18H$_6$**), *p*-*tert*-butylcalix[8]areneH$_8$ (**L19H$_8$**), 2,4-di-tert-butyl-6-(4,5-diphenyl-1H-imidazol-2-yl)phenol (**L20H**), 2,4-di-tert-butyl-6-(phenanthro[9,10-d]oxazol-2-yl)phenol (**L21H**), N,N′-Bis(2,6-diisopropylphenyl)-1,4-diazabutadiene (**L22**), 2,6-bis[1-(2,6-diisopropylphenylimino)-ethyl]pyridine (**L23**), 1-{6-[(2,6-diisopropylphenyl)ethanimidoyl]-2-pyridinyl}-1-ethanone (**L24H**), 1,3-dipropoxy-*p*-*tert*-butyl-calix[4]areneH$_2$ (**L30H$_2$**), *p*-*tert*-butylhexahomotrioxacalix[3]areneH$_3$ (**L31H$_3$**) and tripropoxy-*p*-*tert*-butyl-calix[4]areneH$_3$ (**L32H**) were synthesized following the reported literature procedures.[13-21] Known compounds **1**,[22] **2**,[22] **5**,[22] **6**,[22] **36**,[23] **37**[24] and **38**[24] were synthesized according to the reported literature procedures.

### *5.1.2 Synthesis of Vanadium Complexes*

#### *5.1.2.1 Synthesis of **L1**(VCl$_2$) (**3**)*

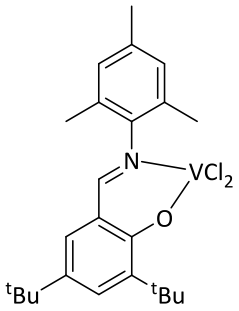


To a solution of **L1H** (0.5 g, 1.4 mmol) in THF (20 ml), $VCl_3(THF)_3$ (1.1 eq., 0.57 g, 1.54 mmol) was added and this solution was stirred for 10 minutes before adding $Et_3N$ (0.21 ml, 1.54 mmol). The solution was stirred at room temperature for 4 hours and then concentrated to approximately 15 ml. The mixture was filtered and recrystallised by diffusion of *n*-hexane (10 ml) to yield complex **3** as a brown powder (0.38 g, 57%). MS (EI, *m/z*): 543.2 $[M]^+$. Found: C, 61.15; H 6.70; N, 3.08. $VCl_2C_{24}H_{32}NO$ (sample dried *in vacuo* for 12h, loss of THF) requires C, 61.02; H, 6.83; N, 2.97%. IR (Nujol, KBr, $cm^{-1}$):

1612s, 1557s, 1544s, 1376s, 1293m, 1257s, 1195m, 1180m, 1144m, 1027m, 994s, 932w, 920w, 907w, 875m, 849s, 801m, 776m, 743m, 714s, 644m, 625m, 614m, 572m, 558m. Magnetic moment μ = 1.69$\mu_B$.

*5.1.2.2 Synthesis of **L2**($VCl_2$) (**4**)*

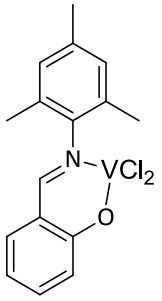


Procedure as described for complex **1** using **L2H** (0.34 g, 1.4 mmol), $VCl_3(THF)_3$ (1.1 eq., 0.57 g, 1.54 mmol) and $Et_3N$ (0.21 ml, 1.54 mmol). Complex **4** was obtained as a red powder (0.29 g, 36%). MS (EI, *m/z*): 359 $[M]^+$. Found: C, 53.18; H 4.38; N, 4.01. $VCl_2C_{16}H_{16}NO$ (sample dried *in vacuo* for 12h, loss of THF) requires C, 53.36; H, 4.48; N, 3.89%. IR (Nujol, KBr, $cm^{-1}$): 1632m (C=N), 1600s, 1558m, 1543m, 1261s, 1225m, 1189s, 1096s, 924w, 856m, 801s, 737w, 704w, 623w. Magnetic moment μ = 2.05$\mu_B$.

*5.1.2.3 Synthesis of **L4**[$VCl_2(THF)_2$]$_2$ (**7**)*

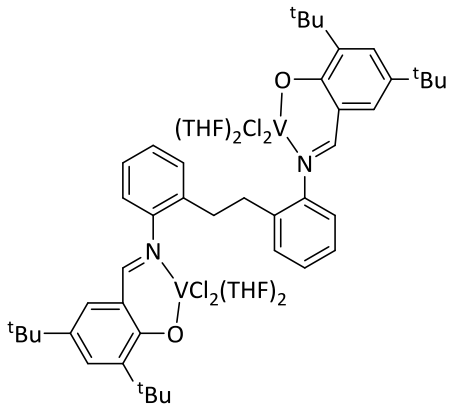


Procedure as described for complex **1** using **L4H$_2$** (0.25 g, 0.388 mmol), $VCl_3(THF)_3$ (2.3 eq., 0.33 g, 0.9 mmol) and $Et_3N$ (0.12 ml, 0.9 mmol). Complex **7** was obtained as dark red crystals (0.57 g, 65%). MS (EI, *m/z*): 693 $[M\text{-}V\text{-}4Cl\text{-}4THF]^+$. Found: C, 61.19; H 7.23; N, 2.38. $V_2Cl_4C_{60}H_{86}N_2O_6$ requires C, 61.33; H, 7.38; N, 2.38%. IR (Nujol, KBr, $cm^{-1}$): 1609w, 1598w, 1539w, 1410w, 705m, 687w, 665w. Magnetic moment μ = 1.90$\mu_B$.

*5.1.2.4 Synthesis of **L5**[VCl2(THF)$_2$]$_2$ (**8**)*

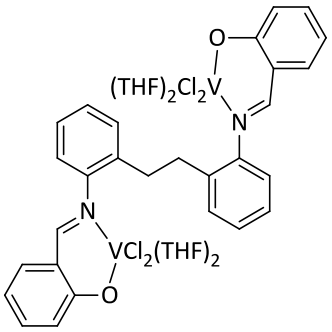


Procedure as described for complex **1** using **L5H$_2$** (0.25 g, 0.6 mmol), $VCl_3(THF)_3$ (2.2 eq., 0.49 g, 1.3 mmol) and $Et_3N$ (0.18 ml, 1.3 mmol). Complex **8** was obtained as a red powder (0.34 g, 61%). MS (EI, *m/z*): 468 $[M\text{-}V\text{-}4Cl\text{-}4THF]^+$. Found: C, 55.65; H 5.60; N, 3.07. $V_2Cl_4C_{44}H_{54}N_2O_6$ requires C, 55.59; H, 5.73; N, 2.95%. IR (Nujol, KBr, $cm^{-1}$): 1608s, 1542m, 1300m, 926w, 862m, 756m, 739m, 705w, 664w, 637m. Magnetic moment $\mu = 2.18\mu_B$.

*5.1.2.5 Synthesis of (**L3**H)$_2$(VOCl$_2$) (**9**)*

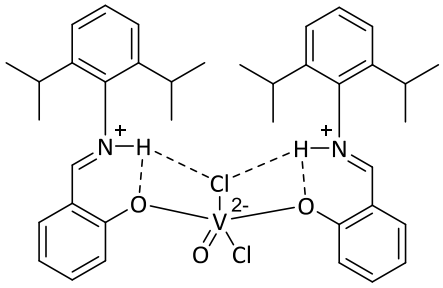


To a solution of **L3H** (0.5 g, 1.7 mmol), which had been held under dynamic vacuum for 5 hours, in toluene (40 ml), $VCl_3(THF)_3$ (0.6 eq., 0.29 g, 1.0 mmol) was added and this solution was refluxed for 12 hours. The solvents were removed *in vacuo* and the residue was extracted into hot acetonitrile (35 ml) affording dark orange needles on cooling (0.49 g, 37%). MS (EI, *m/z*): 646.2 $[M\text{-}MeH\text{-}HCl]^+$ 627.3 $[M\text{-}2HCl]^+$. Found: C, 65.00; H, 6.70; N, 4.12. $VCl_2C_{38}H_{46}N_2O_3$ (sample dried *in vacuo* for 12h, loss of MeCN) requires C, 65.14; H, 6.62; N, 4.00%. IR (Nujol, KBr, $cm^{-1}$): 1605s, 1539s, 1339s, 1301s, 1255s, 1212m, 1164s, 1146s, 987s, 927s, 854s, 795s, 754s, 702m, 650m, 639m, 614s, 516s. Magnetic moment $\mu = 0.98\mu_B$.

*5.1.2.6 Synthesis of **L6**$_2$(VO) (**10**)*

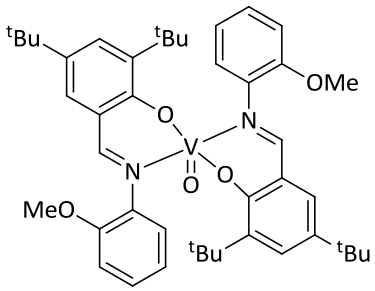


A toluene solution (20 ml) of **L6H** (0.42 g, 1.2 mmol) and vanadium oxytripropoxide (0.6 eq., 0.15ml, 0.68 mmol) was refluxed for 12 h. The solution was cooled to room temperature and volatiles were removed *in vacuo*. The residue was extracted into hot acetonitrile. After cooling to room temperature and prolonged standing (24 h), green needles of **10** formed (0.20 g, 44%). MS (MALDI-TOF) 743.3 $[M]^+$. Found: C, 70.84; H, 7.65; N, 3.62. $C_{44}H_{56}N_2O_5V$ requires C, 71.04; H, 7.59; N, 3.77%. IR (Nujol, KBr, $cm^{-1}$): 2956m, 2905w, 1609s, 1535w, 1492m, 1460w, 1391w, 1253s, 1167m, 1087s, 1019s, 963.6m, 875w, 840m, 795s, 752s, 732s, 694m. EPR (toluene, 298 K): $g_{iso}$= 1.99485, $A_{iso}$= 97.76 G; (toluene, 120 K): $g_{\perp}$= 2.00577, $A_{\perp}$= 61.60 G, g = 1.88861, A = 176.83 G.

*5.1.2.7 Synthesis of **L7**$_2$(VO) (**11**)*

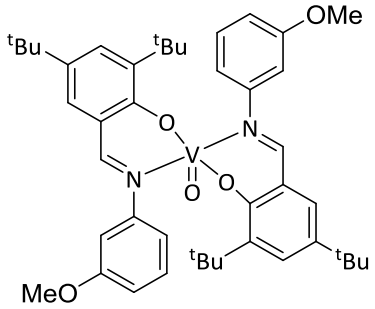


A toluene solution (20 ml) of **L7H** (0.40 g, 1.2 mmol) and vanadium oxytripropoxide (0.6 eq., 0.16 ml, 0.71 mmol) was refluxed for 12 h. The solution was cooled to room temperature and volatiles were removed *in vacuo*. The residue was extracted into hot acetonitrile. After cooling to room temperature and prolonged standing (24 h), brown needles of **11** formed (0.33 g, 37%). MS (MALDI-TOF) 743.3 $[M]^+$. Found: C, 70.49; H, 7.74; N, 3.63. $C_{44}H_{56}N_2O_5V$ requires C, 71.04; H, 7.59; N, 3.77%. IR (Nujol, KBr, $cm^{-1}$): 2951m, 2906w, 2862w, 1609s, 1586s, 1538s, 1483s, 1457m, 1433s, 1388s, 1361m, 1307m, 1254s, 1206w, 1175s, 1142s, 1090w, 1046m, 966s, 889w, 869w, 844s, 779s, 751m, 694s. EPR (toluene, 298 K): $g_{iso}$= 1.99504, $A_{iso}$= 96.00 G; (toluene, 120 K): $g_{\perp}$= 2.00649, $A_{\perp}$= 60.62 G, g = 1.97776, A = 178.73 G.

*5.1.2.8 Synthesis of **L8**$_2$(VO) (**12**)*

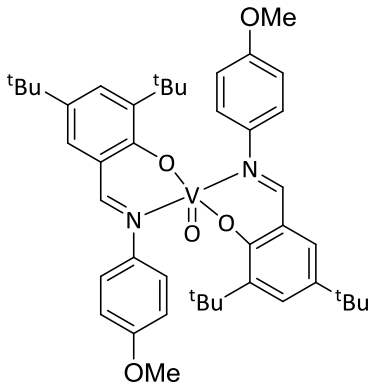


A toluene solution (20 ml) of **L8H** (0.40 g, 1.2 mmol) and vanadium oxytripropoxide (0.6 eq., 0.16 ml, 0.71 mmol) was refluxed for 12 h. The solution was cooled to room temperature and volatiles were removed *in vacuo*. The residue was extracted into hot acetonitrile. After cooling to room temperature and prolonged standing (24 h), dark red needles of **12** formed (0.18 g, 40%). MS (MALDI-TOF) 743.2 $[M]^+$. Found: C, 70.73; H, 7.74; N, 3.66. $C_{44}H_{56}N_2O_5V$ requires C, 71.04; H, 7.59; N, 3.77%. IR (Nujol, KBr, $cm^{-1}$): 2956m, 2905w, 1612s, 1502,s 1431w, 1387w, 1252s, 1169m, 1087s, 1017s, 970s, 874w, 790s, 751m, 687m. EPR (toluene, 298 K): $g_{iso}$= 1.99643, $A_{iso}$= 97.56 G; (toluene, 120 K): $g_{\perp}$= 2.00806, $A_{\perp}$= 61.13 G, g = 1.97845, A = 178.35 G.

*5.1.2.9 Synthesis of **L9**$_2$(VO) (**13**)*

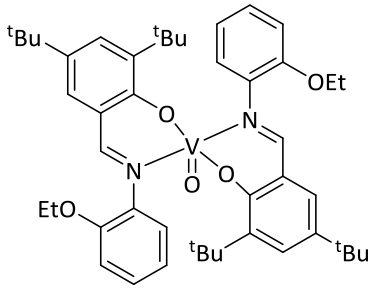


A toluene solution (20 ml) of **L9H** (0.40 g, 0.85 mmol) and vanadium oxytripropoxide (0.6 eq., 0.12 ml, 0.51 mmol) was refluxed for 12 h. The solution was cooled to room temperature and volatiles were removed *in vacuo*. The residue was extracted into hot acetonitrile. After cooling to room temperature and prolonged standing (24 h), brown needles of **13** formed (0.17 g, 50%). MS (MALDI-TOF) 771.3 $[M]^+$. Found: C, 71.50; H, 7.76; N, 3.53. $C_{46}H_{60}N_2O_5V$ requires C, 71.57; H, 7.83; N, 3.63%. IR (Nujol, KBr, $cm^{-1}$): 2949m, 2362m, 2161m, 2027m, 1608s, 1536s, 1486s, 1432w, 1389s, 1359s, 1302w, 1248s, 1170s, 1118m, 968s, 928m, 874w, 839s, 745s. EPR (toluene, 298 K): $g_{iso}$= 1.99452, $A_{iso}$= 94.83 G; (toluene, 120 K): $g_{\perp}$= 2.00701, $A_{\perp}$= 61.46 G, g = 1.97955, A = 178.01 G.

*5.1.2.10 Synthesis of **L10**$_2$(VO) (**14**)*

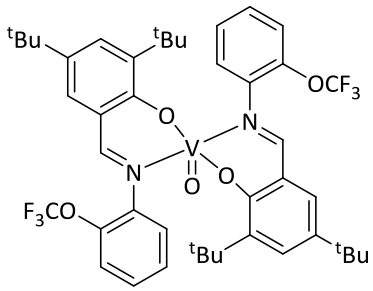


A toluene solution (20 ml) of **L10H** (0.10 g, 0.27 mmol) and vanadium oxytripropoxide (0.6 eq., 0.04 ml, 0.16 mmol) was refluxed for 12 h. The solution was cooled to room temperature and volatiles were removed *in vacuo*. The residue was extracted into hot acetonitrile. After cooling to room temperature and prolonged standing (24 h), dark red needles of **13** formed (0.03 g, 26%). Found: C, 62.21; H, 6.04; N, 3.89. $C_{44}H_{50}F_6N_2O_5V$ requires C, 62.04; H, 5.92; N, 3.29%. IR (Nujol, KBr, $cm^{-1}$): 2954m, 1611s, 1593s, 1540m, 1488m, 1458w, 1434w, 1392m, 1361m, 1248s, 1206s, 1158s, 1109s, 1045w, 968s, 927m, 876m, 839s, 756s, 686w. EPR (toluene, 298 K): $g_{iso}$= 1.99442, $A_{iso}$= 95.22 G; (toluene, 120 K): $g_{\perp}$= 2.00513, $A_{\perp}$= 59.78 G, g = 1.97867, A = 176.67 G.

*5.1.2.11 Synthesis of **L11**$_2$(VO) (**15**)*

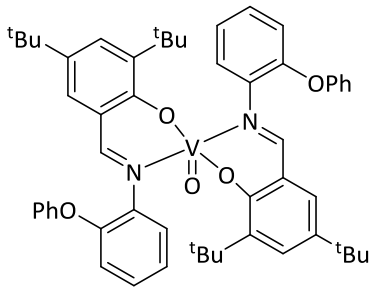


A toluene solution (30 ml) of **L11H** (1.0 g, 2.5 mmol) and vanadium oxytripropoxide (0.6 eq., 0.32 ml, 1.5 mmol) was refluxed for 12 h. The solution was cooled to room temperature and volatiles removed *in vacuo*. The residue was extracted into hot acetonitrile. After cooling to room temperature and prolonged standing (24 h), orange needles of **15** formed. (0.73 g, 67%). MS (EI, *m/z*): 867.3 $[M]^+$. Found: C, 74.53; H 7.05; N, 3.35. $VC_{54}H_{60}N_2O_5$ requires C, 74.72; H, 6.97; N, 3.23. IR (Nujol, KBr, $cm^{-1}$): 2952m, 2867w, 1605s, 1540m, 1483s, 1453m, 1390m, 1357w, 1303w, 1232s, 1203m, 1171s, 1105m, 1070w, 1000m, 968s, 887m, 846s, 785m, 749s, 688s. EPR (toluene, 298K): $g_{iso}$= 1.99552, $A_{iso}$= 97.18 G; (toluene, 120K): $g_{\perp}$= 2.00553, $A_{\perp}$= 61.13 G, $g_{\parallel}$= 1.97617, $A_{\parallel}$= 181.37 G.

*5.1.2.12 Synthesis of* ***L6*****$_2$***[(VO)$_2$(μ-O)$_2$]* (***16***)

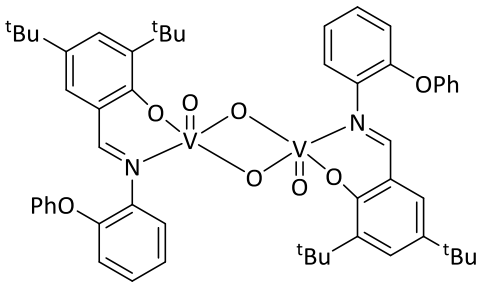


A toluene solution (30 ml) of **L6H** (1.0 g, 2.5 mmol) and vanadium oxytripropoxide (1.1 eq., 0.6 ml, 2.7 mmol) was refluxed for 12 h. The solution was cooled to room temperature and volatiles were removed *in vacuo*. The residue was extracted into hot acetonitrile. After cooling to room temperature and prolonged standing (24 h), dark red needles of **16** formed. (0.65 g, 27%). MS (EI, *m/z*): 966.5 $[M]^+$. Found: C, 67.07; H 6.37; N, 2.82. $V_2C_{54}H_{60}N_2O_8$ requires C, 67.24; H, 6.25; N, 2.90. IR (Nujol, KBr, $cm^{-1}$): 2958m, 1610s, 1588m, 1547m, 1485s, 1458m, 1433m, 1360w, 1302w, 1237s, 1203s, 1179s 1108m, 1022m, 982s, 857m, 797m, 752s. $^1$H NMR ($CDCl_3$): δ = 8.67 (s, 1H, C*H*=N), 7.61 (d, 1H, *J* = 2.6, Ar*H*), 7.57 (dd, 1H, *J* = 1.6, 7.97, Ar*H*), 7.29 (d, 1H, *J* = 2.5, Ar*H*), 7.25 – 7.24 (overlapping m, 2H, Ar*H*), 7.20 – 7.16 (m, 2H, Ar*H*), 7.09 – 7.07 (m, 2H, Ar*H*), 7.00 – 6.97 (m, 2H, Ar*H*), 1.33 (s, 9H, *t*Bu), 1.28 (s, 9 H, *t*Bu). $^{13}$C NMR ($CDCl_3$): δ = 169.5, 157.7, 156.7, 149.5, 143.1, 142.5, 137.9, 131.4, 129.6, 128.1, 127.7, 127.5, 124.7, 123.3, 123.2, 120.0, 119.3 35.1, 34.4, 31.4, 29.5. $^{51}$V NMR ($C_6D_6$): δ = -532.56.

*5.1.2.13 Synthesis of* ***L12*****$_2$***(VO)* (***17***)

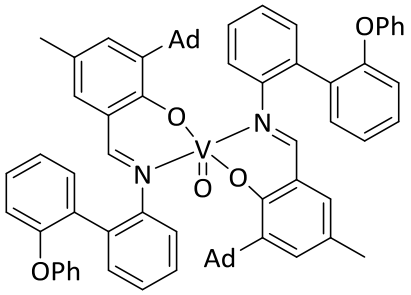


A toluene solution (20 ml) of **L12H** (0.20 g, 0.39 mmol) and vanadium oxytripropoxide (1.1 eq., 0.06 ml, 0.23 mmol) was refluxed for 12 h. The solution was cooled to room temperature and volatiles were removed *in vacuo*. The residue was extracted into hot acetonitrile. After cooling to room temperature and prolonged standing (24 h), dark red needles of **17** formed (0.06 g, 30%). MS (MALDI-TOF) 1091.4 $[M]^+$. Found: C, 79.22; H, 6.21; N, 2.67. $C_{72}H_{68}N_2O_5V$ requires C, 79.17; H, 6.28; N, 2.56%.

IR (Nujol, KBr, $cm^{-1}$): 2897m, 2871m, 2845m, 2030w 1599s, 1539m, 1475s, 1432s, 1384w, 1289m, 1230s, 1191m, 1163m, 1103w, 973s, 874w, 831s, 747s, 688s. EPR (toluene, 298 K): $g_{iso}$= 1.99286, $A_{iso}$= 89.74 G; (toluene, 120 K): $g_{\perp}$= 2.00158, $A_{\perp}$= 63.98 G, g = 1.96095, A = 168.27 G.

*5.1.2.14 Synthesis of **L13**$_2$(VO) (**18**)*

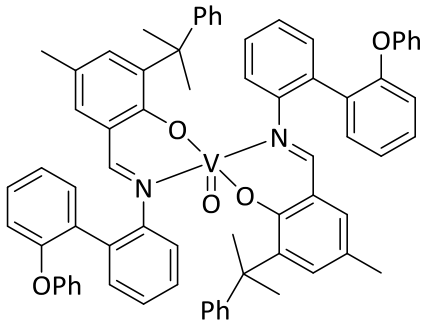


A toluene solution (20 ml) of **L13H** (0.26 g, 0.52 mmol) and vanadium oxytripropoxide (0.6 eq., 0.07 ml, 0.08 mmol) was refluxed for 12 h. The solution was cooled to room temperature and volatiles were removed *in vacuo*. The residue was extracted into hot acetonitrile. After cooling to room temperature and prolonged standing (24 h), dark red needles of **18** formed (0.19 g, 69%). MS (MALDI, *m/z*) : 1059.4 $[M]^+$. Found: C, 79.3; H, 5.79; N, 2.66. $C_{70}H_{60}N_2O_5V$ requires C, 79.3; H, 5.70; N, 2.64%. IR (Nujol, KBr, $cm^{-1}$): 3025w, 2948w, 2168w, 2031w, 1615s, 1595s, 1545s, 1489s, 1471s, 1433s, 1382m, 1293m, 1221s, 1162s, 1125m, 969s, 866m, 825s, 747s, 693s. EPR (toluene, 298 K): $g_{iso}$= 1.98756, $A_{iso}$= 89.74 G; (toluene, 120 K): $g_{\perp}$= 2.00083, $A_{\perp}$= 64.82 G, g = 1.95741, A = 173.98 G.

*5.1.2.15 Synthesis of **L14**(VOCl$_2$) (**19**)*

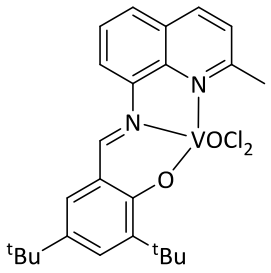


(*E*)-2-(2-methylquinolin-8-ylimino)-4,6-di-*tert*-butylphenol (**L14H**) (0.5 g, 1.33 mmol) was dissolved in tetrahydrofuran (40 ml). Triethylamine (0.2 ml, 1.44 mmol) and vanadium oxytrichloride (1.1 eq., 0.14 ml, 1.46 mmol) were added via syringe and the solution stirred at ambient temperature for 6 h. The volatiles were removed *in vacuo*. Crystallization using hot acetonitrile gave brown plates of the vanadium compound **19**. (0.46 g, 68%). MS (EI, *m/z*): 475.1 $[M\text{-}Cl]^+$. Found: C, 58.82; H 5.87; N, 5.57.

$VC_{25}H_{29}Cl_2N_2O_2$ requires C, 58.72; H, 5.72; N, 5.48. IR (Nujol, KBr, $cm^{-1}$): 1610m, 1588s, 1566m, 1538w, 1505m, 1431m, 1311m, 1232w, 1213m, 1199m, 1170m, 1146s, 972s, 886w, 796s, 764m, 694m. $^1H$ NMR ($CDCl_3$): $\delta$ = 8.94 (s, 1H, C*H*=N), 8.24 (d, 1H, *J* = 8.4, Ar*H*), 7.94 (d, 1H, *J* = 7.4, Ar*H*), 7.81 (d, 1H, *J* = 7.8, Ar*H*), 7.66 (d, 1H, *J* = 2.4, Ar*H*) 7.61 (m, 2H, Ar*H*) 7.48 (d, 1H, J = 2.4, Ar*H*) 3.58 (s, 3H, Ar-*Me*), 1.63 (s, 9H, $^t$Bu), 1.38 (s, 9H, $^t$Bu). $^{51}V$ NMR ($CDCl_3$): $\delta$ = -261.47 ($w_{1/2}$ = 535).

*5.1.2.16 Synthesis of **L14**($VO_2$) (**20**)*

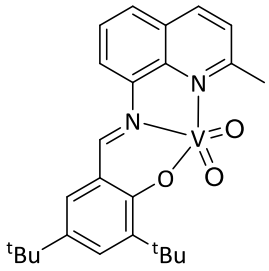


(*E*)-2-(2-methylquinolin-8-ylimino)-4,6-di-*tert*-butylphenol (**L14H**) (0.5 g, 1.33 mmol) was dissolved in toluene (40 ml). Vanadium oxytripropoxide (1.1 eq., 0.34 ml, 1.46 mmol) was added via syringe and the solution refluxed for 16 hours. The solution was allowed to cool to room temperature and the volatiles were removed *in vacuo*. Crystallization using hot acetonitrile gave yellow needles of the vanadium compound **20**. (0.39 g, 64%). MS (EI, *m/z*): 456.1 $[M]^+$, 441.0 $[M\text{-}Me]^+$. Found: C, 65.63; H 6.46; N, 6.23. $VC_{25}H_{29}N_2O_3$ requires C, 65.78; H, 6.40; N, 6.14. IR (Nujol, KBr, $cm^{-1}$): 1613s, 1587s, 1556m, 1538s, 1508m, 1323m, 1253s, 1200m, 1181s, 1171s, 1149m, 1134w, 987w, 969w, 942s, 895w, 843s, 792s, 754m. $^1H$ NMR ($CDCl_3$): $\delta$ = 9.17 (s, 1H, C*H*=N), 8.30 (d, 1H, *J* = 8.4, Ar*H*), 7.93 (d, 1H, *J* = 7.6, Ar*H*), 7.81 (d, 1H, *J* = 8.0, Ar*H*), 7.68 (ABq, 2H, $\Delta v_{AB}$ = 5.7, *J* = 6.7, Ar*H*) 7.60 (d, 1H, *J* = 8.4, Ar*H*) 7.36 (d, 1H, *J* = 2.4, Ar*H*), 3.82 (s, 3H, Ar-*Me*), 1.50 (s, 9H, $^t$Bu), 1.36 (s, 9H, $^t$Bu). $^{13}C$ NMR ($CDCl_3$): $\delta$ = 166.3, 165.7, 163.5, 144.2, 140.9, 140.8, 140.4, 138.9, 134.0, 128.2, 127.6, 127.4, 126.2, 120.8, 115.6, 35.5, 34.3, 31.3, 29.6, 27.5. $^{51}V$ NMR ($CDCl_3$): $\delta$ = -535.93 ($w_{1/2}$ = 535).

*5.1.2.17 Synthesis of **L15**$_2$[$(VO)_2(\mu\text{-}O^nPr)]_2$ (**21**)*

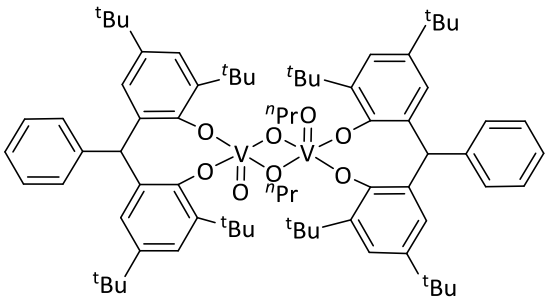

2-(α-(2-hydroxy-3,5-di-*tert*-butylphenyl)benzyl)-4,6-di-*tert*-butylphenol (**L15H$_2$**, 4.1 g, 8.2 mmol) was dissolved in tetrahydrofuran (40 ml). Vanadium oxytripropoxide (1.1 eq., 1.9 ml, 8.4 mmol) was added via syringe and the solution stirred at room temperature for 16 hr. The volatiles were removed *in vacuo*, following which crystallization using warm light petroleum gave red needles of the vanadium dimer, **21**. (3.6 g, 70%). MS (EI, *m/z*): 624.4 $[M]^+$, 564.4 $[M\text{-}OnPr]^+$. IR (Nujol, KBr, $cm^{-1}$): 1599m, 1381m, 1289w, 1220s, 1153s, 1103s, 1060s, 989s, 911w, 875w, 855m, 836s, 800m, 770m, 745m, 705m, 652s, 599m, 503w, 451w. Found: C, 73.11; H, 9.20. $C_{76}H_{106}O_8V_2$ requires C, 73.05; H, 8.55%. $^1$H NMR ($CDCl_3$): δ = 7.3 (4H, d, *J* = 2.3, Ar*H*), 7.27 (4H, d, *J* = 2.3, Ar*H*), 7.21 – 7.15 (4H, m, Ar*H*), 7.00 (4H, d, *J* = 8.0, Ar*H*), 6.38 (2H, s, $Ar_3$-C*H*), 5.37 (4H, t, *J* = 6.0, $OCH_2CH_2$), 1.99 (4H, m, $CH_2CH_2CH_3$), 1.47 (36H, s, *t*Bu), 1.26 (36H, s, *t*Bu), 1.10 (6H, t, *J* = 7.4, $CH_2CH_3$). $^{51}$V NMR ($CDCl_3$): δ = -433.6 ($w_{1/2}$ =170 Hz).

*5.1.2.18 Synthesis of **L16**[VO(O$^n$Pr)(THF)]$_2$ (**22**)*

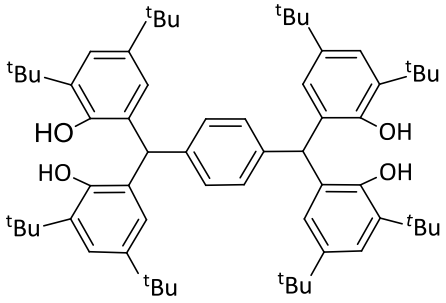


α,α,α',α'-Tetrakis(3,5-di-*tert*-butyl-2-hydroxyphenyl)-*p*-xylene (**L16H$_4$,** 4.1 g, 4.4 mmol) was dissolved in tetrahydrofuran (40 ml). Vanadium oxytripropoxide (2.1 eq., 2.0 ml, 9 mmol) was added via syringe and the solution stirred at room temperature for 16 h. The volatiles were removed *in vacuo,* crystallization using THF/light petroleum gave orange plates of the compound **22**. (2.6 g, 45%). MS (EI, *m/z*) 1170.6 $[M\text{-}2THF]^+$, 1110.5 $[M\text{-}OnPr\text{-}2THF]^+$, 1068.5 $[M\text{-}nPr\text{-}OnPr\text{-}2THF]^+$ IR (Nujol, KBr, $cm^{-1}$): 1597w, 1507m, 1435s, 1402w, 1286w, 1261m, 1221s, 1203s, 1153m, 1118s, 1104s, 1027s, 989s, 908m, 891m, 876s, 837s, 801m, 777m, 767m, 750m, 736w, 702w, 659s, 603m, 578w. Found: C, 71.61; H, 8.42. $C_{70}H_{100}O_8V_2$ (sample dried *in vacuo* for 24 h leads to loss of THF) requires C, 71.77; H, 8.60%. $^1$H NMR ($CDCl_3$): δ= 7.31 (4H, d, *J* = 2.3, Ar*H*), 7.22 (4H, d, *J* = 2.3, Ar*H*), 6.78 (4H, s, Ar*H*), 6.31 (2H, s, $Ar_3$-C*H*), 5.36 (4H, t, *J* = 6.0, $OCH_2CH_2$), 3.75 (THF), 1.86 (4H, m, *J* = 6.7, $CH_2CH_2CH_3$), 1.40 (36H, s, *t*Bu), 1.24 (36H, s, *t*Bu), 1.08 (6H, t, *J* = 7.4, $CH_2CH_3$). $^{51}$V NMR ($CDCl_3$): δ= -433.32 ($w_{1/2}$ =170 Hz).

*5.1.2.19 Synthesis of **L17**[VO(O$^n$Pr)]$_2$ (**23**)*

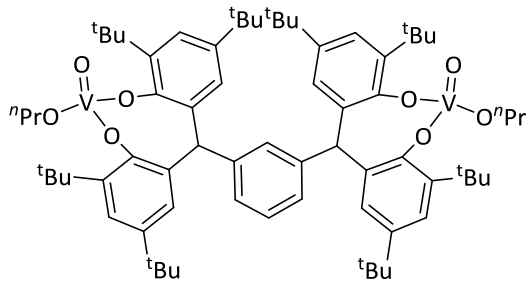

α,α,α′,α′-Tetrakis(3,5-di-*tert*-butyl-2-hydroxyphenyl)-*m*-xylene (**L17H$_4$**, 4.1 g, 4.4 mmol) was dissolved in tetrahydrofuran (40 ml). Vanadium oxytripropoxide (2.1 eq., 2.0 ml, 9 mmol) was added via syringe and the solution stirred at room temperature for 16 hr. The volatiles were removed *in vacuo*, and the residue recrystallization using THF/light petroleum giving orange needles of the compound **23**. (2.0 g, 35%). MS (E.I.) 1170.6 [M-2THF]$^+$, 1110.5 [M-HO*n*Pr-2THF]$^+$. IR (Nujol, KBr, cm$^{-1}$): 1595m, 1406m, 1361s, 1217s, 1154m, 1118s, 1104s, 1030s, 992s, 910w, 882w, 846s, 787s, 720s, 695w, 649s, 601m, 499w, 449w. Found: C, 71.60; H, 8.41. $C_{70}H_{100}O_8V_2$ requires C, 71.77; H, 8.60%. $^1$H NMR ($CDCl_3$): $\delta$= 7.18 (4H, d, *J* = 2.4, Ar*H*), 7.15 (4H, d, *J* = 2.4, Ar*H*), 7.10 (1H, s, Ar*H*), 7.02 (1H, t, *J* = 7.8, Ar*H*), 6.80 (2H, d, *J* = 7.9, Ar*H*), 6.25 (2H, s, $Ar_3CH$), 5.34 (4H, t, *J* = 6.5, $OCH_2CH_2$), 1.98 (4H, m, *J* = 7.0, $CH_2CH_2CH_3$), 1.42 (36H, s, *t*Bu), 1.17 (36H, s, *t*Bu), 1.09 (6H, t, J = 7.4, $CH_2CH_3$). $^{51}$V NMR ($CDCl_3$) $\delta$= -432.52 ($w_{1/2}$ =170 Hz).

***5.1.2.20** Synthesis of [Li(NCMe)$_4$][V$_2$(O)$_2$Li(NCMe)(**L18**H$_2$)$_2$]·8MeCN (**24**·8MeCN)*

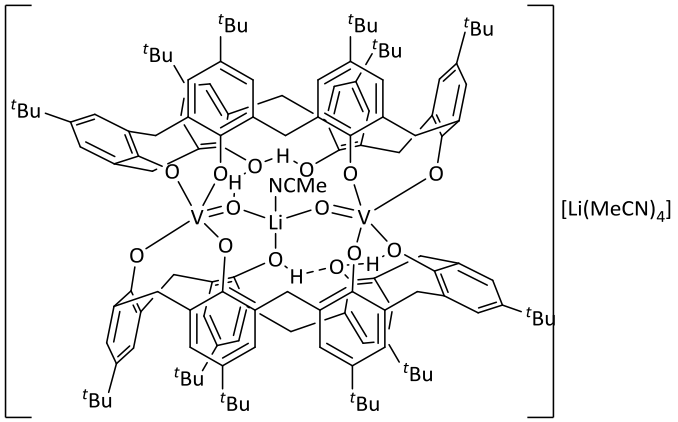


[LiVO(O*t*-Bu)$_4$] (prepared *in-situ* from $VOCl_3$ 0.27 ml, 2.89 mmol and LiO*t*-Bu 0.93 g, 11.62 mmol, at -78 $^o$C in THF (30 ml)) and *p-tert*-butylcalix[6]areneH$_6$ (**L18H$_6$**, 1.40 g, 1.44 mmol) were dissolved in toluene (30 ml). The mixture was refluxed for 12 h. Following removal of solvent, the crude brown product was extracted in acetonitrile (30 ml). Prolonged standing at room temperature afforded **25** as

green blocks (1.19 g, 63%). MS (MALDI, *m/z*): 2089 $[M]^+$ - 13MeCN, 2082 $[M]^+$ - 13MeCN – Li. Found: C, 73.6; H, 7.7; N, 4.6. $C_{142}H_{175}Li_2N_5O_{14}V_2$.3MeCN (sample dried for 12 h *in vacuo* leads to loss of 5MeCN) requires C, 73.6; H, 7.7; N, 4.6%. IR (Nujol, KBr, $cm^{-1}$): 3470bw, 2302w, 2272w, 2249w, 1747w, 1597m, 1416s, 1392s, 1362s, 1290s, 1261s, 1201s, 1152m, 1100bs, 977m, 949m, 915m, 871m, 835s, 799s, 771m, 760m, 728w, 695m, 680w, 635w, 617w. $^1$H NMR ($CDCl_3$): $\delta =$ 10.54 (2H, br s, OH), 7.37 (d, 4H, *J* = 2.0, Ar-H), 7.26 (d, 4H, *J* = 2.3, Ar-H), 7.16 (m, 8H, Ar-H), 7.09 (d, 4H, *J* = 2.3, Ar-H), 7.06 (br s, 4H, Ar-H), 6.74 (br s, 2H, OH), 5.27 (d, 4H, *J* = 13.9, *endo*-$CH_2$), 5.22 (d, 2H, *J* = 20.3, *endo*-$CH_2$), 4.92 (br s, 4H, *endo*-$CH_2$), 4.37 (d, 2H, *J* = 20.3, *endo*-$CH_2$), 4.31 (d, 2H, *J* = 13.4, *exo*-$CH_2$), 3.50 (d, 4H, *J* = 14.0, *exo*-$CH_2$) 3.45 (d, 4H, *J* = 14.0, *exo*-$CH_2$), 3.07 (d, 2H, *J* = 13.4, *exo*-$CH_2$), 1.28 (overlapping s, 54H, $^t$Bu-Ar). $^{51}$V NMR ($CDCl_3$): $\delta =$ -70.5 ($\omega^1/_2$ 535 Hz, minor), -78.8 ($\omega^1/_2$ 770 Hz, major).

*5.1.2.21 Synthesis of [$VO_2$($LiMeCN_2$)$_2$(**L18**$H_2$)] (**25**)*

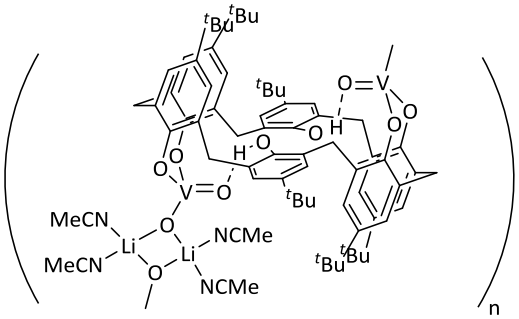


Yield: *ca.* 10 % from synthesis of **24**; elemental analysis calculated for **25**.1$CH_3CN$ – $CH_3CN$, $C_{37}H_{46}LiN_2O_5V$: C 67.7, H 7.1, N 4.3 %; found: C 67.7, H 6.8, N 4.2 %; IR (nujol mull, KBr): 1603m, 1298m, 1285m, 1260s, 1235m, 1193s, 1108m, 1048m, 967m, 921m, 846m, 803m, 722m, 680w, 666w.

*5.1.2.22 Synthesis of [Na(NCMe)$_5$][(VO)$_2$**L19**H]·4MeCN (**26**.4MeCN)*

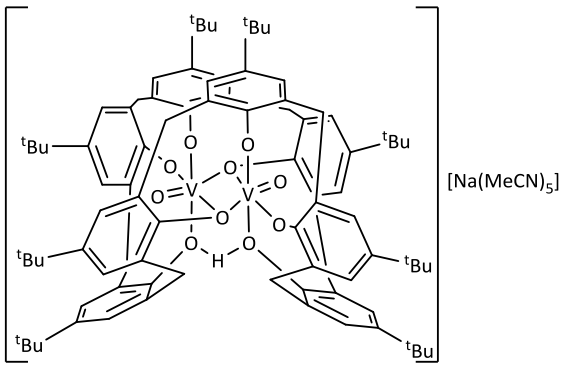


As for **26**, but using [NaVO(O*t*-Bu)$_4$] ($VOCl_3$ 0.27 ml, 2.89 mmol and NaO*t*-Bu 1.12 g, 11.65 mmol) and *p-tert*-butylcalix[8]areneH$_8$ (**L19H$_8$**, 1.87 g, 1.44 mmol), affording **26** as brown blocks (1.23 g, 47%) MS (MALDI, *m/z*): 1651 $[M-H]^+$. Found: C, 70.5; H, 6.8; N, 3.5. $C_{96}H_{117}N_4NaO_{10}V_2$ (sample dried *in-vacuo* for 12 h leads to loss of 5MeCN) requires C, 71.5; H, 7.3; N, 3.5%. IR (Nujol, KBr, $cm^{-1}$): 3176w, 2263w, 1733w, 1610w, 1293s, 1260s, 1203s, 1153m, 1093s, 1018s, 967s, 911m, 869m, 808s, 722s, 670w, 633w, 581w, 572w, 553w, 534w, 521w, 464w, 448w, 430w. $^1$H NMR ($CDCl_3$, 400MHz): $\delta$ = 15.49 (Br s, O-H-O, 1H) 7.30 (s, 4H, aryl*H* ), 7.21 (s, 6H, aryl*H*), 7.17 (s, 2H, aryl*H* ), 7.06 (s, 2H, aryl*H*), 6.97 (s, 2H, Ar-*H*), 5.97 (d, 2H, *J* = 12.6, *endo*-C*H*$_2$), 5.66 (d, 4H, *J* = 13.7, *endo*-C*H*$_2$), 4.66 (d, 2H, *J* =11.8, *endo*-C*H*$_2$), 3.54 (d, 2H, *J* = 13.5, *exo*-C*H*$_2$), 3.49 (d, 2H, *J* = 12.3, *exo*-C*H*$_2$), 3.38 (d, 2H, *J* = 13.7, *exo*-C*H*$_2$), 3.30 (d, 2H, *J* = 11.8, *exo*-C*H*$_2$), 1.30 (overlapping s, 72H, C(C*H*$_3$)$_3$) $^{51}$V NMR ($CDCl_3$): $\delta$ = -202.4 ($\omega^1/_2$ 700 Hz), -333.8 ($\omega^1/_2$ 500 Hz).

*5.1.2.23 Synthesis of [(VO)$_4$L$^8$($\mu^3$-O)$_2$] **27**.3MeCN and **27**.3CH$_2$Cl$_2$*

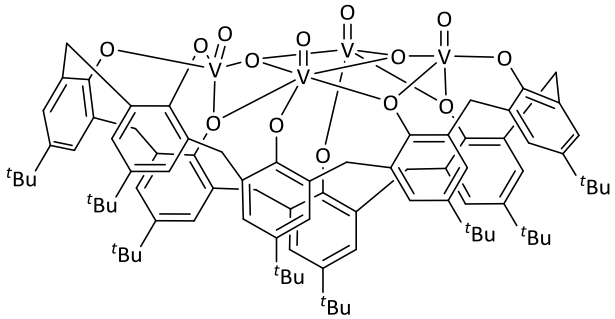


As for **26**, but using [KVO(O*t*-Bu)$_3$] ($VOCl_3$ 0.27 ml, 2.89 mmol and KO*t*-Bu 1.03 g, 8.67 mmol) and **L19H$_8$** (0.93 g, 0.72 mmol), affording **27**.3$CH_3CN$ as black blocks (0.47 g, 38%). Found: C, 65.7; H, 6.3; N, 3.2. $C_{88}H_{104}V_4O_{14}$.3MeCN requires C, 65.9; H, 6.7; N, 2.5%. IR (Nujol, KBr, $cm^{-1}$): 1594w, 1567w,

1303w, 1288w, 1260s, 1226w, 1201m, 1172w, 1098bs, 1022s, 944w, 913w, 875m, 833m, 794s, 734w, 705w, 670w, 653m, 642w, 617w, 574w. MS (MALDI, *m/z*): [$MH^+$] 1589.6 (solvent free). $^1$H NMR ($C_6D_6$, sample dried for 12 h): δ= 7.34 – 6.96 (overlapping m, 16H, Ar-*H*), 5.05 (d, 2H, *J* = 11.7, *endo*-C*H*$_2$), 4.89 (d, 4H, *J* = 14.4 Hz, *endo*-C*H*$_2$), 4.29 (d, 2H, *J* = 12.6, *endo*-C*H*$_2$), 3.14 (d, 2H, *J* = 12.6, *exo*-C*H*$_2$), 2.98 – 2.92 (overlapping m, 4H, J obscured, *exo*-C*H*$_2$), 2.55 (d, 2H, *J* = 14.4, *exo*-C*H*$_2$), 0.95 (s, 36H, C(C*H*$_3$)$_3$), 0.74 (s, 36H, C(C*H*$_3$)$_3$). $^{51}$V NMR ($CDCl_3$): δ= -209.7 ($\omega^1/_2$ 750 Hz), -341.1 ($\omega^1/_2$ 415 Hz). Re-crystallization of the crude product from dichloromethane afforded dark green rod-like crystals of **27**·3$CH_2Cl_2$ (0.41 g, 31%). Found: C, 59.4; H, 5.9. $C_{88}H_{104}V_4O_{14}$ (sample dried *in-vacuo* for 12 h leads to loss of $CH_2Cl_2$) requires: C, 59.3; H, 6.0%. $^{51}$V NMR ($CDCl_3$) δ: -213.6 ($\omega^1/_2$ 1500 Hz), -341.2 ($\omega^1/_2$ 330 Hz), -371.2.

### *5.1.3 Synthesis of Niobium/Tantalum Complexes*

#### *5.1.3.1 Synthesis of **L20**($NbCl_4$) (**28**)*

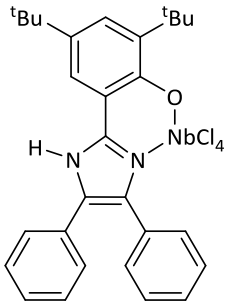


A solution of **L20H** (1.0 g, 2.36 mmol) and $NbCl_5$ (1.1 eq., 0.69 g, 2.60 mmol) in toluene (30 ml) was refluxed for 12 h. The reaction mixture was cooled to room temperature and volatiles were removed *in vacuo*. The solid residue was extracted into hot acetonitrile. After prolonged standing at room temperature, deep red plates of **28**.MeCN formed (0.82 g, 56%). MS (ESI, *m/z*): 658 [$M]^+$, 587 [$M^+$-2Cl]$^+$. Found: C, 53.09; H, 4.62; N, 4.34. $C_{29}H_{31}Cl_4N_2NbO$ requires C, 52.91; H, 4.75; N, 4.26%. IR (Nujol, KBr, $cm^{-1}$): 3279br, 2289w, 2257w, 1587m, 1568w, 1508m, 1402s, 1365m, 1325w, 1146s, 924m, 906w, 877s, 845m, 766m, 732w, 712m, 698s, 670m. $^1$H NMR ($C_6D_6$): δ = 9.87 (s, 1H, NH), 7.60 (dd, 2H, $J_1$ = 15.76, $J_2$ = 2.03, Ar*H*), 7.47 (m, 1H, Ar*H*), 7.45 (d, 1H, *J* = 1.69, Ar*H*), 7.39 – 7.35 (overlapping m, 3H, Ar*H*), 7.30 (m, 3H, Ar*H*), 7.17 (m, 2H, Ar*H*), 2.00 (s, 3H, C*H*$_3$CN), 1.56 (s, 9H, C(C*H*$_3$)$_3$), 1.43 (s, 9H, C(C*H*$_3$)$_3$).

*5.1.3.2 Synthesis of **L20**[$NbOCl_2$(MeCN)] (**29**)*

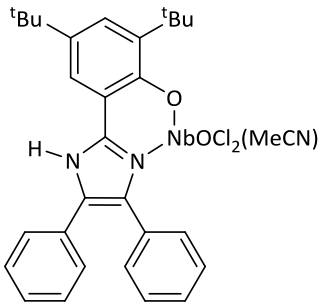


As described for **28** but using $NbOCl_3$ (1.1 eq., 0.28 g, 1.30 mmol) and **L20H** (0.50 g, 1.18 mmol), affording orange prisms of **29**.3(MeCN) (0.41 g, 54%). MS (ESI, *m/z*): 602 $[M\text{-}CH_3CN+H]^+$, 551 $[M^+\text{-}Cl\text{-}O+H]^+$. Found: C, 57.69; H, 5.33; N, 6.45. $C_{31}H_{34}Cl_2N_3NbO_2$ requires C, 57.78; H, 5.32; N, 6.52%. IR (Nujol, KBr, $cm^{-1}$): 3572w, 3405w, 3195br, 2307m, 2278m, 1950w, 1883w, 1810w, 1617s, 1604s, 1589s, 1575m, 1523m, 1500m, 1404s, 1364s, 1201m, 1184m, 1150m, 1126s, 1072s, 975m, 910s, 890m, 846s, 769m, 697s, 668m. $^1$H NMR ($(CD_3)_2CO$): δ = 7.88 (d, 1H, *J* = 2.4, Ar*H*), 7.57 (d, 4H, *J* = 7.0, Ar*H*), 7.40 (overlapping m, 7H, Ar*H*), 2.68 (s, 3H, C$H_3$CN), 1.49 (s, 9H, C(C$H_3$)$_3$), 1.33 (s, 9H, C(C$H_3$)$_3$).

*5.1.3.3 Synthesis of **L20**($TaCl_4$) (**30**)*

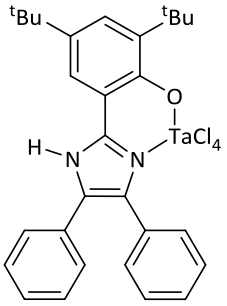


As described for **28** but using $TaCl_5$ (1.1 eq., 0.47 g, 1.30 mmol) and **L20H** (0.50 g, 1.18 mmol), affording dark red plates of **30**.MeCN (0.50 g, 57% yield). MS (ESI, *m/z*): 746.1 $[M]^+$, 675.1 $[M^+\text{-}2Cl]$. Found: C, 46.78; H, 4.07; N, 3.81. $C_{29}H_{31}Cl_4N_2OTa$ requires C, 46.67; H, 4.19; N, 3.75%. IR (Nujol, KBr, $cm^{-1}$): 3283s, 2291w, 2259w, 1597m, 1509s, 1403s, 1326m, 1286s, 1177s, 1147s, 1128s, 971m, 928s, 906m, 881s, 846s, 771s, 734m, 698s. $^1$H NMR ($C_6D_6$): δ = 8.52 (s, 1H), 7.67 – 7.65 (overlapping m, 2H, Ar*H*), 7.23 – 7.15 (overlapping m, 7H, Ar-*H*), 7.04 (s, 1H, Ar*H*), 6.80 (m, 1H, Ar*H*), 6.67 (m, 1H, Ar*H*), 1.67 (s, 9H, C(C$H_3$)$_3$), 1.23 (s, 9H, C(C$H_3$)$_3$).

*5.1.3.4 Synthesis of **L20**[$TaOCl_2$(MeCN)] (**31**)*

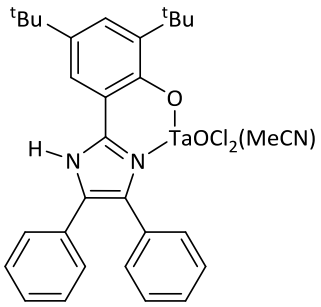


As described for **28** but using $TaOCl_3$(DME) (1.1 eq., 0.47 g, 1.30 mmol) and **L20H** (0.50 g, 1.18 mmol), affording orange powder (0.49 g, 51%). MS (ESI, *m/z*): 590.8 [$M^+$-2Me-2Cl]. Found: C, 50.28; H, 4.24; N, 3.87. $C_{29}H_{31}Cl_2N_2O_2Ta$ (sample dried *in vacuo* for 12hr, loss of MeCN) requires C, 50.38; H, 4.52; N, 4.05%. IR (Nujol, KBr, $cm^{-1}$): 3210m, 2258w, 1672m, 1596m, 1524m, 1364m, 1199w, 1177w, 922s, 872s, 770s, 698s. $^1$H NMR ($C_6D_6$): δ = 7.55 (m, 2H, Ar*H*), 7.46 (s, 1H, Ar*H*), 6.93 (m, 2H, Ar*H*), 6.76 (m, 4H, Ar*H*), 6.61 (m, 1H, Ar*H*), 1.55 (s, 3H, C$H_3$CN), 1.36 (s, 9H, C(C$H_3$)$_3$), 1.07 (s, 9H, C(C$H_3$)$_3$).

*5.1.3.5 Synthesis of **L21**($NbCl_4$) (**32**)*

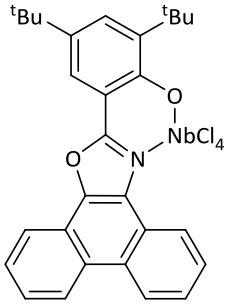


As described for **28** but using $NbCl_5$ (1.1 eq., 0.35 g, 1.30 mmol) and **L21H** (0.50 g, 1.19 mmol), affording red/orange crystals (0.56 g, 72%). MS (ESI, *m/z*): 657 $[M]^+$, 622 $[M^+$-Cl$]^+$, 550 $[M^+$-3Cl$]^+$. Found: C, 53.12; H, 4.22; N, 2.24. $C_{29}H_{28}Cl_4NNbO_2$ requires C, 52.99; H, 4.29; N, 2.13%. IR (Nujol, KBr, $cm^{-1}$): 2297w, 2271w, 1601w, 1572w, 1515m, 1364m, 1316w, 1291w, 1035s, 996m, 958s, 922m, 885m, 851m, 774m, 752s, 731m, 686m. $^1$H NMR ($(CD_3)_2CO$): δ = 8.90 (t, 2H, *J* = 8.4, ArH), 8.6 – 8.54 (overlapping m, 1H, Ar*H*), 8.47 – 8.46 (overlapping m, 1H, Ar*H*), 8.20 (d, 1H, *J* = 2.5, Ar*H*), 8.10 (d, 1H, *J* = 2.5, Ar*H*), 7.84 – 7.68 (overlapping m, 3H, Ar*H*), 7.50 (d, 1H, *J* = 2.5, Ar*H*), 3.68 (s, 3H, C$H_3$CN), 1.46 (s, 9H, C(C$H_3$)$_3$), 1.35 (s, 9H, C(C$H_3$)$_3$).

*5.1.3.6 Synthesis of **L21**[$NbOCl_2$(MeCN)] (**33**)*

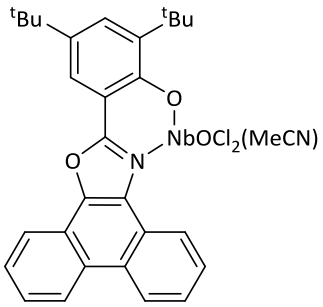


As described for **28** but using $NbOCl_3$ (1.1 eq., 0.20 g, 0.91 mmol) and **L21H** (0.35 g, 0.83 mmol), affording orange/yellow crystals of **33** (0.34 g, 64%). MS (ESI, *m/z*): 603 $[M\text{-}CH_3CN+H]^+$, 566 $[M^+\text{-}CH_3CN\text{-}Cl]^+$. Found: C, 57.91; H, 4.58; N, 2.51. $C_{29}H_{28}Cl_2NNbO_3$ (sample dried *in vacuo* for 12h, loss of MeCN) requires C, 57.83; H, 4.69; N, 2.33%. IR (Nujol, KBr, $cm^{-1}$): 2296w, 2270w, 1601w, 1571w, 1515m, 1315w, 1291w, 1201m, 1157m, 958s, 922m, 885m, 851m, 751s, 731s. $^1$H NMR $(CD_3)_2CO$): δ = 9.0 (t, 2H, *J* = 8.1, ArH), 8.6 (d, 1H, *J* = 7.8, Ar*H*), 8.54 – 8.49 (overlapping m, 1H, Ar*H*), 8.20 (dd, 1H, $J_1$ = 0.5, $J_2$ = 2.5, Ar*H*), 7.95 – 7.73 (overlapping m, 4H, Ar*H*), 7.62 (d, 1H, *J* = 2.4, Ar*H*), 2.68 (s, 6H, 2C$H_3$CN), 1.54 (s, 9H, C(C$H_3$)$_3$), 1.44 (s, 9H, C(C$H_3$)$_3$).

*5.1.3.7 Synthesis of **L21**($TaCl_4$) (**34**)*

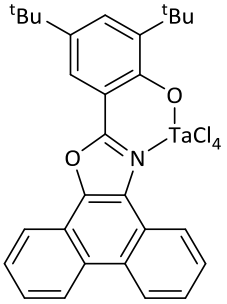


As described for **28** but using $TaCl_5$ (1.1 eq., 0.47 g, 1.30 mmol) and **L21H** (0.5 g, 1.19 mmol), affording red microcrystals (0.64 g, 65%). MS (E.S.): *m/z*: 745.1 $[M]^+$, 706.1 $[M\text{-}Cl]^+$. Found: C, 46.59; H, 3.71; N, 1.84. $C_{29}H_{28}Cl_4NO_2Ta$ requires C, 46.73; H, 3.79; N, 1.88%. IR (Nujol, KBr, $cm^{-1}$): 2291w, 2276w, 1604w, 1582m, 1516m, 1312w, 1297w, 1202w, 1157w, 924m, 877m, 852w, 751s, 732m, 722m, 686w, 570m. $^1$H NMR ($C_6D_6$): δ = 8.31 (d, 1H, *J* = 8.3, ArH), 8.24 (d, 1H, *J* = 7.8, Ar*H*), 8.04 (d, 1H, *J* = 2.2 Ar*H*), 7.84 (d, 1H, *J* = 7.1, Ar*H*), 7.75 (d, 1H, *J* = 2.2 , Ar*H*), 7.61 (d, 1H, *J* = 7.7, Ar*H*), 7.40 – 7.21 (overlapping m, 4H, Ar*H*), 1.62 (s, 9H, C(C$H_3$)$_3$), 1.26 (s, 9H, C(C$H_3$)$_3$).

*5.1.3.8 Synthesis of **L22**($NbCl_4$) (**35**)*

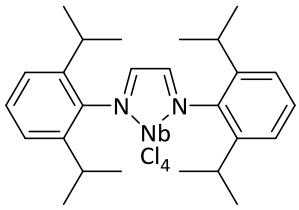


$NbCl_4$(THF) (1.1 eq., 0.39 g, 1.46 mmol) and **L22** (0.50 g, 1.32 mmol) were refluxed in THF (40 ml) for 12 h, and then dried *in vacuo*. The residue was washed with hexane (20 ml x 2) and recrystallized from MeCN to give **25** as an orange powder (0.55 g, 62%). MS (ESI, *m/z*): 576 [M-Cl]+. Found: C, 50.96; H, 5.86; N, 4.48. $C_{26}H_{36}Cl_4N_2Nb$ requires C, 51.08; H, 5.94; N, 4.58%. IR (Nujol, KBr, $cm^{-1}$): 2311m, 2284m, 1645w, 1582w, 1510m, 1320m, 1198m, 1139m, 939m, 782m, 760m, 722w. $^1$H NMR ($CDCl_3$): δ = 7.34 (m, 2H, ArH), 7.24 (m, 2H, ArH), 7.19 (m, 2H, Ar-H), 6.41 (s, 2H, N=CH), 2.85 (m, 4H, $CH(Me)_2$), 1.26 (d, 12H, *J* = 6.6 Hz, $C(CH_3)_2$), 1.19 (d, 12H, *J* = 6.3, $C(CH_3)_2$). EPR (toluene, 298 K) $g_{iso}$: 2.01, $A_{iso}$: 6G.

*5.1.3.9 Synthesis of **L24**$_2$($NbCl_2O)_2$ (**39**)*

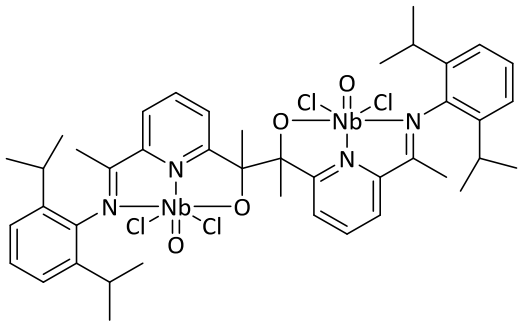


A solution of $NbCl_3$(dme) (0.55 g, 1.88 mmol) and **L24H** (1.00 g, 2.07 mmol) in THF (40 ml) was refluxed for 12 h. The reaction mixture was cooled to room temperature and volatiles were removed *in vacuo.* The residue was washed with hexane (45 ml × 2) and extracted into hot acetonitrile. After prolonged standing at room temperature, yellow plates of **24**.4MeCN formed. (0.12 g, 13%). Found: C, 50.25; H, 5.09; N, 5.43. $C_{42}H_{52}Cl_4N_4Nb_2O_4$ requires C, 50.22; H, 5.22; N, 5.58 %. IR (Nujol, KBr, $cm^{-1}$): 2725w, 1643s, 1588w, 1396w, 1190w, 929w, 865w, 722m, 622w. $^1$H NMR ($CDCl_3$): δ = 7.19 – 7.16 (overlapping m, 12H, Ar*H*), 2.78 (m, 4H, -C*H*$(Me)_2$, 2.36 (s, 6H, C$H_3$CN), 1.25 (s, 6H, C$H_3$C-O), 1.17 (d, 24H, $C(CH_3)_2$).

*5.1.3.10 Synthesis of **L25**($NbCl_4$) (**40**)*

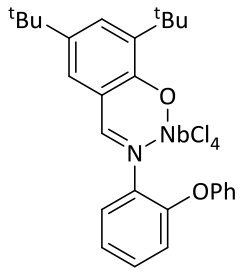


A solution of $NbCl_5$ (1.1 eq., 0.37 g, 1.38 mmol) and **L25H** (0.50 g, 1.25 mmol) in toluene (30 ml) was refluxed for 12 h. The reaction mixture was cooled to room temperature and volatiles removed in vacuo. Extraction of the solid residue into hot acetonitrile, and cooling to room temperature afforded dark yellow/brown plates of complex **40** (0.42 g, 53%). MS (ESI, *m/z*): *m/z*: 635 $[M]^+$, 598 $[M\text{-}Cl]^+$. Found: C, 50.92; N, 2.18; H, 4.74. $NbC_{27}H_{30}Cl_4NO_2$ requires C, 51.05; N, 2.20; H, 4.76%. IR (Nujol, KBr, $cm^{-1}$): 1585m, 1552m, 1484m, 1365m, 1330w, 1202w, 1176w, 1157w, 982w, 923w, 891w, 874m, 753m. $^1H$ NMR ($CDCl_3$): δ = 8.44 (s, 1H, C*H*=N), 7.80 (d, 1H, *J* = 2.2, Ar*H*), 7.50 (dd, 1H, $J_1$ = 7.9, $J_2$ = 2.2, Ar*H*), 7.36 – 7.30 (overlapping m, 3H, Ar*H*), 7.25 – 7.18 (overlapping m, 1H, Ar*H*), 7.13 – 7.06 (overlapping m, 4H, Ar*H*), 6.90 (dd, 1H, $J_1$ = 8.3, $J_2$ = 1.3, Ar*H*), 1.52 (s, 9H, $C(CH_3)_3$), 1.34 (s, 9H, $C(CH_3)_3$).

*5.1.3.11 Synthesis of **L25**($TaCl_4$) (**41**)*

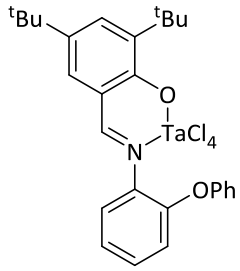


As described for **40**, but using $TaCl_5$ (1.1 eq., 1.02 g, 2.86 mmol) and **L25H** (1.0 g, 2.6 mmol), affording orange needles of compound **41** (0.96 g, 51%). MS (EI, *m/z*): 724 $[MH]^+$, 687 $[MH\text{-}Cl]^+$. Found: C, 44.79; H 4.12; N 2.00. $C_{27}H_{30}Cl_4NO_2Ta$ requires C, 44.84; H, 4.18; N, 1.94%. IR (Nujol, KBr, $cm^{-1}$): 1641m, 1602m, 1586m, 1553m, 1365m, 1201w, 1176m, 925w, 875m, 753m, 699m. $^1H$ NMR ($C_6D_6$): δ = 7.89 (s, 1H, C*H*=N), 7.66 (m, 2H, Ar*H*), 7.14 (m, 2H, Ar*H*), 6.98 (m, 2H, Ar*H*), 6.82 (m, 3H, Ar*H*), 6.72 (m, 2H, Ar*H*), 1.47 (s, 9H, $C(CH_3)_3$), 1.08 (s, 9H, $C(CH_3)_3$).

*5.1.3.12 Synthesis of **L26**($NbCl_4$) (**42**)*

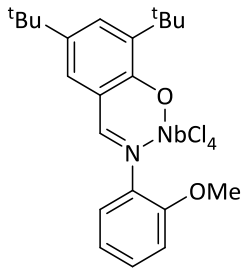


As described for **42** but using $NbCl_5$ (1.1 eq., 0.87 g, 3.24 mmol) and **L26H** (1.0 g, 2.95 mmol), affording dark red plates (0.72 g, 42%). MS (CI, *m/z*): 573 $[M]^+$, 536 $[M\text{-}Cl]^+$, 521 $[M\text{-}MeCl]^+$. Found: C, 45.94; H, 4.80; N, 2.33. $C_{22}H_{28}Cl_4NNbO_2$ requires C, 46.10; H, 4.92; N, 2.44%. IR (Nujol, KBr, $cm^{-1}$): 1589w, 1557w, 1325w, 1218w, 1202w, 1174m, 923w, 869w, 757m, 722w. $^1$H NMR ($C_6D_6$): δ = 7.66 (s, 1H, C*H*=N), 7.61 (d, 1H, *J* = 2.3, Ar*H*), 7.48 (d, 1H, *J* = 7.8, Ar*H*), 7.00 (t, 1H, *J* = 7.9, Ar*H*), 6.77 (t, 1H, *J* = 7.7, Ar*H*), 6.68 (d, 1H, *J* = 2.3, Ar*H*), 6.53 (d, 1H, *J* = 8.4, Ar*H*), 3.33 (s, 3H, O*Me*), 1.48 (s, 9H, C(C$H_3$)$_3$), 1.05 (s, 9H, C(C$H_3$)$_3$).

*5.1.3.13 Synthesis of **L26**($TaCl_4$) (**43**)*

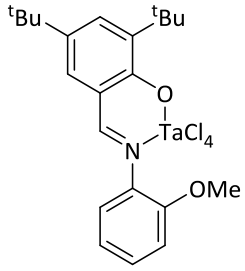


$TaCl_5$ (1.1 eq., 1.16 g, 3.24 mmol) and **L26H** (1.0 g, 2.95 mmol) were stirred at room temperature in toluene (40 ml) for 12 h. The solvents were removed *in vacuo* and the product was recrystallized from MeCN giving an orange powder (0.72 g, 37%). MS (EI, *m/z*): 661 $[M]^+$, 624 $[M\text{-}Cl]^+$, 609 $[M\text{-}Me\text{-}Cl]^+$. Found: C, 39.84; H, 4.14; N, 2.01. $C_{22}H_{28}Cl_4NO_2Ta$ requires C. 39.96; H, 4.27; N, 2.12 %. IR (Nujol, KBr, $cm^{-1}$): 1641w, 1593w, 1555s, 1495w, 1409w, 1301w, 1228w, 927w, 872m, 751m, 723m.$^1$H NMR ($CDCl_3$): δ = 8.35 (s, 1H, C*H*=N), 7.91 (d, 1H, *J* = 8.0, Ar*H*), 7.80 (d, 1H, *J* = 2.4, Ar*H*), 7.41 (d, 1H, *J* = 7.1, Ar*H*), 7.38 (d, 1H, *J* = 2.3, Ar*H*), 7.02 (dd, 1H, *J* = 3.3, 8.2, Ar*H*), 6.93 (dd, 1H, $J_1$ = 8.4, $J_2$ = 3.1, Ar*H*), 3.29 (s, 3H, OMe), 1.30 (s, 9H, C(C$H_3$)$_3$), 1.27 (s, 9H, C(C$H_3$)$_3$).

*5.1.3.14 Synthesis of **L27**($NbCl_4$) (**44**)*

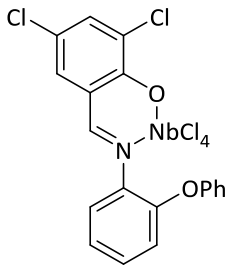


As described for **40**, but using $NbCl_5$ (1.1 eq., 0.83 g, 3.07 mmol) and **L27H** (1.0 g, 2.79 mmol), affording a dark red powder (0.78 g, 47%). MS (EI, *m/z*): 480 $[M\text{-}Ph\text{-}Cl+H]^+$. Found: C, 38.59; H, 1.96; N, 2.45; $C_{19}H_{12}Cl_6NO_2Nb$ requires C, 38.55; H, 2.04; N, 2.37 %. IR (Nujol, KBr, $cm^{-1}$) 1645m, 1583m, 1548m, 1275s, 1217s, 964m, 872s, 693s. $^1H$ NMR ($C_6D_6$): δ = 7.53 (dd, 1H, *J* = 7.6, 1.8, Ar*H*), 7.35 (s, 1H, C*H*=N), 7.11 (overlapping m, 2H, Ar*H*), 7.01 (overlapping m, 2H, Ar*H*), 6.76 (overlapping m, 5H, Ar*H*), 6.16 (d, 1H, *J* = 2.4, Ar*H*).

*5.1.3.15 Synthesis of **L27**($TaCl_4$) (**45**)*

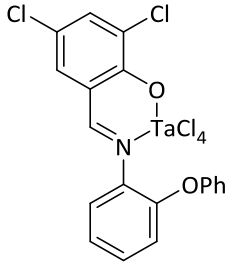


As described for **40**, but using $TaCl_5$ (1.1 eq., 1.10 g, 3.07 mmol) and **L27H** (1.0 g, 2.79 mmol), affording a yellow powder (0.86 g, 44%). MS (EI, *m/z*): 679 $[M]^+$, 644 $[M\text{-}Cl]^+$. Found: C, 33.42; H, 1.71; N, 2.15. $C_{19}H_{12}Cl_6NO_2Ta$ requires C, 33.56; H, 1.78; N, 2.06%. IR (Nujol, KBr, $cm^{-1}$): 2723m, 2251m, 1948w, 1779w, 1646s, 1582s, 1547w, 1297m, 1206m, 907w, 871w, 848m, 755m, 727m, 693m. $^1H$ NMR ($C_6D_6$): δ = 8.81 (s, 1H, C*H*=N), 7.83 (s, 1H, Ar*H*), 7.36 (s, 1H, Ar*H*), 7.04 – 6.96 (m, 3H, Ar*H*), 6.92 – 6.78 (m, 3H, Ar*H*), 6.71 – 6.55 (m, 2H, Ar*H*), 6.30 (d, 1H, *J* = 7.4, Ar*H*) .

*5.1.3.16 Synthesis of **L28**($NbCl_4$) (**46**)*

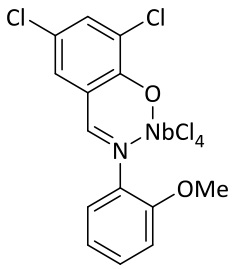


As described for **40**, but using $NbCl_5$ (1.1 eq., 1.00 g, 3.71 mmol) and **L28H** (1.0 g, 3.38 mmol), affording a yellow powder (1.16 g, 65%). Found: C, 31.59; H, 2.03; N, 2.52. $C_{14}H_{10}Cl_6NNbO_2$ requires C, 31.73; H, 1.90; N, 2.64%. MS (EI, *m/z*): 494 $[M\text{-}Cl]^+$, 478 $[M\text{-}Me\text{-}Cl]^+$, 444 $[M\text{-}Me\text{-}2Cl]^+$, IR (Nujol, KBr, $cm^{-1}$): 2738w, 2362w, 1797w, 1634m, 1601m, 1584m, 1543m, 1301m, 1167w, 898m, 875m, 753m, 723m, 633m. $^1$H NMR ($(CD_3)_2CO$): δ = 8.97 (s, 1H, C*H*=N), 7.80 (s, 1H, Ar*H*), 7.71 (d, 1H, *J* = 2.7, Ar*H*), 7.66 (s, 1H, Ar*H*), 7.55 (t, *J* = 7.2, 1H, Ar*H*), 7.23 (overlapping m, 2H, Ar*H*).

*5.1.3.17 Synthesis of **L28**($TaCl_4$) (**47**)*

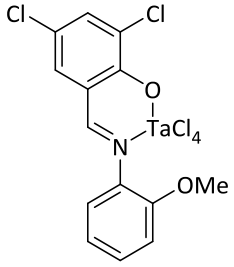


As described for **40**, but using $TaCl_5$ (1.1 eq., 1.33 g, 3.71 mmol) and **L28H** (1.0 g, 3.38 mmol), affording a dark red powder (1.13 g, 54%). MS (EI, *m/z*): 618 $[M+H]^+$, 583 $[M+H\text{-}Cl]^+$. Found: C, 27.13; H, 1.53; N, 2.19. $C_{14}H_{10}Cl_6NO_2Ta$ requires C, 27.21; H, 1.63; N, 2.27 %. IR (Nujol, KBr, $cm^{-1}$): 2723w, 1791w, 1633m, 1583m, 1542w, 1493m, 1317m, 1303m, 1183m, 1168m, 903m, 840m, 753m, 730m, 674w. $^1$H NMR ($C_6D_6$): δ = 8.45 (s, 1H, C*H*=N), 7.73 (d, 1H, *J* = 8.5, Ar*H*), 7.47 (m, 1H, Ar*H*), 7.34 (dd, 1H, *J* = 1.7, 7.9, Ar*H*), 7.21 (d, 1H, *J* = 7.5, Ar*H*), 7.05 (m, 2H, Ar*H*), 3.85 (s, 3H, $OCH_3$).

*5.1.3.18 Synthesis of **L29**($NbCl_4$) (**48**)*

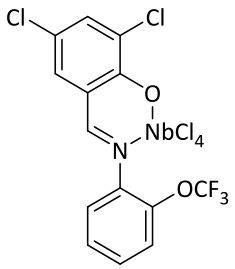


As described for **13**, but using $NbCl_5$ (1.0 eq., 0.743 g, 2.75 mmol) and **L14H** (1.0 g, 2.75 mmol), affording a dark red powder (0.56 g, 35%). MS (EI, *m/z*): 583 $[M]^+$. Found: C, 28.69; H, 1.13; N, 2.34. $C_{14}H_7Cl_6F_3NO_2Nb$ requires C, 28.80; H, 1.21; N, 2.40%. IR (Nujol, KBr, $cm^{-1}$): 2723m, 1775w, 1594m, 1551m, 1298m, 1213w, 1174s, 914w, 900w, 878m, 760m, 723m, 674w. $^1$H NMR ($C_6D_6$): δ = 7.34 (m, 1H, Ar*H*), 7.09 (s, 1H, C*H*=N), 6.96 (m, 1H, Ar*H*), 6.72 (overlapping m, 3H, Ar*H*), 6.21 (d, 1H, *J* = 2.4, Ar*H*). $^{19}$F NMR ($C_6D_6$): δ = -56.4 (s).

*5.1.3.19 Synthesis of (**L26**$^{-Me}$)($TaCl_3$) (**49**)*

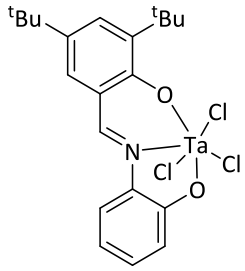


As described for **40**, but using $TaCl_5$ (1.1 eq., 1.16 g, 3.24 mmol) and **L26H** (1.0 g, 2.95 mmol), affording a red powder (0.86 g, 44%). MS (EI, *m/z*): 609 $[M]^+$, 594 $[M\text{-}Me]^+$, 574 $[M\text{-}Cl]^+$, 558 $[M\text{-}Cl\text{-}O]^+$. Found: C, 41.12; H, 3.95; N, 2.33. $C_{21}H_{25}Cl_3NO_2Ta$ requires C. 41.30; H, 4.13; N, 2.29%. IR (Nujol, KBr, $cm^{-1}$): 1651w, 1605s, 1549s, 1481s, 1382s, 1365m, 1326w, 1284s, 1218m, 1188w, 1174w, 924w, 852s, 751m, 696w, 667m. $^1$H NMR ($CDCl_3$): δ = 8.41 (s, 1H), 7.65 (d, 1H, *J* = 1.9, Ar*H*), 7.22 (m, 3H, Ar*H*), 6.87 (t, 1H, *J* = 7.5, Ar*H*), 6.65 (m, 1H,), 1.41 (s, 9H, $C(CH_3)_3$), 1.27 (s, 9H, $C(CH_3)_3$).

*5.1.3.20 Synthesis of **L27H**($TaCl_5$) (**50**)*

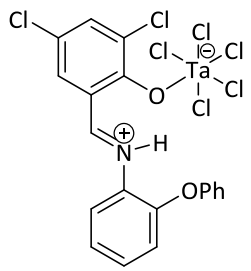

$TaCl_5$ (1.1 eq., 1.10 g, 3.07 mmol) and **L27H** (1.0 g, 2.79 mmol) were heated to reflux temperature under $N_2$, the vessal was sealed and left at this temperature for 8 h. The volatiles were removed *in vacuo*, recrystallisation of the residue from acetonitrile (30 ml) afforded yellow needles of **50** (0.72 g, 32%). MS (EI, *m/z*): 679 $[M\text{-}Cl]^+$, 644 $[M\text{-}2Cl]^+$. Found: C, 31.98; H, 1.74; N, 1.86. $C_{19}H_{13}Cl_7NO_2Ta$ requires C, 31.85; H, 1.83; N, 1.96 %. IR (Nujol, KBr, $cm^{-1}$): 2855m, 2257w, 1781w, 1649s, 1583m, 1297m, 1206m, 1175w, 907w, 871w, 848m, 756m, 728m, 693m, 674w. $^1H$ NMR ($C_6D_6$): δ = 10.49 (br s, 1H, C=N*H*), 8.95 (s, 1H, C*H*=N), 7.86 (s, 1H, Ar*H*), 7.03 – 6.98 (overlapping m, 6H, Ar*H*), 6.62 (overlapping m, 2H, Ar*H*), 6.48 (s, 1H, Ar*H*), 6.31 (d, 1H, *J* = 8.0, Ar*H*).

## *5.1.4 Synthesis of Zinc/Magnesium Bearing Calix[4]arenes*

*5.1.4.1 Synthesis of **L30**($ZnC_6F_5)_2$ (**51**)*

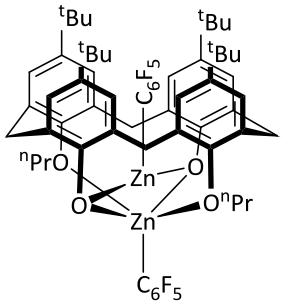

1,3-dipropoxy-*p*-*tert*-butylcalix[4]arene (**$L30H_2$**, 0.75 g, 1.0 mmol) and bis(pentafluorophenyl)zinc.toluene (0.98 g, 2.0 mmol) were dissolved in toluene (30 ml) and refluxed for 16 h. The volatiles were removed *in vacuo*. The residue was extracted into warm acetonitrile and after 24 hours clear blocks of **30** formed. (0.65 g, 54%). MS (EI, *m/z*) 1196 $[M]^+$, 1181 $[M\text{-}Me^+]$. Found: C, 62.06; H, 5.42. $C_{62}H_{66}F_{10}O_4Zn_2$ requires C, 62.27; H, 5.56%. IR (ATR, $cm^{-1}$): 2953m, 1738m, 1632w, 1505m, 1457s, 1363m, 1256m, 1203m, 1097w, 1074m, 1056m, 986m, 953s, 917w, 831w, 755m, 721w, 526m. $^1H$ NMR ($CDCl_3$): 7.13 (s, 4H, Ar-*H*), 6.83 (s, 4H, Ar-*H*), 4.43 (d, 4H, *J* = 17.5, endo-C$H_2$), 3.82 (t, 4H, *J* = 10.0 Hz, OC$H_2$$CH_2$$CH_3$), 3.39 (d, 4H, *J* = 17.5, exo-C$H_2$) 1.54 (m, 4H, $CH_2$C$H_2$$CH_3$), 1.39 (s,

18H, $^{t}$Bu), 0.68 (m, 24H). $^{19}$F ($CDCl_3$): -113.9 (m, 2F, *o*-Ar*F*), -114.0 (m, 2F, *o*-Ar*F*) -154.8 (t, 1F, *J* = 19.3, *p*-Ar*F*), -158.0 (t, 1F, *J* = 19.3, *p*-Ar*F*), -160.5 (m, 2F, *m*-Ar*F*), -164.4 (m, 2F, *m*-Ar*F*).

*5.1.4.2 Synthesis of **L30**[NaZnN(SiMe$_3$)$_2$] (**53**)*

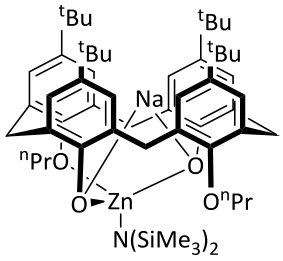


1,3-dipropoxy-*p*-*tert*-butylcalix[4]arene (**L30H$_2$**, 2.0 g, 2.73 mmol) and sodium hydride (140 mg, 5.83 mmol) were dissolved in THF (30ml). The solution was stirred for 1 h and then $ZnCl_2$ (0.37 g, 2.73 mmol) was added as a THF solution (15 ml). The solution was stirred for a further hour, $NaN(SiMe_3)_2$ (2.73 ml, 1M solution in THF) was then added and after 1 h, the volatiles were removed *in vacuo*. The residue was extracted in light petroleum and on standing (2 h) clear rods of compound **53** appeared. (1.32 g, 50%). MS (EI, *m/z*): 977 [M$^+$]. Found: C, 68.44; H 8.72; N, 1.49. $C_{56}H_{84}NNaO_4Si_2Zn$ requires C, 68.65; H, 8.64; N, 1.43%. IR (ATR, cm$^{-1}$): 2954s, 2903m, 2870m, 1453s, 1350m, 1301m, 1249m, 1194m, 1097w, 995m, 930s, 872m, 839s, 752m. $^1$H NMR ($CDCl_3$): $\delta$ = 7.13 (s, 4H, Ar-*H*), 6.70 (s, 2H, Ar-*H*), 6.67 (s, 2H, Ar-*H*), 4.38 (d, 2H, *J* = 13.1, *endo*-C*H*$_2$), 4.32 (d, 2H, *J* = 12.9, *endo*-C*H*$_2$), 4.26 (t, 2H, *J* = 8.02, OC*H*$_2$), 3.77 (t, 2H, *J* = 7.80, OC*H*$_2$), 3.18 (d, 2H, *J* = 13.1, *exo*-C*H*$_2$), 3.13 (d, 4H, *J* = 12.7, *exo*-C*H*$_2$), 1.99 (m, 2H, *J* = 7.68, $OCH_2CH_2CH_3$), 1.46 (m, 2H, *J* = 7.62, $OCH_2CH_2CH_2CH_3$), 1.39 (s, 9H, $^{t}$Bu), 1.37 (s, 9H, $^{t}$Bu), 0.97 (s, 9H, $^{t}$Bu), 0.94 (s, 9H, $^{t}$Bu), 0.91 (t, 3H, *J* = 7.00, $OCH_2CH_2CH_3$), 0.52 (t, 3H, *J* = 7.28, $OCH_2CH_2CH_3$), 0.11 (s, 18H, N(Si*Me*$_3$)$_2$. $^{13}$C NMR ($CDCl_3$): $\delta$ = 162.5, 157.3, 154.0, 153.5, 136.9, 136.0, 132.1, 131.6, 125.5, 125.4, 123.3, 122.2, 78.1, 77.5, 34.2, 34.0, 33.9, 33.7, 33.7, 32.4, 32.1, 31.4, 31.3, 23.0, 22.5, 10.1, 9.5, 5.5, 2.7.

*5.1.4.3 Synthesis of **L30**[ZnN(SiMe$_3$)$_2$]$_2$ (**54**)*

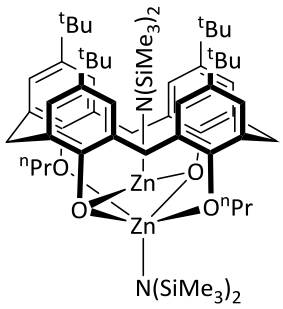


1,3-dipropoxy-*p-tert*-butylcalix[4]arene (**L30H$_2$**, 2.0 g, 2.73 mmol) was dissolved in toluene (30 ml) and zinc bis(bis(trimethylsilyl)amide) (2.2 ml, 5.46 mmol) was added. The solution was heated at reflux for 72 h. The volatiles were removed *in vacuo* and the residue extracted with pentane. The pentane solution was concentrated to 15 ml and left to stand overnight resulting in a yellow microcrystalline solid. (1.39 g, 43%) MS (EI, *m/z*) 1022 [M-ZnN(TMS)$_2^+$]. Found: C, 63.12; H 8.68; N, 2.22. $C_{62}H_{102}N_2NaO_4Si_2Zn$ requires C, 62.97; H, 8.69; N, 2.37%. IR (ATR, cm$^{-1}$): 2955s, 2905m, 2869m, 1478s, 1390m, 1361m, 1303m, 1250m, 1194s, 1124w, 1096w, 995m, 966s, 931s, 870s, 827s, 799m, 754m. $^1$H NMR ($CDCl_3$): $\delta$ = 7.03 (s, 4H, Ar-*H*), 6.76 (s, 4H, Ar-*H*), 4.50 (d, 4H, *J* = 12.1, *endo*-C*H*$_2$), 4.06 (t, 4H, *J* =7.46, OC*H*$_2$), 3.16 (d, 4H, *J* = 12.1, *exo*-C*H*$_2$), 1.91 (m, 4H, *J* = 7.47, $OCH_2CH_2CH_3$), 1.28 (s, 18H, $^t$Bu), 1.03 (t, 6H, *J* = 7.45, $OCH_2CH_2CH_3$), 0.90 (s, 18H, $^t$Bu), 0.11 (overlapping s, 36H, N(Si*Me*$_3$)$_2$. $^{13}$C NMR ($CDCl_3$): $\delta$ = 156.3, 148.4, 145.1, 138.0, 131.2, 131.1, 124.8, 123.3, 79.2, 32.8, 32.6, 30.9, 30.1, 29.9, 19.7, 8.2, 3.9.

*5.1.4.4 Synthesis of **L31**(ZnC$_6$F$_5$)$_3$ (**55**)*

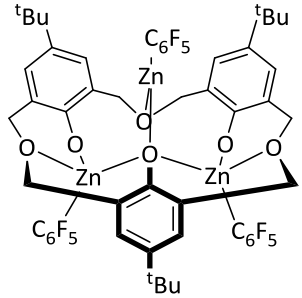


A toluene solution (30 ml) of *p-tert*-butylhexahomotrioxacalix[3]arene (**L31H$_3$**, 0.5 g, 0.87 mmol) and bis(pentafluorophenyl)zinc.toluene (1.27 g, 2.6 mmol) was stirred at ambient temperature for 12 h. The volatiles removed *in vacuo*. The residue was extracted into warm light petroleum, compound **55** immediately formed as a white powder. (0.91 g, 79%). MS (EI, *m/z*): 1270.2 [M]$^+$. IR (Nujol, KBr, cm$^{-1}$):

1634m, 1608m, 1588w, 1532w, 1504s, 1394m, 1304m, 1261s, 1215s, 1052s, 1023s, 974s, 954s, 925m, 915m, 878s, 828m, 799s, 771m, 751m, 659w, 598m, 590m, 534m, 498w, 455m. Found: C, 51.12; H 3.63%. $C_{62}H_{66}F_{10}O_4Zn_2$ requires C, 51.03; H, 3.57%. $^1$H NMR ($CDCl_3$): δ = 7.20 (s, 2H, Ar-*H*), 7.16, 7.13 (ABq, 4H, *J* = 1.91 Hz, Ar-*H*) 5.54 (d, 2H, *J* = 13.6, Ar-*H*), 5.54 (d, 2H, *J* = 13.6, endo-C*H*$_2$), 5.40 (d, 2H, *J* = 10.4, endo-C*H*$_2$), 5.26 (d, 2H, *J* = 10.6, endo-C*H*$_2$), 4.82 (d, 2H, *J* = 10.4, exo-C*H*$_2$), 4.71 (d, 2H, *J* = 10.6, exo-C*H*$_2$), 4.51 (d, 2H, *J* = 13.6, exo-C*H*$_2$), 1.25 (s, 18H, $^t$Bu), 1.17 (s, 9H, $^t$Bu). $^{19}$F ($CDCl_3$): -115.8 (m, 4F, Ar*F*), -116.2 (m, 2F, Ar*F*) -155.5 (t, 2F, *J* = 25.0, Ar*F*), -155.6 (t, 1F, *J* = 25.0, Ar*F*), -161.5 – 162.0 (m, 6F, Ar*F*).

*5.1.4.5 Synthesis of (**L31**)$Zn_6(C_6F_5)(R)(RH)OH{\cdot}5MeCN$ (**56**)*

R = $C_6F_5CH_2$–(*p*-$^t$BuPhenolate–$CH_2OCH_2$–)$_2$–*p*-$^t$BuPhenolate–$CH_2O^-$)$^{3-}$

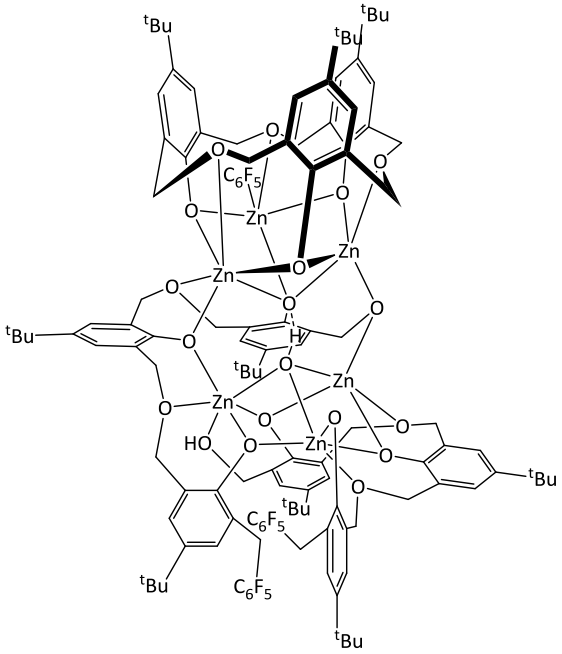

Compound **55** (1.0 g, 0.79 mmol) was dissolved in acetonitrile (30 ml) and heated at reflux for 1 hr. Clear blades of compound **56** formed on cooling to room temperature. (0.11 g, 5% yield). Found: C, 56.26; H 4.72. $C_{126}H_{137}F_{15}O_{19}Zn_6$ requires C, 57.53; H, 4.67%. $^1$H NMR ($CDCl_3$): 7.24 (s, 2H), 7.18-7.14 (m, 1H), 7.11-7.01 (m, 3H), 6.93 (d, 1H, *J* = 2.5), 6.88 (d, 1H, *J* = 2.5), 6.86-6.85 (m, 1H), 6.77 (d, 1H, *J* = 2.45) 6.74 (d, 1H, *J* = 2.25), 6.70 (d, 1H, *J* = 2.35), 6.63 (br t, 2H), 6.58 (d, 1H, *J* = 2.32) 6.56 (d, 1H, *J* =2.32) 6.10-6.02 (m, 2H), 5.94-5.88 (m, 2H), 5.86-5.83 (m, 2H), 5.73-5.67 (m, 2H), 5.58-5.55 (m, 2H), 5.31 (d, 1H, *J* = 9.21), 4.97 (d, 1H, *J* = 13.7), 4.90 (d, 1H, *J* = 10.85), 4.85 (d, 1H, *J* = 13.7), 4.79 (d, 1H, *J* = 11.0), 4.64-4.52 (m, 2H), 4.48 (d, 2H, *J* = 13.6), 4.19 (d, 2H, *J* = 13.6), 4.15 (d, 1H, *J* = 9.45), 4.10 (d, 1H, *J* = 9.10), 4.07-3.96 (m, 4H), 3.88-3.75 (m, 5H), 3.70 (d, 1H, *J* = 13.9), 3.63 (m, 2H), 3.55 (d, 1H, *J* = 10.8), 3.07 (d, 1H, *J* = 17.3), 2.80 (d, 1H, *J* = 14.5), 2.35 (s, 2H), 2.00 (s, 6H), 1.36 (s, 9H), 1.29 (s, 9H), 1.28 (s, 9H), 1.23 (s, 9H), 1.14 (s, 9H), 1.10 (s, 9H) 0.98 (s, 9H) 0.82 (s, 9H) 0.62 (s, 9H). $^{19}$F NMR ($CDCl_3$): -114.8 (m, 2F), -141.8 (m, 2F), -142.3 (m, 2F), -158.3 (t, 1F, *J* = 21.3), -158.8 (t, 1F, *J* = 19.7), -160.14 (t, 1F, *J* = 20.9), -163.2 (m, 2F), -163.6 (m, 2F), -164.2 (m, 2F).[1]

[1] Sample was submitted for mass spectroscopy analysis however the molecular ion of the product was not observed.

*5.1.4.6 Synthesis of **L30**[Li(THF)Mg$^{n}$Bu)] (**57**)*

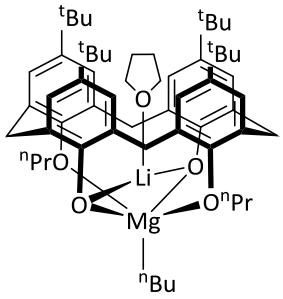


1,3-dipropoxy-*p*-*tert*-butylcalix[4]arene (**L30H$_2$**, 4.0 g, 5.46 mmol) was dissolved in THF (50 ml). The solution was cooled to 0 °C and $^{n}$BuLi (10.93 mmol, 1.6 M in hexanes, 6.83 ml) was added dropwise. The orange solution was allowed to warm to room temperature and stirred for 1 h. The Grignard reagent *n*-BuMgBr (10.93 mmol), prepared from reaction between *n*-BuBr and magnesium turnings in THF and used immediately, was added to the lithiated solution at 0 °C. The solution was allowed to warm to room temperature and stirred for 1 h. The THF solution was extracted and then concentrated to approximately 10 ml, and light petroleum (40 ml) was added. After standing at room temperature overnight, yellow needles of the product formed (1.54 g, 32%). MS (ASAP, *m/z*) 875.6 $[M\text{-}CH_3]^+$, 841.5 [M-Pr-Li+H]. IR (ATR, $cm^{-1}$): 2956s, 2904m, 2872m, 1627w, 1600w, 1479s, 1389m, 1362m, 1308m, 1249w, 1191m, 1123m, 1094m, 1043w, 999w, 870m, 830w, 797w, 531m. Found: C, 78.29; H, 9.44. $C_{58}H_{83}LiMgO_5$ requires C, 78.14; H, 9.38%. $^1$H NMR ($C_6D_6$): $\delta$ = 7.37 (s, 4H, Ar-*H*), 7.20 (s, 4H, Ar-*H*), 4.63 (d, 4H, J = 12.7, *endo*-C*H$_2$*), 4.26 (br t, 4H, OC*H$_2$*), 3.41 (d, 4H, *J* = 12.7, *exo*-C*H$_2$*), 2.48 (m, 2H, $MgCH_2CH_2CH_2CH_3$), 2.05 (m, 2H, *J* = 7.22, $MgCH_2CH_2CH_2CH_3$), 1.90 (m, 4H, *J* = 7.84, $OCH_2CH_2CH_3$), 1.53 (s, 18H, $^{t}$Bu), 1.42 (t, 3H, *J* = 7.31, $MgCH_2CH_2CH_2CH_3$), 1.15 (s, 18H, tBu) 0.73 (t, 6H, *J* = 7.31 Hz, $OCH_2CH_2CH_3$), 0.57 (m, 2H, $MgCH_2CH_2CH_2CH_3$). $^{13}$C NMR ($C_6D_6$): $\delta$ = 152.2, 146.7, 137.6, 134.9, 130.5, 128.6, 125.8, 125.2, 78.8, 35.4, 34.2, 34.1, 33.8, 32.5, 32.4, 31.4, 30.8, 25.2, 23.0, 14.8, 14.0, 9.8, 7.0.

*5.1.4.7 Synthesis of **L32**(Mg$^n$Bu) (**58**)*

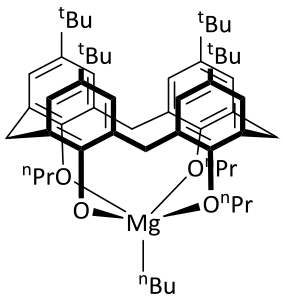


Tripropoxy-*p-tert*-butyl-calix[4]areneH$_3$ (**L32H$_3$**, 2.0 g, 2.58 mmol) was dissolved in THF (30 ml), cooled to 0 °C and $^n$Bu$_2$Mg (1.0 M in heptane, 2.58 mmol, 2.58 ml) was added dropwise. After complete addition the solution was allowed to warm to room temperature and then stirred for 3 h. The volatiles were removed *in vacuo* and the product extracted using light petroleum (30 ml). The petroleum ether solution was concentrated to approximately 15 ml. Upon standing overnight colourless needles formed (1.1 g, 50%). MS (EI, *m/z*) 774 [M-Mg$^n$Bu]$^+$. IR (ATR, cm$^{-1}$): 2956s, 2871s, 1480s, 1390w, 1361m, 1299w, 1261w, 1200m, 1121m, 1105m, 1042m, 1008m, 985m, 870m, 799m, 635w, 532m. Found: C, 79.72; H 9.44. $C_{56}H_{80}MgO_4$ requires C, 79.93; H, 9.58 %. $^1$H NMR ($C_6D_6$): $\delta$ = 7.40 (s, 2H, Ar-*H*), 7.39 (s, 2H, Ar-*H*), 6.99 (s, 4H, Ar-*H*), 4.58 (d, 2H, *J* = 12.3, *endo*-C*H*$_2$), 4.52 (d, 2H, *J* = 12.1, *endo*-C*H*$_2$), 4.33 (m, 4H, OC*H*$_2$), 3.59 (br t, 4H, OC*H*$_2$), 3.46 (d, 4H, *J* = 12.3, *exo*-C*H*$_2$), 3.38 (d, 4H, *J* = 12.1, *exo*-C*H*$_2$), 2.28 (m, 2H, MgCH$_2$C*H*$_2$CH$_2$CH$_3$), 2.07-1.80 (m, 8H), 1.62 (s, 9H, tBu), 1.40 (s, 9H, tBu), 1.31 (t, 3H, J = 7.3 Hz, MgCH$_2$CH$_2$CH$_2$C*H*$_3$), 0.79 (s, 18H, tBu) 0.56 (m, 9H, OCH$_2$CH$_2$C*H*$_3$), 0.28 (m, 2H, MgC*H*$_2$CH$_2$CH$_2$CH$_3$). $^{13}$C NMR ($C_6D_6$): $\delta$ = 160.2, 151.2, 148.8, 148.7, 148.5, 146.3, 135.2, 133.7, 133.8, 130.9, 127.5, 125.4, 123.4, 122.9, 79.6, 78.2, 40.5, 34.8, 33.4, 33.0, 32.6, 32.2, 31.6, 30.4, 29.6, 21.6, 21.5, 13.5, 13.1, 8.2, 7.9, 7.5.

## *5.1.5 Polymerisation Procedures*

### *5.1.5.1 Homogeneous Polyethylene Polymerisation Procedure*

A flame dried (250 ml) flask was purged several times with ethylene gas at 1 bar pressure. This pressure was maintained throughout the polymerisation run. Dry, degassed toluene (100 ml) and ethyltrichloroacetate (ETA, 0.05 – 0.1 ml) were added and stirred for 10 minutes. The required temperature was maintained *via* a water bath, and the co-catalyst was added; the pre-catalyst was then injected as a toluene solution. The polymerisation time was recorded from injection of the pre-catalyst. The polymerisation solution was quenched by addition of methanol and the aluminium

residues dissolved by the addition of acidified water. The solid polyethylene was then filtered and dried.

#### *5.1.5.2 Polycaprolactone Polymerisation Procedure*

A Schlenk flask (250 ml) was charged with the required quantity of pre-catalyst under glove box conditions. The required amount of dry, degassed toluene and alcohol (from an alcohol/toluene solution) was added. The solution was heated to the required temperature. The polymerisation was initiated by addition of the ε-caprolactone and was stirred for the allotted time. Conversion of monomer was determined by $^{1}$H NMR, and the polymerisation was quenched by addition of methanol.

#### *5.1.5.3 Parallel Pressure Reactor Polymerisation Procedure*

A pre-weighed glass vial with stirring paddles was sealed and purged with ethylene. 5 µmol of co-catalyst from a 100 mM heptane solution was added along with co-monomer (if required). Heptane was then added to reach a volume of 4 ml in the reaction vessel and heated to 80 °C. The ethylene pressure was set to 92 psi (6.34 bar). The catalyst (along with ETA if required) was added as a heptane slurry to initiate the run. The run was stirred for 60 minutes and quenched with $CO_2$ (35 % in $N_2$). The glass vial was dried and weighed to calculate yield.

#### *5.1.5.4 Poly(Lactic acid) Polymerisation Procedure*

Solutions of *rac*-lactide and catalyst were prepared separately using the required solvent. The required amount of alcohol, from a standard alcohol solution in toluene, was added to the pre-catalyst. The *rac*-lactide solution was added to the catalyst solution and stirred for the allotted time at the requited temperature under nitrogen. 0.5 – 1.0 ml aliquots were taken out of the stirred solution where required and quenched with 1 drop of 0.5 M HCl. The aliquots were then dried, precipitated polymer was analysed by $^{1}$H NMR spectroscopy and GPC.

### *5.1.6 X-ray Photoelectron Spectroscopy Analysis*

A small amount (mg) of powdered sample was pressed onto adhesive carbon tape. High resolution XPS core level measurements were performed with a VG Escalab 250 in LENNF, Leeds University, equipped with a conventional hemispherical sector analyser and controlled by a VGX900 data system. XPS experiments were carried out using a high intensity monochromated Al-Kα source (1486.6 eV)

operated at 15 kV and 20 mA. V-2*p*, C-1*s* , Cl-2*p* and N-1*s* spectra were recorded using a pass energy of 20 eV. The energy scale of the spectrometer was calibrated to the Ag-$3d_{5/2}$ peak at 368.3 eV. The binding energy scale was calibrated to the C-1s at 284.5 eV. High-resolution peak fitting was performed using CasaXPS software (version 2.3.15).

### *5.1.7 Crystallography*

Crystallographic analysis and solutions were performed by Dr David Hughes (UEA), Dr Joseph Wright (UEA) or Dr Tim Prior (Hull). Crystal structure data was collect either at the University of East Anglia or at the National Crystallography Service at the University of Southampton. Crystals, under oil, were mounted onto glass fibers and fixed under the cold nitrogen stream on a diffractometer. Data for each compound were measured by thin-slice ω and ϕ^^scans on an Oxford Diffraction Xcalibur-3/Sapphire3-CCD diffractometer that was equipped with $Mo_{K\alpha}$ radiation and graphite monochromator and processed using the CrysAlisPro-CCD and -RED[25] programs or measured on an AFC12 (Right), Kappa 3-circle diffractometer with a Rigaku Saturn724+ CCD detector, molybdenum radiation and a confocal monochromator at the National Crystallography Service at the University of Southampton and were processed by using the CrystalClear-SM Expert 2.0 r7 programs.[26] The structures of all of the structures were determined by the direct methods routines in the SHELXS program[27] or with SIR-2004[28] and refined by full-matrix least-squares methods on $F^2$ in SHELXL.[27] The non-hydrogen atoms in most structures were refined with anisotropic thermal parameters. Hydrogen atoms were included at idealised positions and their $U_{iso}$ values were set to ride on the $U_{eq}/U_{iso}$ values of the parent carbon or nitrogen atoms. Crystal data and structural refinement for each structure are collated in the appendix. Scattering factors for the neutral atoms were taken from Ref. The computer programs that were used in this analysis are noted above and were run on a Dell Precision 370 PC with WinGX[29] at the University of East Anglia.

## 5.2 References


[1] P. B. Hitchcock, D. L. Hughes, G. Jeffery Leigh, J. Roger Sanders, J. S. de Souza, *J. Chem. Soc., Dalton Trans.* **1999**, 1161.

[2] F. Marchetti, G. Pampaloni, S. Zacchini, *Dalton Trans.* **2008**, 7026.

[3] S. F. Pedersen, J. B. Hartung, E. J. Roskamp, P. S. Dragovich, C. J. Ruffing, B. A. Klein, in *Inorg. Synth.*, John Wiley & Sons, Inc., **2007**, pp. 119-123.

[4] D. A. Walker, T. J. Woodman, D. L. Hughes, M. Bochmann, *Organometallics* **2001**, *20*, 3772.

[5] D. J. Darensbourg, M. W. Holtcamp, G. E. Struck, M. S. Zimmer, S. A. Niezgoda, P. Rainey, J. B. Robertson, J. D. Draper, J. H. Reibenspies, *J. Am. Chem. Soc.* **1998**, *121*, 107.

[6] A. Maisse-Franois, L. Azor, A.-L. Schmitt, A. Coquel, L. Brelot, R. Welter, S. Bellemin-Laponnaz, S. Dagorne, *J. Organomet. Chem.* **2012**, *696*, 4248

[7] G. J. Clarkson, V. C. Gibson, P. K. Y. Goh, M. L. Hammond, P. D. Knight, P. Scott, T. M. Smit, A. J. P. White, D. J. Williams, *Dalton Trans.* **2006**, 5484

[8] D. Gong, B. Wang, X. Jia, X. Zhang, *Dalton Trans.* **2014**, *43*, 4169

[9] J. Ma, K.-Q. Zhao, M. J. Walton, J. A. Wright, J. W. A. Frese, M. R. J. Elsegood, Q. Xing, W.-H. Sun, C. Redshaw, *Dalton Trans.* **2014**, *43*, 8300

[10] P. A. Cameron, V. C. Gibson, C. Redshaw, J. A. Segal, A. J. P. White, D. J. Williams, *J. Chem. Soc., Dalton Trans.* **2002**, 415

[11] C. Redshaw, M. Walton, L. Clowes, D. L. Hughes, A.-M. Fuller, Y. Chao, A. Walton, V. Sumerin, P. Elo, I. Soshnikov, W. Zhao, W.-H. Sun, *Chem. Eur. J.* **2013**, *19*, 8884

[12] D. J. Jones, V. C. Gibson, S. M. Green, P. J. Maddox, A. J. P. White, D. J. Williams, *J. Am. Chem. Soc.* **2005**, *127*, 11037.

[13] L. Tang, E. P. Wasserman, D. R. Neithamer, R. D. Krystosek, Y. Cheng, P. C. Price, Y. He, T. J. Emge, *Macromolecules* **2008**, *41*, 7306.

[14] Q.-S. Shi, X. Hao, C. Redshaw, W.-H. Sun, *Chin. J. Polym. Sci.* **2013**, *31*, 769.

[15] C. Bianchini, G. Mantovani, A. Meli, F. Migliacci, F. Zanobini, F. Laschi, A. Sommazzi, *Eur. J. Inorg. Chem.* **2003**, *2003*, 1620.

[16] L. Jafarpour, E. D. Stevens, S. P. Nolan, *J. Organomet. Chem.* **2000**, *606*, 49.

[17] C. D. Gutsche, B. Dhawan, M. Leonis, D. Stewart, *Org. Synth.* **1990**, *68*, 238.

[18] J. H. Munch, C. D. Gutsche, *Org. Synth.* **1990**, *68*, 243.

[19] G. J. P. Britovsek, V. C. Gibson, S. J. McTavish, G. A. Solan, A. J. P. White, D. J. Williams, G. J. P. Britovsek, B. S. Kimberley, P. J. Maddox, *Chem. Commun.* **1998**, 849.

[20] A. O. Eseola, W. Li, W.-H. Sun, M. Zhang, L. Xiao, J. A. O. Woods, *Dyes Pigm.* **2011**, *88*, 262.

[21] L. Benisvy, A. J. Blake, D. Collison, E. S. Davies, C. D. Garner, E. J. L. McInnes, J. McMaster, G. Whittaker, C. Wilson, *Chem. Commun.* **2001**, 1824.

[22] J.-Q. Wu, L. Pan, N.-H. Hu, Y.-S. Li, *Organometallics* **2008**, *27*, 3840.

[23] H. Tsurugi, T. Saito, H. Tanahashi, J. Arnold, K. Mashima, *J. Am. Chem. Soc.* **2011**, *133*, 18673.

[24] Y. Nakayama, N. Maeda, T. Shiono, in *Stud. Surf. Sci. Catal., Vol. Volume 161* (Eds.: K. N. Takeshi Shiono, T. Minoru), Elsevier, **2006**, pp. 165-170.

[25] Oxford Diffraction Ltd, Abingdon, UK, **2010**.

[26] Rigaku Corporation, Tokyo, Japan **2011**.

[27] G. Sheldrick, *Acta Crystallogr., Sect. A: Found. Crystallogr.* **2008**, *64*, 112.

[28] A. J. Florence, N. Shankland, K. Shankland, W. I. F. David, E. Pidcock, X. Xu, A. Johnston, A. R. Kennedy, P. J. Cox, J. S. O. Evans, G. Steele, S. D. Cosgrove, C. S. Frampton, *J. Appl. Crystallogr.* **2005**, *38*, 249.

[29] L. Farrugia, *J. Appl. Crystallogr.* **1999**, *32*, 837.

# Chapter 6 – Appendix

**Table 6.1** Crystal structure data for compounds reported in this thesis.

| **Compound** | **7** | **9** | **10** | **11** | **12** | **13** | **14** |
|---|---|---|---|---|---|---|---|
| Formula | $C_{60}H_{86}Cl_4N_2O_6V_2$ | $C_{38}H_{46}Cl_2N_2O_3V.$ $2CH_3CN$ | $C_{44}H_{56}N_2O_5V.2CH_3CN$ | $C_{44}H_{56}N_2O_5V$ | $C_{44}H_{56}N_2O_5V.2CH_3CN$ | $C_{46}H_{60}N_2O_5V$ | $C_{44}H_{50}F_6N_2O_5V$ |
| Formula weight | 1175.0 | 782.72 | 825.96 | 743.85 | 825.96 | 771.90 | 851.80 |
| Crystal system | Orthorhombic | Orthorhombic | Monoclinic | Triclinic | Triclinic | Monoclinic | Triclinic |
| Space group | Pbca | $P2_1nb$ | $P2_1/n$ | $P\ \bar{1}$ | $P\ \bar{1}$ | $P2_1/n$ | $P\ \bar{1}$ |
| Unit cell dimensions | | | | | | | |
| a (Å) | 15.4851(3) | 11.0873(5) | 17.946(4) | 15.165(3) | 10.979(2) | 13.997(3) | 14.096(3) |
| b (Å) | 12.3449(2) | 17.9157(8) | 9.2015(18) | 18.182(4) | 13.256(3) | 18.580(4) | 15.274(3) |
| c (Å) | 33.0323(6) | 20.6832(14) | 28.165(6) | 19.034(4) | 15.575(3) | 17.898(4) | 24.527(5) |
| α (°) | 90 | 90 | 90 | 66.33(3) | 101.47(3) | 90 | 87.65(3) |
| β (°) | 90 | 90 | 95.87(3) | 67.40(3) | 91.71(3) | 104.38(3) | 75.73(3) |
| γ (°) | 90 | 90 | 90 | 67.40(3) | 92.44(3) | 90 | 64.15(3) |
| V ($Å^3$) | 6314.5(2) | 4108.4(4) | 4626.6(16) | 4433.0(15) | 2217.7(8) | 4508.7(16) | 4592.1(16) |
| Z | 4 | 4 | 4 | 4 | 2 | 4 | 4 |
| Temperature (K) | 140(1) | 100(2) | 173(2) | 173(2) | 173(2) | 173(2) | 173(2) |
| $D_{calcd}$ ($Mg/m^{-3}$) | 1.236 | 1.262 | 1.186 | 1.115 | 1.237 | 1.137 | 1.232 |
| Absorption coefficient, μ ($mm^{-1}$) | 0.512 | 0.414 | 0.262 | 0.266 | 0.273 | 0.263 | 0.283 |
| Crystal size ($mm^3$) | 0.43 x 0.41 x 0.09 | 0.22 x 0.01 x 0.01 | 0.30 × 0.27 × 0.05 | 0.41 × 0.33 × 0.26 | 0.50 × 0.44 × 0.25 | 0.50 × 0.46 × 0.35 | 0.32 × 0.18 × 0.14 |
| $2\vartheta_{max}$ (°) | 25 | 25 | 25.00 | 25.00 | 27.52 | 25.00 | 25.00 |
| Reflections measured | 104961 | 9744 | 25257 | 32972 | 28054 | 25974 | 35870 |
| Unique reflections, $R_{int}$ | 5557, 0.072 | 5871, 0.048 | 8083, 0.0639 | 15504, 0.0497 | 10097, 0.0576 | 7916, 0.0619 | 16108, 0.0739 |
| Transmission factors (max., min.) | 1.020 and 0.982 | 1.000 and 0.480 | 0.9870 and 0.9255 | 0.9330 and 0.8998 | 0.9345 and 0.8759 | 0.9128 and 0.8794 | 0.9615 and 0.9149 |
| Number of parameters | 339 | 471 | 570 | 996 | 539 | 532 | 1069 |
| $R_1$ [$F^2 > 2\sigma(F^2)$] | 0.061 | 0.051 | 0.0830 | 0.0661 | 0.064 | 0.0857 | 0.1081 |
| $wR_2$ (all data) | 0.113 | 0.098 | 0.2740 | 0.1833 | 0.210 | 0.2769 | 0.3372 |
| GOOF, *S* | 1.199 | 1.037 | 1.218 | 1.069 | 1.040 | 1.222 | 1.111 |
| Largest difference peak and hole (e $Å^{-3}$) | 0.39 and -0.31 | 0.31 and -0.29 | 0.714 and -0.773 | 0.353 and -0.293 | 0.461 and -0.579 | 0.882 and -0.717 | 1.095 and -0.679 |

| **Compound** | **15** | **15'** | **16** | **17** | **18** | **19** | **20** |
|---|---|---|---|---|---|---|---|
| Formula | $C_{54}H_{60}N_2O_5V$ | $C_{54}H_{60}N_2O_5V.1.5CH_3CN$ | $C_{54}H_{60}N_2O_8V_2$ | $C_{72}H_{68}N_2O_5V$ | $C_{70}H_{60}N_2O_5V$ | $C_{25}H_{29}Cl_2N_2O_2V$ | $C_{25}H_{29}N_2O_3V.$ $0.67CH_3CN$ |
| Formula weight | 867.98 | 929.56 | 966.92 | 1092.22 | 1060.14 | 511.34 | 483.81 |
| Crystal system | Triclinic | Triclinic | Monoclinic | Triclinic | Triclinic | Triclinic | Monoclinic |
| Space group | $P\ \bar{1}$ | $P\ \bar{1}$ | $P2_1/c$ | $P\ \bar{1}$ | $P\ \bar{1}$ | $P\ \bar{1}$ | $P2_1/n$ |
| Unit cell dimensions | | | | | | | |
| a (Å) | 11.896(2) | 15.3075(16) | 11.9699(5) | 13.457(3) | 12.286(3) | 8.9979(4) | 26.127(17) |
| b (Å) | 14.224(3) | 18.0329(18) | 15.6408(6) | 15.049(3) | 13.190(3) | 12.6300(6) | 10.845(8) |
| c (Å) | 15.568(3) | 20.191(2) | 13.9536(5) | 16.071(3) | 19.728(4) | 13.0073(9) | 26.44(2) |
| α (°) | 108.49(3) | 76.0289(15) | 90.00 | 70.73(3) | 70.80(3) | 61.214(4) | 90 |
| β (°) | 90.94(3) | 81.7168(15) | 99.3405(6) | 68.07(3) | 74.35(3) | 78.851(6) | 91.646(12) |
| γ (°) | 109.43(3) | 78.9101(15) | 90.00 | 79.53(3) | 87.75(3) | 70.715(5) | 90 |
| V ($Å^3$) | 2334.2(8) | 5279.7(9) | 2577.74(17) | 2843.8(10) | 2902.9(11) | 1221.78(12) | 7489(9) |
| Z | 2 | *4* | 2 | 2 | 2 | 2 | 12 |
| Temperature (K) | 173(2) | 150(2) | 150(2) | 173(2) | 173(2) | 100(2) | 100(2) |
| $D_{calcd}$ ($Mg/m^{-3}$) | 1.235 | 1.169 | 1.246 | 1.276 | 1.213 | 1.390 | 1.287 |
| Absorption coefficient, μ ($mm^{-1}$) | 0.262 | 0.237 | 0.416 | 0.230 | 0.224 | 0.649 | 0.428 |
| Crystal size ($mm^3$) | 0.40 × 0.17 × 0.11 | 0.62 × 0.38 × 0.08 | 0.58 × 0.20 × 0.12 | 0.536 × 0.422 × 0.254 | 0.58 × 0.20 × 0.12 | 0.10 × 0.40 × 0.01 | 0.17 × 0.05 × 0.01 |
| $2\vartheta_{max}$ (°) | 25.00 | 22.50 | 30.56 | 25.00 | 30.56 | 27.47 | 31.48 |
| Reflections measured | 25233 | 44050 | 29752 | 30994 | 29752 | 16140 | 60185 |
| Unique reflections, $R_{int}$ | 8209, 0.0692 | 13810, 0.0659 | 7812, 0.0315 | 15504, 0.0497 | 7812, 0.0315 | 5555, 0.0385 | 22162, 0.0892 |
| Transmission factors (max., min.) | 0.9727 and 0.9031 | 0.9813 and 0.8670 | 0.9518 and 0.7945 | 1.0000 and 0.5983 | 0.9518 and 0.7945 | 1.000, 0.872 | 0.996, 0.931 |
| Number of parameters | 559 | 1250 | 304 | 831 | 304 | 296 | 1265 |
| $R_1$ [$F^2 > 2\sigma(F^2)$] | 0.0590 | 0.0485 | 0.0378 | 0.0782 | 0.0378 | 0.0389 | 0.1250 |
| $wR_2$ (all data) | 0.2345 | 0.1303 | 0.1069 | 0.2527 | 0.1069 | 0.0966 | 0.1893 |
| GOOF, *S* | 1.023 | 1.049 | 1.024 | 1.092 | 1.024 | 1.062 | 1.194 |
| Largest difference peak and hole (e $Å^{-3}$) | 0.827 and -0.801 | 0.445 and -0.276 | 0.440 and -0.399 | 1.197 and -0.677 | 0.440 and -0.399 | 0.718 and –0.488 | 0.508 and –0.839 |

| **Compound** | **20'** | **21** | **22** | **23** | **24** | **24'** | **25** |
|---|---|---|---|---|---|---|---|
| Formula | $C_{25}H_{29}N_2O_3V$ | $C_{76}H_{106}O_8V_2$ | $C_{78}H_{116}O_{10}V_2.2C_4H_8O$ | $C_{78}H_{116}O_{10}V_2$ | $C_{142}H_{175}Li_2N_5O_{14}V_2{\cdot}8CH_3CN$ | $C_{142}H_{175}Li_2N_5O_{14}V_2{\cdot}9.69CH_3CN$ | $C_{37}H_{46}LiN_2O_5V{\cdot}CH_3CN$ |
| Formula weight | 456.44 | 1249.49 | 1459.80 | 1315.66 | 2620.06 | 2689.23 | 697.69 |
| Crystal system | Monoclinic | Triclinic | Orthorhombic | Monoclinic | monoclinic | monoclinic | Triclinic |
| Space group | P $2_1$/c | P $\bar{1}$ | Pbca | P 2/n | C2/c | C2/c | P $\bar{1}$ |
| Unit cell dimensions | | | | | | | |
| a (Å) | 11.9806(4) | 11.3476(8) | 23.8164(16) | 20.18(2) | 61.082(3) | 61.03(4) | 12.0813(7) |
| b (Å) | 10.2865(4) | 12.2819(9) | 18.9585(7) | 15.820(16) | 20.4495(10) | 20.308(18) | 12.7544(8) |
| c (Å) | 17.9031(12) | 16.8097(11) | 18.6002(6) | 26.50(3) | 25.7085(12) | 25.59(2) | 14.2206 |
| α (°) | 90 | 100.861(4) | 90 | 90 | 90 | 90 | 90.879(6) |
| β (°) | 98.769(7) | 99.097(4) | 90 | 110.686(11) | 90.0954(8) | 90.11(2) | 94.563(7) |
| γ (°) | 90 | 108.087(5) | 90 | 90 | 90 | 90 | 117.961(8) |
| V (Å$^3$) | 2180.56(18) | 2127.4(3) | 8398.4(7) | 7915(14) | 32112(3) | 31716(43) | 1925.9(2) |
| Z | 4 | 1 | 4 | 4 | 8 | 8 | 2 |
| Temperature (K) | 100(2) | 100(2) | 100(2) | 100(2) | 150(2) | 100(2) | 100(2) |
| $D_{calcd}$ (Mg/m$^{-3}$) | 1.390 | 0.975 | 1.155 | 1.021 | 1.084 | 1.126 | 1.203 |
| Absorption coefficient, μ (mm$^{-1}$) | 0.485 | 0.263 | 0.279 | 0.264 | 0.176 | 0.180 | 0.301 |
| Crystal size (mm$^3$) | 0.10 × 0.40 × 0.01 | 0.07 x 0.06 x 0.03 | 0.09 x 0.08 x 0.03 | 0.04 × 0.04 × 0.01 | 0.52 × 0.45 × 0.34 | 0.10 × 0.06 × 0.03 | 0.09 × 0.04 × 0.01 |
| $2\vartheta_{max}$ (°) | 27.48 | 27.49 | 27.46 | | 25.0 | 22.5 | 25.0 |
| Reflections measured | 15333 | 9683 | 57655 | 30414 | 115060 | 132839 | 20767 |
| Unique reflections, $R_{int}$ | 4999, 0.0353 | 9683, 0.000 | 9280, 0.1195 | 6040, 0.2574 | 28282, 0.0691 | 20718, 0.225 | 6765, 0.094 |
| Transmission factors (max., min.) | 1.000, 0.718 | 0.9921 and 0.9818 | 0.9917 and 0.9753 | 1.000 and 0.355 | 0.914 and 0.943 | 0.982 and 0.995 | 0.973 and 0.997 |
| Number of parameters | 287 | 392 | 464 | 578 | 1883 | 1997 | 458 |
| $R_1$ [$F^2 > 2\sigma(F^2)$] | 0.0535 | 0.0566 | 0.0484 | 0.2176 | 0.1179 | 0.1715 | 0.0737 |
| $wR_2$ (all data) | 0.1586 | 0.1587 | 0.1110 | 0.5275 | 0.3571 | 0.3415 | 0.2118 |
| GOOF, *S* | 1.075 | 1.057 | 0.913 | 1.522 | 1.110 | 1.279 | 1.021 |
| Largest difference peak and hole (e Å$^{-3}$) | 0.567 and -1.175 | 0.631 and -0.502 | 0.346 and -0.454 | 0.777 and -0.463 | 1.184 and –0.393 | 0.725 and -0.446 | 0.823 and -0.437 |

| Compound | 26 | 27 | 27’ | 28 | 29 | 30 | 33 | 39 |
|---|---|---|---|---|---|---|---|---|
| Formula | $C_{98}H_{120}V_2N_5NaO_{10}\cdot 4CH_3CN$ | $C_{88}H_{104}V_4O_{14}\cdot 3CH_3CN$ | $C_{88}H_{104}V_4O_{14}\cdot 3CH_2Cl_2$ | $C_{29}H_{31}Cl_4N_2NbO.CH_3CN$ | $C_{31}H_{34}Cl_2N_3NbO_2.3CH_3CN$) | $C_{29}H_{31}Cl_4N_2OTa.CH_3CN$ | $C_{31}H_{31}Cl_2N_2NbO_3$ | $C_{42}H_{52}Cl_4N_4O_4$-$Nb_2.4CH_3CN$ |
| Formula weight | 1817.08 | 1712.63 | 1844.25 | 699.3 | 767.6 | 787.4 | 643.4 | 1168.71 |
| Crystal system | Monoclinic | Triclinic | Triclinic | Orthorhombic | Orthorhombic | Orthorhombic | Triclinic | Monoclinic |
| Space group | $P\,2_1/n$ | $P\,\bar{1}$ | $P\,\bar{1}$ | Pbca | Pbcn | Pbca | $P\,\bar{1}$ | $P2_1/c$ |
| Unit cell dimensions | | | | | | | | |
| a (Å) | 12.4731(7) | 13.763(6) | 13.870(2) | 12.1825(3) | 26.4887(6) | 12.20751(12) | 9.2530(3) | 17.3058(5) |
| b (Å) | 31.3969(17) | 18.382(8) | 18.180(3) | 19.4186(5) | 14.1088(2) | 19.4381(2) | 9.6926(3) | 10.4825(3) |
| c (Å) | 27.8042(15) | 18.985(8) | 18.983(5) | 26.5342(5) | 20.7568(5) | 26.5521(3) | 16.9423(4) | 15.1775(5) |
| α (°) | 90 | 74.641(6) | 75.296(2) | 90 | 90 | 90 | 91.042(2) | 90 |
| β (°) | 102.8887(8) | 86.251(6) | 86.178(2) | 90 | 90 | 90 | 102.538(2) | 93.632(3) |
| γ (°) | 90 | 79.451(7) | 77.749(2) | 90 | 90 | 90 | 100.719(2) | 90 |
| V ($Å^3$) | 10614.2(10) | 4553(3) | 4524.0(13) | 6277.1(3) | 7757.3(3) | 6300.55(11) | 1454.64(7) | 2747.79(14) |
| Z | 4 | 2 | 2 | 8 | 8 | 8 | 2 | 2 |
| Temperature (K) | 150(2) | 150(2) | 150(2) | 140(1) | 140(1) | 140(1) | 140(1) | 140(1) |
| $D_{calcd}$ ($Mg/m^{-3}$) | 1.137 | 1.249 | 1.354 | 1.480 | 1.314 | 1.660 | 1.469 | 1.413 |
| Absorption coefficient, μ ($mm^{-1}$) | 0.238 | 0.460 | 0.638 | 0.753 | 0.487 | 3.858 | 0.632 | 0.660 |
| Crystal size ($mm^3$) | 0.45 × 0.28 × 0.27 | 0.19 × 0.07 × 0.02 | 0.26 × 0.05 × 0.04 | 0.24 x 0.15 x 0.015 | 0.33 x 0.18 x 0.18 | 0.42 x 0.22 x 0.06 | 0.30 x 0.18 x 0.12 | 0.27 x 0.16 x 0.09 |
| $2\theta_{max}$ (°) | 27.19 | 24.0 | 26.7 | 25.0 | 25.0 | 30.0 | 27.5 | 32.53 |
| Reflections measured | 99178 | 57516 | 71017 | 79369 | 104864 | 119629 | 24291 | 57508 |
| Unique reflections, $R_{int}$ | 23497, 0.0832 | 15616, 0.1565 | 20773, 0.0921 | 5518, 0.143 | 6819, 0.076 | 9179, 0.058 | 6659, 0.053 | 9513, 0.106 |
| Transmission factors (max., min.) | 0.900 and 0.939 | 0.918 and 0.991 | 0.852 and 0.975 | 1.081 and 0.912 | 1.094 and 0.889 | 1.204 and 0.650 | 1.087 and 0.896 | 1.000 and 0.761 |
| Number of parameters | 1320 | 1114 | 1058 | 362 | 440 | 362 | 353 | 309 |
| $R_1$ [$F^2 > 2\sigma(F^2)$] | 0.0609 | 0.0829 | 0.0932 | 0.034 | 0.064 | 0.021 | 0.032 | 0.055 |
| $wR_2$ (all data) | 0.1905 | 0.2291 | 0.2706 | 0.047 | 0.142 | 0.039 | 0.082 | 0.129 |
| GOOF, S | 1.038 | 0.970 | 1.066 | 0.743 | 1.197 | 0.893 | 0.983 | 0.967 |
| Largest difference peak and hole (e $Å^{-3}$) | 1.060 and –0.535 | 0.738 and –0.814 | 3.393 and –1.442 | 0.90 and -0.58 | 0.83 and -1.26 | 0.70 and -0.56 | 0.73 and -0.55 | 0.98 and -0.54 |

| Compound | 40 | 41 | 42 | 44 | 50 | 51 |
|---|---|---|---|---|---|---|
| Formula | $C_{27}H_{30}Cl_4NNbO_2$ | $C_{27}H_{30}Cl_4NO_2Ta$ | $2(C_{22}H_{28}Cl_4NNbO_2)\cdot CH_3CN$ | $C_{19}H_{12}Cl_6NNbO_2$ | $C_{19}H_{13}Cl_7NO_2Ta.CH_3CN$ | $C_{62}H_{66}F_{10}O_4Zn_2$ |
| Formula weight | 635.23 | 723.27 | 1187.38 | 591.91 | 757.46 | 1195.89 |
| Crystal system | triclinic | triclinic | triclinic | orthorhombic | monoclinic | triclinic |
| Space group | $P\bar{1}$ | $P\bar{1}$ | $P\bar{1}$ | $P2_12_12_1$ | $P2_1/n$ | $P\bar{1}$ |
| Unit cell dimensions | | | | | | |
| a (Å) | 12.1954(2) | 12.1398(6) | 13.0985(7) | 10.868(4) | 8.183(2) | 10.935(3) |
| b (Å) | 12.6842(2) | 12.6559(6) | 13.7170(7) | 11.314(4) | 13.749(4) | 15.653(4) |
| c (Å) | 18.5633(4) | 18.4905(13) | 17.7489(8) | 35.538(10) | 22.878(6) | 18.150(5) |
| α (°) | 89.5122(14) | 89.558(6) | 99.982(4) | 90 | 90 | 95.911(4) |
| β (°) | 86.343(2) | 86.364(6) | 101.996(4) | 90 | 94.750(4) | 105.236(3) |
| γ (°) | 86.3393(14) | 86.546(6) | 118.206(5) | 90 | 90 | 105.822(4) |
| V ($Å^3$) | 2859.81(9) | 2830.0(3) | 2608.9(2) | 4370(2) | 2565.2(11) | 2832.4(13) |
| Z | 4 | 4 | 2 | 8 | 4 | 2 |
| Temperature (K) | 140(1) | 100(2) | 140(1) | 100(2) | 100(2) | 120(2) |
| $D_{calcd}$ ($Mg/m^{-3}$) | 1.475 | 1.698 | 1.511 | 1.799 | 1.961 | 1.402 |
| Absorption coefficient, μ ($mm^{-1}$) | 0.819 | 4.286 | 0.892 | 1.301 | 5.04 | 0.926 |
| Crystal size ($mm^3$) | 0.31 x 0.22 x 0.15 | 0.04 x 0.03 x 0.01 | 0.3 x 0.2 x 0.01 | 0.38 x 0.04 x 0.02 | 0.40 x 0.07 x 0.03 | 0.18 x 0.05 x 0.02 |
| $2\theta_{max}$ (°) | 30.0 | 25.0 | 22.5 | 27.53 | 30.0 | 26.00 |
| Reflections measured | 56330 | 27028 | 28059 | 27674 | 26828 | 24992 |
| Unique reflections, $R_{int}$ | 16648, 0.047 | 9890, 0.071 | 6787, 0.083 | 9973, 0.051 | 7472, 0.043 | 11859, 0.0418 |
| Reflections with $F^2 > 2\sigma(F^2)$ | 13655 | 7902 | 5308 | 9191 | 6847 | 7447 |
| Transmission factors (max., min.) | 1.000 and 0.853 | 1.000 and 0.702 | 1.000 and 0.890 | 1.000 and 0.791 | 1.000 and 0.752 | 0.982 and 0.851 |
| Number of parameters | 631 | 362 | 569 | 524 | 299 | 888 |
| $R_1$ [$F^2 > 2\sigma(F^2)$] | 0.037 | 0.087 | 0.058 | 0.048 | 0.036 | 0.0456 |
| $wR_2$ (all data) | 0.083 | 0.216 | 0.128 | 0.094 | 0.064 | 0.1167 |
| GOOF, S | 1.035 | 1.153 | 1.064 | 1.083 | 1.093 | 0.988 |
| Largest difference peak and hole (e $Å^{-3}$) | 1.66 and -0.89 | 4.86 and -3.47 | 1.92 and -1.06 | 1.12 and -1.01 | 1.44 and -1.38 | 0.388 and -0.332 |

| **Compound** | **52** | **53** | **56** | **57** | **58** |
|---|---|---|---|---|---|
| Formula | $C_{52}H_{72}O_4Zn_2$ | $C_{56}H_{84}NNaO_4Si_2Zn$ | $C_{126}H_{137}F_{15}O_{19}Zn_6.5CH_3CN$ | $C_{58}H_{83}LiMgO_5$ | $C_{57}H_{82}MgO_4.C_5H_{12}$ |
| Formula weight | 891.89 | 979.83 | 2837.84 | 891.49 | 927.68 |
| Crystal system | Triclinic | Triclinic | Triclinic | Monoclinic | Monoclinic |
| Space group | $P\ \bar{1}$ | $P\ \bar{1}$ | $P\ \bar{1}$ | $C2/c$ | $P2_1/c$ |
| Unit cell dimensions | | | | | |
| a (Å) | 12.4407(9) | 10.0724(7) | 16.9733 (14) | 26.5541(19) | 16.4117(7) |
| b (Å) | 13.4833(9) | 12.3152(9) | 20.4715 (17) | 22.8307(16) | 13.4182(7) |
| c (Å) | 24.1096(17) | 22.8866(16) | 21.2759 (17) | 21.4201(15) | 25.8860(18) |
| α (°) | 90.508(5) | 81.897(3) | 91.246 (6) | 90 | 90 |
| β (°) | 100.609(6) | 88.440(3) | 109.931 (8) | 124.770(2) | 93.318(7) |
| γ (°) | 113.943(7) | 89.093(3) | 102.477 (7) | 90 | 90 |
| V (Å$^3$) | 3617.2(5) | 2809.3(3) | 6749.0 (10) | 10667.2(13) | 5690.9(6) |
| Z | 3 | 2 | 2 | 8 | 4 |
| Temperature (K) | 100(2) | 100(2) | 100(2) | 100(2) | 100(2) |
| $D_{calcd}$ (Mg/m$^{-3}$) | 1.228 | 1.058 | 1.396 | 1.110 | 1.083 |
| Absorption coefficient, μ (mm$^{-1}$) | 1.036 | 0.526 | 1.14 | 0.079 | 0.075 |
| Crystal size (mm$^3$) | 0.050 x 0.040 x 0.020 | 0.18 x 0.13 x 0.05 | 0.11 × 0.02 × 0.01 | 0.01 × 0.07 × 0.17 | 0.02 × 0.10 × 0.11 |
| $2\vartheta_{max}$ (°) | 27.5 | 27.5 | 22.5 | 27.5 | 27.5 |
| Reflections measured | 42558 | 49433 | 60159 | 64853 | 26366 |
| Unique reflections, $R_{int}$ | 16159, 0.0754 | 12822, 0.0389 | 17582, 0.340 | 12206 | 9632 |
| Reflections with $F^2 > 2\sigma(F^2)$ | 11427 | 12053 | 5403 | 7056 | 5353 |
| Transmission factors (max., | 1.000 and 0.757 | 1.000 and 0.747 | 0.994 and 0.885 | 1.000 and 0.635 | 1.000 and 0.299 |
| Number of parameters | 808 | 603 | 1766 | 625 | 621 |
| $R_1$ [$F^2 > 2\sigma(F^2)$] | 0.0789 | 0.0406 | 0.086 | 0.074 | 0.090 |
| $wR_2$ (all data) | 0.2282 | 0.1156 | 0.142 | 0.192 | 0.275 |
| GOOF, *S* | 1.041 | 1.055 | 0.81 | 1.046 | 1.040 |
| Largest difference peak and hole (e Å$^{-3}$) | 2.818 and -1.586 | 0.901 and -0.806 | 0.50 and -0.44 | 0.728 and −0.354 | 0.922 and −0.339 |